

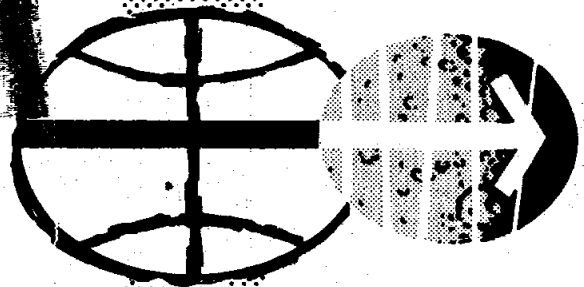
348 pages

MSC-00171



NATIONAL AERONAUTICS AND SPACE ADMINISTRATION

APOLLO 11 MISSION REPORT



MANNED SPACECRAFT CENTER  
HOUSTON, TEXAS  
NOVEMBER 1969

*Green Det*

APOLLO SPACECRAFT FLIGHT HISTORY

<u>Mission</u>	<u>Spacecraft</u>	<u>Description</u>	<u>Launch date</u>	<u>Launch site</u>
PA-1	BP-6	First pad abort	Nov. 7, 1963	White Sands Missile Range, N. Mex.
A-001	BP-12	Transonic abort	May 13, 1964	White Sands Missile Range, N. Mex.
AS-101	BP-13	Nominal launch and exit environment	May 28, 1964	Cape Kennedy, Fla.
AS-102	BP-15	Nominal launch and exit environment	Sept. 18, 1964	Cape Kennedy, Fla.
A-002	BP-23	Maximum dynamic pressure abort	Dec. 8, 1964	White Sands Missile Range, N. Mex.
AS-103	BP-16	Micrometeoroid experiment	Feb. 16, 1965	Cape Kennedy, Fla.
A-003	BP-22	Low-altitude abort (planned high- altitude abort)	May 19, 1965	White Sands Missile Range, N. Mex.
AS-104	BP-26	Micrometeoroid experiment and service module RCS launch environment	May 25, 1965	Cape Kennedy, Fla.
PA-2	BP-23A	Second pad abort	June 29, 1965	White Sands Missile Range, N. Mex.
AS-105	BP-9A	Micrometeoroid experiment and service module RCS launch environment	July 30, 1965	Cape Kennedy, Fla.
A-004	SC-002	Power-on tumbling boundary abort	Jan. 20, 1966	White Sands Missile Range, N. Mex.
AS-201	SC-009	Supercircular entry with high heat rate	Feb. 26, 1966	Cape Kennedy, Fla.
AS-202	SC-011	Supercircular entry with high heat load	Aug. 25, 1966	Cape Kennedy, Fla.

(Continued inside back cover)

MSC-00171

APOLLO 11 MISSION REPORT

PREPARED BY

Mission Evaluation Team

APPROVED BY

A handwritten signature in cursive script that reads "George M. Low". The signature is written in black ink and is positioned above a solid horizontal line.

George M. Low  
Manager, Apollo Spacecraft Program

NATIONAL AERONAUTICS AND SPACE ADMINISTRATION  
MANNED SPACECRAFT CENTER  
HOUSTON, TEXAS  
November 1969



"Houston, the Eagle has landed."



## CONTENTS

Section		Page
1.0	<u>SUMMARY</u> . . . . .	1-1
2.0	<u>INTRODUCTION</u> . . . . .	2-1
3.0	<u>MISSION DESCRIPTION</u> . . . . .	3-1
4.0	<u>PILOTS' REPORT</u> . . . . .	4-1
4.1	PRELAUNCH ACTIVITIES . . . . .	4-1
4.2	LAUNCH . . . . .	4-1
4.3	EARTH ORBIT COAST AND TRANSLUNAR INJECTION . . . . .	4-1
4.4	TRANSPOSITION AND DOCKING . . . . .	4-2
4.5	TRANSLUNAR COAST . . . . .	4-2
4.6	LUNAR ORBIT INSERTION . . . . .	4-3
4.7	LUNAR MODULE CHECKOUT . . . . .	4-4
4.8	DESCENT PREPARATION . . . . .	4-4
4.9	UNDOCKING AND SEPARATION . . . . .	4-7
4.10	LUNAR MODULE DESCENT . . . . .	4-7
4.11	COMMAND MODULE SOLO ACTIVITIES . . . . .	4-9
4.12	LUNAR SURFACE OPERATIONS . . . . .	4-10
4.13	LAUNCH PREPARATION . . . . .	4-16
4.14	ASCENT . . . . .	4-17
4.15	RENDEZVOUS . . . . .	4-17
4.16	COMMAND MODULE DOCKING . . . . .	4-18
4.17	TRANSEARTH INJECTION . . . . .	4-19
4.18	TRANSEARTH COAST . . . . .	4-19
4.19	ENTRY . . . . .	4-20
4.20	RECOVERY . . . . .	4-20
5.0	<u>LUNAR DESCENT AND ASCENT</u> . . . . .	5-1
5.1	DESCENT TRAJECTORY LOGIC . . . . .	5-1
5.2	PREPARATION FOR POWERED DESCENT . . . . .	5-2
5.3	POWERED DESCENT . . . . .	5-4

Section		Page
5.4	LANDING DYNAMICS . . . . .	5-6
5.5	POSTLANDING SPACECRAFT OPERATIONS . . . . .	5-7
5.6	ASCENT . . . . .	5-8
5.7	RENDEZVOUS . . . . .	5-10
6.0	<u>COMMUNICATIONS</u> . . . . .	6-1
7.0	<u>TRAJECTORY</u> . . . . .	7-1
7.1	LAUNCH PHASE . . . . .	7-1
7.2	EARTH PARKING ORBIT . . . . .	7-1
7.3	TRANSLUNAR INJECTION . . . . .	7-1
7.4	MANEUVER ANALYSIS . . . . .	7-2
7.5	COMMAND MODULE ENTRY . . . . .	7-4
7.6	SERVICE MODULE ENTRY . . . . .	7-5
7.7	LUNAR ORBIT TARGETING . . . . .	7-5
7.8	LUNAR ORBIT NAVIGATION . . . . .	7-6
8.0	<u>COMMAND AND SERVICE MODULE PERFORMANCE</u> . . . . .	8-1
8.1	STRUCTURAL AND MECHANICAL SYSTEMS . . . . .	8-1
8.2	ELECTRICAL POWER . . . . .	8-4
8.3	CRYOGENIC STORAGE . . . . .	8-5
8.4	VHF RANGING . . . . .	8-5
8.5	INSTRUMENTATION . . . . .	8-5
8.6	GUIDANCE, NAVIGATION, AND CONTROL . . . . .	8-6
8.7	REACTION CONTROL . . . . .	8-19
8.8	SERVICE PROPULSION . . . . .	8-19
8.9	ENVIRONMENTAL CONTROL SYSTEM . . . . .	8-23
8.10	CREW STATION . . . . .	8-24
8.11	CONSUMABLES . . . . .	8-25
9.0	<u>LUNAR MODULE PERFORMANCE</u> . . . . .	9-1
9.1	STRUCTURAL AND MECHANICAL SYSTEMS . . . . .	9-1
9.2	THERMAL CONTROL . . . . .	9-1
9.3	ELECTRICAL POWER . . . . .	9-2

Section		Page
9.4	COMMUNICATIONS EQUIPMENT . . . . .	9-2
9.5	INSTRUMENTATION . . . . .	9-3
9.6	GUIDANCE AND CONTROL . . . . .	9-3
9.7	REACTION CONTROL . . . . .	9-19
9.8	DESCENT PROPULSION . . . . .	9-22
9.9	ASCENT PROPULSION . . . . .	9-27
9.10	ENVIRONMENTAL CONTROL SYSTEM . . . . .	9-29
9.11	RADAR . . . . .	9-29
9.12	CREW STATION . . . . .	9-30
9.13	CONSUMABLES . . . . .	9-30
10.0	<u>EXTRAVEHICULAR MOBILITY UNIT PERFORMANCE</u> . . . . .	10-1
11.0	<u>THE LUNAR SURFACE</u> . . . . .	11-1
11.1	LUNAR GEOLOGY EXPERIMENT . . . . .	11-3
11.2	LUNAR SURFACE MECHANICS EXPERIMENT . . . . .	11-12
11.3	EXAMINATION OF LUNAR SAMPLES . . . . .	11-14
11.4	PASSIVE SEISMIC EXPERIMENT . . . . .	11-17
11.5	LASER RANGING RETRO-REFLECTOR EXPERIMENT . . . . .	11-22
11.6	SOLAR WIND COMPOSITION EXPERIMENT . . . . .	11-23
11.7	PHOTOGRAPHY . . . . .	11-23
12.0	<u>BIOMEDICAL EVALUATION</u> . . . . .	12-1
12.1	BIOINSTRUMENTATION AND PHYSIOLOGICAL DATA . . . . .	12-1
12.2	MEDICAL OBSERVATIONS . . . . .	12-2
12.3	EXTRAVEHICULAR ACTIVITY . . . . .	12-5
12.4	PHYSICAL EXAMINATIONS . . . . .	12-5
12.5	LUNAR CONTAMINATION AND QUARANTINE . . . . .	12-6
13.0	<u>MISSION SUPPORT PERFORMANCE</u> . . . . .	13-1
13.1	FLIGHT CONTROL . . . . .	13-1
13.2	NETWORK PERFORMANCE . . . . .	13-2
13.3	RECOVERY OPERATIONS . . . . .	13-3

Section	Page
14.0	<u>ASSESSMENT OF MISSION OBJECTIVES</u> . . . . . 14-1
14.1	LOCATION OF LANDED LUNAR MODULE . . . . . 14-1
14.2	LUNAR FIELD GEOLOGY . . . . . 14-2
15.0	<u>LAUNCH VEHICLE SUMMARY</u> . . . . . 15-1
16.0	<u>ANOMALY SUMMARY</u> . . . . . 16-1
16.1	COMMAND AND SERVICE MODULES . . . . . 16-1
16.2	LUNAR MODULE . . . . . 16-9
16.3	GOVERNMENT-FURNISHED EQUIPMENT . . . . . 16-21
17.0	<u>CONCLUSIONS</u> . . . . . 17-1
APPENDIX A -	<u>VEHICLE DESCRIPTIONS</u> . . . . . A-1
A.1	COMMAND AND SERVICE MODULES . . . . . A-1
A.2	LUNAR MODULE . . . . . A-1
A.3	EXTRAVEHICULAR MOBILITY UNIT . . . . . A-5
A.4	EXPERIMENT EQUIPMENT . . . . . A-8
A.5	LAUNCH VEHICLE . . . . . A-10
A.6	MASS PROPERTIES . . . . . A-10
APPENDIX B -	<u>SPACECRAFT HISTORIES</u> . . . . . B-1
APPENDIX C -	<u>POSTFLIGHT TESTING</u> . . . . . C-1
APPENDIX D -	<u>DATA AVAILABILITY</u> . . . . . D-1
APPENDIX E -	<u>GLOSSARY</u> . . . . . E-1

SYMBOLS AND ABBREVIATIONS

A	ampere
ac	alternating current
AGS	abort guidance system
A-h	ampere-hour
ALDS	Apollo launch data system
arc sec	arc second
ARIA	Apollo range instrumentation aircraft
BDA	Bermuda
Btu	British thermal unit
CAPCOM	capsule communicator
CATS	command and telemetry system
c.d.t.	central daylight time
cm	centimeter
CMC	command module computer
CRO	Carnarvon, Australia
CSM	command and service modules
CYI	Canary Islands
D	down
dB	decibel (also used as dBm)
dc	direct current
deg	degree
D/T	delayed time
E	east
e.s.t.	eastern standard time
FM	frequency modulation
ft/sec	feet per second
g	gravity of earth
G&N	guidance and navigation
GDS	Goldstone, California
G.m.t.	Greenwich mean time

HAW	Hawaii
hr	hour
HSK	Honeysuckle, Australia
Hz	hertz
I	inertia
in-lb	inch-pound
kpps	kilopulses per second
kW-h	kilowatt-hour
lb/hr	pounds per hour
lb/ft <sup>2</sup>	pounds per square foot
LGC	lunar module guidance computer
LM	lunar module
M	mega-
MAD	Madrid, Spain
mERU	milli-earth rate unit
mg	milligram
MILA	Merritt Island Launch Area, Florida
min	minute
mm	millimeter
msec	millisecond
MSFN	Manned Space Flight Network
N	north
NA	not available
P	pressure (transducer location)
PAM	pulse amplitude modulation
PCM	pulse code modulation
PM	phase modulation
ppm	parts per million
psf	pounds per square foot
psi	pounds per square inch
q	dynamic pressure
RED	Redstone tracking ship

REFSMAT	REFErence Stable Member MATrix
S	south
S-IC, S-II, S-IVB	first, second, and third stages of Saturn V launch vehicle
T	temperature (transducer location)
TAN	Tananarive
US	United States
V	volt
VAN	Vanguard tracking ship
VHF	very high frequency
VOX	voice-operated transmitter
W	west
W-h	watt-hour
X, Y, Z	spacecraft axes
°C	degrees Centigrade
°F	degrees Fahrenheit
$\alpha$	angle of attack
$\mu$	micro-

## 1.0 SUMMARY

The purpose of the Apollo 11 mission was to land men on the lunar surface and to return them safely to earth. The crew were Neil A. Armstrong, Commander; Michael Collins, Command Module Pilot; and Edwin E. Aldrin, Jr., Lunar Module Pilot.

The space vehicle was launched from Kennedy Space Center, Florida, at 8:32:00 a.m., e.s.t., July 16, 1969. The activities during earth orbit checkout, translunar injection, transposition and docking, spacecraft ejection, and translunar coast were similar to those of Apollo 10. Only one midcourse correction, performed at about 27 hours elapsed time, was required during translunar coast.

The spacecraft was inserted into lunar orbit at about 76 hours, and the circularization maneuver was performed two revolutions later. Initial checkout of lunar module systems was satisfactory, and after a planned rest period, the Commander and Lunar Module Pilot entered the lunar module to prepare for descent.

The two spacecraft were undocked at about 100 hours, followed by separation of the command and service modules from the lunar module. Descent orbit insertion was performed at approximately 101-1/2 hours, and powered descent to the lunar surface began about 1 hour later. Operation of the guidance and descent propulsion systems was nominal. The lunar module was maneuvered manually approximately 1100 feet downrange from the nominal landing point during the final 2-1/2 minutes of descent. The spacecraft landed in the Sea of Tranquillity at 102:45:40. The landing coordinates were 0 degrees 41 minutes 15 seconds north latitude and 23 degrees 26 minutes east longitude referenced to lunar map ORB-II-6(100), first edition, December 1967. During the first 2 hours on the surface, the two crewmen performed a postlanding checkout of all lunar module systems. Afterwards, they ate their first meal on the moon and elected to perform the surface operations earlier than planned.

Considerable time was deliberately devoted to checkout and donning of the back-mounted portable life support and oxygen purge systems. The Commander egressed through the forward hatch and deployed an equipment module in the descent stage. A camera in this module provided live television coverage of the Commander descending the ladder to the surface, with first contact made at 109:24:15 (9:56:15 p.m. e.s.t., July 20, 1969). The Lunar Module Pilot egressed soon thereafter, and both crewmen used the initial period on the surface to become acclimated to the reduced gravity and unfamiliar surface conditions. A contingency sample was taken from the surface, and the television camera was deployed so that most of the lunar module was included in its view field. The crew activated the scientific experiments, which included a solar wind detector, a passive



seismometer, and a laser retro-reflector. The Lunar Module Pilot evaluated his ability to operate and move about, and was able to translate rapidly and with confidence. Forty-seven pounds of lunar surface material were collected to be returned for analysis. The surface exploration was concluded in the allotted time of 2-1/2 hours, and the crew reentered the lunar module at 111-1/2 hours.

Ascent preparation was conducted efficiently, and the ascent stage lifted off the surface at 124-1/4 hours. A nominal firing of the ascent engine placed the vehicle into a 45- by 9-mile orbit. After a rendezvous sequence similar to that of Apollo 10, the two spacecraft were docked at 128 hours. Following transfer of the crew, the ascent stage was jettisoned, and the command and service modules were prepared for transearth injection.

The return flight started with a 150-second firing of the service propulsion engine during the 31st lunar revolution at 135-1/2 hours. As in translunar flight, only one midcourse correction was required, and passive thermal control was exercised for most of transearth coast. Inclement weather necessitated moving the landing point 215 miles downrange. The entry phase was normal, and the command module landed in the Pacific Ocean at 195-1/4 hours. The landing coordinates, as determined from the onboard computer, were 13 degrees 19 minutes north latitude and 169 degrees 09 minutes west longitude.

After landing, the crew donned biological isolation garments. They were then retrieved by helicopter and taken to the primary recovery ship, USS Hornet. The crew and lunar material samples were placed in the Mobile Quarantine Facility for transport to the Lunar Receiving Laboratory in Houston. The command module was taken aboard the Hornet about 3 hours after landing.

With the completion of Apollo 11, the national objective of landing men on the moon and returning them safely to earth before the end of the decade had been accomplished.

## 2.0 INTRODUCTION

The Apollo 11 mission was the eleventh in a series of flights using Apollo flight hardware and was the first lunar landing mission of the Apollo Program. It was also the fifth manned flight of the command and service modules and the third manned flight of the lunar module. The purpose of the mission was to perform a manned lunar landing and return safely to earth.

Because of the excellent performance of the entire spacecraft, only the systems performance that significantly differed from that of previous missions is reported. The ascent, descent, and landing portions of the mission are reported in section 5, and the lunar surface activities are reported in section 11.

A complete analysis of all flight data is not possible within the time allowed for preparation of this report. Therefore, report supplements will be published for the guidance and control system, propulsion, the biomedical evaluation, the lunar surface photography, the lunar sample analysis, and the trajectory analysis. Other supplements will be published as need is identified.

In this report, all actual times are elapsed time from range zero, established as the integral second before lift-off. Range zero for this mission was 13:32:00 G.m.t., July 16, 1969. All references to mileage distance are in nautical miles.

### 3.0 MISSION DESCRIPTION

The Apollo 11 mission accomplished the basic mission of the Apollo Program; that is, to land two men on the lunar surface and return them safely to earth. As a part of this first lunar landing, three basic experiment packages were deployed, lunar material samples were collected, and surface photographs were taken. Two of the experiments were a part of the early Apollo scientific experiment package which was developed for deployment on the lunar surface. The sequence of events and the flight plan of the Apollo 11 mission are shown in table 3-I and figure 3-1, respectively.

The Apollo 11 space vehicle was launched on July 16, 1969, at 8:32 a.m. e.s.t., as planned. The spacecraft and S-IVB were inserted into a 100.7- by 99.2-mile earth parking orbit. After a 2-1/2-hour checkout period, the spacecraft/S-IVB combination was injected into the translunar phase of the mission. Trajectory parameters after the translunar injection firing were nearly perfect, with the velocity within 1.6 ft/sec of that planned. Only one of the four options for midcourse corrections during the translunar phase was exercised. This correction was made with the service propulsion system at approximately 26-1/2 hours and provided a 20.9 ft/sec velocity change. During the remaining periods of free-attitude flight, passive thermal control was used to maintain spacecraft temperatures within desired limits. The Commander and Lunar Module Pilot transferred to the lunar module during the translunar phase to make an initial inspection and preparations for systems checks shortly after lunar orbit insertion.

The spacecraft was inserted into a 60- by 169.7-mile lunar orbit at approximately 76 hours. Four hours later, the lunar orbit circularization maneuver was performed to place the spacecraft in a 65.7- by 53.8-mile orbit. The Lunar Module Pilot entered the lunar module at about 81 hours for initial power-up and systems checks. After the planned sleep period was completed at 93-1/2 hours, the crew donned their suits, transferred to the lunar module, and made final preparations for descent to the lunar surface. The lunar module was undocked on time at about 100 hours. After the exterior of the lunar module was inspected by the Command Module Pilot, a separation maneuver was performed with the service module reaction control system.

The descent orbit insertion maneuver was performed with the descent propulsion system at 101-1/2 hours. Trajectory parameters following this maneuver were as planned, and the powered descent initiation was on time at 102-1/2 hours. The maneuver lasted approximately 12 minutes, with engine shutdown occurring almost simultaneously with the lunar landing in the Sea of Tranquillity. The coordinates of the actual landing point

were 0 degree 41 minutes 15 seconds north latitude and 23 degrees 26 minutes east longitude, compared with the planned landing point of 0 degree 43 minutes 53 seconds north latitude and 23 degrees 38 minutes 51 seconds east longitude. These coordinates are referenced to Lunar Map ORB-II-6 (100), first edition, dated December 1967.

A 2-hour postlanding checkout was completed, followed by a partial power-down of the spacecraft. A crew rest period was planned to precede the extravehicular activity to explore the lunar surface. However, the crew elected to perform the extravehicular portion of the mission prior to the sleep period because they were not overly tired and were adjusting easily to the 1/6 gravity. After the crew donned their portable life support systems and completed the required checkouts, the Commander egressed at about 109 hours. Prior to descending the ladder, the Commander deployed the equipment module in the descent stage. The television camera located in the module operated satisfactorily and provided live television coverage of the Commander's descent to the lunar surface. The Commander collected the contingency lunar material samples, and approximately 20 minutes later, the Lunar Module Pilot egressed and dual exploration of the lunar surface began.

During this exploration period, the television camera was deployed and the American flag was raised on the lunar surface. The solar wind experiment was also deployed for later retrieval. Both crewmen evaluated their mobility on the lunar surface, deployed the passive seismic and laser retro-reflector experiments, collected about 47 pounds of lunar material, and obtained photographic documentation of their activities and the conditions around them. The crewmen reentered the lunar module after about 2 hours 14 minutes of exploration.

After an 8-hour rest period, the crew began preparations for ascent. Lift-off from the lunar surface occurred on time at 124:22:00.8. The spacecraft was inserted into a 48.0- by 9.4-mile orbit from which a rendezvous sequence similar to that for Apollo 10 was successfully performed.

Approximately 4-1/2 hours after lunar module ascent, the command module performed a docking maneuver, and the two spacecraft were docked. The ascent stage was jettisoned in lunar orbit and the command and service modules were prepared for transearth injection at 135-1/2 hours.

The activities during transearth coast were similar to those during translunar flight. The service module was separated from the command module 15 minutes before reaching the entry interface at 400 000 feet altitude. After an automatic entry sequence and landing system deployment, the command module landed in the Pacific Ocean at 195-1/2 hours. The postlanding procedures involving the primary recovery ship, USS Hornet, included precautions to avoid back-contamination by any lunar organisms, and the crew and samples were placed in quarantine.

After reaching the Manned Spacecraft Center, the spacecraft, crew, and samples entered the Lunar Receiving Laboratory quarantine area for continuation of the postlanding observation and analyses. The crew and spacecraft were released from quarantine on August 10, 1969, after no evidence of abnormal medical reactions was observed.

TABLE 3-I.- SEQUENCE OF EVENTS

Event	Time, hr:min:sec
Range zero - 13:32:00 G.m.t., July 16, 1969	
Lift-off	00:00:00.6
S-IC outboard engine cutoff	00:02:41.7
S-II engine ignition (command)	00:02:43.0
Launch escape tower jettison	00:03:17.9
S-II engine cutoff	00:09:08.3
S-IVB engine ignition (command)	00:09:12.2
S-IVB engine cutoff	00:11:39.3
Translunar injection maneuver	02:44:16.2*
Command and service module/S-IVB separation	03:17:04.6
First docking	03:24:03.1
Spacecraft ejection	04:16:59.1
Separation maneuver (from S-IVB)	04:40:01.8*
First midcourse correction	26:44:58.7*
Lunar orbit insertion	75:49:50.4*
Lunar orbit circularization	80:11:36.8*
Undocking	100:12:00
Separation maneuver (from lunar module)	100:39:52.9*
Descent orbit insertion	101:36:14*
Powered descent initiation	102:33:05.2*
Lunar landing	102:45:39.9
Egress (hatch opening)	109:07:33
Ingress (hatch closing)	111:39:13
Lunar lift-off	124:22:00.8*
Coelliptic sequence initiation	125:19:36*
Constant differential height maneuver	126:17:49.6*
Terminal phase initiation	127:03:51.8*

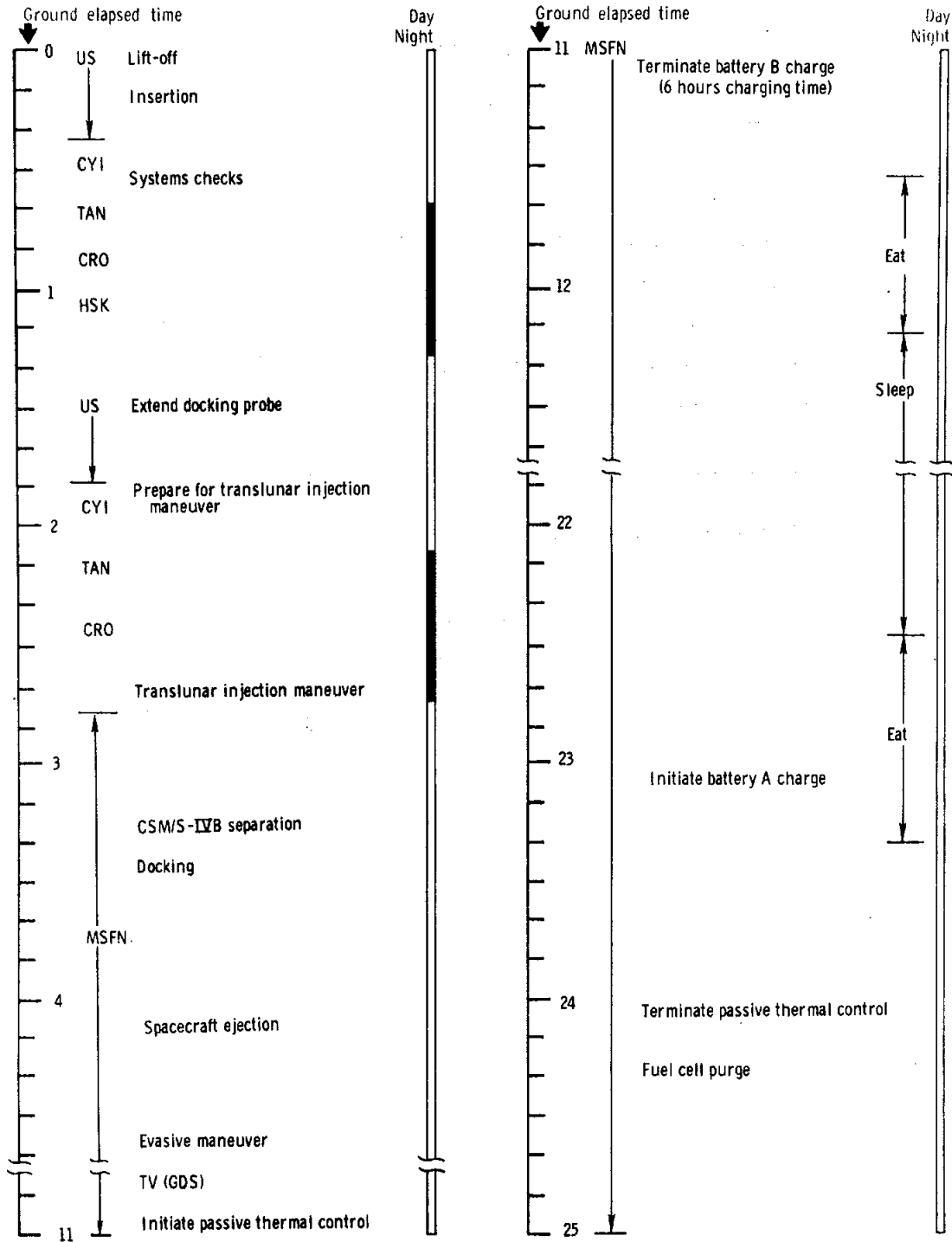
\*Engine ignition time.

TABLE 3-I.- SEQUENCE OF EVENTS - Concluded

Event	Time, hr:min:sec
Docking	128:03:00
Ascent stage jettison	130:09:31.2
Separation maneuver (from ascent stage)	130:30:01*
Transearth injection maneuver	135:23:42.3*
Second midcourse correction	150:29:57.4*
Command module/service module separation	194:49:12.7
Entry interface	195:03:05.7
Landing	195:18:35

\*Engine ignition time.

NASA-S-69-3700

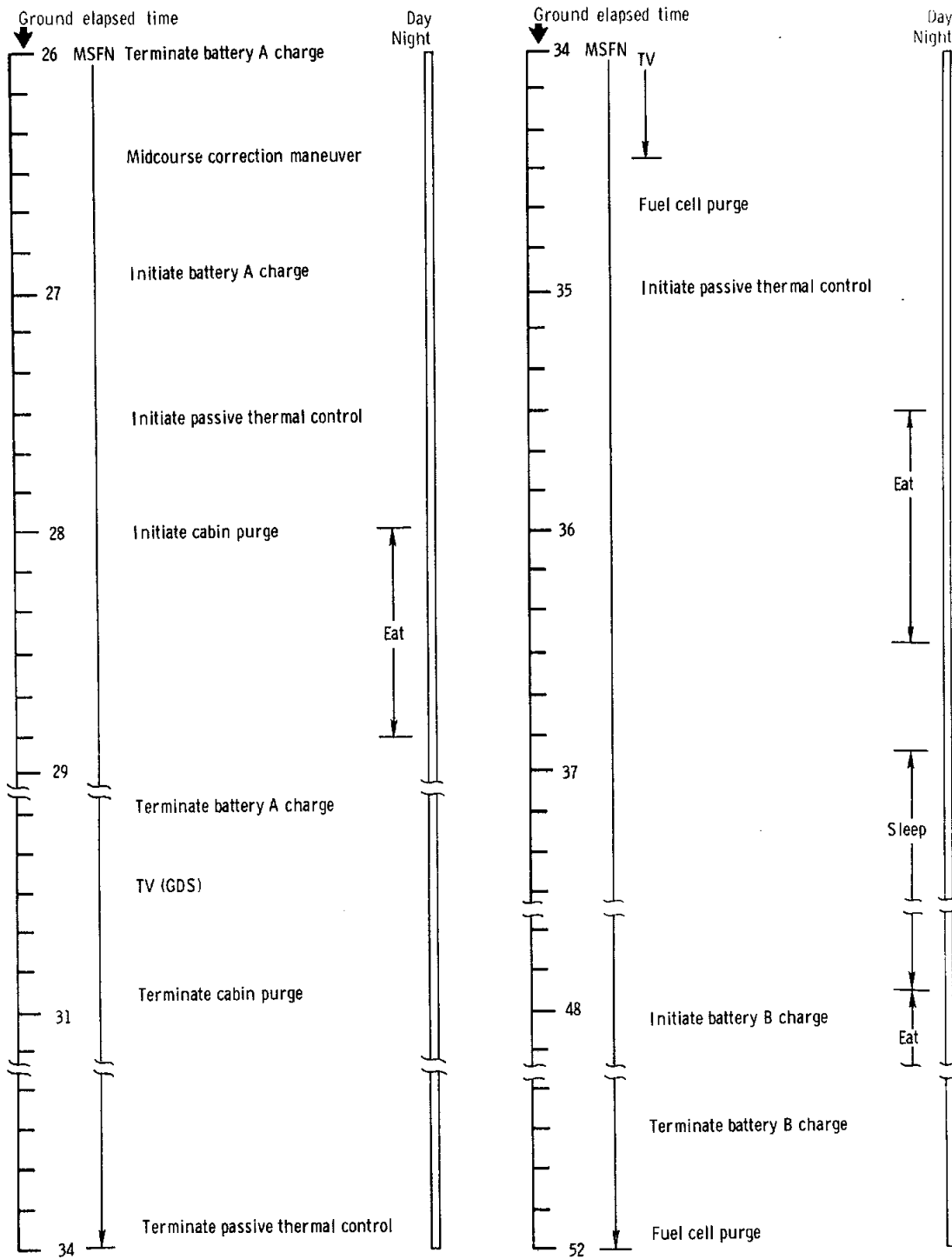


(a) 0 to 25 hours.

Figure 3-1. - Flight plan activities.

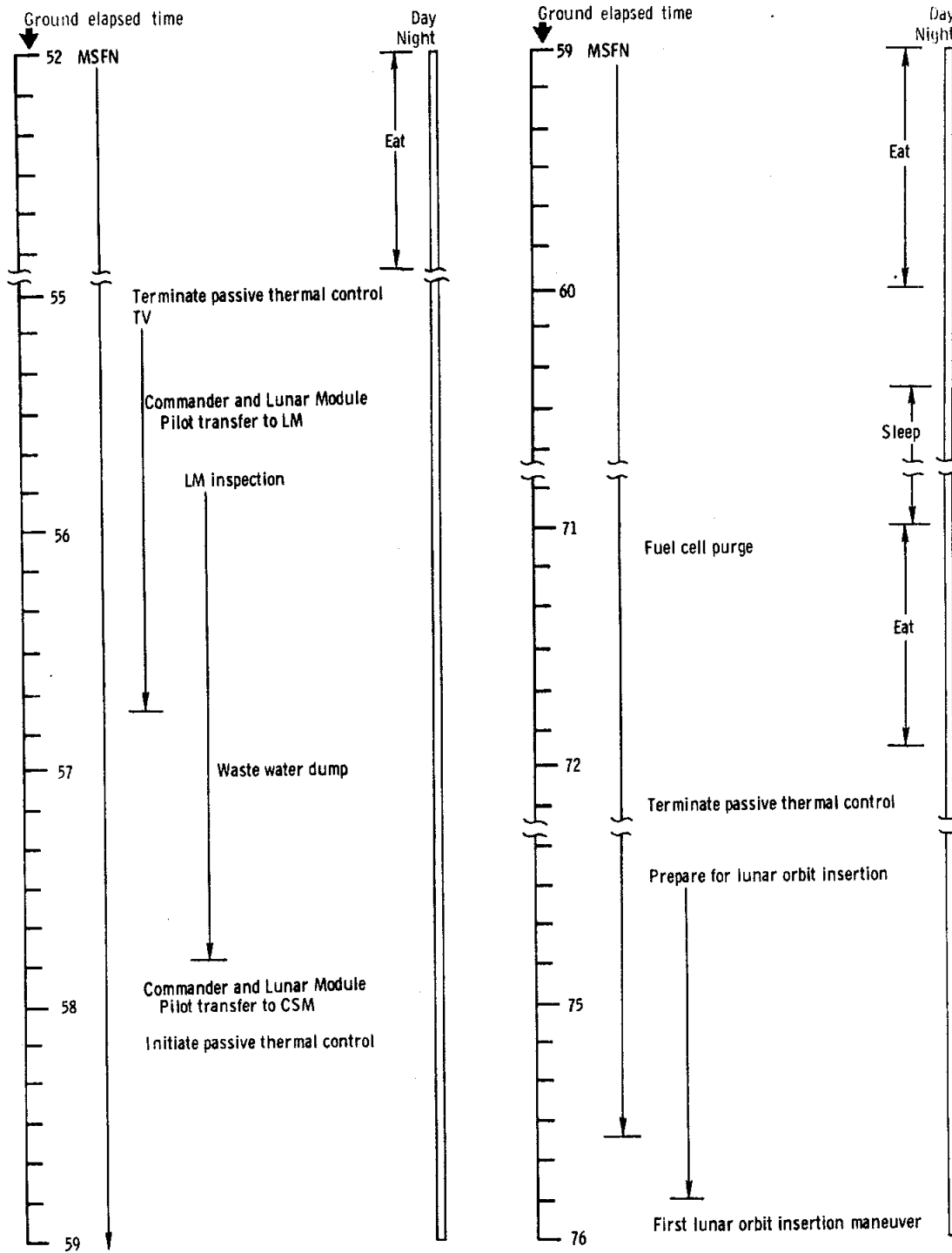


NASA-S-69-3701



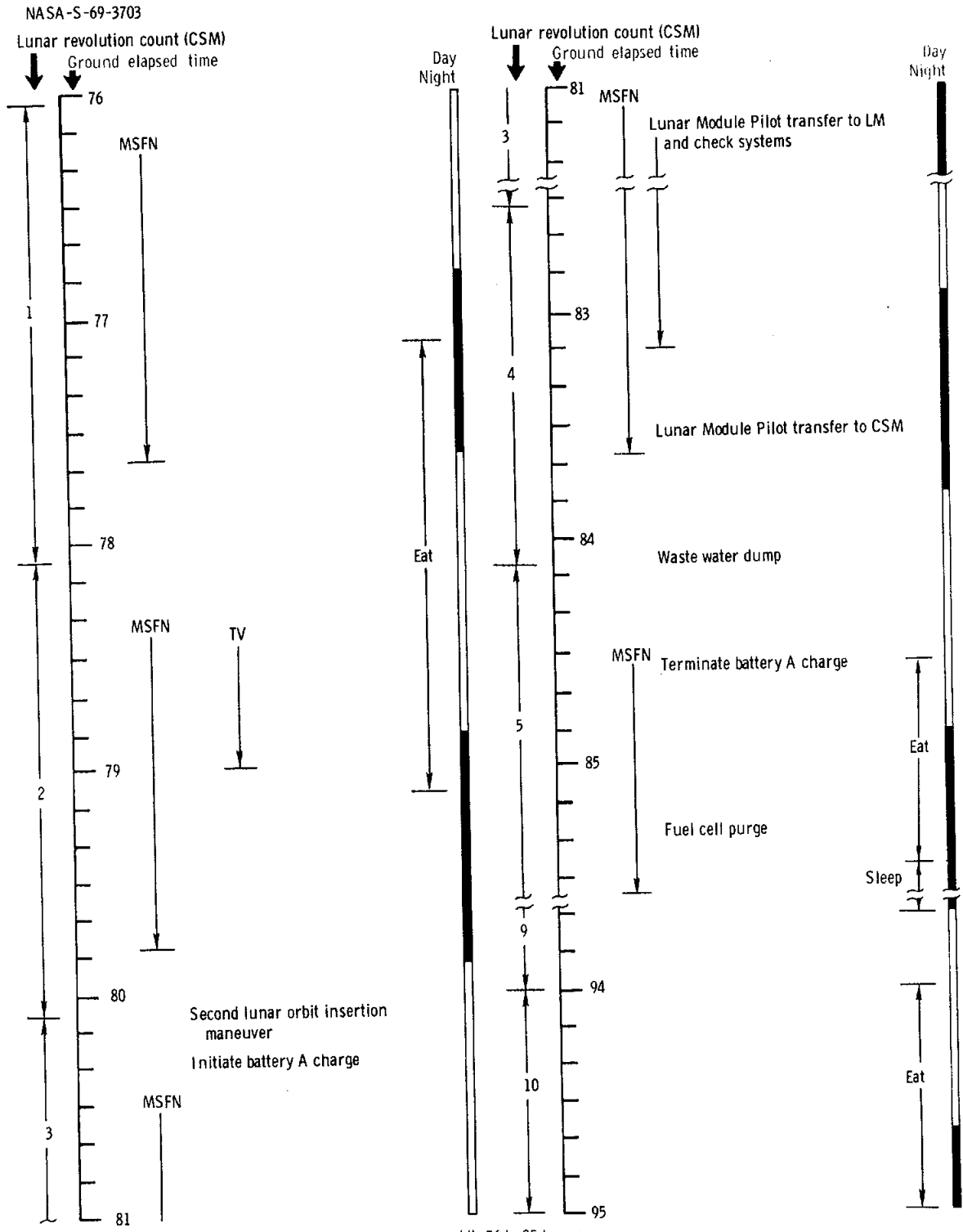
(b) 26 to 52 hours.

Figure 3-1. - Continued.



(c) 52 to 76 hours.

Figure 3-1. - Continued.

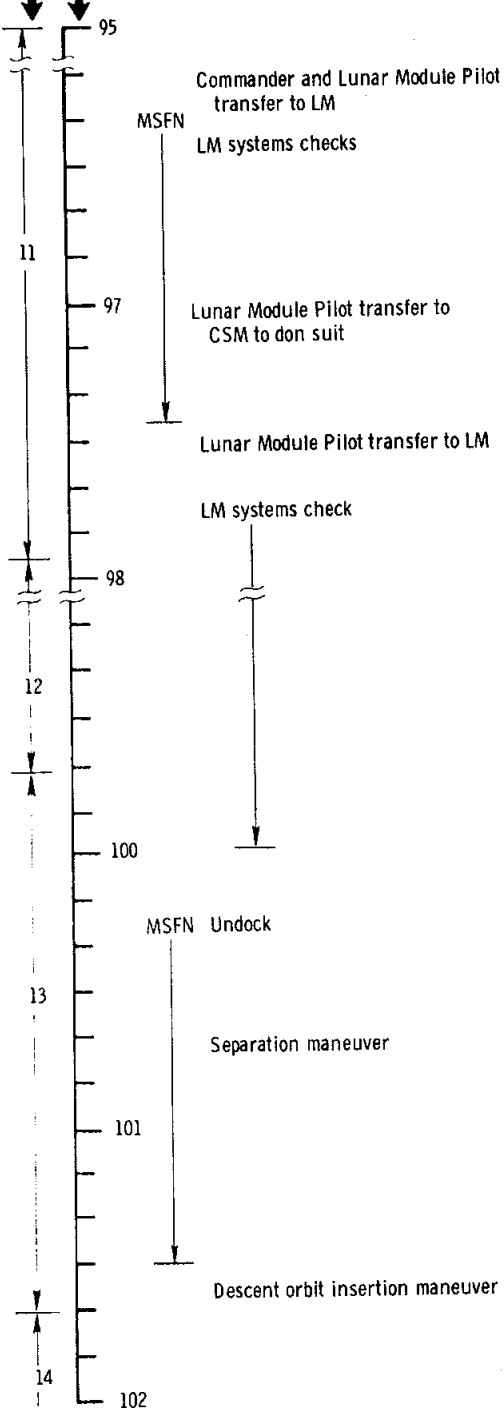


(d) 76 to 95 hours.  
 Figure 3-1. - Continued.

NASA-S-69-3704

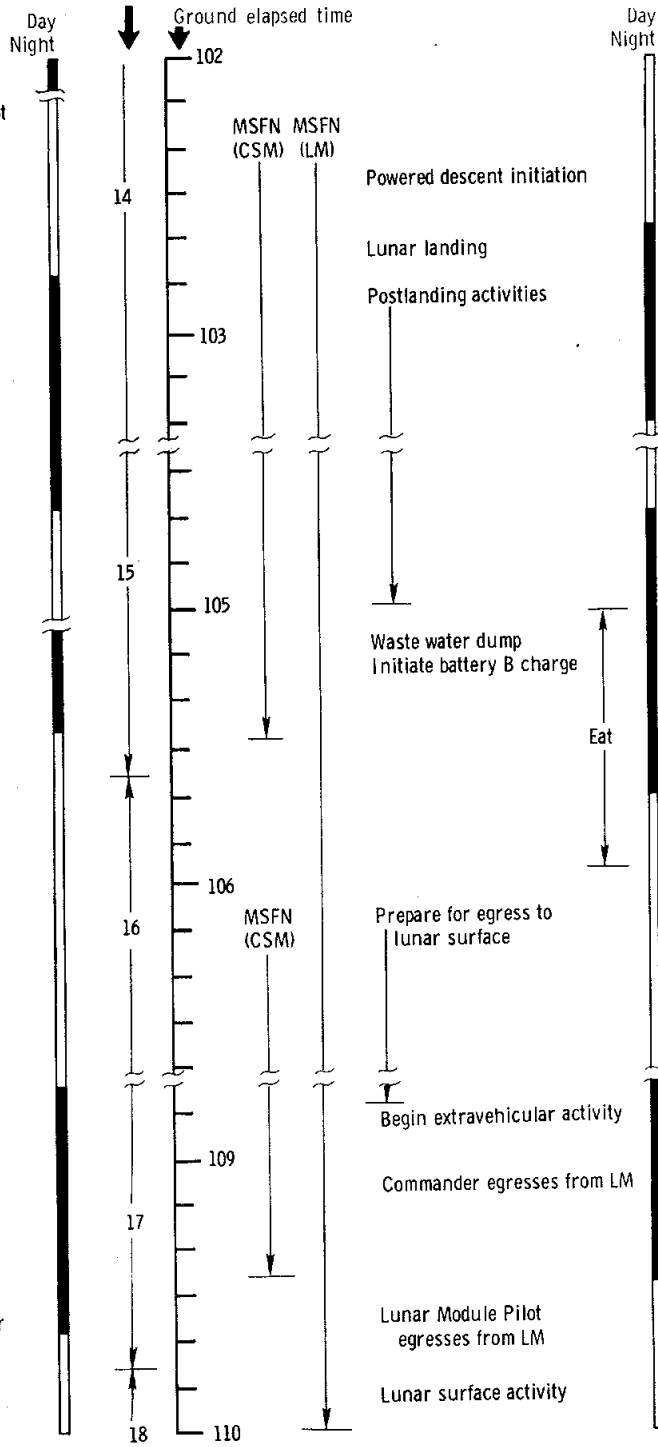
Lunar revolution count (CSM)

Ground elapsed time



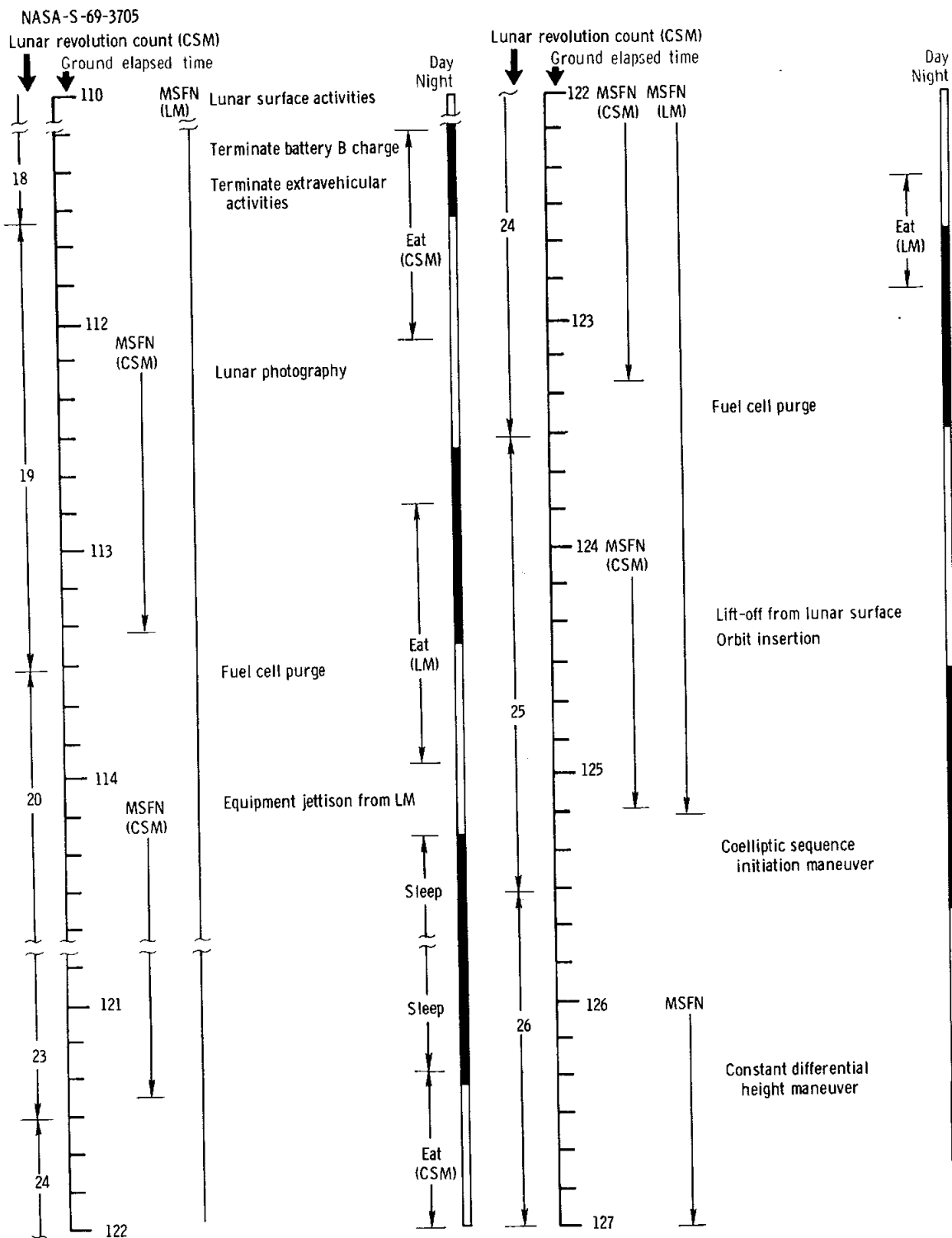
Lunar revolution count (CSM)

Ground elapsed time



(e) 95 to 110 hours.

Figure 3-1. - Continued.

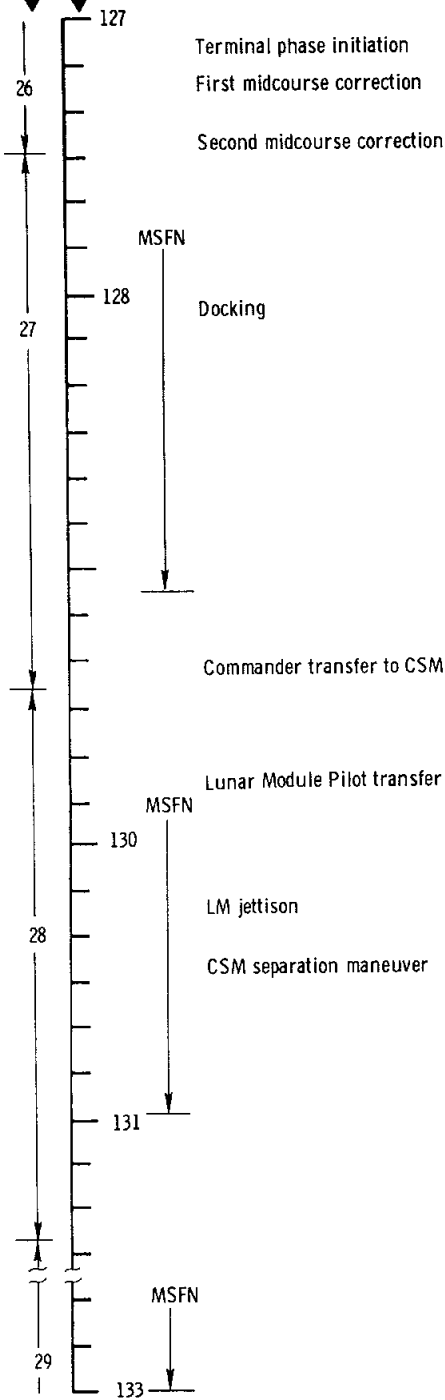


(f) 110 to 127 hours.

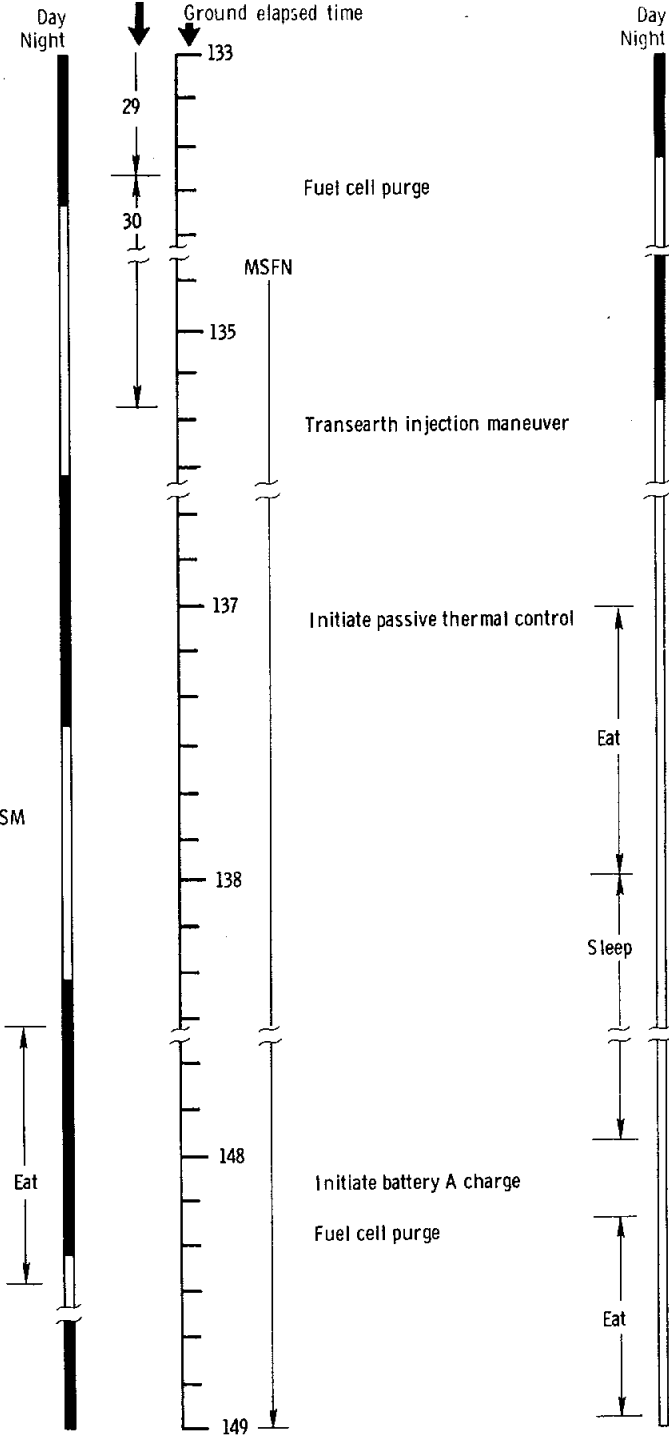
Figure 3-1. - Continued.

NASA-S-69-3706

Lunar revolution count (CSM)  
Ground elapsed time



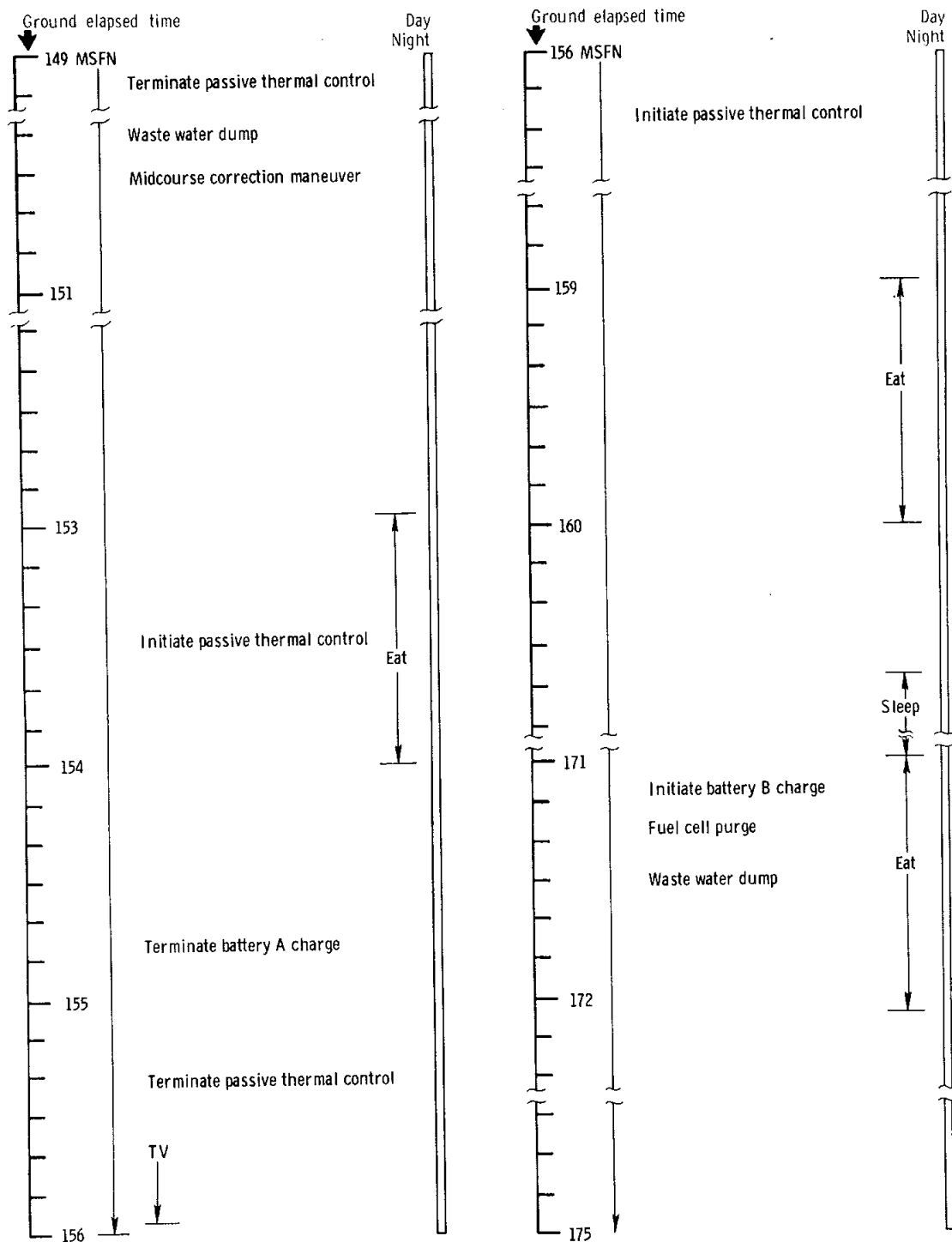
Lunar revolution count (CSM)  
Ground elapsed time



(g) 127 to 149 hours.

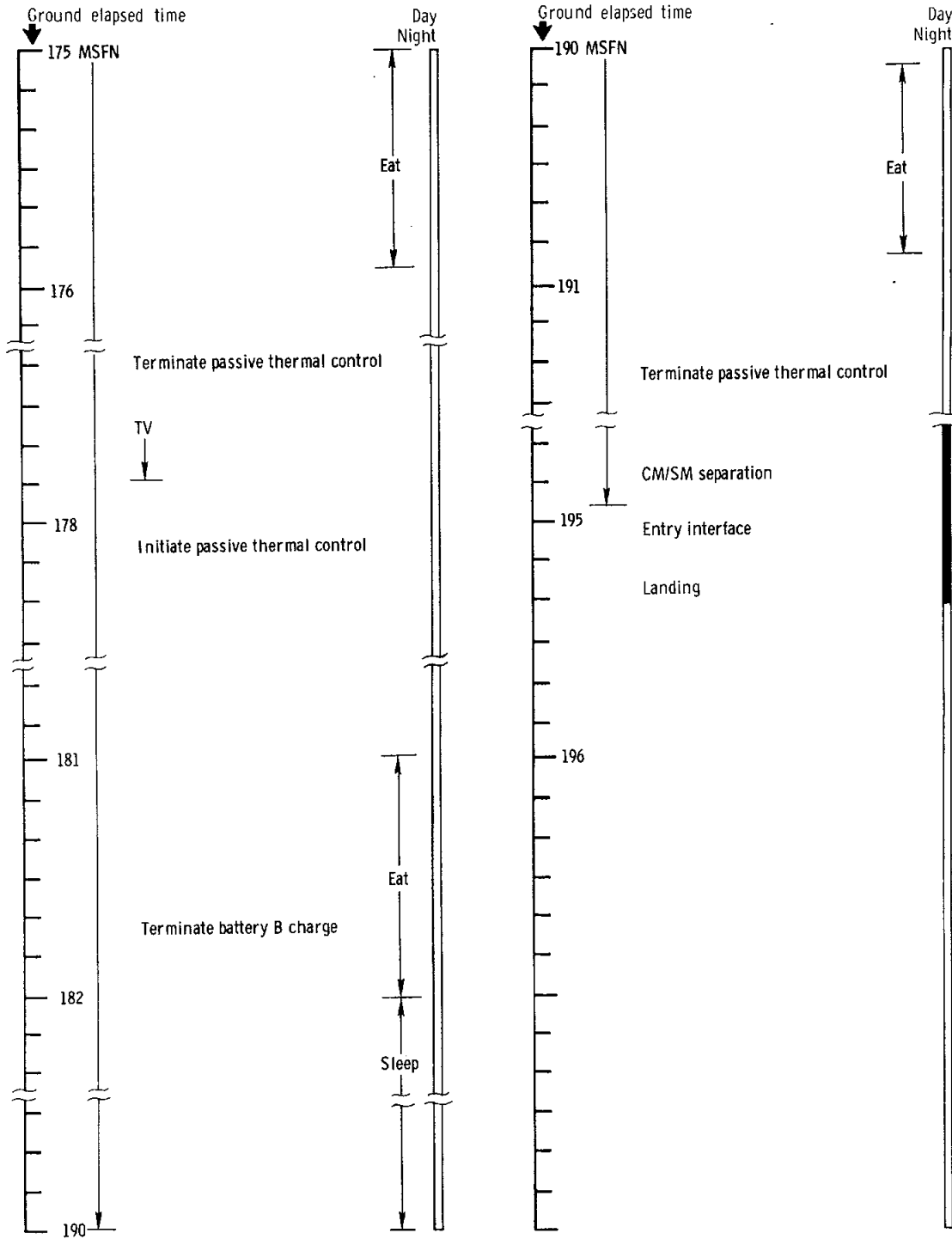
Figure 3-1. - Continued.

NASA-S-69-3707



(h) 149 to 175 hours.

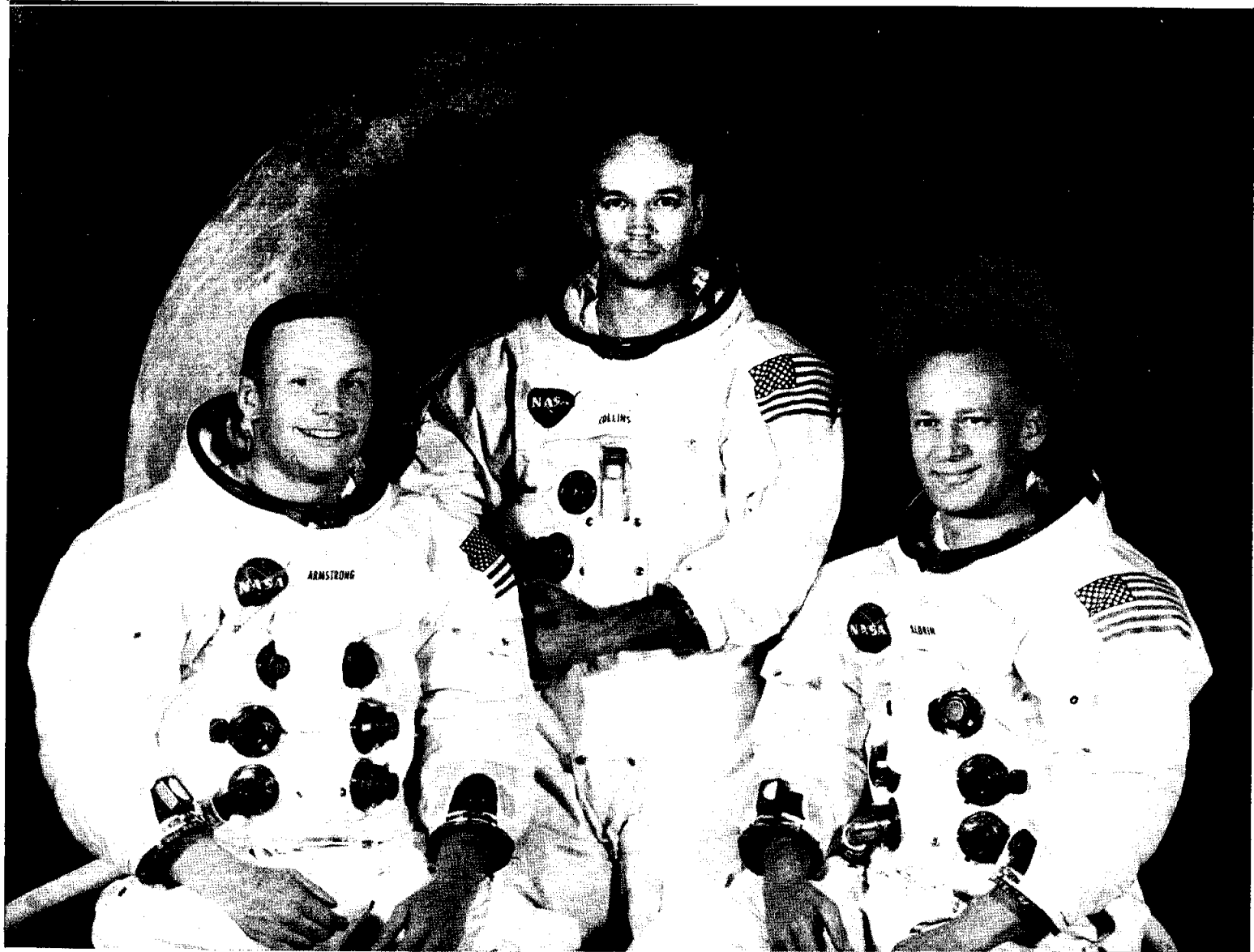
Figure 3-1.- Continued.



(i) 175 to 196 hours.

Figure 3-1. - Concluded.





Commander Neil A. Armstrong, Command Module Pilot Michael Collins, and Lunar Module Pilot Edwin E. Aldrin, Jr.

## 4.0 PILOTS' REPORT

### 4.1 PRELAUNCH ACTIVITIES

All prelaunch systems operations and checks were completed on time and without difficulty. The configuration of the environmental control system included operation of the secondary glycol loop and provided comfortable cockpit temperature conditions.

### 4.2 LAUNCH

Lift-off occurred precisely on time with ignition accompanied by a low rumbling noise and moderate vibration that increased significantly at the moment of hold-down release. The vibration magnitudes decreased appreciably at the time tower clearance was verified. The yaw, pitch, and roll guidance-program sequences occurred as expected. No unusual sounds or vibrations were noted while passing through the region of maximum dynamic pressure and the angle of attack remained near zero. The S-IC/S-II staging sequence occurred smoothly and at the expected time.

The entire S-II stage flight was remarkably smooth and quiet and the launch escape tower and boost protective cover were jettisoned normally. The mixture ratio shift was accompanied by a noticeable acceleration decrease. The S-II/S-IVB staging sequence occurred smoothly and approximately at the predicted time. The S-IVB insertion trajectory was completed without incident and the automatic guidance shutdown yielded an insertion-orbit ephemeris, from the command module computer, of 102.1 by 103.9 miles. Communication between crew members and the Network were excellent throughout all stages of launch.

### 4.3 EARTH ORBIT COAST AND TRANSLUNAR INJECTION

The insertion checklist was completed and a series of spacecraft systems checks disclosed no abnormalities. All tests of the navigation equipment, including alignments and drift checks, were satisfactory. The service module reaction control thrusters were fired in the minimum impulse mode and verified by telemetry.

No abnormalities were noted during preparation for translunar injection. Initiation of translunar injection was accompanied by the proper onboard indications and the S-IVB propellant tanks were repressurized on schedule.

The S-IVB stage reignited on time at 2:44:16 without ignition or guidance transients. An apparent 0.5- to 1.5-degree pitch-attitude error on the attitude indicators was not confirmed by the command module computer, which indicated that the attitude and attitude rate duplicated the reference trajectory precisely (see section 8.6). The guided cutoff yielded a velocity very close to that expected, as indicated by the on-board computer. The entry monitor system further confirmed that the forward velocity error for the translunar injection maneuver was within 3.3 ft/sec.

#### 4.4 TRANSPOSITION AND DOCKING

The digital autopilot was used for the transposition maneuver scheduled to begin 20 seconds after spacecraft separation from the S-IVB. The time delay was to allow the command and service modules to drift about 70 feet prior to thrusting back toward the S-IVB. Separation and the beginning of transposition were on time. In order to assure a pitch-up maneuver for better visibility through the hatch window, pitch axis control was retained in a manual mode until after a pitch-up rate of approximately 1 deg/sec was attained. Control was then given to the digital autopilot to continue the combined pitch/roll maneuver. However, the autopilot stopped pitching up at this point, and it was necessary to re-establish manual control (see section 8.6 for more discussion of this subject). This cycle was repeated several times before the autopilot continued the transposition maneuver. Consequently, additional time and reaction control fuel (18 pounds above preflight nominal) were required, and the spacecraft reached a maximum separation distance of at least 100 feet from the S-IVB.

The subsequent closing maneuvers were made normally under digital autopilot control, using a 2-deg/sec rate and 0.5-degree deadband control mode. Contact was made at an estimated 0.1 ft/sec, without side velocity, but with a small roll misalignment. Subsequent tunnel inspection revealed a roll index angle of 2.0 degrees and a contact mark on the drogue 4 inches long. Lunar module extraction was normal.

#### 4.5 TRANSLUNAR COAST

The S-IVB was targeted to achieve a translunar injection cutoff velocity 6.5 ft/sec in excess of that required to place it on the desired free-return trajectory. This overspeed was then cancelled by a service propulsion correction of 20 ft/sec at 23 minutes after spacecraft ejection.

Two periods of cislunar midcourse navigation, using the command module computer program (P23), were planned and executed. The first, at 6 hours, was primarily to establish the apparent horizon altitude for optical marks in the computer. The first determination was begun at a distance of approximately 30 000 miles, while the second, at 24 hours, was designed to accurately determine the optical bias errors. Excess time and fuel were expended during the first period because of difficulty in locating the substellar point of each star. Ground-supplied gimbal angles were used rather than those from the onboard computer. This technique was devised because computer solutions are unconstrained about the optics shaft axis; therefore, the computer is unable to predict if lunar module structure might block the line of sight to the star. The ground-supplied angles prevented lunar module structure from occulting the star, but were not accurate in locating the precise substellar point, as evidenced by the fact that the sextant reticle pattern was not parallel to the horizon. Additional maneuvers were required to achieve a parallel reticle pattern near the point of horizon-star superposition.

The second period of navigation measurements was less difficult, largely because the earth appeared much smaller and trim maneuvers to the substellar point could be made much more quickly and economically.

The digital autopilot was used to initiate the passive thermal control mode at a positive roll rate of 0.3 deg/sec, with the positive longitudinal axis of the spacecraft pointed toward the ecliptic north pole during translunar coast (the ecliptic south pole was the direction used during transearth coast). After the roll rate was established, thruster firing was prevented by turning off all 16 switches for the service module thrusters. In general, this method was highly successful in that it maintained a satisfactory spacecraft attitude for very long periods of time and allowed the crew to sleep without fear of either entering gimbal lock or encountering unacceptable thermal conditions. However, a refinement to the procedure in the form of a new computer routine is required to make it foolproof from an operator's viewpoint. [Editor's note: A new routine (routine 64) is available for Apollo 12.] On several occasions and for several different reasons, an incorrect computer-entry procedure was used, resulting in a slight waste of reaction control propellants. Satisfactory platform alignments (program P52, option 3) using the optics in the resolved mode and medium speed were possible while rotating at 0.3 deg/sec.

#### 4.6 LUNAR ORBIT INSERTION

The spacecraft was inserted into a 169.9- by 60.9-mile orbit based on the onboard computer with a 6-minute service propulsion maneuver. Procedurally, this firing was the same as all the other service propulsion

maneuvers, except that it was started using the bank-B propellant valves instead of bank-A. The steering of the docked spacecraft was exceptionally smooth, and the control of applied velocity change was extremely accurate, as evidenced by the fact that residuals were only 0.1 ft/sec in all axes.

The circularization maneuver was targeted for a 66- by 54-mile orbit, a change from the 60-mile circular orbit which had been executed in previous lunar flights. The firing was normally accomplished using bank-A propellant valves only, and the onboard solution of the orbit was 66.1 by 54.4 miles. The ellipticity of this orbit was supposed to slowly disappear because of irregularities in the lunar gravitational field, such that the command module would be in a 60-mile circular orbit at the time of rendezvous. However, the onboard estimate of the orbit during the rendezvous was 63.2 by 56.8 miles, indicating the ellipticity decay rate was less than expected. As a result the rendezvous maneuver solutions differed from preflight estimates.

#### 4.7 LUNAR MODULE CHECKOUT

Two entries were made into the lunar module prior to the final activation on the day of landing. The first entry was made at about 57 hours, on the day before lunar orbit insertion. Television and still cameras were used to document the hatch probe and drogue removal and initial entry into the lunar module. The command module oxygen hoses were used to provide circulation in the lunar module cabin. A leisurely inspection period confirmed the proper positioning of all circuit breaker and switch settings and stowage items. All cameras were checked for proper operation.

#### 4.8 DESCENT PREPARATION

##### 4.8.1 Lunar Module

The crew was awakened according to the flight plan schedule. The liquid cooling garment and biomedical harnesses were donned. In anticipation, these items had been unstowed and repositioned the evening before. Following a hearty breakfast, the Lunar Module Pilot transferred into the lunar module to accomplish initial activation before returning to the command module for suiting. This staggered suiting sequence served to expedite the final checkout and resulted in only two crewmembers in the command module during each suiting operation.

The sequence of activities was essentially the same as that developed for Apollo 10, with only minor refinements. Numerous Network simulations and training sessions, including suited operations of this mission phase, insured the completion of this exercise within the allotted time. As in all previous entries into the lunar module, the repressurization valve produced a loud "bang" whenever it was positioned to CLOSE or AUTO with the cabin regulator off. Transfer of power from the command module to the lunar module and electrical power system activation were completed on schedule.

The primary glycol loop was activated about 30 minutes early, with a slow but immediate decrease in glycol temperature. The activation continued to progress smoothly 30 to 40 minutes ahead of schedule. With the Commander entering the lunar module early, the Lunar Module Pilot had more than twice the normally allotted time to don his pressure suit in the command module.

The early powerup of the lunar module computer and inertial measurement unit enabled the ground to calculate the fine gyro torquing angles for aligning the lunar module platform to the command module platform before the loss of communications on the lunar far side. This early alignment added over an hour to the planned time available for analyzing the drift of the lunar module guidance system.

After suiting, the Lunar Module Pilot entered the lunar module, the drogue and probe were installed, and the hatch was closed. During the ascent-battery checkout, the variations in voltage produced a noticeable pitch and intensity variation in the already loud noise of the glycol pump. Suit-loop pressure integrity and cabin regulator repressurization checks were accomplished without difficulty. Activation of the abort guidance system produced only one minor anomaly. An illuminated portion of one of the data readout numerics failed, and this resulted in some ambiguity in data readout (see section 16.2.7).

Following command module landmark tracking, the vehicle was maneuvered to obtain steerable antenna acquisition and state vectors were up-linked into the primary guidance computer. The landing gear deployment was evidenced by a slight jolt to the vehicle. The reaction control, descent propulsion, and rendezvous radar systems were activated and checked out. Each pressurization was confirmed both audibly and by instrument readout.

The abort guidance system calibration was accomplished at the pre-planned vehicle attitude. As the command and service modules maneuvered both vehicles to the undocking attitude, a final switch and circuit breaker configuration check was accomplished, followed by donning of helmets and gloves.

#### 4.8.2 Command Module

Activities after lunar orbit circularization were routine, with the time being used primarily for photographs of the lunar surface. The activation of the lunar module in preparation for descent was, from the viewpoint of the Command Module Pilot, a well organized and fairly leisurely period. During the abort guidance system calibration, the command module was maintained at a fixed attitude for several minutes without firing thrusters. It was easy to stabilize the spacecraft with minimum impulse control prior to the required period so that no thruster firings were needed for at least 10 minutes.

The probe, drogue, and hatch all functioned perfectly, and the operation of closing out the tunnel, preloading the probe, and cocking the latches was done routinely. Previous practice with installation and removal of the probe and drogue during translunar coast was most helpful.

Two periods of orbital navigation (P22) were scheduled with the lunar module attached. The first, at 83 hours, consisted of five marks on the Crater Kamp in the Foaming Sea. The technique used was to approach the target area in an inertial attitude hold mode, with the X-axis being roughly horizontal when the spacecraft reached an elevation angle of 35 degrees from the target, at which point a pitch down of approximately 0.3 deg/sec was begun. This technique was necessary to assure a 2-1/2 minute mark period evenly distributed near the zenith and was performed without difficulty.

The second navigation exercise was performed on the following day shortly prior to separation from the lunar module. A series of five marks was taken on a small crater on the inner north wall of crater 130. The previously described technique was used, except that two forward firing thrusters (one yaw and one pitch) were inhibited to preclude thrust impingement on the deployed rendezvous-radar and steerable antennas. The reduced pitch authority doubled the time required, to approximately 3 seconds when using acceleration command, to achieve a 0.3 deg/sec pitch-down rate. In both cases, the pitch rate was achieved without reference to any onboard rate instrumentation by simply timing the duration of acceleration-command hand controller inputs, since the Command Module Pilot was in the lower equipment bay at the time.

To prevent the two vehicles from slipping and hence upsetting the docked lunar module platform alignment, roll thruster firings were inhibited after probe preload until the tunnel had been vented to approximately 1 psi. Only single roll jet authority was used after the 1 psi point was reached and until the tunnel pressure was zero.

## 4.9 UNDOCKING AND SEPARATION

Particular care was exercised in the operation of both vehicles throughout the undocking and separation sequences to insure that the lunar module guidance computer maintained an accurate knowledge of position and velocity.

The undocking action imparted a velocity to the lunar module of 0.4 ft/sec, as measured by the lunar module primary guidance system. The abort guidance system disagreed with the primary system by approximately 0.2 ft/sec, which is well within the preflight limit. The velocity was nulled, assuming the primary system to be correct. The command module undocking velocity was maintained until reaching the desired inspection distance of 40 feet, where it was visually nulled with respect to the lunar module.

A visual inspection by the Command Module Pilot during a lunar module 360-degree yaw maneuver confirmed proper landing gear extension. The lunar module maintained position with respect to the command module at relative rates believed to be less than 0.1 ft/sec. The 2.5-ft/sec, radially downward separation maneuver was performed with the command and service modules at 100 hours to enter the planned equiperiod separation orbit.

## 4.10 LUNAR MODULE DESCENT

The first optical alignment of the inertial platform in preparation for descent orbit insertion was accomplished shortly after entering darkness following separation. The torquing angles were approximately 0.3 degree, indicating an error in the docked alignment or some platform drift. A rendezvous radar lock was achieved manually, and the radar boresight coincided with that of the crew optical sight. Radar range was substantiated by the VHF ranging in the command module.

### 4.10.1 Descent Orbit Insertion

The descent orbit insertion maneuver was performed with the descent engine in the manual throttle configuration. Ignition at the minimum throttle setting was smooth, with no noise or sensation of acceleration. After 15 seconds, the thrust level was advanced to 40 percent, as planned. Throttle response was smooth and free of oscillations. The guided cutoff left residuals of less than 1 ft/sec in each axis. The X- and Z-axis residuals were reduced to zero using the reaction control system. The computer-determined ephemeris was 9.1 by 57.2 miles, as compared with the



predicted value of 8.5 by 57.2 miles. The abort guidance system confirmed that the magnitude of the maneuver was correct. An additional evaluation was performed using the rendezvous radar to check the relative velocity between the two spacecraft at 6 and 7 minutes subsequent to the maneuver. These values corresponded to the predicted data within 0.5 ft/sec.

#### 4.10.2 Alignment and Navigation Checks

Just prior to powered descent, the angle between the line of sight to the sun and a selected axis of the inertial platform was compared with the onboard computer prediction of that angle and this provided a check on inertial platform drift. Three such measurements were all within the specified tolerance, but the 0.08-degree spread between them was somewhat larger than expected.

Visual checks of downrange and crossrange position indicated that ignition for the powered descent firing would occur at approximately the correct location over the lunar surface. Based on measurements of the line-of-sight rate of landmarks, the estimates of altitudes converged on a predicted altitude at ignition of 52 000 feet above the surface. These measurements were slightly degraded because of a 10- to 15-degree yaw bias maintained to improve communications margins.

#### 4.10.3 Powered Descent

Ignition for powered descent occurred on time at the minimum thrust level, and the engine was automatically advanced to the fixed throttle point (maximum thrust) after 26 seconds. Visual position checks indicated the spacecraft was 2 or 3 seconds early over a known landmark, but with very little crossrange error. A yaw maneuver to a face-up position was initiated at an altitude of about 45 900 feet approximately 4 minutes after ignition. The landing radar began receiving altitude data immediately. The altitude difference, as displayed from the radar and the computer, was approximately 2800 feet.

At 5 minutes 16 seconds after ignition, the first of a series of computer alarms indicated a computer overload condition. These alarms continued intermittently for more than 4 minutes, and although continuation of the trajectory was permissible, monitoring of the computer information display was occasionally precluded (see section 16.2.5).

Attitude thruster firings were heard during each major attitude maneuver and intermittently at other times. Thrust reduction of the descent propulsion system occurred nearly on time (planned at 6 minutes 24 seconds after ignition), contributing to the prediction that the

landing would probably be downrange of the intended point, inasmuch as the computer had not been corrected for the observed downrange error.

The transfer to the final-approach-phase program (P64) occurred at the predicted time. After the pitch maneuver and the radar antenna position change, the control system was transferred from automatic to the attitude hold mode and control response checked in pitch and roll. Automatic control was restored after zeroing the pitch and yaw errors.

After it became clear that an automatic descent would terminate in a boulder field surrounding a large sharp-rimmed crater, manual control was again assumed, and the range was extended to avoid the unsatisfactory landing area. The rate-of-descent mode of throttle control (program P66) was entered in the computer to reduce altitude rate so as to maintain sufficient height for landing-site surveillance.

Both the downrange and crossrange positions were adjusted to permit final descent in a small relatively level area bounded by a boulder field to the north and sizeable craters to the east and south. Surface obscuration caused by blowing dust was apparent at 100 feet and became increasingly severe as the altitude decreased. Although visual determination of horizontal velocity, attitude, and altitude rate were degraded, cues for these variables were adequate for landing. Landing conditions are estimated to have been 1 or 2 ft/sec left, 0 ft/sec forward, and 1 ft/sec down; no evidence of vehicle instability at landing was observed.

#### 4.11 COMMAND MODULE SOLO ACTIVITIES

The Command Module Pilot consolidated all known documentation requirements for a single volume, known as the Command Module Pilot Solo Book, which was very useful and took the place of a flight plan, rendezvous book, updates book, contingency extravehicular checklist, and so forth. This book was normally anchored to the Command Module Pilot by a clip attached to the end of his helmet tie-down strap. The sleep period was timed to coincide with that of the lunar module crew so that radio silence could be observed. The Command Module Pilot had complete trust in the various systems experts on duty in the Mission Control Center and therefore was able to sleep soundly.

The method used for target acquisition (program P22) while the lunar module was on the surface varied considerably from the docked case. The optical alignment sight reticle was placed on the horizon image, and the resulting spacecraft attitude was maintained at the orbital rate manually in the minimum impulse control mode. Once stabilized, the vehicle maintained this attitude long enough to allow the Command Module Pilot to

move to the lower equipment bay and take marks. He could also move from the equipment bay to the hatch window in a few seconds to cross-check attitude. This method of operation in general was very satisfactory.

Despite the fact that the Command Module Pilot had several uninterrupted minutes each time he passed over the lunar module, he could never see the spacecraft on the surface. He was able to scan an area of approximately 1 square mile on each pass, and ground estimates of lunar module position varied by several miles from pass to pass. It is doubtful that the Command Module Pilot was ever looking precisely at the lunar module and more likely was observing an adjacent area. Although it was not possible to assess the ability to see the lunar module from 60 miles, it was apparent there were no flashes of specular light with which to attract his attention.

The visibility through the sextant was good enough to allow the Command Module Pilot to acquire the lunar module (in flight) at distances of over 100 miles. However, the lunar module was lost in the sextant field of view just prior to powered descent initiation (120-mile range) and was not regained until after ascent insertion (at an approximate range of 250 miles), when it appeared as a blinking light in the night sky.

In general, more than enough time was available to monitor systems and perform all necessary functions in a leisurely fashion, except during the rendezvous phase. During that 3-hour period when hundreds of computer entries, as well as numerous marks and other manual operations, were required, the Command Module Pilot had little time to devote to analyzing any off-nominal rendezvous trends as they developed or to cope with any systems malfunctions. Fortunately, no additional attention to these details was required.

## 4.12 LUNAR SURFACE OPERATIONS

### 4.12.1 Postlanding Checkout

The postlanding checklist was completed as planned. Venting of the descent oxidizer tanks was begun almost immediately. When oxidizer pressure was vented to between 40 and 50 psi, fuel was vented to the same pressure level. Apparently, the pressure indications received on the ground were somewhat higher and were increasing with time (see section 16.2.2). At ground request, the valves were reopened and the tanks vented to 15 psi.

Platform alignment and preparation for early lift-off were completed on schedule without significant problems. The mission timer malfunctioned and displayed an impossible number that could not be correlated with any specific failure time. After several unsuccessful attempts to recycle this timer, it was turned off for 11 hours to cool. The timer was turned on for ascent and it operated properly and performed satisfactorily for the remainder of the mission (see section 16.2.1).

#### 4.12.2 Egress Preparation

The crew had given considerable thought to the advantage of beginning the extravehicular activity as soon as possible after landing instead of following the flight plan schedule of having the surface operations between two rest periods. The initial rest period was planned to allow flexibility in the event of unexpected difficulty with postlanding activities. These difficulties did not materialize, the crew were not overly tired, and no problem was experienced in adjusting to the 1/6-g environment. Based on these facts, the decision was made at 104:40:00 to proceed with the extravehicular activity prior to the first rest period.

Preparation for extravehicular activity began at 106:11:00. The estimate of the preparation time proved to be optimistic. In simulations, 2 hours had been found to be a reasonable allocation; however, everything had also been laid out in an orderly manner in the cockpit, and only those items involved in the extravehicular activity were present. In fact, there were checklists, food packets, monoculars, and other miscellaneous items that interfered with an orderly preparation. All these items required some thought as to their possible interference or use in the extravehicular activity. This interference resulted in exceeding the timeline estimate by a considerable amount. Preparation for egress was conducted slowly, carefully, and deliberately, and future missions should be planned and conducted with the same philosophy. The extravehicular activity preparation checklist was adequate and was closely followed. However, minor items that required a decision in real time or had not been considered before flight required more time than anticipated.

An electrical connector on the cable that connects the remote control unit to the portable life support system gave some trouble in mating (see section 16.3.2). This problem had been occasionally encountered using the same equipment before flight. At least 10 minutes were required to connect each unit, and at one point it was thought the connection would not be successfully completed.

Considerable difficulty was experienced with voice communications when the extravehicular transceivers were used inside the lunar module. At times communications were good but at other times were garbled on the

ground for no obvious reason. Outside the vehicle, there were no appreciable communication problems. Upon ingress from the surface, these difficulties recurred, but under different conditions. That is, the voice dropouts to the ground were not repeatable in the same manner.

Depressurization of the lunar module was one aspect of the mission that had never been completely performed on the ground. In the various altitude chamber tests of the spacecraft and the extravehicular mobility unit, a complete set of authentic conditions was never present. The depressurization of the lunar module through the bacteria filter took much longer than had been anticipated. The indicated cabin pressure did not go below 0.1 psi, and some concern was experienced in opening the forward hatch against this residual pressure. The hatch appeared to bend on initial opening, and small particles appeared to be blown out around the hatch when the seal was broken (see section 16.2.6).

#### 4.12.3 Lunar Module Egress

Simulation work in both the water immersion facility and the 1/6-g environment in an airplane was reasonably accurate in preparing the crew for lunar module egress. Body positioning and arching-the-back techniques that were required to exit the hatch were performed, and no unexpected problems were experienced. The forward platform was more than adequate to allow changing the body position from that used in egressing the hatch to that required for getting on the ladder. The first ladder step was somewhat difficult to see and required caution and forethought. In general, the hatch, porch, and ladder operation was not particularly difficult and caused little concern. Operations on the platform could be performed without losing body balance, and there was adequate room for maneuvering.

The initial operation of the lunar equipment conveyor in lowering the camera was satisfactory, but after the straps had become covered with lunar surface material, a problem arose in transporting the equipment back into the lunar module. Dust from this equipment fell back onto the lower crewmember and into the cabin and seemed to bind the conveyor so as to require considerable force to operate it. Alternatives in transporting equipment into the lunar module had been suggested before flight, and although there was no opportunity to evaluate these techniques, it is believed they might be an improvement over the conveyor.

#### 4.12.4 Surface Exploration

Work in the 1/6-g environment was a pleasant experience. Adaptation to movement was not difficult and seemed to be quite natural. Certain specific peculiarities, such as the effect of the mass versus the lack of traction, can be anticipated but complete familiarization need not be pursued.

The most effective means of walking seemed to be the lope that evolved naturally. The fact that both feet were occasionally off the ground at the same time, plus the fact that the feet did not return to the surface as rapidly as on earth, required some anticipation before attempting to stop. Although movement was not difficult, there was noticeable resistance provided by the suit.

On future flights, crewmembers may want to consider kneeling in order to work with their hands. Getting to and from the kneeling position would be no problem, and being able to do more work with the hands would increase the productive capability.

Photography with the Hasselblad cameras on the remote control unit mounts produced no problems. The first panorama was taken while the camera was hand-held; however, it was much easier to operate on the mount. The handle on the camera was adequate, and very few pictures were triggered inadvertently.

The solar wind experiment was easily deployed. As with the other operations involving lunar surface penetration, it was only possible to penetrate the lunar surface material about 4 or 5 inches. The experiment mount was not quite as stable as desired, but it stayed erect.

The television system presented no difficulties except that the cord was continually getting in the way. At first, the white cord showed up well, but it soon became covered with dust and was therefore more difficult to see. The cable had a "set" from being coiled around the reel and would not lie completely flat on the surface. Even when it was flat, however, a foot could still slide under, and the Commander became entangled several times (see section 16.3.1).

Collecting the bulk sample required more time than anticipated because the modular equipment stowage assembly table was in deep shadow, and collecting samples in that area was far less desirable than taking those in the sunlight. It was also desirable to take samples as far from the exhaust plume and propellant contamination as possible. An attempt was made to include a hard rock in each sample, and a total of about twenty trips were required to fill the box. As in simulations, the difficulty of scooping up the material without throwing it out as the scoop

became free created some problem. It was almost impossible to collect a full scoop of material, and the task required about double the planned time.

Several of the operations would have been easier in sunlight. Although it was possible to see in the shadows, time must be allowed for dark adaptation when walking from the sunlight into shadow. On future missions, it would be advantageous to conduct a yaw maneuver just prior to landing so that the descent stage work area is in sunlight.

The scientific experiment package was easy to deploy manually, and some time was saved here. The package was easy to manage, but finding a level area was quite difficult. A good horizon reference was not available, and in the 1/6-g environment, physical cues were not as effective as in one-g. Therefore, the selection of a deployment site for the experiments caused some problems. The experiments were placed in an area between shallow craters in surface material of the same consistency as the surrounding area and which should be stable. Considerable effort was required to change the slope of one of the experiments. It was not possible to lower the equipment by merely forcing it down, and it was necessary to move the experiment back and forth to scrape away the excess surface material.

No abnormal conditions were noted during the lunar module inspection. The insulation on the secondary struts had been damaged from the heat, but the primary struts were only singed or covered with soot. There was much less damage than on the examples that had been seen before flight.

Obtaining the core tube samples presented some difficulty. It was impossible to force the tube more than 4 or 5 inches into the surface material, yet the material provided insufficient resistance to hold the extension handle in the upright position. Since the handle had to be held upright, this precluded using both hands on the hammer. In addition, the resistance of the suit made it difficult to steady the core tube and still swing with any great force. The hammer actually missed several times. Sufficient force was obtained to make dents in the handle, but the tube could only be driven to a depth of about 6 inches. Extraction offered little or virtually no resistance. Two samples were taken.

Insufficient time remained to take the documented sample, although as wide a variety of rocks was selected as remaining time permitted.

The performance of the extravehicular mobility unit was excellent. Neither crewman felt any thermal discomfort. The Commander used the minimum cooling mode for most of the surface operation. The Lunar Module Pilot switched to the maximum diverter valve position immediately after

sublimator startup and operated at maximum position for 42 minutes before switching to the intermediate position. The switch remained in the intermediate position for the duration of the extravehicular activity. The thermal effect of shadowed areas versus those areas in sunlight was not detectable inside the suit.

The crewmen were kept physically cool and comfortable and the ease of performing in the 1/6-g environment indicate that tasks requiring greater physical exertion may be undertaken on future flights. The Commander experienced some physical exertion while transporting the sample return container to the lunar module, but his physical limit had not been approached.

#### 4.12.5 Lunar Module Ingress

Ingress to the lunar module produced no problems. The capability to do a vertical jump was used to an advantage in making the first step up the ladder. By doing a deep knee bend, then springing up the ladder, the Commander was able to guide his feet to the third step. Movements in the 1/6-g environment were slow enough to allow deliberate foot placement after the jump. The ladder was a bit slippery from the powdery surface material, but not dangerously so.

As previously stated, mobility on the platform was adequate for developing alternate methods of transferring equipment from the surface. The hatch opened easily, and the ingress technique developed before flight was satisfactory. A concerted effort to arch the back was required when about half way through the hatch, to keep the forward end of the portable life support system low enough to clear the hatch. There was very little exertion associated with transition to a standing position.

Because of the bulk of the extravehicular mobility unit, caution had to be exercised to avoid bumping into switches, circuit breakers, and other controls while moving around the cockpit. One circuit breaker was in fact broken as a result of contact (see section 16.2.11).

Equipment jettison was performed as planned, and the time taken before flight in determining the items not required for lift-off was well spent. Considerable weight reduction and increase in space was realized. Discarding the equipment through the hatch was not difficult, and only one item remained on the platform. The post-ingress checklist procedures were performed without difficulty; the checklist was well planned and was followed precisely.



#### 4.12.6 Lunar Rest Period

The rest period was almost a complete loss. The helmet and gloves were worn to relieve any subconscious anxiety about a loss of cabin pressure and presented no problem. But noise, lighting, and a lower-than-desired temperature were annoying. It was uncomfortably cool in the suits, even with water-flow disconnected. Oxygen flow was finally cut off, and the helmets were removed, but the noise from the glycol pumps was then loud enough to interrupt sleep. The window shades did not completely block out light, and the cabin was illuminated by a combination of light through the shades, warning lights, and display lighting. The Commander was resting on the ascent engine cover and was bothered by the light entering through the telescope. The Lunar Module Pilot estimated he slept fitfully for perhaps 2 hours and the Commander did not sleep at all, even though body positioning was not a problem. Because of the reduced gravity, the positions on the floor and on the engine cover were both quite comfortable.

#### 4.13 LAUNCH PREPARATION

Aligning the platform before lift-off was complicated by the limited number of stars available. Because of sun and earth interference, only two detents effectively remained from which to select stars. Accuracy is greater for stars close to the center of the field, but none were available at this location. A gravity/one-star alignment was successfully performed. A manual averaging technique was used to sample five successive cursor readings and then five spiral readings. The result was then entered into the computer. This technique appeared to be easier than taking and entering five separate readings. Torquing angles were close to 0.7 degree in all three axes and indicated that the platform did drift. (Editor's note: Platform drift was within specification limits.)

After the alignment, the navigation program was entered. It is recommended that future crews update the abort guidance system with the primary guidance state vector at this point and then use the abort guidance system to determine the command module location. The primary guidance system cannot be used to determine the command module range and range rate, and the radar will not lock on until the command module is within 400 miles range. The abort guidance system provides good data as this range is approached.

A cold-fire reaction control system check and abort guidance system calibration were performed, and the ascent pad was taken. About 45 minutes prior to lift-off, another platform alignment was performed. The landing site alignment option at ignition was used for lift-off. The torquing angles for this alignment were on the order of 0.09 degree.

In accordance with ground instructions, the rendezvous radar was placed in the antenna SLEW position with the circuit breakers off for ascent to avoid recurrence of the alarms experienced during descent.

Both crewmembers had forgotten the small helium pressure decrease indication that the Apollo 10 crew experienced when the ascent tanks were pressurized and the crew initially believed that only one tank had pressurized. This oversight was temporary and delayed crew verification of proper pressurization of both tanks.

#### 4.14 ASCENT

The pyrotechnic noises at descent stage separation were quite loud, but ascent-engine ignition was inaudible. The yaw and pitch maneuvers were very smooth. The pitch- and roll-attitude limit cycles were as expected and were not accompanied by any physiological difficulties. Both the primary and abort guidance systems indicated the ascent to be a duplicate of the planned trajectory. The guided cutoff yielded residuals of less than 2 ft/sec; and the inplane components were nulled to within 0.1 ft/sec with the reaction control system. Throughout the trajectory, the ground track could be visually verified, although a pitch attitude confirmation by use of the horizon in the overhead window was found to be quite difficult because of the horizon lighting condition.

#### 4.15 RENDEZVOUS

At orbital insertion, the primary guidance system showed an orbit of 47.3 by 9.5 miles, as compared to the abort guidance system solution of 46.6 by 9.5 miles. Since radar range-rate data were not available, the Network quickly confirmed that the orbital insertion was satisfactory.

In the preflight planning, stars had been chosen that would be in the field of view and require a minimum amount of maneuvering to get through alignment and back in plane. This maintenance of a nearly fixed attitude would permit the radar to be turned on and the acquisition conditions designated so that marks for a coelliptic sequence initiation solution would be immediately available. For some reason during the simulations, these preselected stars had not been correctly located relative to the horizon, and some time and fuel were wasted in first maneuvering to these stars, failing to mark on them, and then maneuvering to an alternate pair. Even with these problems, the alignment was finished about 28 minutes before coelliptic sequence initiation, and it was possible to proceed with radar lock-on.

All four sources for the coelliptic sequence initiation solution agreed to within 0.2 ft/sec, an accuracy that had never been observed before. The Commander elected to use the primary guidance solution without any out-of-plane thrusting.

The coelliptic sequence initiation maneuver was accomplished using the plus Z thrusters, and radar lock-on was maintained throughout the firing. Continued navigation tracking by both vehicles indicated a plane change maneuver of about 2-1/2 ft/sec, but the crew elected to defer this small correction until terminal phase initiation. The very small out-of-plane velocities that existed between the spacecraft orbits indicated a highly accurate lunar surface alignment. As a result of the higher-than-expected ellipticity of the command module orbit, backup chart solutions were not possible for the first two rendezvous maneuvers, and the constant differential height maneuver had a higher-than-expected vertical component. The computers in both spacecraft agreed closely on the maneuver values, and the lunar module primary guidance computer solution was executed, using the minus X thrusters.

During the coelliptic phase, radar tracking data were inserted into the abort guidance system to obtain an independent intercept guidance solution. The primary guidance solution was 6-1/2 minutes later than planned. However, the intercept trajectory was quite nominal, with only two small midcourse corrections of 1.0 and 1.5 ft/sec. The line-of-sight rates were low, and the planned braking schedule was used to reach a station-keeping position.

In the process of maneuvering the lunar module to the docking attitude, while at the same time avoiding direct sunlight in the forward windows, the platform inadvertently reached gimbal lock. The docking was completed using the abort guidance system for attitude control.

#### 4.16 COMMAND MODULE DOCKING

Pre-docking activities in the command module were normal in all respects, as was docking up to the point of probe capture. After the Command Module Pilot ascertained that a successful capture had occurred, as indicated by "barberpole" indicators, the CMC-FREE switch position was used and one retract bottle fired. A right yaw excursion of approximately 15 degrees immediately took place for 1 or 2 seconds. The Command Module Pilot went back to CMC-AUTO and made hand-controller inputs to reduce the angle between the two vehicles to zero. At docking thruster firings occurred unexpectedly in the lunar module when the retract mechanism was actuated, and attitude excursions of up to 15 degrees were observed. The lunar module was manually realigned. While

this maneuver was in progress, all twelve docking latches fired and docking was completed successfully. (See section 8.6.1 for further discussion.)

Following docking, the tunnel was cleared and the probe and drogue were stowed in the lunar module. The items to be transferred to the command module were cleaned using a vacuum brush attached to the lunar module suit return hose. The suction was low and made the process rather tedious. The sample return containers and film magazines were placed in appropriate bags to complete the transfer, and the lunar module was configured for jettison according to the checklist procedure.

#### 4.17 TRANSEARTH INJECTION

The time between docking and transearth injection was more than adequate to clean all equipment contaminated with lunar surface material and return it to the command module for stowage so that the necessary preparations for transearth injection could be made. The transearth injection maneuver, the last service propulsion engine firing of the flight, was nominal. The only difference between it and previous firings was that without the docked lunar module the start transient was apparent.

#### 4.18 TRANSEARTH COAST

During transearth coast, faint spots or scintillations of light were observed within the command module cabin. This phenomenon became apparent to the Commander and Lunar Module Pilot after they became dark-adapted and relaxed. [Editor's note: The source or cause of the light scintillations is as yet unknown. One explanation involves primary cosmic rays, with energies in the range of billions of electron volts, bombarding an object in outer space. The theory assumes that numerous heavy and high-energy cosmic particles penetrate the command module structure, causing heavy ionization inside the spacecraft. When liberated electrons recombine with ions, photons in the visible portion of the spectrum are emitted. If a sufficient number of photons are emitted, a dark-adapted observer could detect the photons as a small spot or a streak of light. Two simple laboratory experiments were conducted to substantiate the theory, but no positive results were obtained in a 5-psi pressure environment because a high enough energy source was not available to create the radiation at that pressure. This level of radiation does not present a crew hazard.]

Only one midcourse correction, a reaction control system firing of 4.8 ft/sec, was required during transearth coast. In general, the transearth coast period was characterized by a general relaxation on the part of the crew, with plenty of time available to sample the excellent variety of food packets and to take photographs of the shrinking moon and the growing earth.

#### 4.19 ENTRY

Because of the presence of thunderstorms in the primary recovery area (1285 miles downrange from the entry interface of 400 000 feet), the targeted landing point was moved to a range of 1500 miles from entry interface. This change required the use of computer program P65 (skip-up control routine) in the computer, in addition to those programs used for the planned shorter range entry. This change caused the crew some apprehension, since such entries had rarely been practiced in preflight simulations. However, during the entry, these parameters remained within acceptable limits. The entry was guided automatically and was nominal in all respects. The first acceleration pulse reached approximately 6.5g and the second 6.0g.

#### 4.20 RECOVERY

On the landing, the 18-knot surface wind filled the parachutes and immediately rotated the command module into the apex down (stable II) flotation position prior to parachute release. Moderate wave-induced oscillations accelerated the uprighting sequence, which was completed in less than 8 minutes. No difficulties were encountered in completing the postlanding checklist.

The biological isolation garments were donned inside the spacecraft. Crew transfer into the raft was followed by hatch closure and by decontamination of the spacecraft and crew members by germicidal scrubdown.

Helicopter pickup was performed as planned, but visibility was substantially degraded because of moisture condensation on the biological isolation garment faceplate. The helicopter transfer to the aircraft carrier was performed as quickly as could be expected, but the temperature increase inside the suit was uncomfortable. Transfer from the helicopter into the mobile quarantine facility completed the voyage of Apollo 11.

## 5.0 LUNAR DESCENT AND ASCENT

### 5.1 DESCENT TRAJECTORY LOGIC

The lunar descent trajectory, shown in figure 5-1, began with a descent orbit insertion maneuver targeted to place the spacecraft into a 60- by 8.2-mile orbit, with the pericyynthion longitude located about 260 miles uprange from the landing site. Powered descent, shown in figure 5-2, was initiated at pericynthion and continued down to landing.

The powered descent trajectory was designed considering such factors as optimum propellant usage, navigation uncertainties, landing radar performance, terrain uncertainties, and crew visibility restrictions. The basic premise during trajectory design was to maintain near-optimum use of propellant during initial braking and to provide a standard final approach from which the landing area can be assessed and a desirable landing location selected. The onboard guidance capability allows the crew to re-designate the desired landing position in the computer for automatic execution or, if late in the trajectory, to take over manually and fly the lunar module to the desired point. To provide these descent characteristics, compatibility between the automatic and manually controlled trajectories was required, as well as acceptable flying quality under manual control. Because of guidance dispersions, site-selection uncertainties, visibility restriction, and undefined surface irregularities, adequate flexibility in the terminal-approach technique was provided the crew, with the principal limitation being descent propellant quantity.

The major phases of powered descent are the braking phase (which terminates at 7700 feet altitude), the approach or visibility phase (to approximately 500 feet altitude), and the final landing phase. Three separate computer programs, one for each phase, in the primary guidance system execute the desired trajectory such that the various position, velocity, acceleration, and visibility constraints are satisfied. These programs provide an automatic guidance and control capability for the lunar module from powered descent initiation to landing. The braking phase program (P63) is initiated at approximately 40 minutes before descent engine ignition and controls the lunar module until the final approach phase program (P64) is automatically entered to provide trajectory conditions and landing site visibility.

If desired during a nominal descent, the crew may select the manual landing phase program (P66) prior to the completion of final approach phase program P64. If the manual landing phase program P66 is not entered, the automatic landing program (P65) would be entered automatically when

time-to-go equals 12 seconds at an altitude of about 150 feet. The automatic landing phase program P65 initiates an automatic descent by nulling the horizontal velocity relative to the surface and maintaining the rate of descent at 3 ft/sec. The manual landing phase P66 is initiated when the crew changes the position of the primary guidance mode control switch from automatic to attitude-hold and then actuates the rate-of-descent control switch. Vehicle attitude changes are then controlled manually by the crew, the descent engine throttle is under computer control, and the Commander can introduce 1-ft/sec increments in the descent rate using the rate-of-descent switch.

Throughout the descent, maximum use was made onboard, as well as on the ground, of all data, system responses, and cues, based on vehicle position with respect to designated lunar features, to assure proper operation of the onboard systems. The two onboard guidance systems provided the crew with a continuous check of selected navigation parameters. Comparisons were made on the ground between data from each of the onboard systems and comparable information derived from tracking data. A powered flight processor was used to simultaneously reduce Doppler tracking data from three or more ground stations and calculate the required parameters. A filtering technique was used to compute corrections to the Doppler tracking data and thereby define an accurate vehicle state vector. The ground data were used as a voting source in case of a slow divergence between the two onboard systems.

## 5.2 PREPARATION FOR POWERED DESCENT

The crew entered and began activation of the lunar module following the first sleep period in lunar orbit (see section 4.8). A listing of significant events for lunar module descent is presented in table 5-I.

Undocking was accomplished on schedule just prior to acquisition of signal on lunar revolution 13. After the lunar module inspection by the Command Module Pilot, a separation maneuver was performed by the command and service modules, and 20 minutes later, the rendezvous radar and VHF ranging outputs were compared. The two systems agreed and indicated 0.7-mile in range. The inertial measurement unit was aligned optically for the first time, and the resulting gyro torquing angles were well within the platform drift criteria for a satisfactory primary system. Descent orbit insertion was performed on time approximately 8 minutes after loss of Network line-of-sight. Table 5-II contains the trajectory information on descent orbit insertion, as reported by the crew following acquisition of signal on revolution 14. A relatively large Z-axis residual for the abort guidance system was caused by an incorrectly loaded target vector. With this exception, the residuals were well within the three-sigma dispersion (plus or minus 0.6 ft/sec) predicted before flight.

Following descent orbit insertion, rendezvous radar data were recorded by the Lunar Module Pilot and used to predict that the pericyynthion point would be at approximately 50 000 feet altitude. Initial checks using the landing point designator capability produced close agreement by indicating 52 000 feet. The crew also reported that a solar sighting, performed following descent orbit insertion and using the alignment telescope, was well within the powered descent initiation go/no-go criterion of 0.25 degree. The solar sighting consisted of acquiring the sun through the telescope and comparing the actual gimbal angles to those theoretically required and computed by the onboard computer for this observation. This check is an even more accurate indication of platform performance if the 0.07-degree bias correction for the telescope rear detent position is subtracted from the recorded data.

The comparison of velocity residuals between ground tracking data and the onboard system, as calculated along the earth-moon line-of-sight, provided an additional check on the performance of the primary guidance system. A residual of 2 ft/sec was recorded at acquisition of signal and provided confidence that the onboard state vector would have only small altitude and downrange velocity magnitude errors at powered descent initiation. The Doppler residual was computed by comparing the velocity measured along the earth-moon line-of-sight by ground tracking with the same velocity component computed by the primary system. As the lunar module approached powered descent initiation, the Doppler residual began to increase in magnitude to about 13 ft/sec. Since the earth-moon line-of-sight vector was almost normal to the velocity vector at this point, the residual indicated that the primary system estimate of its state vector was approximately 21 000 feet uprange of the actual state vector. This same error was also reflected in the real-time comparisons made using the powered flight processor previously mentioned. Table 5-III is a comparison of the latitude, longitude, and altitude between the best-estimated-trajectory state vector at powered descent initiation, that carried onboard, and the preflight-calculated trajectory. The onboard state-vector errors at powered descent initiation resulted from a combination of the following:

- a. Uncoupled thruster firings during the docked landmark tracking exercise
- b. Unaccounted for velocity accrued during undocking and subsequent inspection and station-keeping activity
- c. Descent orbit insertion residual
- d. Propogated errors in the lunar potential function
- e. Lunar module venting.



### 5.3 POWERED DESCENT

The powered descent maneuver began with a 26-second thrusting period at minimum throttle. Immediately after ignition, S-band communications were interrupted momentarily but were reestablished when the antenna was switched from the automatic to the slew position. The descent maneuver was initiated in a face-down attitude to permit the crew to make time marks on selected landmarks. A landing-point-designator sighting on the crater Maskelyne W was approximately 3 seconds early, confirming the suspected downrange error. A yaw maneuver to face-up attitude was initiated following the landmark sightings at an indicated altitude of about 45 900 feet. The maneuver took longer than expected because of an incorrect setting of a rate display switch.

Landing radar lock-on occurred before the end of the yaw maneuver, with the spacecraft rotating at approximately 4 deg/sec. The altitude difference between that calculated by the onboard computer and that determined by the landing radar was approximately 2800 feet, which agrees with the altitude error suspected from the Doppler residual comparison. Radar altitude updates of the onboard computer were enabled at 102:38:45, and the differences converged within 30 seconds. Velocity updates began automatically 4 seconds after enabling the altitude update. Two altitude-difference transients occurred during computer alarms and were apparently associated with incomplete radar data readout operations (see section 16.2.5).

The reduction in throttle setting was predicted to occur 384 seconds after ignition; actual throttle reduction occurred at 386 seconds, indicating nominal performance of the descent engine.

The first of five computer alarms occurred approximately 5 minutes after initiation of the descent. Occurrences of these alarms are indicated in table 5-I and are discussed in detail in section 16.2.5. Although the alarms did not degrade the performance of any primary guidance or control function, they did interfere with an early assessment by the crew of the landing approach.

Arrival at high gate (end of braking phase) and the automatic switch to final approach phase program P64 occurred at 7129 feet at a descent rate of 125 ft/sec. These values are slightly lower than predicted but within acceptable boundaries. At about 5000 feet, the Commander switched his control mode from automatic to attitude-hold to check manual control in anticipation of the final descent.

After the pitchover at high gate, the landing point designator indicated that the approach path was leading into a large crater. An unplanned redesignation was introduced at this time. To avoid the crater, the

Commander again switched from automatic to attitude-hold control and manually increased the flight-path angle by pitching to a nearly vertical attitude for range extension. Manual control began at an altitude of approximately 600 feet. Ten seconds later, at approximately 400 feet, the rate-of-descent mode was activated to control descent velocity. In this manner, the spacecraft was guided approximately 1100 feet downrange from the initial aim point.

Figure 5-3 contains histories of altitude compared with altitude-rate from the primary and abort guidance systems and from the Network powered flight processor. The altitude difference existing between the primary system and the Network at powered descent initiation can be observed in this figure. All three sources are initialized to the primary guidance state vector at powered descent initiation. The primary system, however, is updated by the landing radar, and the abort guidance system is not. As indicated in the figure, the altitude readouts from both systems gradually diverge so as to indicate a lower altitude for the primary system until the abort system was manually updated with altitude data from the primary system.

The powered flight processor data reflect both the altitude and downrange errors existing in the primary system at powered descent initiation. The radial velocity error is directly proportional to the downrange position error such that a 1000-foot downrange error will cause a 1-ft/sec radial velocity error. Therefore, the 20 000-foot downrange error existing at powered descent initiation was also reflected as a 20-ft/sec radial velocity residual. This error is apparent on the figure in the altitude region near 27 000 feet, where an error of approximately 20 ft/sec is evident. The primary-system altitude error in existence at powered descent initiation manifests itself at touchdown when the powered flight processor indicates a landing altitude below the lunar surface. Figure 5-4 contains a similar comparison of lateral velocity from the three sources. Again, the divergence noted in the final phases in the abort guidance system data was caused by a lack of radar updates.

Figure 5-5 contains a time history of vehicle pitch attitude, as recorded by the primary and abort guidance systems. The scale is set up so that a pitch of zero degrees would place the X-axis of the vehicle vertical at the landing site. Two separate designations of the landing site are evident in the phase after manual takeover. Figure 5-6 contains comparisons for the pitch and roll attitude and indicates the lateral corrections made in the final phase.

Figure 5-7 is an area photograph, taken from a Lunar Orbiter flight, showing the landing site ellipse and the ground track flown to the landing point. Figure 5-8 is an enlarged photograph of the area adjacent to the lunar landing site and shows the final portions of the ground track to landing. Figure 5-9 contains a preliminary attempt at reconstructing the surface terrain viewed during descent, based upon trajectory and radar

data and known surface features. The coordinates of the landing point, as obtained from the various real-time and postflight sources, are shown in table 5-IV. The actual landing point is 0 degree 41 minutes 15 seconds north latitude and 23 degrees 26 minutes east longitude, as compared with the targeted landing point of 0 degree 43 minutes 53 seconds north latitude and 23 degrees 38 minutes 51 seconds east longitude as shown in figure 5-10. Figure 5-10 is the basic reference map for location of the landing point in this report. As noted, the landing point dispersion was caused primarily by errors in the onboard state vector prior to powered descent initiation.

Figure 5-11 is a time history of pertinent vehicle control parameters during the entire descent phase. Evidence of fuel slosh was detected in the attitude-rate information following the yaw maneuver. The slosh effect increased to the point where reaction control thruster firings were required to damp the rate prior to throttle recovery. The dynamic behavior at this point and through the remainder of descent was comparable to that observed in simulations and indicates nominal control system performance.

Approximately 95 pounds of reaction control propellant were used during powered descent, as compared to the predicted value of 40 pounds. Plots of propellant consumption for the reaction control and descent propulsion systems are shown in figure 5-12. The reaction control propellant consumption while in the manual descent control mode was 51 pounds, approximately 1-1/2 times greater than that for the automatic mode. This increase in usage rate is attributed to the requirement for greater attitude and translation maneuvering in the final stages of descent. The descent propulsion system propellant usage was greater than predicted because of the additional time required for the landing site redesignation.

#### 5.4 LANDING DYNAMICS

Landing on the surface occurred at 102:45:39.9 with negligible forward velocity, approximately 2.1 ft/sec to the crew's left and 1.7 ft/sec vertically. Body rate transients occurred, as shown in figure 5-13, and indicate that the right and the forward landing gear touched almost simultaneously, giving a roll-left and a pitch-up motion to the vehicle. The left-directed lateral velocity resulted in a slight yaw right transient at the point of touchdown. These touchdown conditions, obtained from attitude rates and integration of accelerometer data, were verified qualitatively by the at-rest positions of the lunar surface sensing probes and by surface buildup around the rims of the foot pads. Figure 11-17 shows the probe boom nearly vertical on the inboard side of the minus Y foot pad, indicating a component of velocity in the minus Y direction. Lunar material

can be seen as built up outboard of the pad, which also indicates a lateral velocity in this direction. The probe position and lunar material disturbance produced by the minus Z gear assembly, shown in the same figure, indicate a lateral velocity in the minus Y direction. Figure 11-16 shows in greater detail the surface material disturbance on the minus Y side of the minus Z foot pad. The plus Y landing gear assembly supports the conclusion of a minus Y velocity, since the probe was on the outboard side and material was piled inboard of the pad.

The crew reported no sensation of rockup (post-contact instability) during the touchdown phase. A postflight simulation of the landing dynamics indicates that the maximum rockup angle was only about 2 degrees, which is indicative of a stable landing. In the simulation, the maximum foot pad penetration was 2.5 to 3.5 inches, with an associated vehicle slideout (skidding) of 1 to 3 inches. The landing gear struts stroked less than 1 inch, which represents about 10 percent of the energy absorption capability of the low-level primary-strut honeycomb cartridge. Examination of photographs indicates agreement with this analytical conclusion.

## 5.5 POSTLANDING SPACECRAFT OPERATIONS

Immediately after landing, the lunar module crew began a simulated launch countdown in preparation for the possibility of a contingency lift-off. Two problems arose during this simulated countdown. First, the mission timer had stopped and could not be restarted; therefore, the event timer was started using a mark from the ground. Second, the descent stage fuel-helium heat exchanger froze, apparently with fuel trapped between the heat exchanger and the valves, causing the pressure in the line to increase. See section 16.2.1 and 16.2.2 for further discussion of these problems.

The inertial measurement unit was aligned three times during this period using each of the three available lunar surface alignment options. The alignments were satisfactory, and the results provided confidence in the technique. The simulated countdown was terminated at 104-1/2 hours, and a partial power-down of the lunar module was initiated.

During the lunar surface stay, several unsuccessful attempts were made by the Command Module Pilot to locate the lunar module through the sextant using sighting coordinates transmitted from the ground. Estimates of the landing coordinates were obtained from the lunar module computer, the lunar surface gravity alignment of the platform, and the limited interpretation of the geological features during descent. Figure 5-14 shows the areas that were tracked and the times of closest approach that were

used for the sightings. It can be seen that the actual landing site, as determined from films taken during the descent, did not lie near the center of the sextant field of view for any of the coordinates used; therefore, the ability to acquire the lunar module from a 60-mile orbit can neither be established nor denied. The Command Module Pilot reported it was possible to scan only one grid square during a single pass.

Because of the unsuccessful attempts to sight the lunar module from the command module, the decision was made to track the command module from the lunar module using the rendezvous radar. The command module was acquired at a range of 79.9 miles and a closing rate of 3236 ft/sec, and loss of track occurred at 85.3 miles with a receding range-rate of 3531 ft/sec (fig. 5-15).

The inertial measurement unit was successfully aligned two more times prior to lift-off, once to obtain a drift check and once to establish the proper inertial orientation for lift-off. The drift check indicated normal system operation, as discussed in section 9.6. An abort guidance system alignment was also performed prior to lift-off; however, a procedural error caused an azimuth misalignment which resulted in the out-of-plane velocity error discussed in section 9.6.2.

## 5.6 ASCENT

Preparations for ascent began after the end of the crew rest period at 121 hours. The command module state vector was updated from the ground, with coordinates provided for crater 130, a planned landmark. This crater was tracked using the command module sextant on the revolution prior to lift-off to establish the target orbit plane. During this same revolution, the rendezvous radar was used to track the command module, as previously mentioned, and the lunar surface navigation program (P22) was exercised to establish the location of the lunar module relative to the orbit plane. Crew activities during the preparation for launch were conducted as planned, and lift-off occurred on time.

The ascent phase was initiated by a 10-second period of vertical rise, which allowed the ascent stage to clear safely the descent stage and surrounding terrain obstacles, as well as provide for rotation of the spacecraft to the correct launch azimuth. The pitchover maneuver to a 50-degree attitude with respect to the local vertical began when the ascent velocity reached 40 ft/sec. Powered ascent was targeted to place the spacecraft in a 10- by 45-mile orbit to establish the correct initial conditions for the rendezvous. Figure 5-16 shows the planned ascent trajectory as compared with the actual ascent trajectory.

The crew reported that the ascent was smooth, with normal reaction control thruster activity. The ascent stage appeared to "wallow," or traverse the attitude deadbands, as expected. Figure 5-17 contains a time history of selected control system parameters during the ascent maneuver. A data dropout occurred immediately after lift-off, making it difficult to determine accurately the fire-in-the-hole forces. The body rates recorded just prior to the data dropout were small (less than 5 deg/sec), but were increasing in magnitude at the time of the dropout. However, crew reports and associated dynamic information during the data loss period do not indicate that any rates exceeded the expected ranges.

The predominant disturbance torque during ascent was about the pitch axis and appears to have been caused by thrust vector offset. Figure 5-18 contains an expanded view of control system parameters during a selected period of the ascent phase. The digital autopilot was designed to control about axes offset approximately 45 degrees from the spacecraft body axes and normally to fire only plus X thrusters during powered ascent. Therefore, down-firing thrusters 2 and 3 were used almost exclusively during the early phases of the ascent and were fired alternately to control the pitch disturbance torque. These jets induced a roll rate while counteracting the pitch disturbance; therefore, the accompanying roll motion contributed to the wallowing sensation reported by the crew. As the maneuver progressed, the center of gravity moved toward the thrust vector, and the resulting pitch disturbance torque and required thruster activity decreased until almost no disturbance was present. Near the end of the maneuver, the center of gravity moved to the opposite side of the thrust vector, and proper thruster activity to correct for this opposite disturbance torque can be observed in figure 5-17.

The crew reported that the velocity-to-be-gained display in the abort guidance system indicated differences of 50 to 100 ft/sec with the primary system near the end of the ascent maneuver. The reason for this difference appears to be unsynchronized data displayed from the two systems (see section 9.6).

Table 5-V contains a comparison of insertion conditions between those calculated by various onboard sources and the planned values, and satisfactory agreement is indicated by all sources. The powered flight processor was again used and indicated performance well within ranges expected for both systems.

## 5.7 RENDEZVOUS

Immediately after ascent insertion, the Commander began a platform alignment using the lunar module telescope. During this time, the ground relayed the lunar module state vector to the command module computer to permit execution of navigation updates using the sextant and the VHF ranging system. The lunar module platform alignment took somewhat longer than expected; consequently, the coelliptic sequence initiation program was entered into the computer about 7 minutes later than planned. This delay allowed somewhat less than the nominal 18 radar navigation updates between insertion and the first rendezvous maneuver. Also, the first range rate measurement for the backup solution was missed; however, this loss was not significant, since both the lunar module and command module guidance systems were performing normally. Figure 5-19 shows the ascent and rendezvous trajectory and their relationship in lunar orbit.

Prior to coelliptic sequence initiation, the lunar module out-of-plane velocity was computed by the command module to be minus 1.0 ft/sec, a value small enough to be deferred until terminal phase initiation. The final lunar module solution for coelliptic sequence was a 51.5-ft/sec maneuver to be performed with the Z-axis reaction control thrusters, with a planned ignition time of 125:19:34.7.

Following the coelliptic sequence initiation maneuver, the constant differential height program was called up in both vehicles. Operation of the guidance systems continued to be normal, and successful navigation updates were obtained using the sextant, the VHF ranging system, and the rendezvous radar. It was reported by the Lunar Module Pilot that the backup range-rate measurement at 36 minutes prior to the constant differential height maneuver was outside the limits of the backup chart. Post-flight trajectory analysis has shown that the off-nominal command module orbit (62 by 56 miles) caused the range rate to be approximately 60 ft/sec below nominal at the 36-minute data point. The command module was near pericyynthion and the lunar module was near apocynthion at the measurement point. These conditions, which decreased the lunar module closure rate to below the nominal value, are apparent from figure 5-20, a relative motion plot of the two vehicles between insertion and the constant differential height maneuver. Figure 5-20 was obtained by forward and backward integration of the last available lunar module state vector prior to loss of signal following insertion and the final constant differential height maneuver vector integrated backward to the coelliptic sequence initiation point. The dynamic range of the backup charts has been increased for future landing missions. The constant differential height maneuver was accomplished at the lunar module primary guidance computer time of 126:17:49.6.

The constant differential height maneuver was performed with a total velocity change of 19.9 ft/sec. In a nominal coelliptic flight plan with a circular target orbit for the command module, this maneuver would be zero. However, the ellipticity of the command module orbit required a real-time change in the rendezvous plan prior to lift-off to include approximately 5 ft/sec, applied retrograde, to compensate for the change in differential height upon arriving at this maneuver point and approximately 11 ft/sec, applied vertically, to rotate the line of apsides to the correct angle. Actual execution errors in ascent insertion and coelliptic sequence initiation resulted in an additional velocity change requirement of about 8 ft/sec, which yielded the actual total of 19.9 ft/sec.

Following the constant differential height maneuver, the computers in both spacecraft were configured for terminal phase initiation. Navigation updates were made and several computer recycles were performed to obtain an early indication of the maneuver time. The final computation was initiated 12 minutes prior to the maneuver, as planned. Ignition had been computed to occur at 127:03:39, or 6 minutes 39 seconds later than planned.

Soon after the terminal phase initiation maneuver, the vehicles passed behind the moon. At the next acquisition, the vehicles were flying formation in preparation for docking. The crew reported that the rendezvous was nominal, with the first midcourse maneuver less than 1 ft/sec and the second about 1.5 ft/sec. The midcourse maneuvers were performed by thrusting the body axis components to zero while the lunar module plus Z axis remained pointed at the command module. It was also reported that line-of-sight rates were small, and the planned braking was used for the approach to station-keeping. The lunar module and command module maneuver solutions are summarized in tables 5-VI and 5-VII, respectively.

During the docking maneuver, two unexpected events occurred. In the alignment procedure for docking, the lunar module was maneuvered through the platform gimbal-lock attitude and the docking had to be completed using the abort guidance system for attitude control. The off-nominal attitude resulted from an added rotation to avoid sunlight interference in the forward windows. The sun elevation was about 20 degrees higher than planned because the angle for initiation of the terminal phase was reached about 6 minutes late.

The second unexpected event occurred after docking and consisted of relative vehicle alignment excursions of up to 15 degrees following initiation of the retract sequence. The proper docking sequence consists of initial contact, lunar module plus-X thrusting from initial contact to capture latch, switch the command module control from the automatic (CMC AUTO) to the manual (CMC FREE) mode and allow relative motions to be



damped to within plus or minus 3 degrees, and then initiate retract to achieve hard docking. The Commander detected the relatively low velocity at initial contact and applied plus X thrusting; however, the thrusting was continued until after the misalignment excursion had developed, since the Commander had received no indication of the capture event. To further complicate the dynamics, the Command Module Pilot also noticed the excursions and reversed the command module control mode from CMC FREE to CMC AUTO. At this time, both the lunar module and the command module were in minimum-deadband attitude-hold, thereby causing considerable thruster firing until the lunar module was placed in maximum deadband. The vehicles were stabilized using manual control just prior to achieving a successful hard dock. The initial observed misalignment excursion is considered to have been caused by the continued lunar module thrusting following capture, since the thrust vector does not pass through the center of gravity of the command and service modules.

The rendezvous was successful and similar to that for Apollo 10, with all guidance and control systems operating satisfactorily. The Command Module Pilot reported that the VHF ranging broke lock about 25 times following ascent insertion; however, lock-on was reestablished each time, and navigation updates were successful. The lunar module reaction control propellant usage was nearly nominal.

TABLE 5-I.- LUNAR DESCENT EVENT TIMES

Time, hr:min:sec	Event
102:17:17	Acquisition of data
102:20:53	Landing radar on
102:24:40	Align abort guidance to primary guidance
102:27:32	Yaw maneuver to obtain improved communications
102:32:55	Altitude of 50 000 feet
102:32:58	Propellant-settling firing start
102:33:05	Descent engine ignition
102:33:31	Fixed throttle position (crew report)
102:36:57	Face-up yaw maneuver in process
102:37:51	Landing radar data good
102:37:59	Face-up maneuver complete
102:38:22	1202 alarm (computer determined)
102:38:45	Enable radar updates
102:38:50	Altitude less than 30 000 feet (inhibit X-axis override)
102:38:50	Velocity less than 2000 ft/sec (start landing radar velocity update)
102:39:02	1202 alarm
102:39:31	Throttle recovery
102:41:32	Enter program P64
102:41:37	Landing radar antenna to position 2
102:41:53	Attitude-hold (handling qualities check)
102:42:03	Automatic guidance
102:42:18	1201 alarm (computer determined)
102:42:19	Landing radar low scale (less than 2500 feet)
102:42:43	1202 alarm (computer determined)
102:42:58	1202 alarm (computer determined)
102:43:09	Landing point redesignation
102:43:13	Attitude-hold
102:43:20	Update abort guidance attitude
102:43:22	Enter program P66
102:44:11	Landing radar data not good
102:44:21	Landing radar data good
102:44:28	Red-line low-level sensor light
102:44:59	Landing radar data not good
102:45:03	Landing radar data good
102:45:40	Landing
102:45:40	Engine off

TABLE 5-II.- MANEUVER RESIDUALS - DESCENT ORBIT INSERTION

Axis	Velocity residual, ft/sec	
	Before trimming	After trimming
X	-0.1	0.0
Y	-0.4	-0.4
Z	-0.1	0.0

TABLE 5-III.- POWERED DESCENT INITIATION STATE VECTORS

Parameter	Operational trajectory	Best estimate trajectory	Primary guidance computer
Latitude, deg	0.9614	1.037	1.17
Longitude, deg	39.607	39.371	39.48
Altitude, ft	50 000	49 376	49 955

TABLE 5-IV.- LUNAR LANDING COORDINATES<sup>a</sup>

Data source for solution	Latitude <sup>b</sup> , deg north	Longitude, deg east	Radius of Landing Site 2, miles
Primary guidance onboard vector	0.649	23.46	937.17
Abort guidance onboard vector	0.639	23.44	937.56
Powered flight processor (based on 4-track solu- tion)	0.631	23.47	936.74
Alignment optical tele- scope	0.523	23.42	
Rendezvous radar	0.636	23.50	937.13
Best estimate trajectory accelerometer recon- struction	0.647	23.505	937.14
Lunar module targeted	0.691	23.72	937.05
Photography	0.647 or <sup>c</sup> 0°41'15"	23.505 or <sup>c</sup> 23°26'00"	

<sup>a</sup>Following the Apollo 10 mission, a difference was noted (from the landmark tracking results) between the trajectory coordinate system and the coordinate system on the reference map. In order to reference trajectory values to the 1:100 000 scale Lunar Map ORB-II-6 (100), dated December 1967, correction factors of plus 2'25" in latitude and minus 4'17" in longitude must be applied to the trajectory values.

<sup>b</sup>All latitude values are corrected for the estimated out-of-plane position error at powered descent initiation.

<sup>c</sup>These coordinate values are referenced to the map and include the correction factors.

TABLE 5-V.- INSERTION SUMMARY

Source	Altitude, ft	Radial velocity, ft/sec	Downrange velocity, ft/sec
Primary guidance	60 602	33	5537.0
Abort guidance	60 019	30	5537.9
Network tracking	61 249	35	5540.7
Operational trajectory	60 085	32	5536.6
Reconstructed from accelerometers	60 337	33	5534.9
Actual (best estimate trajectory)	60 300	32	5537.0
Target values*	60 000	32	5534.9

\*Also, crossrange displacement of 1.7 miles was to be corrected.

The following velocity residuals were calculated by the primary guidance:

$$X = -2.1 \text{ ft/sec}$$

$$Y = -0.1 \text{ ft/sec}$$

$$Z = +1.8 \text{ ft/sec}$$

The orbit resulting after residuals were trimmed was:

$$\text{Apocynthion altitude} = 47.3 \text{ miles}$$

$$\text{Pericynthion altitude} = 9.5 \text{ miles}$$

TABLE 5-VI.- LUNAR MODULE MANEUVER SOLUTIONS

Maneuver	Primary guidance			Abort guidance		Real-time nominal		Actual	
	Solution	Time, hr:min:sec	Velocity, ft/sec	Time, hr:min:sec	Velocity, ft/sec	Time, hr:min:sec	Velocity, ft/sec	Time, hr:min:sec	Velocity, ft/sec
Coelliptic sequence initiation	Initial	125:19:35.48	49.4 posigrade	125:19:34.70	51.3 posigrade	125:19:35	52.9 posigrade	125:19:35	51.6 posigrade 0.7 south 0.1 down
	Final	125:19:35.48	51.5 posigrade						
Constant differential height	Initial	126:17:46.36	8.1 retrograde 1.8 south 17.7 up	(a)	(a)	126:17:42	5.1 retrograde 11.0 up	126:17:50	8.0 retrograde 1.7 south 18.1 up
	Final	126:17:46.36	8.1 retrograde 18.2 up						
Terminal phase initiation <sup>b,c</sup>	Initial	127:03:16.12	25.2 forward 1.9 right 0.4 down	127:03:39	23.4 total	126:57:00	22.4 posigrade 0.2 north 11.7 up	127:03:52	22.9 posigrade 1.4 north 11.0 up
	Final	127:03:31.60	25.0 forward 2.0 right 0.7 down						
First midcourse correction	Final	127:18:30.8	0.0 forward 0.4 right 0.9 down	(a)	(a)	127:12:00	0.0	(d)	(d)
Second midcourse correction	Final	127:33:30.8	0.1 forward 1.2 right 0.5 down	(a)	(a)	127:27:00	0.0	(d)	(d)

<sup>a</sup>Solution not obtained.

<sup>b</sup>Body-axis reference frame; all other solutions for local-vertical reference frame.

<sup>c</sup>For comparing the primary guidance solution for terminal phase initiation with the real-time nominal and actual values, the following components are equivalent to those listed but with a correction to a local-vertical reference frame: 22.7 posigrade, 1.5 north, and 10.6 up.

<sup>d</sup>Data not available because of moon occultation.

TABLE 5-VII.- COMMAND MODULE SOLUTIONS

Maneuver	Time, hr:min:sec	Solution, ft/sec
Coelliptic sequence initiation	125:19:34.70	51.3 retrograde 1.4 south 0.0 up/down
Constant differential height	126:17:46.00	9.1 posigrade 2.4 north 14.6 down
Terminal phase initiation	127:02:34.50 <sup>a</sup> 127:03:30.8 <sup>b</sup>	22.9 retrograde 1.7 south 11.9 down
First midcourse correction	127:18:30.8	1.3 retrograde 0.6 south
Second midcourse correction	127:33:30.8	0.1 retrograde 1.0 south 0.6 down

<sup>a</sup>Initial computed time of ignition using nominal elevation angle of 208.3 degrees for terminal phase initiation.

<sup>b</sup>Final solution using lunar module time of ignition.

NOTE: All solutions in local horizontal coordinate frame.

NASA-S-69-3709

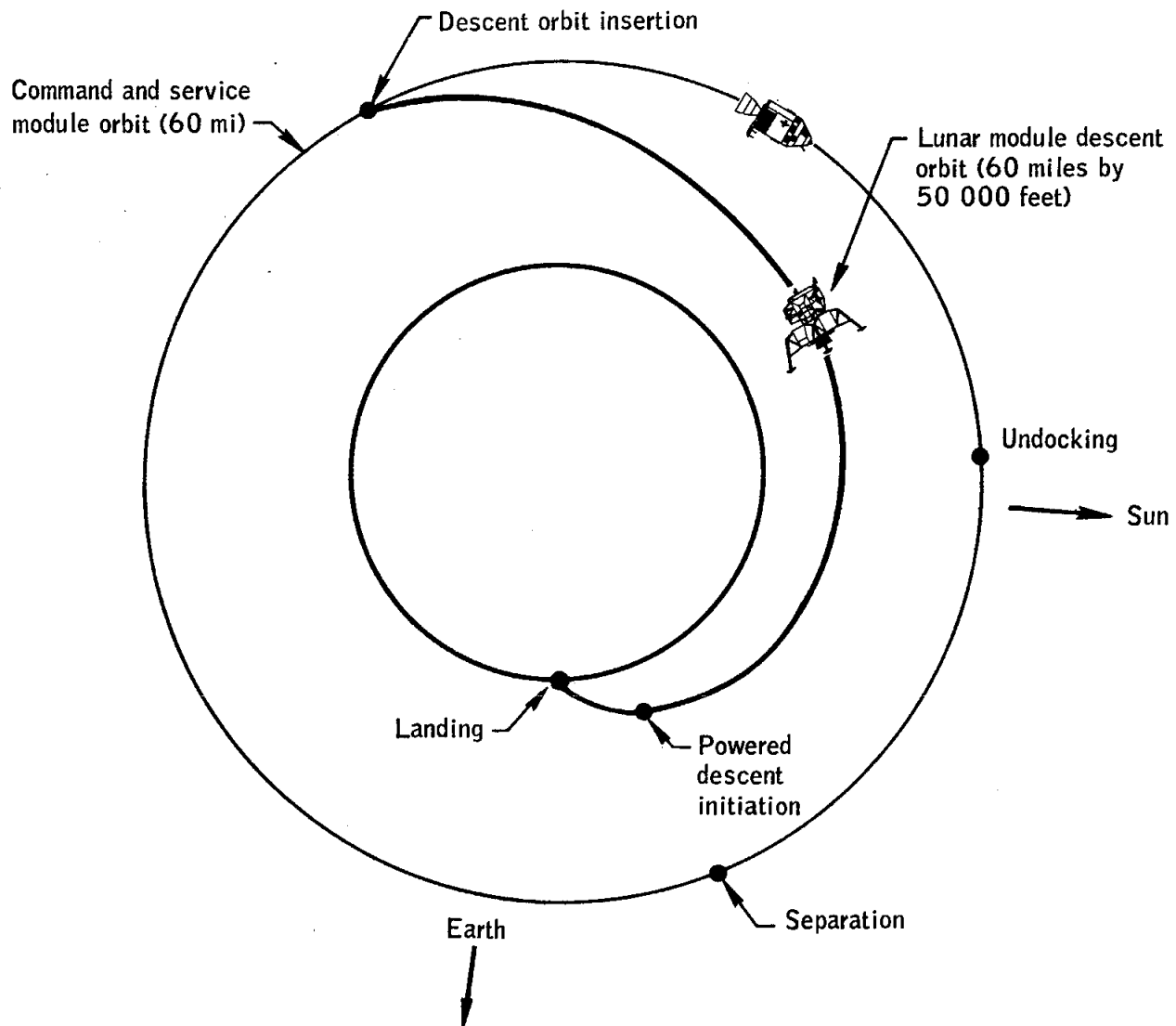


Figure 5-1 . - Lunar descent orbital events .



NASA-S-69-3710

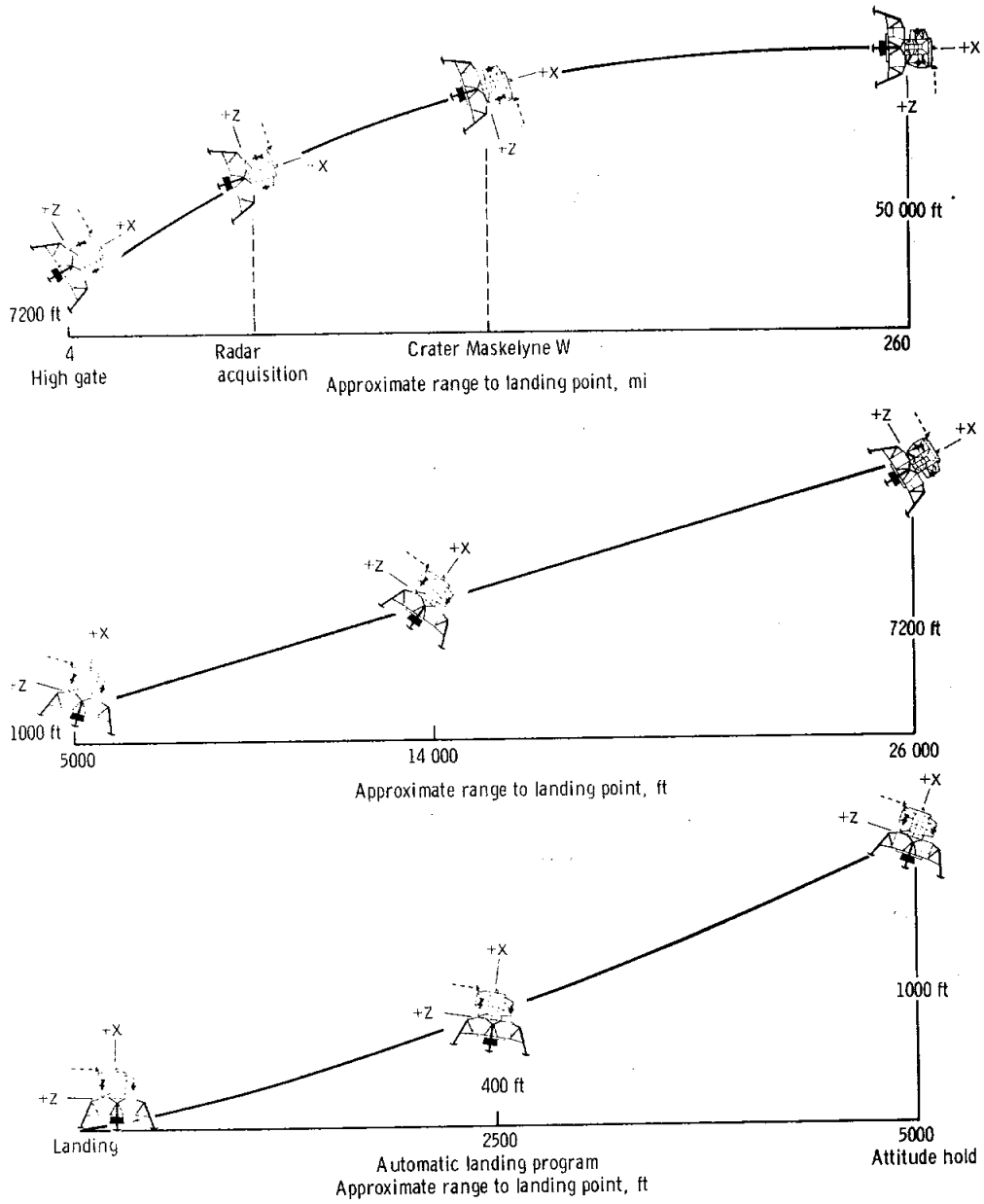


Figure 5-2. - Spacecraft attitudes during powered descent.

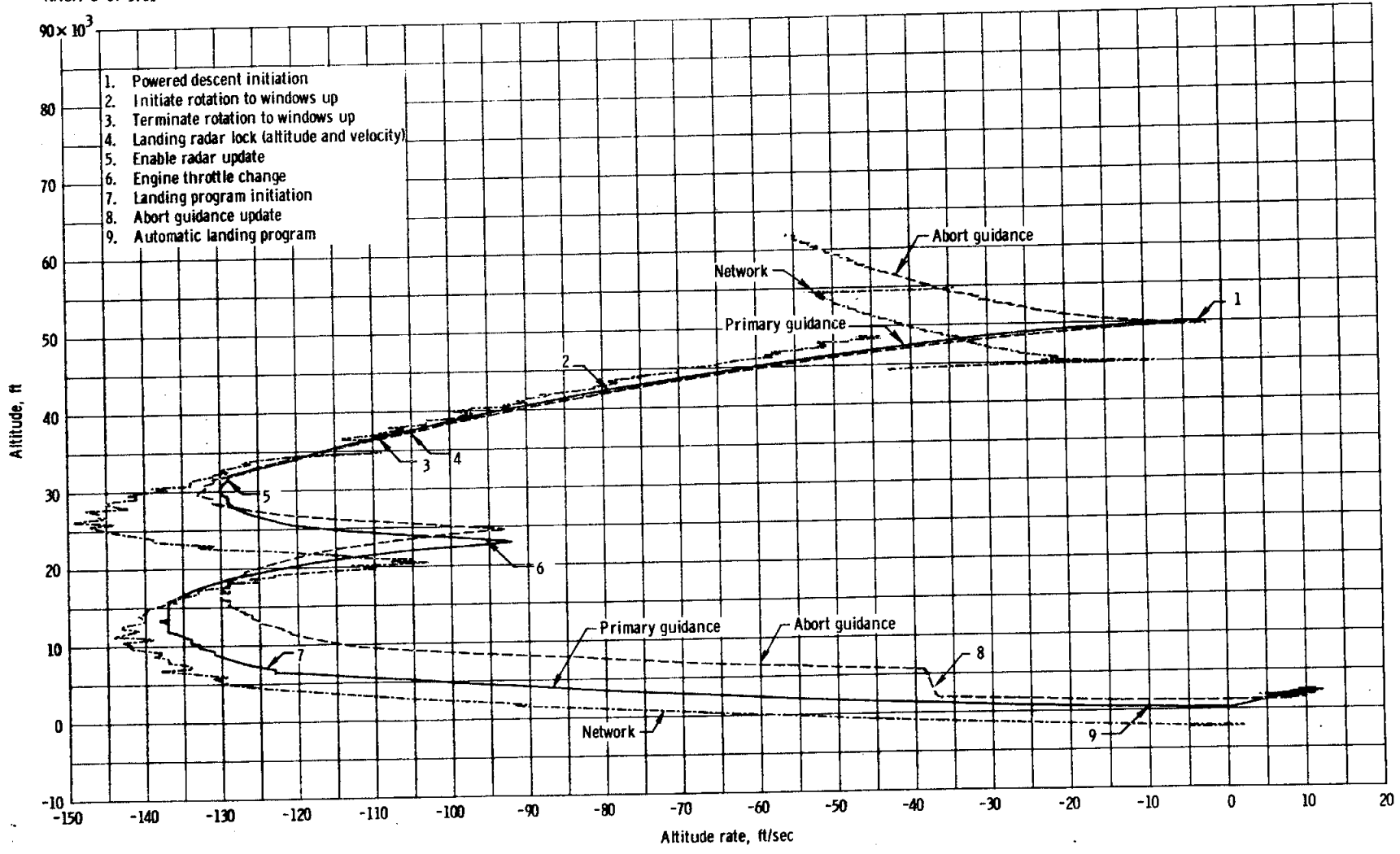


Figure 5-3. - Comparison of altitude and altitude rate during descent.

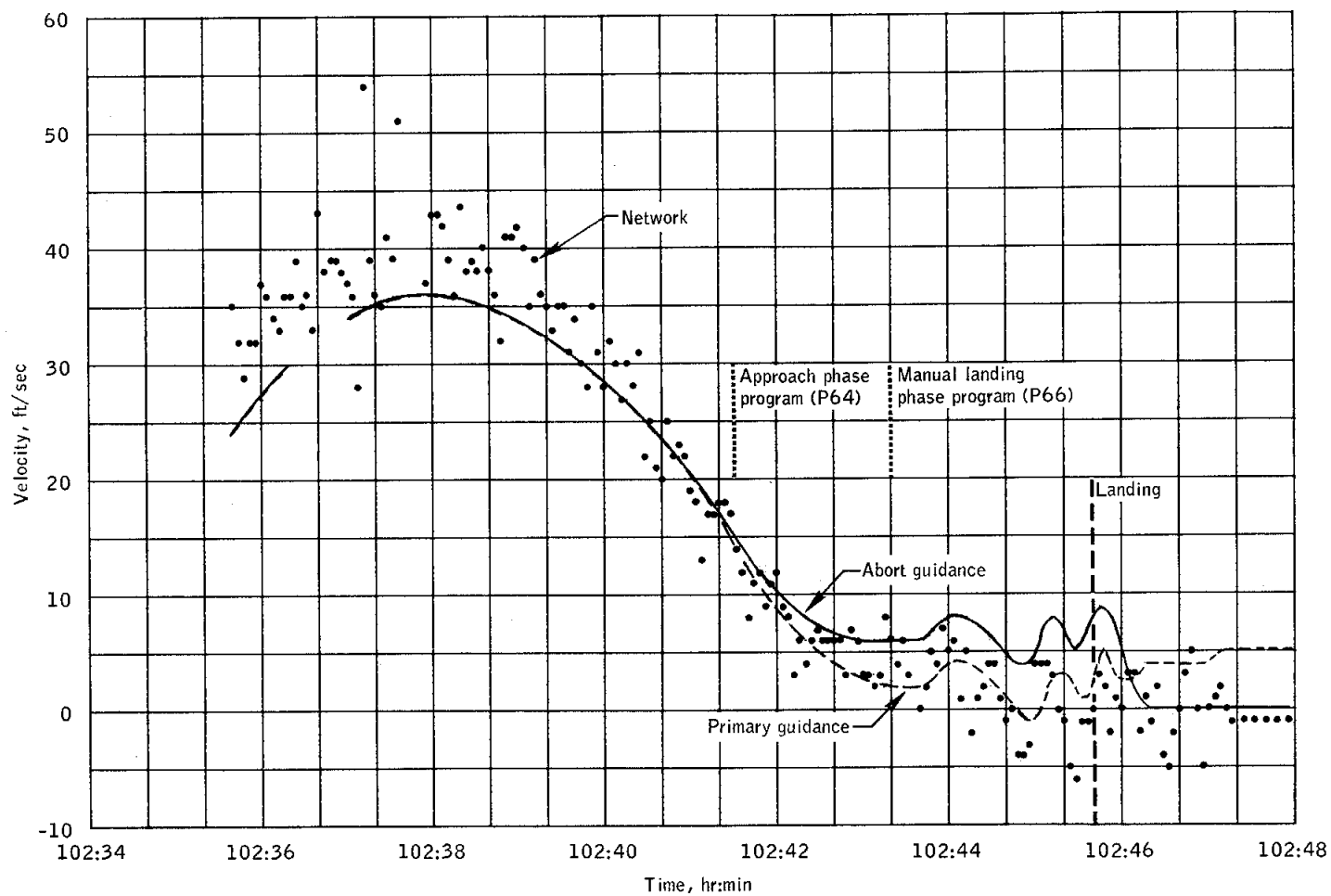


Figure 5-4.- Comparison of lateral velocity.

NASA-S-69-3713

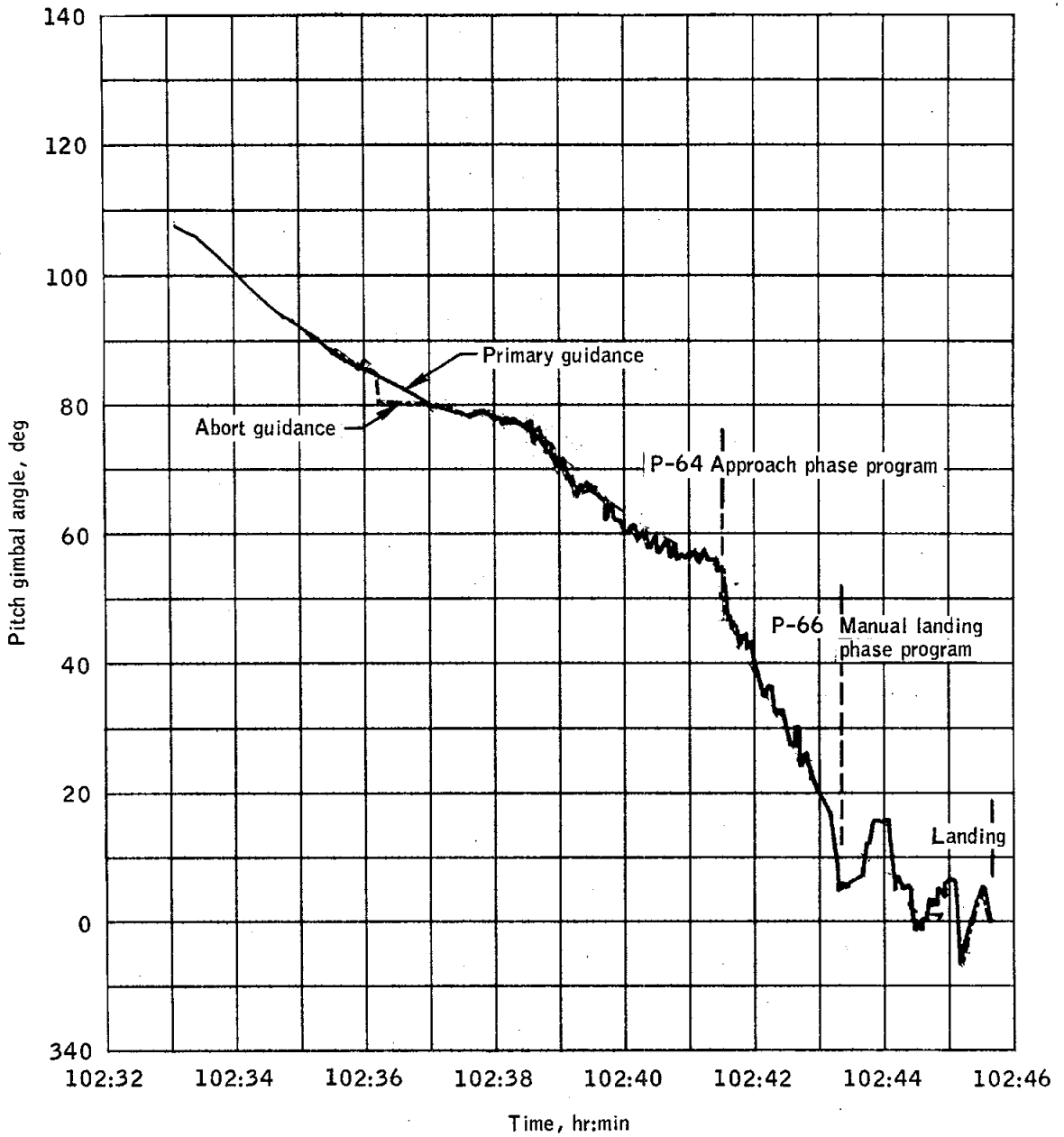
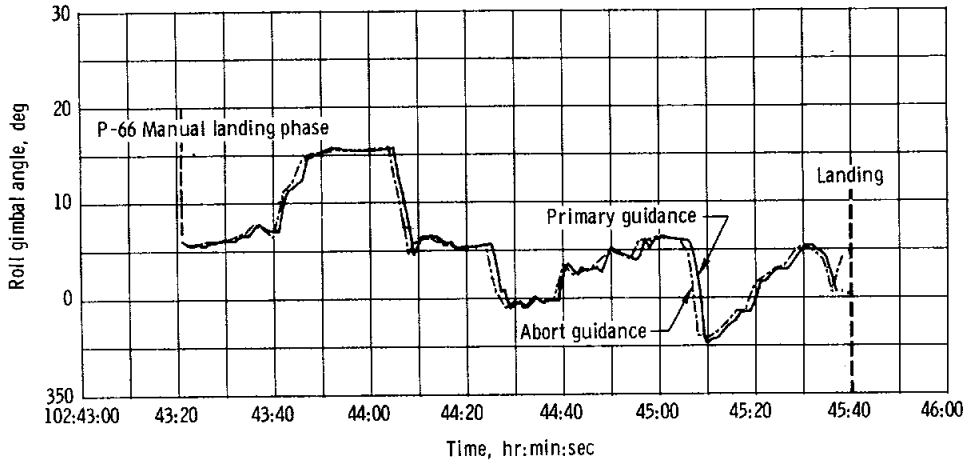
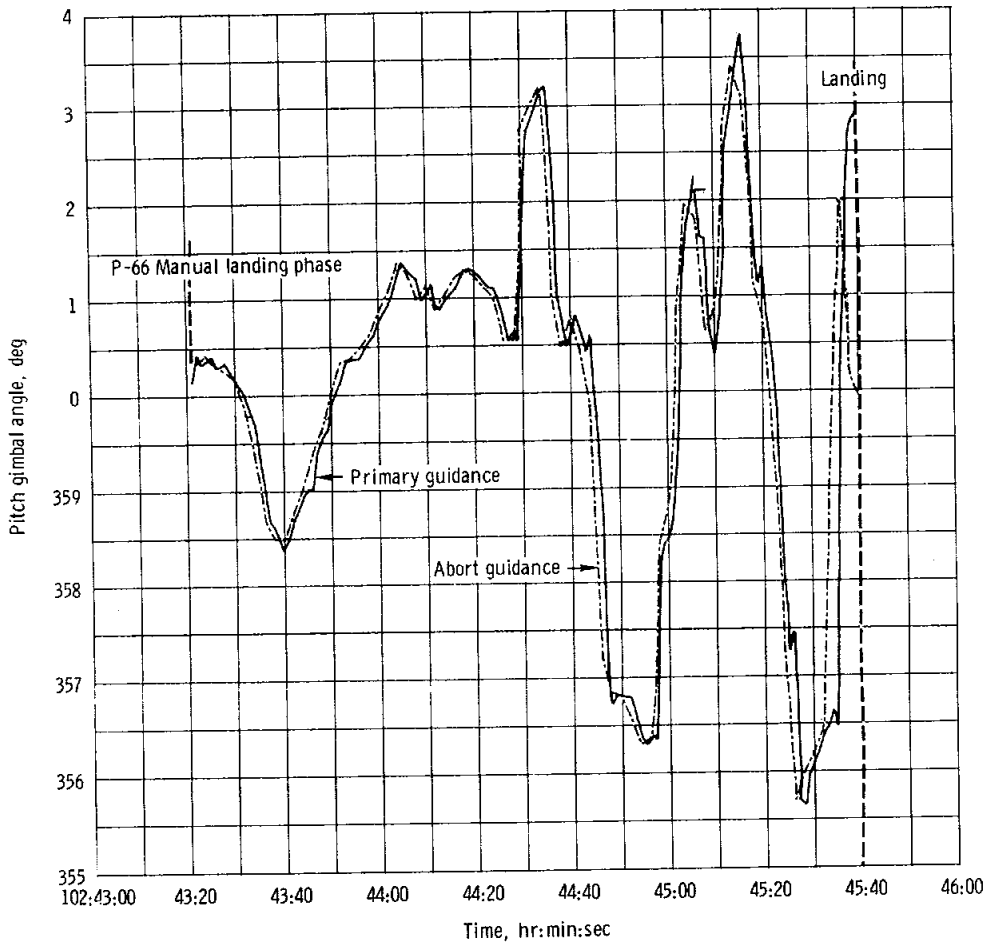


Figure 5-5.- Pitch attitude time history during descent.

NASA-S-69-3714



(a) Roll gimbal angle.



(b) Pitch gimbal angle.

Figure 5-6. - Expanded pitch and roll attitude time histories near landing.

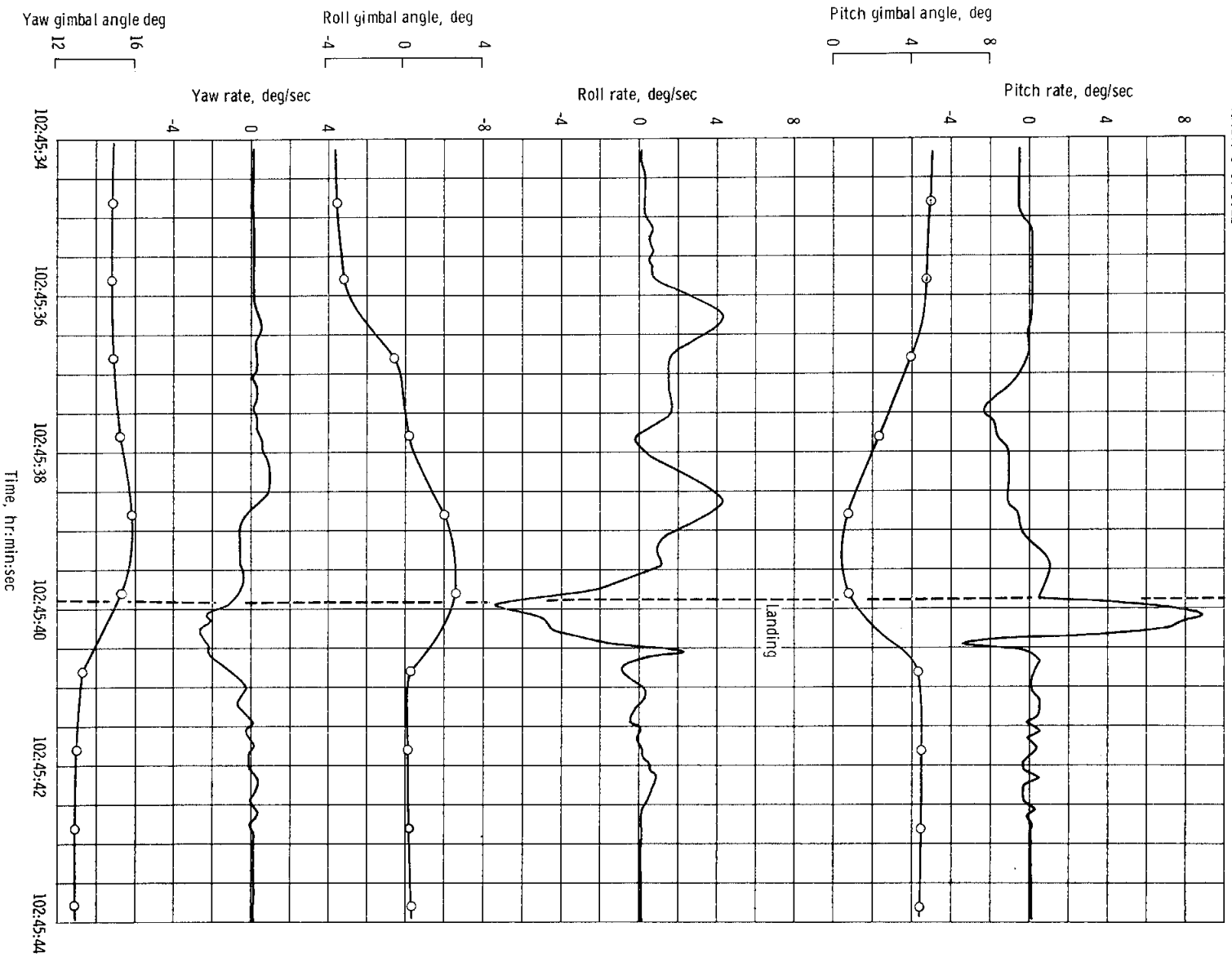


Figure 5-13. - Spacecraft dynamics during lunar touchdown.

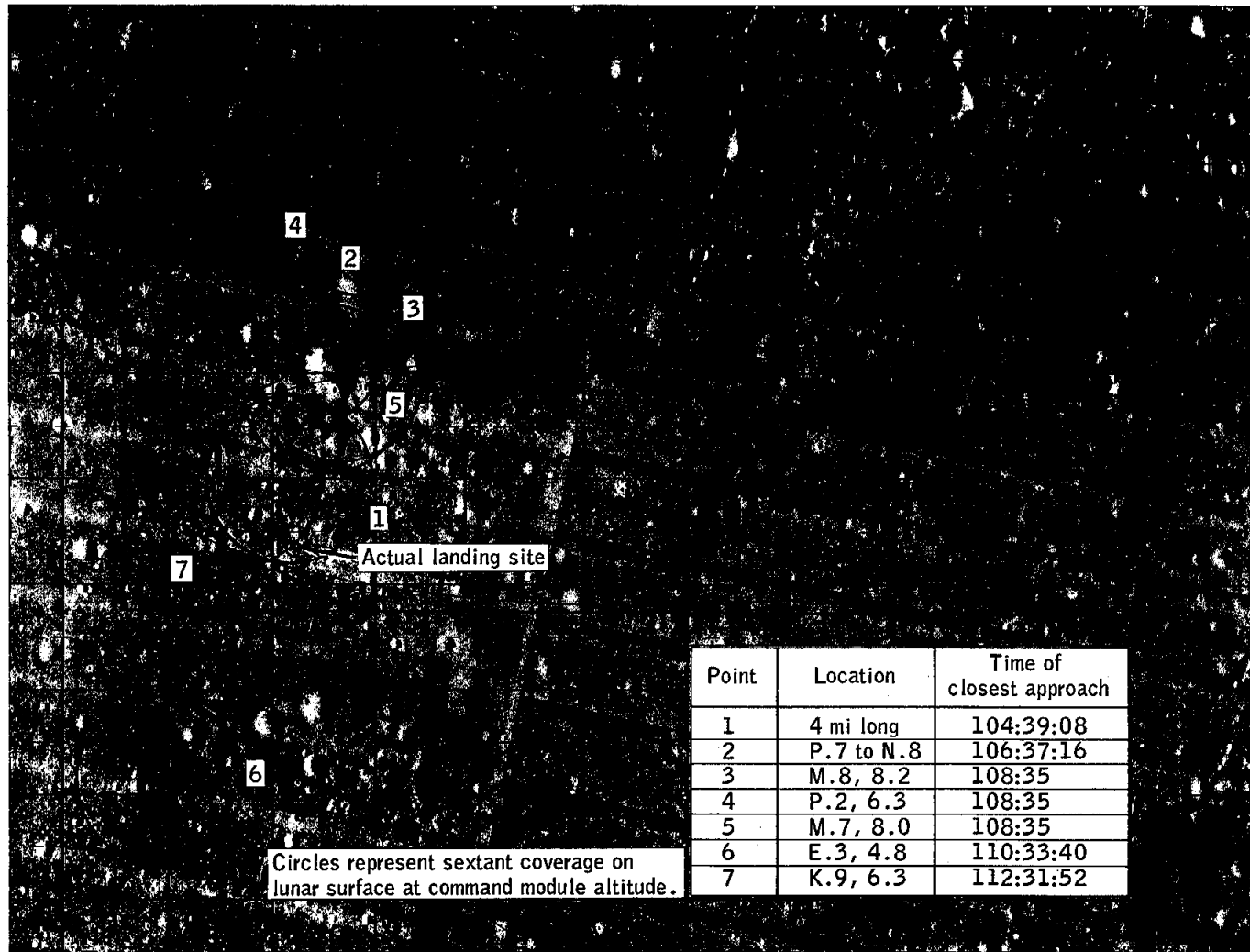


Figure 5-14.- Command module sighting history during lunar stay.

NASA-S-69-3724

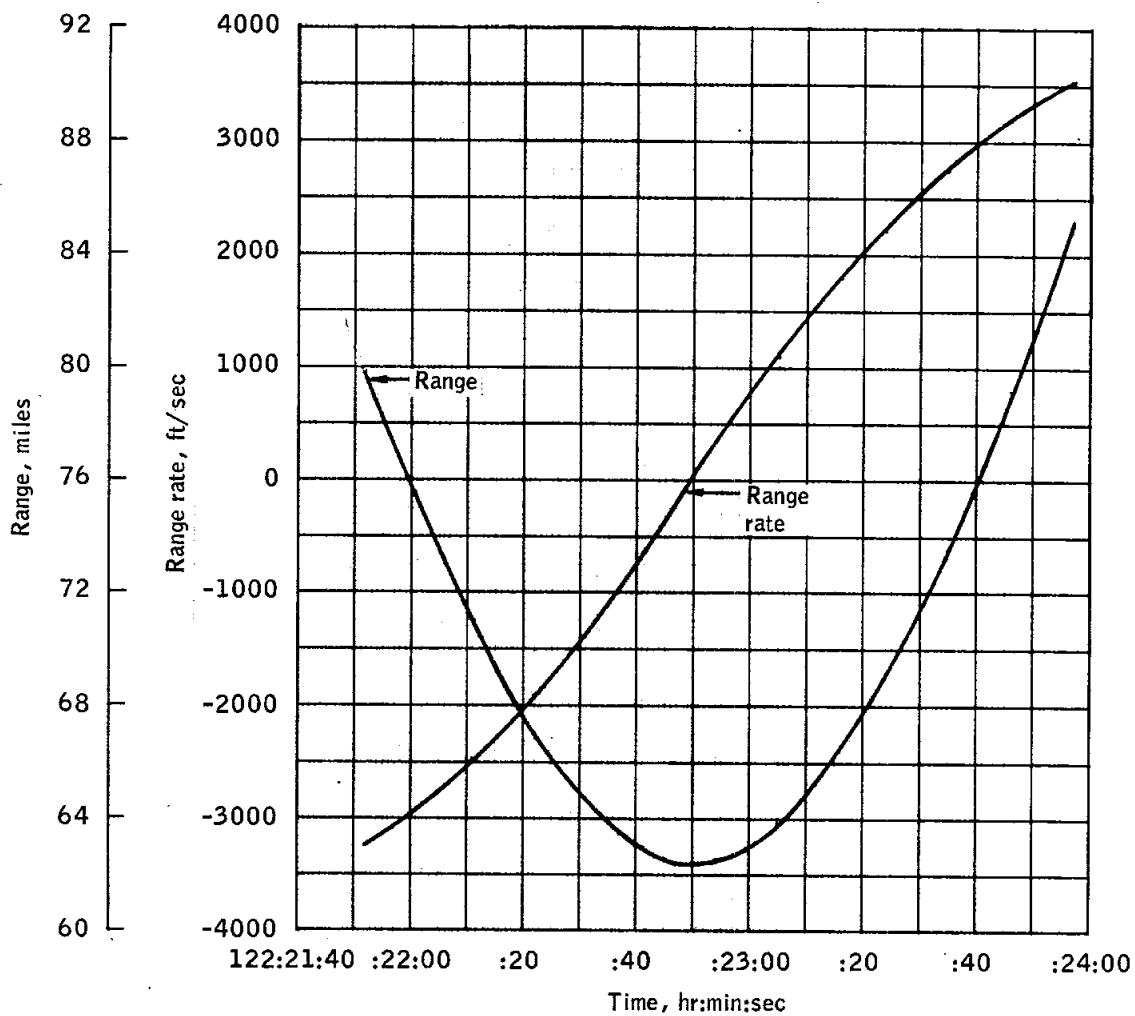
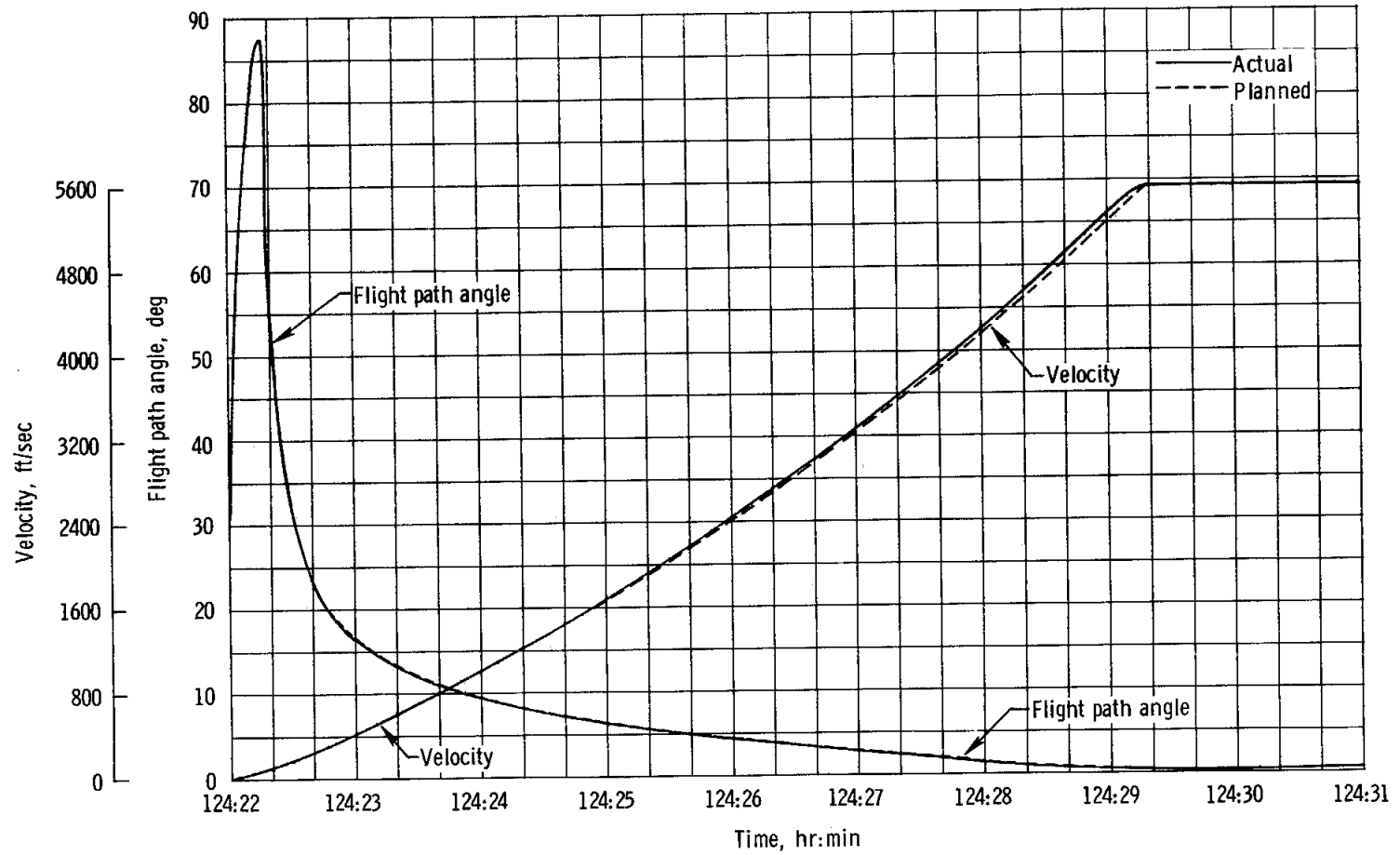


Figure 5-15.- Rendezvous radar tracking of the command module while LM was on lunar surface.

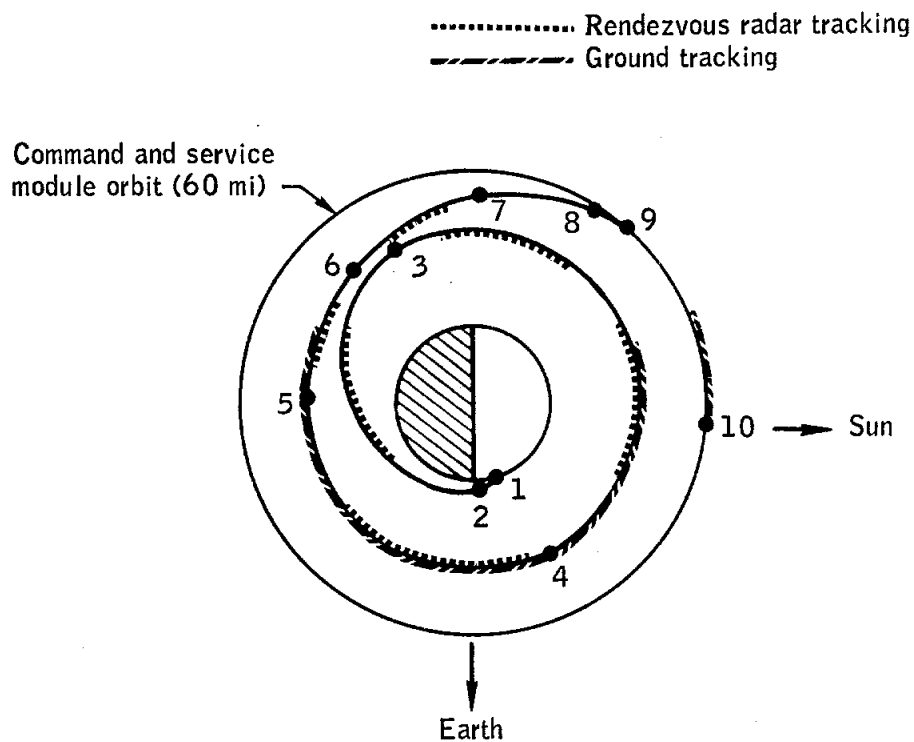




(a) Velocity and flight-path angle.

Figure 5-16. - Trajectory parameters for lunar ascent phase.

NASA-S-69-3730



	Event	Time
1	Lift-off	124:22:00.8
2	Lunar module insertion	124:29:15.7
3	Coelliptic sequence initiation	125:19:35.0
4	Constant differential height	126:17:49.6
5	Terminal phase initiation	127:03:51.8
6	First midcourse correction	127:18:30.8
7	Second midcourse correction	127:33:30.8
8	Begin braking	127:36:57.3
9	Begin stationkeeping	127:52:05.3
10	Docking	128:03:00.0

Figure 5-19.- Ascent and rendezvous trajectory.

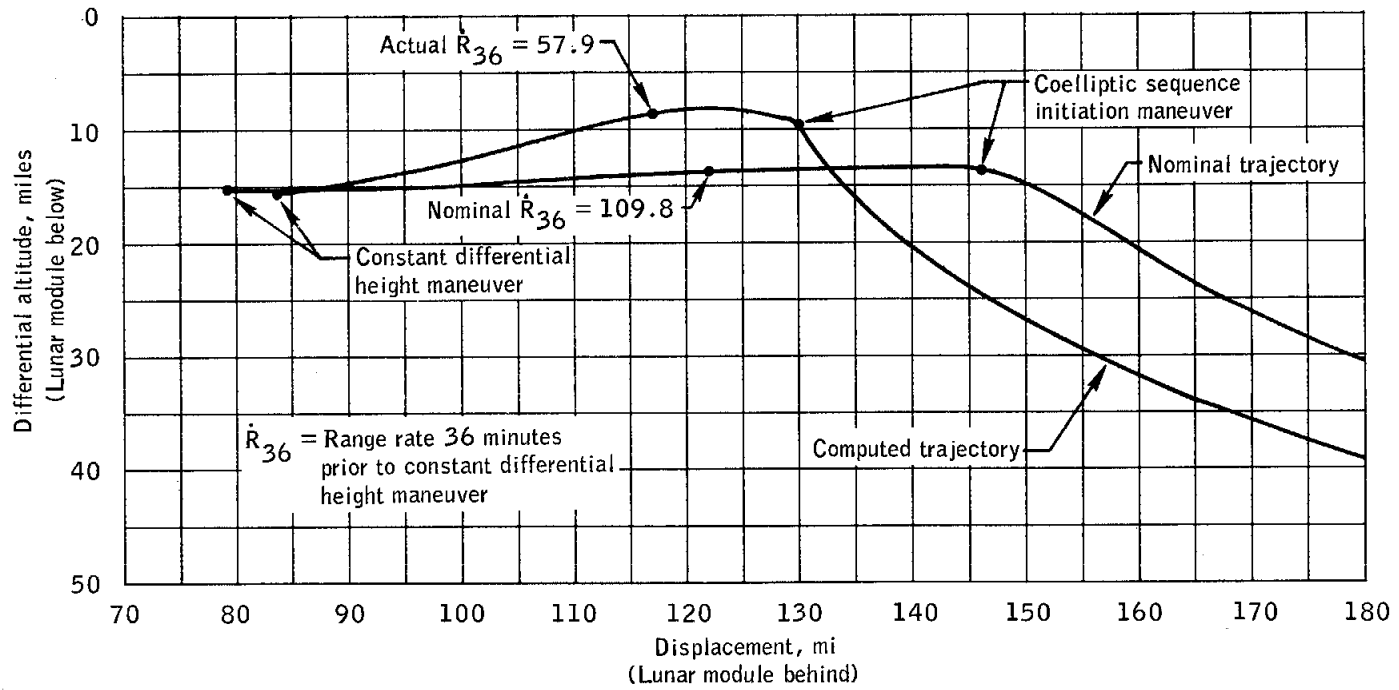


Figure 5-20.- Relative spacecraft motion during rendezvous.

## 6.0 COMMUNICATIONS

Performance of all communications systems (see sections 8, 9, 10, and 13), including those of the command module, lunar module, portable life support system, and Manned Space Flight Network, was generally as expected. This section presents only those aspects of communication system performance which were unique to this flight. The performance of these systems was otherwise consistent with that of previous flights. The S-band communication system provided good quality voice, as did the VHF link within its range capability. The performance of command module and lunar module up-data links was nominal, and real-time and playback telemetry performance was excellent. Color television pictures of high quality were received from the command module. Good quality black-and-white television pictures were received and converted to standard format during lunar surface operations. Excellent quality tracking data were obtained for both the command and lunar modules. The received uplink and downlink signal powers corresponded to preflight predictions. Communications system management, including antenna switching, was generally good.

Two-way phase lock with the command module S-band equipment was maintained by the Merritt Island, Grand Bahama Island, Bermuda, and USNS Vanguard stations through orbital insertion, except during S-IC/S-II staging, interstage jettison, and station-to-station handovers. A complete loss of uplink lock and command capability was encountered between 6 and 6-1/2 minutes after earth lift-off because the operator of the ground transmitter at the Grand Bahama Island station terminated transmission 30 seconds early. Full S-band communications capability was restored at the scheduled handover time when the Bermuda station established two-way phase lock. During the Merritt Island station's coverage of the launch phase, PM and FM receivers were used to demodulate the received telemetry data. (Normally, only the PM data link is used.) The purpose of this configuration was to provide additional data on the possibility of improving telemetry coverage during S-IC/S-II staging and interstage jettison using the FM receiver. There was no loss of data through the FM receiver at staging. On the other hand, the same event caused a 9-second loss of data at the PM receiver output (see fig. 6-1). However, the loss of data at interstage jettison was approximately the same for both types of receivers.

The television transmission attempted during the first pass over the Goldstone station was unsuccessful because of a shorted patch cable in the ground station television equipment. Also, the tracking coverage during this pass was limited to approximately 3 minutes by terrain obstructions. All subsequent transmissions provided high-quality television.

The USNS Redstone and Mercury ships and the Hawaii station provided adequate coverage of translunar injection. A late handover of the command module and instrument unit uplinks from the Redstone to the Mercury and an early handover of both uplinks from the Mercury to Hawaii were performed because of command computer problems at the Mercury. Approximately 58 seconds of command module data were lost during these handovers. The loss of data during the handover from the Mercury to Hawaii was caused by terrain obstructions.

Communications between the command module and the ground were lost during a portion of transposition and docking because the crew failed to switch omnidirectional antennas during the pitch maneuver. Two-way phase lock was regained when the crew acquired the high gain antenna in the narrow beamwidth. The telemetry data recorded onboard the spacecraft during this phase were subsequently played back to the ground. Between 3-1/2 and 4 hours, the downlink voice received at the Mission Control Center was distorted by equipment failures within the Goldstone station.

During the fourth lunar orbit revolution, lunar module communications equipment was activated for the first time. Good quality normal and back-up down-voice and high and low bit rate telemetry were received through the 210-foot Goldstone antenna while the spacecraft was transmitting through an omnidirectional antenna. As expected, telemetry decommutation frame synchronization could not be maintained in the high-bit-rate mode using the 85-foot antenna at Goldstone for reception.

Between acquisition of the lunar module signal at 102:16:30 and the pitch-down maneuver during powered descent, valid steerable antenna auto-track could not be achieved, and received uplink and downlink carrier powers were 4 to 6 dB below nominal. Coincidentally, several losses of phase-lock were experienced (fig. 6-2). Prior to the unscheduled yaw maneuver initiated at 102:27:22, the line of sight from the lunar module steerable antenna to earth was obstructed by a reaction control thruster plume deflector (see section 16.2.4). Therefore, the antenna was more susceptible in this attitude to incidental phase and amplitude modulation resulting from multipath effects off either the lunar module or the lunar surface. The sharp losses of phase lock were probably caused by the build-up of oscillations in steerable antenna motion as the frequencies of the incidental amplitude and phase modulation approached multiples of the antenna switching frequency (50 hertz). After the yaw maneuver, auto-track with the correct steerable antenna pointing angles was not attempted until 102:40:12. Subsequently, valid auto-track was maintained through landing.

As shown in figure 6-2, the performance of the downlink voice and telemetry channels was consistent with the received carrier power. The long periods of loss of PCM synchronization on data received at the 85-foot station distinctly illustrate the advantage of scheduling the descent maneuver during coverage by a 210-foot antenna.

After landing, the lunar module steerable antenna was switched to the slew (manual) mode and was used for all communications during the lunar surface stay. Also, the Network was configured to relay voice communications between the two spacecraft.

This configuration provided good-quality voice while the command module was transmitting through the high gain antenna. However, the lunar module crewmen reported that the noise associated with random keying of the voice-operated amplifier within the Network relay configuration was objectionable when the command module was transmitting through an omnidirectional antenna. This noise was expected with operation on an omnidirectional antenna, and use of the two-way voice relay through the Network was discontinued, as planned, after the noise was reported. During the subsequent extravehicular activity, a one-way voice relay through the Network to the command module was utilized.

Primary coverage of the extravehicular activity was provided by 210-foot antennas at Goldstone, California, and Parkes, Australia. Backup coverage was provided by 85-foot antennas at Goldstone, California, and Honeysuckle Creek, Australia. Voice communications during this period were satisfactory; however, voice-operated-relay operations caused breakup of the voice received at the Network stations (see section 13.2 and 16.2.8). This breakup was primarily associated with the Lunar Module Pilot. Throughout the lunar surface operation, an echo was heard on the ground 2.6 seconds after uplink transmissions because uplink voice was turned around and transmitted on the lunar module S-band downlink (see section 16.2.9). The Parkes receiving station was largely used by the Mission Control Center as the primary receiving station for real-time television transmissions. The telemetry decommutation system and the PAM-to-PCM converter maintained frame synchronization on the lunar module telemetry data and the portable-life-support-system status data, respectively, throughout the lunar surface activities.

An evaluation of data recorded by the Honeysuckle station during lunar surface activities was accomplished to determine whether an 85-foot station could have supported this mission phase without deployment of the lunar module erectable antenna. The results were compared with those of a similar evaluation recorded at the Goldstone station using the 210-foot antenna. A comparison of slow-scan television signals received at the two stations shows that, although there was a 4-dB difference in signal-to-noise ratios, there was no appreciable difference in picture quality. The differences in downlink voice intelligibility and telemetry data quality were not significant. There is no perceptible difference in the quality of biomedical data received at the 85- and 210-foot stations. Playback of portable-life-support-system status data for the Lunar Module Pilot shows that frame synchronization was maintained 88 and 100 percent of the time for the 85- and 210-foot stations, respectively. Based on these comparisons, the 85-foot ground station could

have supported the lunar surface activities without deployment of the erectable antenna with slightly degraded data.

The performance of the communication system during the ascent and rendezvous phases was nominal except for a 15-second loss of downlink phase lock at ascent engine ignition. The data indicate this loss can be attributed to rapid phase perturbations caused by transmission through the ascent engine plume. During future Apollo missions, a wider carrier tracking loop bandwidth will be selected by the Network stations prior to powered ascent. This change will minimize the possibility of loss of lock due to rapid phase perturbations.

NASA-S-69-3732

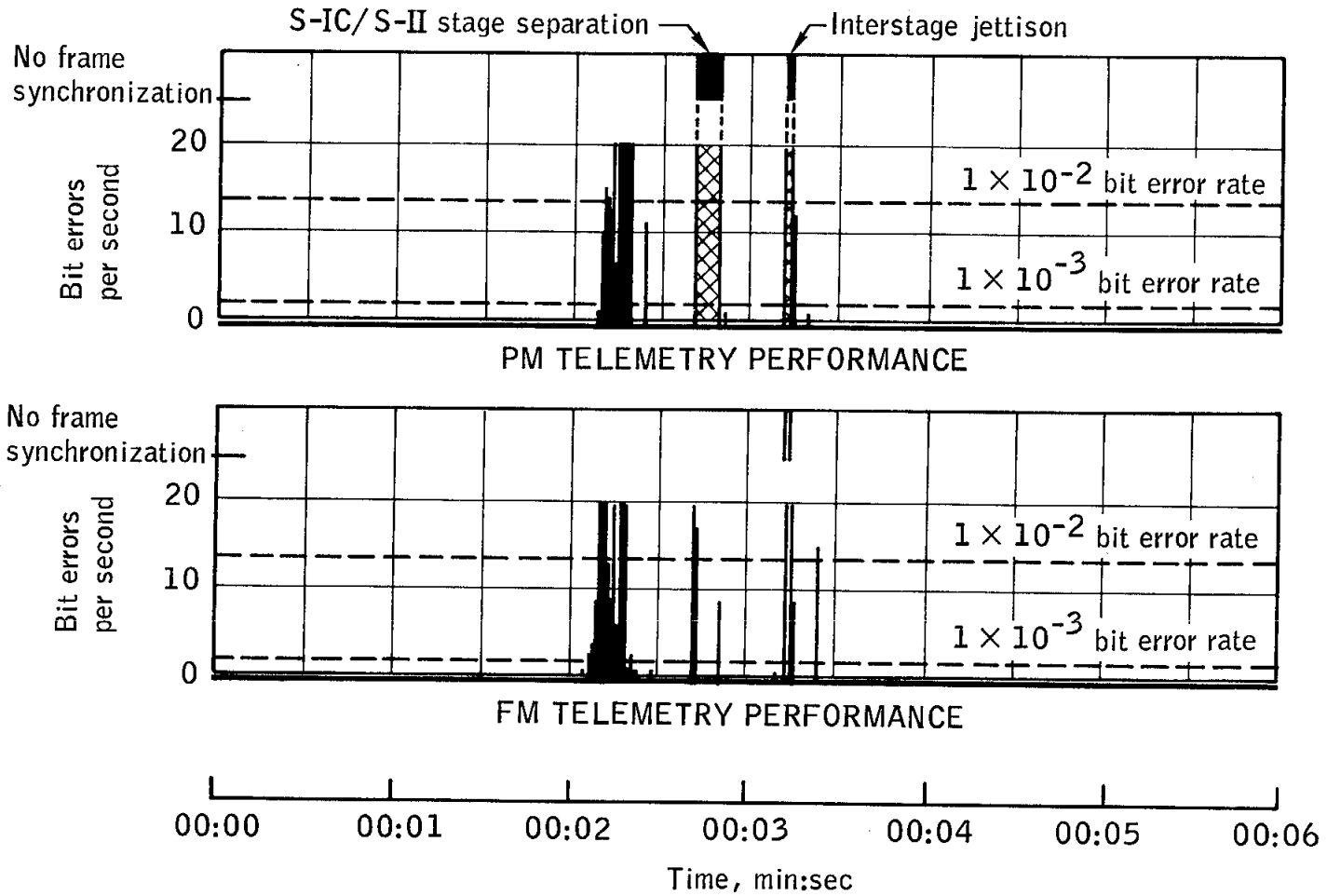


Figure 6-1.- Communications system performance (downlink) during launch.



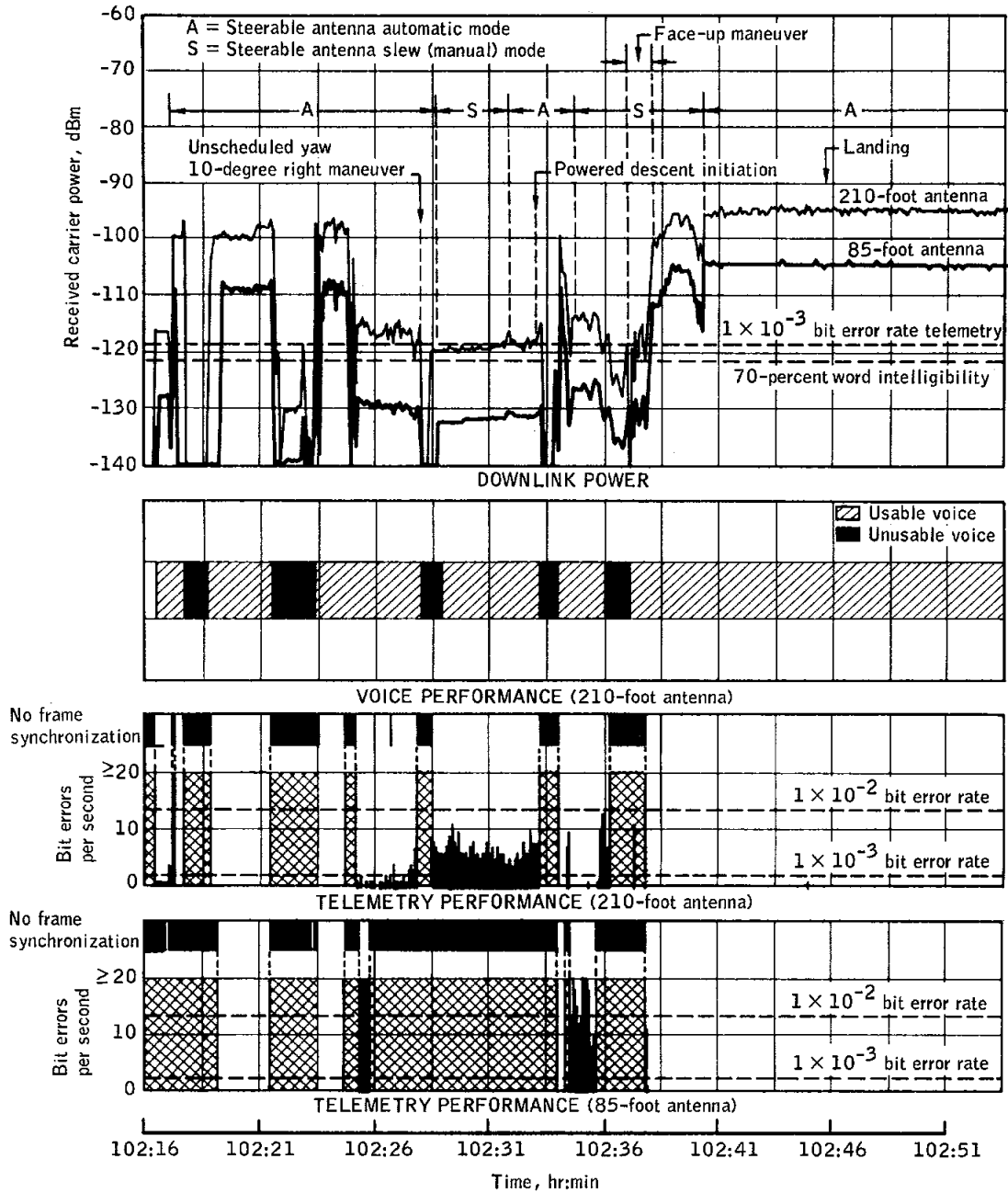


Figure 6-2.- Communications system (downlink) performance during final descent.

## 7.0 TRAJECTORY

The analysis of the trajectory from lift-off to spacecraft/S-IVB separation was based on Marshall Space Flight Center results (ref. 1) and tracking data from the Manned Space Flight Network. After separation, the actual trajectory information was based on the best estimated trajectory generated after the flight from Network tracking and telemetry data.

The earth and moon models used for the trajectory analysis are geometrically described as follows: (1) the earth model is a modified seventh-order expansion containing geodetic and gravitational constants representative of the Fischer ellipsoid, and (2) the moon model is a spherical harmonic expansion containing the  $R_2$  potential function, which is defined in reference 2. Table 7-I defines the trajectory and maneuver parameters.

### 7.1 LAUNCH PHASE

The launch trajectory was essentially nominal and was nearly identical to that of Apollo 10. A maximum dynamic pressure of  $735 \text{ lb/ft}^2$  was experienced. The S-IC center and outboard engines and the S-IVB engine cut off within 1 second of the planned times, and S-II outboard engine cutoff was 3 seconds early. At S-IVB cutoff, the altitude was high by 9100 feet, the velocity was low by 6.0 ft/sec, and the flight-path angle was high by 0.01 degree all of which were within the expected dispersions.

### 7.2 EARTH PARKING ORBIT

Earth parking orbit insertion occurred at 0:11:49.3. The parking orbit was perturbed by low-level hydrogen venting of the S-IVB stage until 2:34:38, the time of S-IVB restart preparation.

### 7.3 TRANSLUNAR INJECTION

The S-IVB was reignited for the translunar injection maneuver at 2:44:16.2, or within 1 second of the predicted time, and cutoff occurred at 2:50:03. All parameters were nominal and are shown in figure 7-1.

## 7.4 MANEUVER ANALYSIS

The parameters derived from the best estimated trajectory for each spacecraft maneuver executed during the translunar, lunar orbit, and transearth coast phases are presented in table 7-II. Tables 7-III and 7-IV present the respective pericyynthion and free-return conditions after each translunar maneuver. The free-return results indicate conditions at entry interface produced by each maneuver, assuming no additional orbit perturbations. Tables 7-V and 7-VI present the respective maneuver summaries for the lunar orbit and the transearth coast phases.

### 7.4.1 Translunar Injection

The pericynthion altitude resulting from translunar injection was 896.3 miles, as compared with the preflight prediction of 718.9 miles. This altitude difference is representative of a 1.6 ft/sec accuracy in the injection maneuver. The associated free-return conditions show an earth capture of the spacecraft.

### 7.4.2 Separation and Docking

The command and service modules separated from the S-IVB and successfully completed the transposition and docking sequence. The spacecraft were ejected from the S-IVB at 4 hours 17 minutes. The effect of the 0.7-ft/sec ejection maneuver was a change in the predicted pericynthion altitude to 827.2 miles. The separation maneuver performed by the service propulsion system was executed precisely and on time. The resulting trajectory conditions indicate a pericynthion altitude reduction to 180.0 miles, as compared to the planned value of 167.7 miles. The difference indicates a 0.24-ft/sec execution error.

### 7.4.3 Translunar Midcourse Correction

The computed midcourse correction for the first option point was only 17.1 ft/sec. A real-time decision was therefore made to delay the first midcourse correction until the second option point at translunar injection plus 24 hours because of the small increase to only 21.2 ft/sec in the corrective velocity required. The first and only translunar midcourse correction was initiated on time and resulted in a pericynthion altitude of 61.5 miles, as compared with the desired value of 60.0 miles. Two other opportunities for midcourse correction were available during the translunar phase, but the velocity changes required to satisfy planned pericynthion altitude and nodal position targets were well below the

levels at which normal lunar orbit insertion can be retargeted. Therefore, no further translunar midcourse corrections were required. The translunar trajectory was very similar to that of Apollo 10.

#### 7.4.4 Lunar Orbit Insertion and Circularization

The lunar orbit insertion and circularization targeting philosophy for Apollo 11 differed from that of Apollo 10 in two ways. First, targeting for landing site latitude was biased to account for the orbit plane regression observed in Apollo 10; and secondly, the circularization maneuver was targeted for a noncircular orbit of 65.7 by 53.7 miles, as compared with the 60-mile-circular orbit targeted for Apollo 10. A discussion of these considerations is presented in section 7.7. The representative ground track of the spacecraft during the lunar orbit phase of the mission is shown in figure 7-2.

The sequence of events for lunar orbit insertion was initiated on time, and the orbit achieved was 169.7 by 60.0 miles. The firing duration was 4.5 seconds less than predicted because of higher than predicted thrust (see section 8.8).

The circularization maneuver was initiated two revolutions later and achieved the desired target orbit to within 0.1 mile. The spacecraft was placed into a 65.7- by 53.8-mile orbit, with pericyynthion at approximately 80 degrees west, as planned. The R2 orbit prediction model predicted a spacecraft orbit at 126 hours (revolution 13) of 59.9 by 59.3 miles. However, the orbit did not circularize during this period (fig. 7-3). The effects of the lunar potential were sufficient to cause this prediction to be in error by about 2.5 miles. The actual spacecraft orbit at 126 hours was 62.4 by 56.6 miles.

#### 7.4.5 Undocking and Command Module Separation

The lunar module was undocked from the command module at about 100 hours during lunar revolution 13. The command and service modules then performed a three-impulse separation sequence, with an actual firing time of 9 seconds and a velocity change of 2.7 ft/sec. As reported by the crew, the lunar module trajectory perturbations resulting from undocking and station-keeping were uncompensated for in the descent orbit insertion maneuver one-half revolution later. These errors directly affected the lunar module state vector accuracy at the initiation of powered descent.

#### 7.4.6 Lunar Module Descent

The descent orbit insertion maneuver was executed at 101-1/2 hours, and about 57 minutes later, the powered descent sequence began. The detailed trajectory analysis for the lunar module descent phase is presented in section 5.1. The trajectory parameters and maneuver results are presented in tables 7-II and 7-V.

#### 7.4.7 Lunar Module Ascent and Rendezvous

The lunar module ascent stage lifted off the lunar surface at 124:22:00.8 after staying on the surface for 21 hours 36.35 minutes. Lunar orbit insertion and the rendezvous sequence were normal. The terminal phase was completed by 128 hours. The detailed trajectory analysis for ascent and rendezvous is presented in sections 5.6 and 5.7. Tables 7-II and 7-V present the trajectory parameters and maneuver results for these phases.

#### 7.4.8 Transearth Injection

The transearth injection maneuver was initiated on time and achieved a velocity change of only 1.2 ft/sec less than planned. This maneuver exceeded the real-time planned duration by 3.4 seconds because of a slightly lower-than-expected thrust (see section 8.8). The transearth injection would not have achieved acceptable earth entry conditions. The resulting perigee altitude solution was 69.4 miles, as compared with the nominal value of 20.4 miles.

#### 7.4.9 Transearth Midcourse Correction

At the fifth midcourse-correction option point, the first and only transearth midcourse correction of 4.8 ft/sec was made with the reaction control system, which corrected the trajectory to the predicted entry flight-path angle of minus 6.51 degrees.

### 7.5 COMMAND MODULE ENTRY

The best estimated trajectory for the command module during entry was obtained from a digital postflight reconstruction. The onboard telemetry recorder was inoperative during entry, and since the spacecraft experienced communications blackout during the first portion of entry,

complete telemetry information was not recorded. A range instrumentation aircraft received a small amount of data soon after the entry interface was reached and again approximately 4 minutes into the entry. These data, combined with the best estimated trajectory, produced the postflight data presented herein. Table 7-VII presents the actual conditions at entry interface.

The flight-path angle at entry was 0.03-degree shallower than predicted at the last midcourse correction, causing a peak load factor of 6.56g, which was slightly higher than planned.

The spacecraft landed in the Pacific Ocean at 169.15 degrees west and 13.30 degrees north.

## 7.6 SERVICE MODULE ENTRY

The service module entry was recorded on film by aircraft. This film shows the service module entering the earth's atmosphere and disintegrating near the command module. According to preflight predictions, the service module should have skipped out of the earth's atmosphere into a highly elliptical orbit. The Apollo 11 crew observed the service module about 5 minutes after separation and indicated that its reaction control thrusters were firing and the module was rotating. A more complete discussion of this anomaly is contained in section 16.1.11.

## 7.7 LUNAR ORBIT TARGETING

The targeting philosophy for the lunar orbit insertion maneuver differed in two ways from that of Apollo 10. First, the landing site latitude targeting was biased in an attempt to account for the orbit plane regression noted in Apollo 10. During Apollo 10, the lunar module passed approximately 5 miles south of the landing site on the low-altitude pass following descent orbit insertion. The Apollo 11 target bias of minus 0.37 degree in latitude was based on the Langley Research Center 13-degree, 13-order lunar gravity model. Of all gravity models investigated, this one came the closest to predicting the orbit inclination and longitude of ascending node rates observed from Apollo 10 data. During the lunar landing phase in revolution 14, the lunar module latitude was 0.078 degree north of the desired landing site latitude. A large part of this error resulted because the targeted orbit was not achieved at lunar orbit insertion. The difference between the predicted and actual values was approximately 0.05 degree, which represents the prediction error from the 13-degree, 13-order model over 14 revolutions. However,

the amount of lunar module plane change required during descent was reduced from the 0.337 degree that would have been required for a landing during Apollo 10 to 0.078 degree in Apollo 11 by biasing the lunar orbit insertion targeting. A comparison between Apollo 10 and 11 latitude targeting results is presented in table 7-VIII.

The second change from Apollo 10 targeting was that the circularization maneuver was targeted for a noncircular orbit of 53.7 by 65.7 miles. The R2 lunar potential model predicted this orbit would decay to a 60-mile circular orbit at nominal time for rendezvous, thereby conserving ascent stage propellants. Although the R2 model is currently the best for predicting in-plane orbital elements, it cannot predict accurately over long intervals. Figure 7-3 shows that the R2 predictions, using the revolution 3 vector, matched the observed altitudes for approximately 12 revolutions. It should be noted that the command and service module separation maneuver in lunar orbit was taken into account for both the circularization targeting and the R2 prediction. If the spacecraft had been placed into a nearly circular orbit, as in Apollo 10, estimates show that a degenerated orbit of 55.7 by 67.3 miles would have resulted by the time of rendezvous. The velocity penalty at the constant differential height maneuver for the Apollo 10 approach would have been at least 23 ft/sec, as compared to the actual 8 ft/sec resulting from the executed circularization targeting scheme. A comparison between Apollo 11 and Apollo 10 circularization results is presented in table 7-IX.

## 7.8 LUNAR ORBIT NAVIGATION

The preflight plan for lunar orbit navigation, based on Apollo 8 and 10 postflight analyses, was to fit tracking data from two near side lunar passes with the orbit plane constrained to the latest, one-pass solution. For descent targeting, it was planned to use the landing site coordinates determined from landmark sightings during revolution 12, if it appeared that the proper landmark had been tracked. If not, the best preflight estimate of coordinates from Lunar Orbiter data and Apollo 10 sightings was to be used. In addition, these coordinates were to be adjusted to account for a two-revolution propagation of radial errors determined in revolutions 3 through 10. The predicted worst-case estimate of navigation accuracy was approximately 3000 feet in both latitude and longitude.

Several unanticipated problems severely affected navigation accuracy. First, there was a greater inconsistency and larger errors in the one-pass orbit plane estimates than had been observed on any previous mission (fig. 7-4).

These errors were the result of a known deficiency in the R2 lunar potential model. This condition should not occur on future missions because different lunar inclination angles will be flown.

A second problem, closely related to the first, was that the two-revolution propagation errors for crosstrack, or latitude, errors were extremely inconsistent. The average propagation error based on five samples at the end of revolution 10 was 2900 feet; but the uncertainty in this estimate was plus or minus 9000 feet. On the other hand, the propagation errors for radial and downtrack, or longitude, errors were within expected limits. No adjustment was made for either latitude or longitude propagation errors because of the large uncertainty in the case of latitude and the small correction (800 feet) required in the case of longitude.

The coordinates obtained from the landmark tracking during revolution 12 deviated from the best preflight estimate of the center of the landing site ellipse by 0.097 degree north, 0.0147 degree east, and 0.038 mile below. These errors are attributed to the R2 potential model deficiencies. The large difference in latitude resulted from an error in the spacecraft state vector estimate of the orbit plane; these were the data used to generate the sighting angles. The difference in longitude could also have been caused by an error in the estimated state vector or from tracking the wrong landmark.

The third problem area was the large number of trajectory perturbation in revolutions 11 through 13 because of uncoupled attitude maneuvers, such as hot firing tests of the lunar module thrusters, undocking impulse, station-keeping activity, sublimator operation and possibly tunnel and cabin venting. The net effect of these perturbations was a sizeable down-range miss.

A comparison between the lunar landing point coordinates generated from various data sources is presented in table 5-IV. The difference, or miss distance, was 0.0444 degree south and 0.2199 degree east, or approximately 4440 and 21 990 feet, respectively. The miss in latitude was caused by neglecting the two-revolution orbit plane propagation error, and the miss in longitude resulted from the trajectory perturbations during revolutions 11 through 13.

The coordinates used for ascent targeting were the best preflight estimate of landing site radius and the onboard-guidance estimate of latitude and longitude at touchdown (corrected for initial state vector errors from ground tracking). The estimated errors in targeting coordinates were a radius 1500 feet less than desired and a longitude 4400 feet to the west.



TABLE 7-I.- DEFINITION OF TRAJECTORY AND ORBITAL PARAMETERS

<u>Trajectory Parameters</u>	<u>Definition</u>
Geodetic latitude	Spacecraft position measured north or south from the earth's equator to the local vertical vector, deg
Selenographic latitude	Spacecraft position measured north or south from the true lunar equatorial plane to the local vertical vector, deg
Longitude	Spacecraft position measured east or west from the body's prime meridian to the local vertical vector, deg
Altitude	Perpendicular distance from the reference body to the point of orbit intersect, ft or miles; altitude above the lunar surface is referenced to Landing Site 2
Space-fixed velocity	Magnitude of the inertial velocity vector referenced to the body-centered, inertial reference coordinate system, ft/sec
Space-fixed flight-path angle	Flight-path angle measured positive upward from the body-centered, local horizontal plane to the inertial velocity vector, deg
Space-fixed heading angle	Angle of the projection of the inertial velocity vector onto the local body-centered, horizontal plane, measured positive eastward from north, deg
Apogee	Maximum altitude above the oblate earth model, miles
Perigee	Minimum altitude above the oblate earth model, miles
Apocynthion	Maximum altitude above the moon model, referenced to Landing Site 2, miles
Pericynthion	Minimum altitude above the moon model, referenced to Landing Site 2, miles
Period	Time required for spacecraft to complete 360 degrees of orbit rotation, min
Inclination	Acute angle formed at the intersection of the orbit plane and the reference body's equatorial plane, deg
Longitude of the ascending node	Longitude where the orbit plane crosses the reference body's equatorial plane from below, deg

TABLE 7-II.- TRAJECTORY PARAMETERS

Event	Ref. body	Time, hr:min:sec	Latitude, deg	Longitude, deg	Altitude, miles	Space-fixed velocity, ft/sec	Space-fixed flight-path angle, deg	Space-fixed heading angle, deg E of N
Translunar Phase								
S-IVB second ignition	Earth	2:44:16.2	5.03S	172.55E	105.8	25 562	0.02	57.78
S-IVB second cutoff	Earth	2:50:03.2	9.52N	165.61W	173.3	35 567	6.91	59.93
Translunar injection	Earth	2:50:13.2	9.98N	164.84W	180.6	35 546	7.37	60.07
Command module/S-IVB separation	Earth	3:17:04.6	31.16N	88.76W	4 110.9	24 456.8	46.24	95.10
Docking	Earth	3:24:03.1	30.18N	81.71W	5 317.6	22 662.5	44.94	99.57
Spacecraft/S-IVB separation (ejection)	Earth	4:16:59.1	23.18N	67.70W	3 506.5	16 060.8	62.01	110.90
Separation maneuver								
Ignition	Earth	4:40:01.8	21.16N	68.46W	16 620.8	14 680.0	64.30	113.73
Cutoff	Earth	4:40:04.7	21.16N	68.46W	16 627.3	14 663.0	64.25	113.74
First midcourse correction								
Ignition	Earth	26:44:58.7	5.99N	11.16W	109 475.3	5 025.0	77.05	120.86
Cutoff	Earth	26:45:01.8	6.00N	11.17W	109 477.2	5 010.0	76.88	120.87
Lunar Orbit Phase								
Lunar orbit insertion								
Ignition	Moon	75:49:50.4	1.57S	169.58W	86.7	8 250.0	-9.99	-62.80
Cutoff	Moon	75:55:48.0	0.16N	167.13E	60.1	5 479.0	-0.20	-66.89
Lunar orbit circularization								
Ignition	Moon	80:11:36.8	0.02S	170.09E	61.8	5 477.3	-0.49	-66.55
Cutoff	Moon	80:11:53.5	0.02S	169.16E	61.6	5 338.3	0.32	-66.77
Undocking	Moon	100:12:00.0	1.11N	116.21E	62.9	5 333.8	0.16	-89.13
Separation								
Ignition	Moon	100:39:52.9	0.99N	31.86E	62.7	5 332.7	-0.13	-106.89
Cutoff	Moon	100:40:01.9	1.05N	31.41E	62.5	5 332.2	-0.16	-106.90
Descent orbit insertion								
Ignition	Moon	101:36:14.0	1.12S	140.20W	56.4	5 364.9	0.10	-75.70
Cutoff	Moon	101:36:44	1.16S	141.88W	57.8	5 284.9	-0.06	-75.19
Powered descent initiation	Moon	102:33:05.	1.02N	39.39E	6.4	5 564.9	0.03	-104.23
Lunar orbit engine cutoff	Moon	124:29:15.7	0.73N	12.99E	10.0	5 537.9	0.28	-108.15
Coelliptic sequence initiation								
Ignition	Moon	125:19:35.0	0.98S	147.12W	47.4	5 328.1	0.11	-77.98
Cutoff	Moon	125:20:22.0	0.91S	149.57W	48.4	5 376.6	0.09	-76.98
Terminal phase initiation								
Ignition	Moon	127:03:51.8	1.17S	110.28W	44.1	5 391.5	-0.16	-93.16
Cutoff	Moon	127:04:14.5	1.17S	111.46W	44.0	5 413.2	-0.03	-92.65
Terminal phase finalize	Moon	127:46:09.8	0.80N	118.61E	7.6	5 339.7	0.42	-70.45
Docking	Moon	128:03:00.0	1.18N	67.31E	60.6	5 341.5	0.16	-87.63
Ascend stage jettison	Moon	130:09:31.2	1.10N	41.85E	61.6	5 335.9	0.15	-97.81
Final separation								
Ignition	Moon	130:30:01.0	0.06N	20.19W	62.7	5 330.1	-0.05	-52.86
Cutoff	Moon	130:30:08.1	0.19N	20.58W	62.7	5 326.9	-0.02	-52.73
Transearth injection								
Ignition	Moon	135:23:42.3	0.16S	164.02E	52.4	5 376.0	-0.03	-62.77
Cutoff	Moon	135:26:13.7	0.50N	154.02E	58.1	8 589.0	5.13	-62.60
Transearth Coast Phase								
Second midcourse correction								
Ignition	Earth	150:29:57.4	13.16S	37.79W	169 087.2	4 075.0	-80.34	129.30
Cutoff	Earth	150:30:07.4	13.16S	37.83W	169 080.6	4 074.0	-80.41	129.30
Command module/service module separation	Earth	194:49:12.7	35.09S	122.54E	1 778.3	29 615.5	-35.26	69.27

TABLE 7-III.- TRANSLUNAR MANEUVER SUMMARY

Maneuver	System	Ignition time, hr:min:sec	Firing time, sec	Velocity change, ft/sec	Resultant pericyynthion conditions				
					Altitude, miles	Velocity, ft/sec	Latitude, deg	Longitude, deg	Arrival time, hr:min:sec
Translunar injection	S-IVB	2:44:16.2	347.3	10 441.0	896.3	6640	0.11S	174.13W	75:05:21
Command and service module/S-IVB separation	Reaction control	3:17:04.6	7.1	0.7	827.2	6728	0.09S	174.89W	75:07:47
Spacecraft/S-IVB separation	Service propulsion	4:40:01.8	2.9	19.7	180.8	7972	0.18N	175.97E	75:39:30
First midcourse correction	Service propulsion	26:44:58.7	3.1	20.9	61.5	8334	0.17N	173.57E	75:53:35

TABLE 7-IV.- FREE RETURN CONDITIONS FOR TRANSLUNAR MANEUVERS

Vector description	Vector time, hr:min:sec	Entry interface conditions				
		Velocity, ft/sec	Flight-path angle, deg	Latitude, deg	Longitude, deg	Arrival time, hr:min:sec
After translunar injection	2:50:03.0	36 076	-64.06	1.93N	66.40E	162:12:04
After command and service module/S-IVB separation	4:40:01.0	36 079	-67.43	0.19S	98.05E	160:32:27
After separation maneuver	11:28:00.0	36 139	-48.95	37.38S	59.95E	146:39:27
After first midcourse correction	26:45:01.5	36 147	-10.25	18.46S	168.10E	145:05:28
Before lunar orbit insertion	70:48:00	36 147	-9.84	17.89S	169.01E	145:04:32

TABLE 7-V.- LUNAR ORBIT MANEUVER SUMMARY

Maneuver	System	Ignition time, hr:min:sec	Firing time, sec	Velocity change, ft/sec	Resultant orbit	
					Apocynthion, miles	Pericynthion, miles
Lunar orbit insertion	Service propulsion	75:49:50.4	357.5	2917.5	169.7	60.0
Lunar orbit circularization	Service propulsion	80:11:36.8	16.8	158.8	66.1	54.5
Command module/lunar module separation	Service module reaction control	100:39:52.9	5.2	1.4	63.7	56.0
Descent orbit insertion	Descent propulsion	101:36:14.0	30.0	76.4	64.3	55.6
Powered descent initiation	Descent propulsion	102:33:05	756.3	6930	58.5	7.8
Lunar orbit insertion	Ascent propulsion	124:22:00.8	434.9	6070.1	48.0	9.4
Coelliptic sequence initiation	Lunar module reaction control	125:19:35.5	47.0	51.5	49.3	45.7
Constant differential height	Lunar module reaction control	126:17:49.6	17.8	19.9	47.4	42.1
Terminal phase initiation	Lunar module reaction control	127:03:51.8	22.7	25.3	61.7	43.7
Terminal phase finalize	Lunar module reaction control	127:46:09.8	28.4	31.4	63.0	56.5
Final separation	Lunar module reaction control	130:30:01.0	7.2	2.2	62.7	54.0

TABLE 7-VI.- TRANSEARTH MANEUVER SUMMARY

Event	System	Ignition time, hr:min:sec	Firing time, sec	Velocity change, ft/sec	Resultant entry interface conditions				
					Flight-path angle, deg	Velocity, ft/sec	Latitude, deg	Longitude, deg	Arrival time, hr:min:sec
Transearth injection	Service propulsion	135:23:42.3	151.4	3279.0	-0.70	36 195	4.29N	180.15E	195:05:57
Second midcourse correction	Service module reaction control	150:29:57.4	11.2	4.8	-6.46	36 194	3.17S	171.99E	195:03:08

TABLE 7-VII.- ENTRY TRAJECTORY PARAMETERS

Entry interface (400 000 feet altitude)

Time, hr:min:sec . . . . .	195:03:05.7
Geodetic latitude, deg south . . . . .	3.19
Longitude, deg east . . . . .	171.96
Altitude, miles . . . . .	65.8
Space-fixed velocity, ft/sec . . . . .	36 194.4
Space-fixed flight-path angle, deg . . . . .	-6.48
Space-fixed heading angle, deg east of north . . . . .	50.18

Maximum conditions

Velocity, ft/sec . . . . .	36 277.4
Acceleration, g . . . . .	6.51

Drogue deployment

Time, hr:min:sec . . . . .	195:12:06.9
Geodetic latitude, deg south	
Recovery ship report . . . . .	13.25
Onboard guidance . . . . .	13.30
Target . . . . .	13.32
Longitude, deg west	
Recovery ship report . . . . .	169.15
Onboard guidance . . . . .	169.15
Target . . . . .	169.15

TABLE 7-VIII.- LATITUDE TARGETING SUMMARY

	Landing site latitude on the landing revolutions, deg	
	Apollo 10	Apollo 11
Desired	0.691	0.691
Actual	0.354	0.769
Error	0.337 south	0.078 north

TABLE 7-IX.- CIRCULARIZATION ALTITUDE TARGETING

		Orbit altitude, miles	
		Apollo 10	Apollo 11
At circularization	Desired	60.0 by 60.0	53.7 by 65.7
	Actual	61.0 by 62.8	54.5 by 66.1
	Error	1.0 by 2.8	0.8 by 0.4
At rendezvous	Desired	60.0 by 60.0	60.0 by 60.0
	Actual	58.3 by 65.9	56.5 by 62.6
	Error	-1.9 by 5.9	-3.5 by 2.6

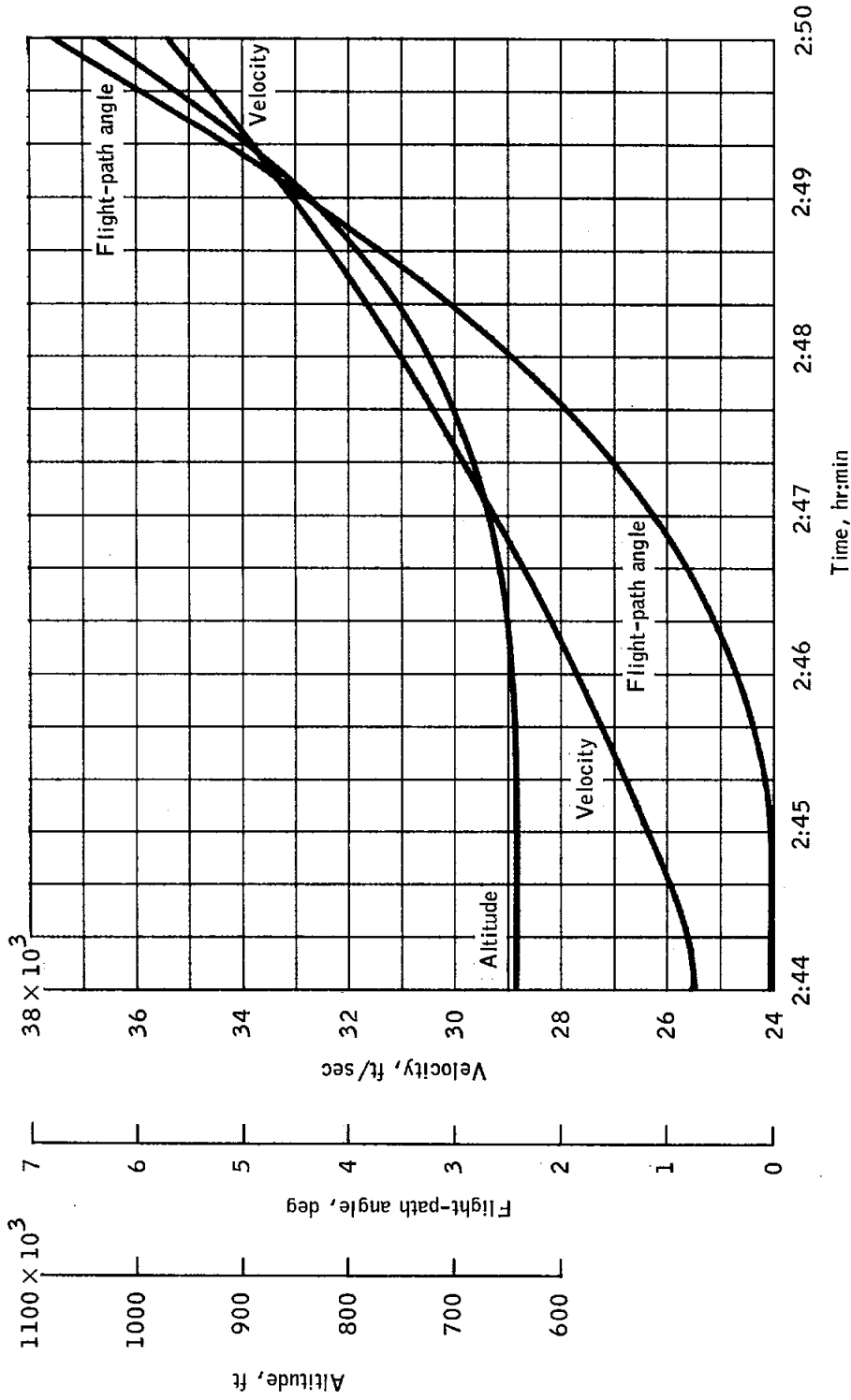


Figure 7-1.- Trajectory parameters during translunar injection firing.

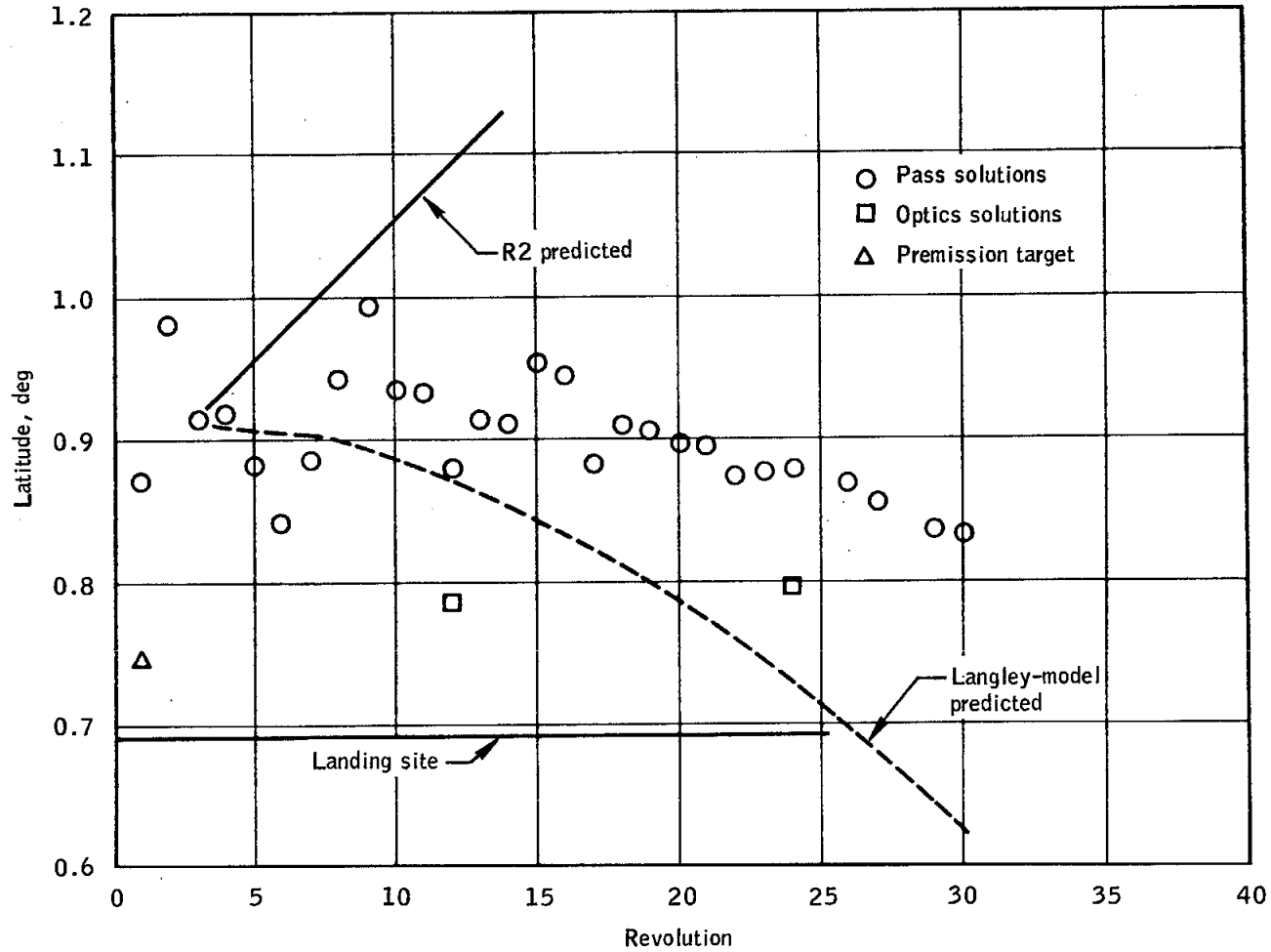


Figure 7-4.- Selenographic latitude estimates based on a one pass solution using R2 model.



## 8.0 COMMAND AND SERVICE MODULE PERFORMANCE

Performance of command and service module systems is discussed in this section. The sequential, pyrotechnic, thermal protection, earth landing, power distribution, and emergency detection systems operated as intended and are not discussed further. Discrepancies and anomalies are generally mentioned in this section but are discussed in greater detail in section 16, Anomaly Summary.

### 8.1 STRUCTURAL AND MECHANICAL SYSTEMS

At earth lift-off, measured winds both at the 60-foot level and in the region of maximum dynamic pressure indicate that structural loads were well below the established limits. During the first stage of flight, accelerations measured in the command module were nominal and similar to those measured during Apollo 10. The predicted and calculated spacecraft loads at lift-off, in the region of maximum dynamic pressure, at the end of first stage boost, and during staging are shown in table 8.1-I.

Command module accelerometer data indicate that sustained low-frequency longitudinal oscillations were limited to 0.15g during S-IC boost. Structural loads during S-II and S-IVB boost, translunar injection, both docking operations, all service propulsion maneuvers, and entry were well within design limits.

As with all other mechanical systems, the docking system performed as required for both the translunar and lunar orbit docking events. The following information concerning the two docking operations at contact is based on crew comments:

Contact conditions	Translunar docking	Lunar orbit docking
Axial velocity, ft/sec	0.1 to 0.2	0.1
Lateral velocity, ft/sec	0	0
Angular velocity, deg/sec	0	0
Angular alignment, deg	0	0
Miss distance, in.	4	0

The probe retract time for both events was between 6 and 8 seconds. During the gas retract phase of lunar orbit docking, the crew detected a relative yaw misalignment that was estimated to have been as much as 15 degrees. See sections 4.15 and 5.7 for further discussion. The unexpected vehicle motions were not precipitated by the docking hardware and did not prevent accomplishment of a successful hard dock. Computer simulations of the lunar orbit docking event indicate that the observed vehicle misalignments can be caused by lunar module plus X thrusting after the command module is placed in an attitude-free control mode (see section 8.6).

TABLE 8.1-I.- MAXIMUM SPACECRAFT LOADS DURING LAUNCH PHASE

Interface	Load	Lift-off		Maximum q <sub>a</sub>		End of first-stage boost		Staging	
		Calculated <sup>a</sup>	Predicted <sup>b</sup>	Calculated <sup>a</sup>	Predicted <sup>c</sup>	Calculated <sup>a</sup>	Predicted <sup>d</sup>	Calculated <sup>a</sup>	Predicted <sup>e</sup>
Launch escape system/command module	Bending moment, in-lb . . .	520 000	1 000 000	136 000	310 000	110 000	173 000	230 000	110 000
	Axial force, lb . . . . .	-12 100	-11 000	-22 200	-24 000	-34 600	-36 000	5 000	8 000
Command module/service module	Bending moment, in-lb . . .	680 000	1 320 000	166 000	470 000	340 000	590 000	300 000	140 000
	Axial force, lb . . . . .	-28 600	-36 000	-88 200	-88 000	-81 600	-89 600	11 000	19 000
Service module/adaptor	Bending moment, in-lb . . .			696 000	1 620 000	2 000 000	2 790 000	1 220 000	1 540 000
	Axial force, lb . . . . .			-193 300	-200 000	-271 000	-296 000	34 000	60 000
Adapter/instrument unit	Bending moment, in-lb . . .			2 263 000	4 620 000	2 600 000	5 060 000	1 400 000	1 440 000
	Axial force, lb . . . . .			-297 800	-300 000	-415 000	-441 000	51 000	90 000

NOTE: Negative axial force indicates compression.

The flight conditions at maximum q<sub>a</sub> were:

Condition	Measured	Predicted <sup>c</sup>
Flight time, sec . . . . .	89.0	87.2
Mach no. . . . .	2.1	1.9
Dynamic pressure, psf . . .	695	727
Angle of attack, deg . . . .	1.43	1.66
Maximum q <sub>a</sub> , psf-deg . . . .	994	1210

The accelerations at the end of first-stage boost were:

Acceleration	Measured	Predicted <sup>d</sup>
Longitudinal, g . . . . .	3.88	4.0
Lateral, g . . . . .	0.06	0.05

<sup>a</sup>Calculated from flight data.

<sup>b</sup>Predicted Apollo 11 loads based on wind induced launch vehicle bending moment measured prior to launch.

<sup>c</sup>Predicted Apollo 11 loads based on measured winds aloft.

<sup>d</sup>Predicted Apollo 11 loads for block II spacecraft design verification conditions.

<sup>e</sup>Predicted Apollo 11 loads based on AS-506 static test thrust decay data.

## 8.2 ELECTRICAL POWER

### 8.2.1 Batteries

The bus voltages of the entry and pyrotechnic batteries were maintained at normal levels, and battery charging was nominal. All three entry batteries contained the cellophane separators, whereas only battery B used this type of separator for Apollo 10. The improved performance of the cellophane separators is evident from voltage/current data, which show, at a 15-ampere load, that the cellophane type batteries maintain an output 1 to 2 volts higher than the Permion-type batteries.

The only departure from expected performance was when battery A was placed on main bus A for the translunar midcourse correction. During this maneuver, normal current supplied by each battery is between 4 and 8 amperes, but current from battery A was initially 25 amperes and gradually declined to approximately 10 amperes just prior to removal from the main bus. This occurrence can be explained by consideration of two conditions: (1) fuel cell 1 on main bus A had a lower (400° F) than average skin temperature, causing it to deliver less current than usual; and (2) battery A had been fully charged just prior to the maneuver. Both these conditions, combined to result in the higher than usual current delivery by battery A. Performance was normal thereafter.

The total battery capacity was continuously maintained above 103 A-h until separation of the command module from the service module.

### 8.2.2 Fuel Cells

The fuel cells and radiators performed satisfactorily during the prelaunch and flight phases. All three fuel cells were activated 68 hours prior to launch, and after a 3-1/2-hour conditioning load, they were placed on open-circuit inline heater operation until 3 hours prior to launch. After that time, the fuel cells provided full spacecraft power.

During the 195 hours of the mission, the fuel cells supplied approximately 393 kW-h of energy at an average spacecraft current of 68.7 amperes (22.9 amperes per fuel cell) and an average command module bus voltage of 29.4 volts. The maximum deviation from equal load sharing between individual fuel cells was an acceptable 4.5 amperes.

All thermal parameters, including condenser exit temperature, remained within normal operating ranges and agreed favorably with predicted flight values. The condenser exit temperature on fuel cell 2 fluctuated periodically every 3 to 8 minutes throughout the flight. This disturbance was similar to that noted on all other flights and is discussed in more detail in reference 3. The periodic disturbance has been shown to have no effect on fuel cell performance.

### 8.3 CRYOGENIC STORAGE

The cryogenic storage system satisfactorily supplied reactants to the fuel cells and metabolic oxygen to the environmental control system. At launch, the total oxygen quantity was 615 pounds (79 pounds above the minimum red-line limit), and the hydrogen quantity was 54.1 pounds (1.0 pound above the minimum red-line limit). The overall consumption from the system was nominal during the flight.

During the flight, it was discovered that one heater in oxygen tank 2 was inoperative. Records show that it had failed between the times of the countdown demonstration test and the actual countdown, and current measurements indicate that the element had an open circuit. This anomaly is discussed in detail in section 16.1.2.

### 8.4 VHF RANGING

The operation of the VHF ranging system was nominal during descent and from lunar lift-off until orbital insertion. Following insertion, a number of tracking dropouts were experienced. These dropouts resulted from negative circuit margins caused by use of the lunar module aft VHF antenna instead of the forward antenna. After the antennas were switched, VHF ranging operation returned to normal. A maximum range of 246 miles was measured, and a comparison of the VHF ranging data with rendezvous radar data and the predicted trajectory showed very close agreement.

### 8.5 INSTRUMENTATION

The instrumentation system, including the data storage equipment, the central timing equipment, and the signal conditioning equipment, supported the mission.

The data storage equipment did not operate during entry because the circuit breaker was open. The circuit breaker which supplies ac power to the recorder also controls operation of the S-band FM transmitter. When the television camera and associated monitor were to be powered without transmitting to a ground station, the circuit breaker was opened to disable the S-band FM transmitter. This breaker was inadvertently left open after the last television transmission.

At approximately 5 hours 20 minutes during a scheduled cabin oxygen enrichment (see section 16.1.8), the oxygen flow-rate transducer indicated a low oxygen flow rate. Comparison of the oxygen manifold pressure, oxygen-flow-restrictor differential pressures, and cryogenic oxygen values indicated that the flow-rate-transducer output calibration had shifted downward. To compensate for the uncertainties associated with the oxygen flow indications, cabin enrichment procedures were extended from 8 hours to 9 hours.

## 8.6 GUIDANCE, NAVIGATION, AND CONTROL

The command module guidance, navigation, and control system performance was satisfactory throughout the mission. Earth-launch, earth-orbit, and translunar-injection monitoring functions were normal except that the crew reported a 1.5-degree pitch deviation from the expected flight director attitude indicator reading during the translunar injection maneuver. The procedure was designed for the crew to align the flight director attitude indicator/orbit-rate drive electronics assembly (ORDEAL) at approximately 4 deg/min while the launch vehicle was maintaining local vertical. One error of 0.5 degree is attributed to the movement of the S-IVB while the flight director attitude indicator and the orbit-rate drive electronics are being aligned. An additional 0.2-degree resulted from an error in orbit-rate drive electronics initialization. Further, the reading accuracy of the flight director attitude indicator is 0.25 degree. An additional source of error for Apollo 11 was a late trajectory modification which changed the ignition attitude by 0.4 degree. The accumulation of errors from these four sources accounts for the error reported by the crew. The present procedure is considered adequate; therefore, no change is being prepared for later missions.

### 8.6.1 Transposition and Docking

Two unexpected indications reported by the crew later proved to be normal operation of the respective systems. The 180-degree pitch transposition maneuver was to be performed automatically under digital autopilot control with a manually initiated angular rate. The crew reported that each time the digital autopilot was activated, it stopped the manually induced rate and maintained a constant attitude. The cause of the apparent discrepancy was procedural; although the digital autopilot was correctly initialized for the maneuver, in each case the rotational hand controller was moved out of detent prior to enabling the digital autopilot. Normally, when the out-of-detent signal is received by the computer, the digital autopilot is switched from an automatic to an attitude-hold function until reenabled. After four attempts, the maneuver was initiated properly and proceeded according to plan.

The other discrepancy concerned the entry monitor system velocity counter. The crew reported biasing the counter to minus 100 ft/sec prior to separation, thrusting forward until the counter indicated 100.6, then thrusting aft until the counter indicated 100.5. After the transposition maneuver, the counter indicated 99.1, rather than the expected 100.5. The cause of this apparent discrepancy was also procedural. The transposition maneuver was made at an average angular velocity of 1.75 deg/sec. The entry monitor system is mounted approximately 12 feet from the center of rotation. The resulting centripetal acceleration integrated over the time necessary to move 180 degrees yields a 1.2-ft/sec velocity change and accounts for the error observed. The docking maneuver following transposition was normal, with only small transients.

#### 8.6.2 Inertial Reference System Alignments

The inertial measurement unit was aligned as shown in table 8.6-I. Results were normal and comparable to those of previous missions.

#### 8.6.3 Translation Maneuvers

A summary of pertinent parameters for each of the service propulsion maneuvers is contained in table 8.6-II. All maneuvers were as expected, with very small residuals. Monitoring of these maneuvers by the entry monitor system was excellent, as shown in table 8.6-III. The velocity initializing the entry monitor velocity counter prior to each firing is biased by the velocity expected to be accrued during thrust tail-off. When in control of a maneuver, the entry monitor issues an engine-off discrete signal when the velocity counter reaches zero to avoid an overburn, and the bias includes an allowance for the predicted tail-off.

The crew was concerned with the duration of the transearth injection maneuver. When the firing appeared to be approximately 3 seconds longer than anticipated, the crew issued a manual engine-off command. Further discussion of this problem is contained in section 8.8. The data indicate that a computer engine-off discrete appeared simultaneously with actual engine shutdown. Therefore, the manual input, which is not instrumented, was either later than, or simultaneous with, the automatic command.

#### 8.6.4 Attitude Control

All attitude control functions were satisfactorily performed throughout the mission. The passive thermal control roll maneuver was used during translunar and transearth coast.

After entry into lunar orbit, and while still in the docked configuration, the crew reported a tendency of the spacecraft to position itself along the local vertical with the lunar module positioned down. This effect was apparently a gravity gradient torque, which can be as large as 0.86 ft-lb when the longitudinal axis of the vehicle is oriented 45 degrees from the local vertical. A thruster duty cycle of once every 15 to 18 seconds would be consistent with a disturbance torque of this magnitude.

#### 8.6.5 Midcourse Navigation

Midcourse navigation using star/horizon sightings was performed during the translunar and transearth coast phases. The first two groups of sightings, at 43 600 and 126 800 miles, were used to calibrate the height of the horizon for updating the computer. Although several procedural problems were encountered during early attempts, the apparent horizon altitude was determined to be 35 kilometers. Table 8.6-IV contains a synopsis of the navigation sightings performed.

#### 8.6.6 Landmark Tracking

Landmark tracking was performed in lunar orbit as indicated in table 8.6-V. The objective of the sightings was to eliminate part of the relative uncertainty between the landing site and the command module orbit and thus improve the accuracy of descent targeting. The sightings also provided an independent check on the overall targeting scheme. The pitch technique provided spacecraft control while the sextant was in use. The landmark tracking program was also used to point the optics in several unsuccessful attempts to locate and track the lunar module on the lunar surface (see section 5.5).

#### 8.6.7 Entry

The entry was performed under automatic control as planned. No telemetry data are available for the period during blackout; however, all indications are that the system performed as intended.

The onboard calculations for inertial velocity and flight-path angle at the entry interface were 36 195 ft/sec and minus 6.488 degrees, respectively, and compare favorably with the 36 194 ft/sec and minus 6.483 degrees determined from tracking. Figure 13-1 shows a summary of landing point data. The onboard computer indicated a landing at 169 degrees 9 minutes west longitude and 13 degrees 18 minutes north latitude, or 1.69 miles from the desired target point. Since no telemetry nor radar



was available during entry, a final evaluation of navigation accuracy cannot be obtained. However, a simulated best estimate trajectory shows a landing point 1.03 miles from the target and confirms the onboard solution. Indications are that the entry monitor system performed as intended.

#### 8.6.8 Inertial Measurement Unit Performance

Preflight performance of the inertial components is summarized in table 8.6-VI. This table also shows the average value of the accelerometer bias measurements and gyro null bias drift measurements made in flight and the accompanying updates.

The gyro drift compensation updates were not as successful as expected, probably because of the change in sign of the compensation values. With the change in the torquing current, a bias difference apparently occurred as a result of residual magnetization in the torquer winding. The difference was small, however, and had no effect on the mission.

Figure 8.6-1 contains a comparison of velocity measured by the inertial measurement unit with that from the launch-vehicle guidance system during earth ascent. These velocity differences reflect the errors in the inertial component compensation values. One set of error terms that would cause these velocity errors is shown in table 8.6-VII. The divergence between the two systems is well within the expected limits and indicates excellent performance, although a momentary saturation of the launch vehicle guidance system Y-axis accelerometer caused an initial 5 ft/sec error between the two systems. The remainder of the divergence in this axis was primarily caused by a misalignment during gyrocompassing of the spacecraft guidance system. The 60-ft/sec out-of-plane velocity error at insertion is equivalent to a misalignment of 0.11 degree; this is corroborated by the Z-axis gyro torquing angle calculated during the initial optical alignment in earth orbit.

#### 8.6.9 Computer

The computer performed as intended throughout the mission. A number of alarms occurred, but all were caused by procedural errors or were intended to caution the respective crewman.

#### 8.6.10 Optics

The sextant and the scanning telescope performed normally throughout the mission. After the coelliptic sequence maneuver, the Command Module Pilot reported that, after selecting the rendezvous tracking program (P20),

the optics had to be "zeroed" before automatic tracking of the lunar module would begin. Data indicate that the optics mode switch was in the "computer" position when the command module was set up for the contingency mirror image coelliptic sequence maneuver. In this maneuver program, the service propulsion engine gimbals are trimmed by the computer through the digital-to-analog converter outputs of the optics coupling data units. These same converters are used to drive the optics shaft and trunnion when the optics are in "computer" mode. To avoid driving the optics with a gimbal drive signal, or vice versa, the computer issues discrettes which enable or disable the appropriate output. With the optics drive disengaged, the trunnion in this unit was observed during preflight testing to drift toward the positive stop. The drift is caused by an anti-backlash spring.

A register in the computer tracks trunnion position but is not large enough to provide an unambiguous value for the full range of allowable trunnion angles. Therefore, the register is biased to provide unambiguous readouts for the normally used range of minus 10 degrees to plus 64.7 degrees. In this case, the trunnion drifted beyond 64.7 degrees, the register overflowed, and the computer lost track of actual trunnion position. When the automatic optics positioning routine was entered after selection of the rendezvous tracking program (P20), the computer drive commands, based on the invalid counter contents, drove the trunnion to the positive stop. Zeroing the system reestablished synchronization and proper operation.

#### 8.6.11 Entry Monitor System

Operation of the entry monitor system was normal, although one segment on the electroluminescent numerical display for the velocity counter failed to operate during the mission (see section 16.1.4).

TABLE 8.6-I.- PLATFORM ALIGNMENT SUMMARY

Time, hr:min	Program option*	Star used	Gyro torquing angle, deg			Star angle difference, deg	Gyro drift, mERU			Comments
			X	Y	Z		X	Y	Z	
0:48	3	30 Menkent, 37 Nunki	+0.018	+0.033	+0.152	0.01	--	--	--	Check star 34 Atria
5:35	3	17 Regor, 34 Atria	-0.172	-0.050	-0.060	0.02	+2.4	+0.7	-0.8	Not torqued
5:39	3	17 Regor, 34 Atria	-0.171	-0.052	-0.055	0.02	+2.4	+0.7	-0.8	
9:36	1	30 Menkent, 32 Alphecca	+1.005	-0.368	-0.737	0.01	--	--	--	Check star 33 Antares
24:14	3	36 Vega, 37 Nunki	-0.493	-0.191	-0.024	0.00	+2.3	+0.9	-0.1	
53:00	3	10 Mirfak, 16 Procyon	+0.103	+0.366	-0.004	0.01	-1.1	-1.4	0.0	
57:26	3	31 Arcturus, 35 Rasalhague	+0.111	+0.128	+0.014	0.01	-1.7	-1.9	-0.2	
73:08	3	40 Altair, 45 Fomalhaut	+0.285	+0.281	-0.006	0.01	-1.2	-1.2	0.0	
73:33	1	6 Acamar, 42 Peacock	-0.423	+0.508	+0.111	0.01	--	--	--	
79:10	3	33 Antares, 41 Dabih	+0.100	+0.159	+0.044	0.02	-1.2	-1.9	+0.5	Check star 33 Antares
81:05	3	37 Nunki, 44 Enif	+0.046	+0.051	-0.028	0.02	-1.6	-1.8	-1.0	
96:55	1	4 Achernar, 34 Atria	+0.170	+0.342	-0.023	0.00	-0.7	-1.5	-0.1	
101:15	3	1 Alpheratz, 6 Acamar	+0.084	+0.124	-0.010	0.01	-1.3	-1.9	-0.2	
103:00	3	10 Mirfak, 12 Rigel	+0.032	+0.009	+0.001	0.02	-1.2	-0.3	0.0	Check star 7 Menkar
107:30	3	43 Deneb, 44 Enif	+0.057	+0.166	-0.022	0.01	-0.8	-2.4	-0.3	
112:52	1	33 Antares, 41 Dabih	+0.057	+0.213	-0.081	0.00	--	--	--	
121:15	3	25 Acrux, 42 Peacock	+0.165	+0.186	-0.039	0.00	-1.3	-1.5	-0.3	
124:41	3		+0.064	+0.100	+0.021		-1.2	-1.9	+0.4	
134:34	3	1 Alpheratz, 11 Aldebaran	+0.166	+0.212	-0.019	0.01	-1.1	-1.4	-0.1	Check star 1 Alpheratz
136:51	1	1 Alpheratz, 43 Deneb	+0.469	-0.217	+0.383	0.02	--	--	--	
149:19	3	14 Canopus, 16 Procyon	+0.265	+0.268	+0.012	0.01	-1.5	-1.5	+0.1	Check star 11 Aldebaran
171:16	3		+0.445	+0.451	+0.006	0.01	-1.4	-1.4	0.0	Check star 12 Rigel
192:12	1	2 Diphda, 4 Achernar	-1.166	-0.690	+0.456	0.00	--	--	--	Check stars 10 Mirfak, 1 Alpheratz, 45 Fomalhaut, 3 Navl
193:35	3	1 Alpheratz, 45 Fomalhaut	+0.016	-0.040	-0.010	0.01	-0.8	+1.9	-0.5	

\*1 - Preferred; 2 - Nominal; 3 - REFSMMAT.

TABLE 8.6-II.- MANEUVER SUMMARY

Parameter	Service propulsion maneuver				
	Separation	First midcourse correction	Lunar orbit insertion	Lunar orbit circularization	Transearth injection
Time					
Ignition, hr:min:sec	4:40:01.72	26:44:58.64	75:49:50.37	80:11:36.75	135:23:42.28
Cutoff, hr:min:sec	4:40:04.65	26:45:01.77	75:55:47.90	80:11:53.63	135:26:13.69
Duration, sec	2.93	3.13	357.53	16.88	151.41
Velocity, ft/sec (actual/desired)					
X	-9.76/-9.74	-14.19/-14.68	+327.12/+327.09	+92.53/+92.51	+932.77/+932.74
Y	+14.94/+14.86	+13.17/+13.14	+2361.28/+2361.29	+118.18/+118.52	-2556.06/-2555.81
Z	+8.56/+8.74	+7.56/+7.66	+1681.85/+1681.79	+51.61/+51.93	-1835.66/-1834.60
Velocity residual after trim- ming, ft/sec					
X	0.0	+0.3	-0.1	+0.3	0.0
Y	0.0	0.0	0.0	0.0	+0.7
Z	-0.1	+0.5	+0.1	-0.1	+0.1
Entry monitor system	-0.3	-0.5	+0.5	-0.7	-2.7
Engine gimbal position, deg					
Initial					
Pitch	+0.93	+0.97	+0.97	+1.65	-0.55
Yaw	-0.15	-0.15	-0.15	-0.69	+0.69
Maximum excursion					
Pitch	+0.40	+0.30	+0.30	+0.31	-1.73
Yaw	-0.46	-0.42	-0.38	-0.33	+1.55
Steady-state					
Pitch	+1.15	+1.15	+1.23	+1.90	-0.12
Yaw	-0.06	-0.02	-0.06	-0.32	+0.48
Cutoff					
Pitch	+1.28	+1.19	+2.03	+1.81	-0.33
Yaw	-0.19	-0.19	-0.57	-0.44	-0.94
Maximum rate excursion, deg/sec					
Pitch	-0.08	+0.12	+0.07	-0.04	+1.00*
Yaw	+0.21	+0.16	+0.14	-0.20	-1.00*
Roll	-0.14	-0.21	-0.18	-0.13	-1.00*
Maximum attitude error, deg					
Pitch	Negligible	Negligible	0.2	-0.3	-0.4
Yaw	Negligible	-0.1	0.2	+0.2	+0.5
Roll	Negligible	-0.3	-5.0	+2.6	±5.0

\*Saturated.

NOTE: Velocities are in earth- or moon-centered inertial coordinates; velocity residuals in body coordinates.

TABLE 8.6-III.- ENTRY MONITOR SYSTEM VELOCITY SUMMARY

Maneuver	Total velocity to be gained along X-axis, minus residual, ft/sec	Velocity set into entry monitor system counter, ft/sec	Planned residual, ft/sec	Actual residual, ft/sec	Corrected entry monitor error, ft/sec
Separation	19.8	15.2	-4.6	-4.0	+0.6
First midcourse correction	20.9	16.8	-4.1	-3.8	+0.3
Lunar orbit insertion	2917.4	2910.8	-6.6	-6.8	-0.2
Lunar orbit circularization	159.3	153.1	-6.2	-5.2	+1.0
Transearth injection	3283.2	3262.5	-20.7	-17.9	+2.8
Second midcourse correction	4.7	4.8	+0.1	+0.2	+0.1

NOTE: A correction factor of 0.2 ft/sec was applied to determine the corrected error.

TABLE 8.6-IV.- MIDCOURSE NAVIGATION

Group	Set/Marks	Star	Horizon	Time, hr:min	Distance from earth, miles	Remarks
1	1/4	2 Diphda	Earth near	6:36	43 600	Optics calibration determined as -0.003 deg; was not entered. Encountered difficulty in locating star because of procedural problems. *First sighting on star 40 was re- jected; had the wrong horizon.  Sightings were misaligned in the measurement plane, up to 50 deg; resulted from improper instructions from the ground.
	2/3*	40 Altair	Earth far			
	3/6	45 Fomalhaut	Earth near			
	4/3	2 Diphda	Earth near	8:08		
2	1/3	1 Alpheratz	Earth near	24:20	126 800	Optics calibration was zero. Not entered. Computed automatic maneu- ver onboard which did not consider the lunar module; therefore, diffi- culty in locating first star was encountered as optics pointed at lunar module. Ground-computed ma- neuver was used and sightings pro- ceeded satisfactorily.
	2/3	2 Diphda	Earth near			
	3/4	45 Fomalhaut	Earth far	25:20		

TABLE 8.6-V.- LANDMARK TRACKING

Time, hr:min:sec	Landmark identification	Number of marks	Optics mode
82:43:00	A1 (altitude landmark)	5	Sextant, manual - resolved
98:49:00	130	5	Sextant, manual - resolved
104:39:00	130	5	Sextant, manual - resolved
122:24:00	130	5	Sextant, manual - resolved

TABLE 8.6-VI.- INERTIAL COMPONENT PREFLIGHT HISTORY - COMMAND MODULE

Error	Sample mean	Standard deviation	No. of samples	Countdown value	Flight load	Flight average before update	Flight average after update
Accelerometers							
X - Scale factor error, ppm . . . . .	35	46	8	50	40	--	--
Bias, cm/sec <sup>2</sup> . . . . .	-0.23	0.07	9	-0.25	-0.26	-0.26	-0.26
Y - Scale factor error, ppm . . . . .	-22	56	8	-98	-80	--	--
Bias, cm/sec <sup>2</sup> . . . . .	-0.05	0.11	8	0.04	-0.13 <sup>a</sup>	+0.08	+0.08
Z - Scale factor error, ppm . . . . .	-43	50	8	-101	-30	--	--
Bias, cm/sec <sup>2</sup> . . . . .	0.20	0.14	8	0.15	0.14 <sup>b</sup>	0.00	+0.01
Gyroscopes							
X - Null bias drift, mERU . . . . .	-1.2	1.7	9	0.4	-1.8 <sup>c</sup>	+2.4	-1.2
Acceleration drift, spin reference axis, mERU/g . . . . .	-5.4	3.8	9	-3.3	-6.0		
Acceleration drift, input axis, mERU/g . . . . .	13.7	3.9	9	14.4	15.0		
Y - Null bias drift, mERU . . . . .	-1.5	1.1	9	-2.4	-0.6 <sup>d</sup>	+0.7	-1.4
Acceleration drift, spin reference axis, mERU/g . . . . .	1.7	2.0	8	1.3	3.0		
Acceleration drift, input axis, mERU/g . . . . .	7.1	5.6	14	9.0	5.0		
Z - Null bias drift, mERU . . . . .	-0.9	1.6	9	-2.3	-0.2 <sup>e</sup>	-0.6	-0.1
Acceleration drift, spin reference axis, mERU/g . . . . .	8.4	6.6	8	20.4	5.0		
Acceleration drift, input axis, mERU/g . . . . .	0.8	6.4	9	-4.7	1.0		

<sup>a</sup>Updated to +0.08 at 31 hours.<sup>b</sup>Updated to +0.02 at 31 hours.<sup>c</sup>Updated to +0.44 at 31 hours.<sup>d</sup>Updated to +0.26 at 31 hours.<sup>e</sup>Updated to -0.31 at 31 hours.



TABLE 8.6-VII.- INERTIAL SUBSYSTEM ERRORS DURING LAUNCH

Error term	Uncompensated error	One-sigma specification
Offset velocity, ft/sec . . . . .	4.2	--
Bias, cm/sec <sup>2</sup> - X . . . . .	-0.046*	0.2
- Y . . . . .	0.150*	
- Z . . . . .	0.001*	
Null bias drift, mERU - X . . . . .	2.4*	2.0
- Y . . . . .	0.7*	
- Z . . . . .	-0.8*	
Acceleration drift, input axis, mERU/g - X . . . . .	-6.8	8.0
- Y . . . . .	2.0	8.0
- Z . . . . .	-0.7	8.0
Acceleration drift, spin reference axis, mERU/g - Y . . . . .	-8.0	5.0
Acceleration drift, output axis, mERU/g - X . . . . .	-2.3	2 to 5
- Y . . . . .	-0.8	2 to 5
- Z . . . . .	-3.0	
Uncorrelated platform misalignment about X axis, arc sec . . . . .	-13	50
Uncorrelated platform misalignment about Y axis, arc sec . . . . .	-26	50

\*Averaged for entire flight.

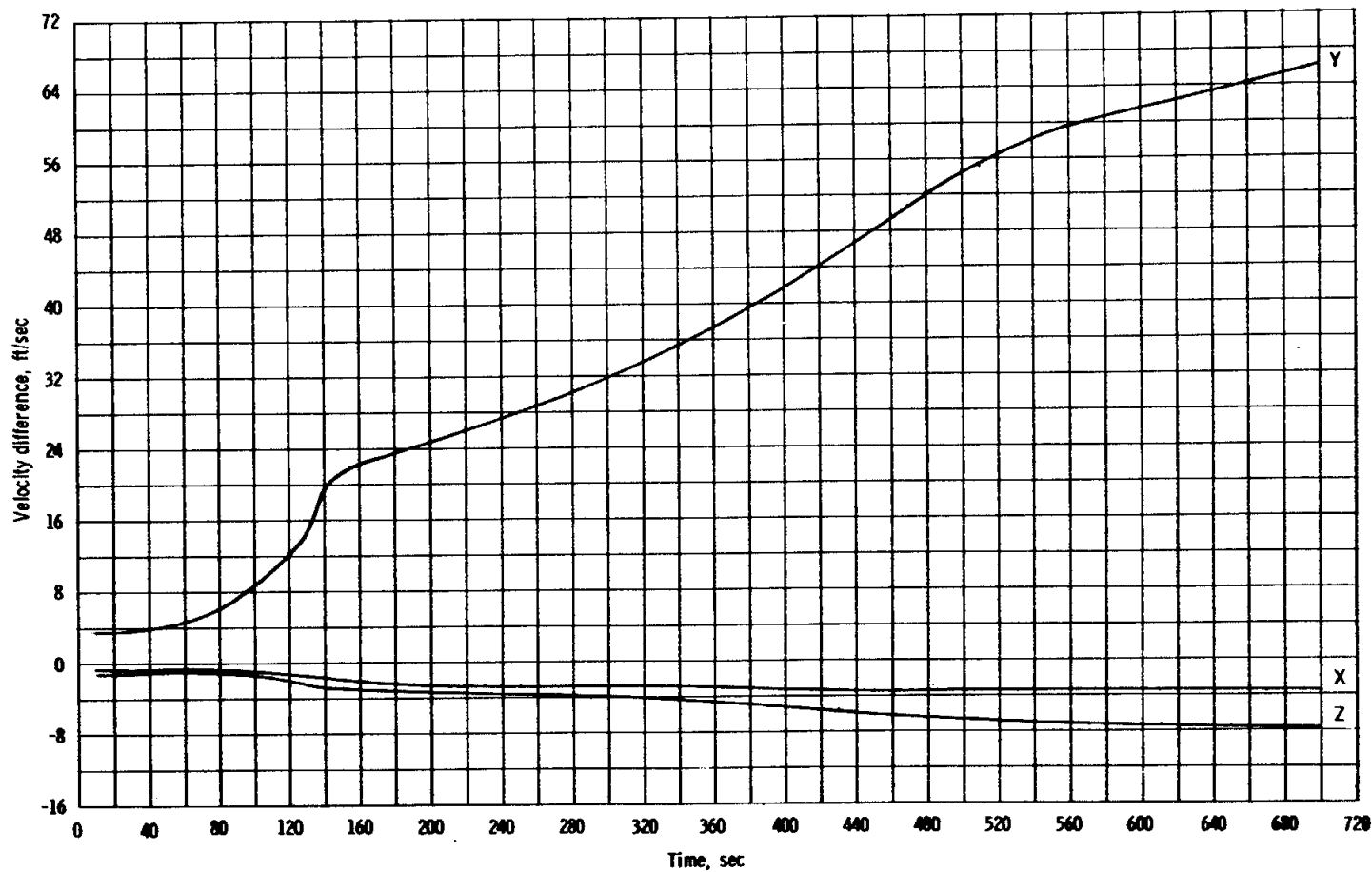


Figure 8.6-1. - Velocity comparison between instrument unit and spacecraft guidance during ascent.

## 8.7 REACTION CONTROL

### 8.7.1 Service Module

Performance of the service module reaction control system was normal throughout the mission. Total propellant consumed up to command module/service module separation was 560 pounds, 30 pounds less than predicted. During all mission phases, the system pressures and temperatures remained well within their normal operating ranges.

At the time the command and service modules separated from the S-IVB, the crew reported that the propellant isolation valve indicators for quad B indicated the "barber-pole" position. This indication corresponds to at least one primary and one secondary valve being in the closed position. Twenty to thirty seconds after closure, the crew reopened the valves according to checklist procedures, and no further problems were experienced (see section 16.1.6).

### 8.7.2 Command Module

After command module/service module separation, the crew reported that the minus-yaw engine in system 1 was not responding properly to firing commands through the automatic coils. Postflight data confirm that this engine produced very low, but detectable, thrust when the automatic coils were activated. Also, the response to direct coil commands was normal, which indicates that, mechanically, the two valves were operating properly and that one of the two valves was operating when the automatic coils were energized. Postflight tests confirmed that an intermittent circuit existed on a terminal board in the valve electronics. Section 16.1.3 contains a discussion of this anomaly.

All measured system pressures and temperatures were normal throughout the mission, and except for the problem with the yaw engine, both systems operated as expected during entry. About 1 minute after command module/service module separation, system 2 was disabled and system 1 was used for entry control, as planned. Forty-one pounds of propellant were used during entry.

## 8.8 SERVICE PROPULSION

Service propulsion system performance was satisfactory during each of the five maneuvers, with a total firing time of 531.9 seconds. The actual ignition times and firing durations are listed in table 8.6-II.

The longest engine firing was for 357.5 seconds during the lunar orbit insertion maneuver. The fourth and fifth service propulsion firings were preceded by a plus-X reaction control translation to effect propellant settling, and all firings were conducted under automatic control.

The steady-state performance during all firings was satisfactory. The steady-state pressure data indicate essentially nominal performance; however, the gaging system data indicate a mixture ratio of 1.55 rather than the expected 1.60 to 1.61.

The engine transient performance during all starts and shutdowns was satisfactory. The chamber pressure overshoot during the start of the spacecraft separation maneuver from the S-IVB was approximately 120 psia, which corresponds to the upper specification limit for starts using only one bank of propellant valves. On subsequent firings, the chamber pressure overshoots were all less than 120 psia. During the separation firing, minor oscillations in the measured chamber pressure were observed beginning approximately 1.5 seconds after the initial firing signal. However, the magnitude of the oscillations was less than 30 psi (peak-to-peak), and by approximately 2.2 seconds after ignition, the chamber pressure data were indicating normal steady-state operation.

The helium pressurization system functioned normally throughout the mission. All system temperatures were maintained within their red-line limits without heater operation.

The propellant utilization and gaging system operated satisfactorily throughout the mission. The mode selection switch for the gaging system was set in the normal position for all service propulsion firings; as a result, only the primary system data were used. The propellant utilization valve was in the "normal" position during the separation and first midcourse firings and for the first 76 seconds of the lunar orbit insertion firing. At that time, the valve was moved to the "increase" position and remained there through the first 122 seconds of the transearth injection firing. The valve position was then moved to "normal" for approximately 9 seconds and then to "decrease" for most of the remainder of the transearth injection firing.

Figure 8.8-1 shows the indicated propellant unbalance, as computed from the data. The indicated unbalance history should reflect the unbalance history displayed in the cabin, within the accuracy of the telemetry system. As expected, based on previous flights, the indicated unbalance following the start of the lunar orbit insertion firing showed decrease readings. The initial decrease readings were caused primarily by the oxidizer level in the sump tank exceeding the maximum gageable height. This condition occurs because oxidizer is transferred from the storage tank to the sump tank as a result of helium absorption from the sump tank ullage. This phenomenon, in combination with a known storage

tank oxidizer gaging error, is known to cause both the initial decrease readings and a step increase in the unbalance at crossover. The crew were briefed on these conditions prior to flight and, therefore, expected both the initial decrease readings and a step increase at crossover of 150 to 200 pounds. When the unbalance started to increase (approach zero) prior to crossover, the crew, in anticipation of the increase, properly interpreted the unbalance meter movement as an indication of a low mixture ratio and moved the propellant utilization valve to the "increase" position. As shown in figure 8.8-1, the unbalance then started to decrease in response to the valve change, and at crossover the expected step increase did occur. At the end of the firing, the crew reported that the unbalance was a 50-pound increase, which agrees well with the telemetered data shown in figure 8.8-1. This early recognition of a lower mixture ratio and the movement of the propellant utilization valve to the "increase" position during lunar orbit insertion resulted in a higher-than-predicted average thrust for the firing and a duration of 4.5 seconds less than predicted.

The duration of the firing as determined by Mission Control, was decreased to reflect the higher thrust level experienced on the lunar orbit insertion firing. However, during the transearth injection firing, the propellant utilization valve was cycled from the normal to the decrease position two times. This resulted in less than the expected thrust and consequently resulted in an overburn of 3.4 seconds above the recalculated transearth injection firing prediction.

Preliminary calculations, which were based on the telemetered gaging data and the predicted effects of propellant utilization valve position, yielded mixture ratios for the "normal" valve position of about 1.55, compared to an expected range of 1.60 to 1.61. Less-than-expected mixture ratios were also experienced during Apollo 9 and 10, and sufficient pre-flight analyses were made prior to this flight to verify that the propellant utilization and gaging system was capable of correcting for mixture ratio shifts of the magnitudes experienced. The reason for the less-than-expected mixture ratios during the last three flights is still under investigation.

An abnormal decay in the secondary (system B) nitrogen pressure was observed during the lunar orbit insertion service propulsion firing, indicating a leak in the system which operates the engine upper bipropellant valve bank. No further leakage was indicated during the remainder of the mission. This anomaly is discussed in greater detail in section 16.1.1.

NASA-S-69-3740

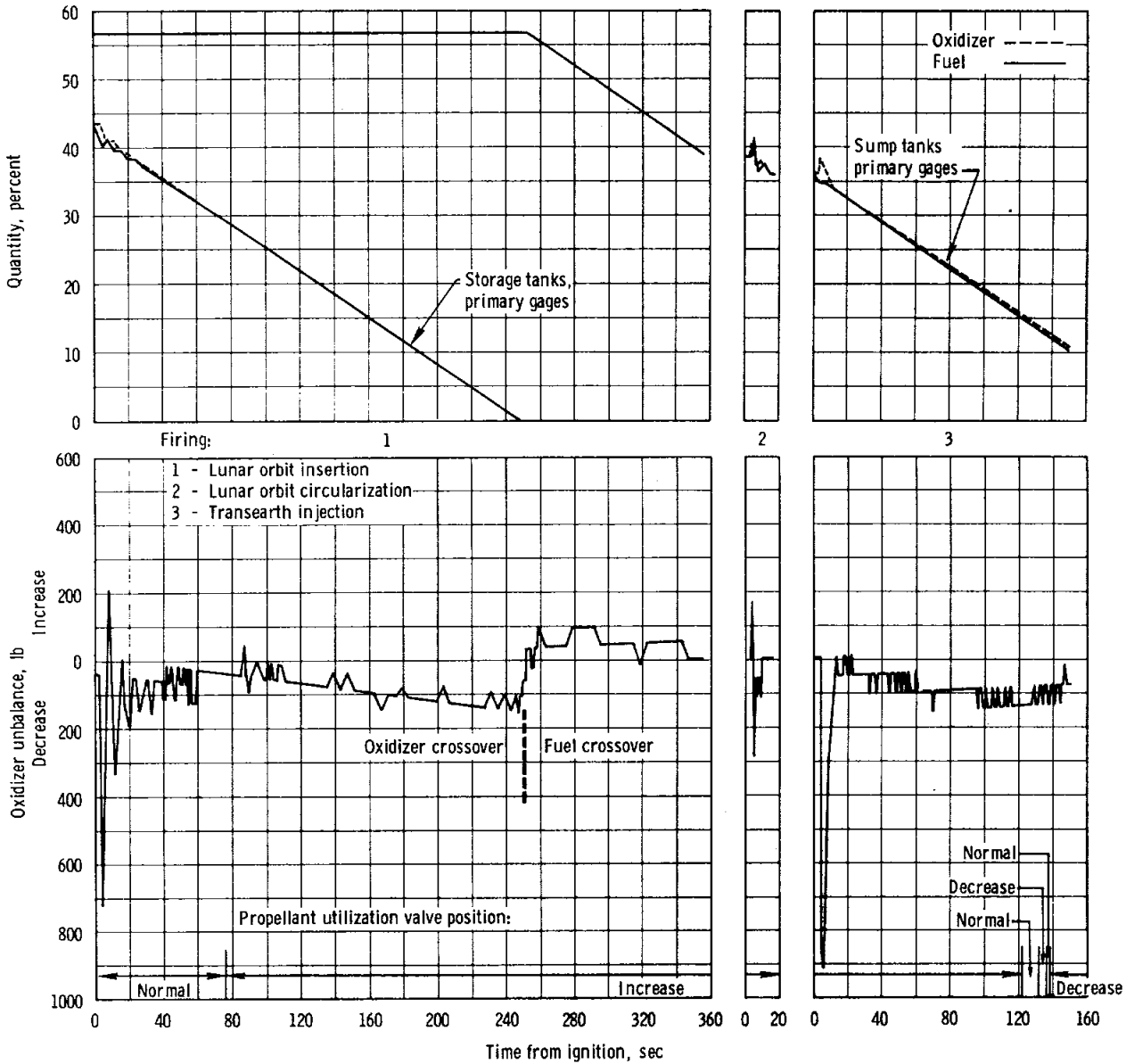


Figure 8.8-1. - Service propulsion propellant unbalance.

## 8.9 ENVIRONMENTAL CONTROL SYSTEM

The environmental control system performed satisfactorily throughout the mission and provided a comfortable environment for the crew and adequate thermal control of spacecraft equipment.

### 8.9.1 Oxygen Distribution

The cabin pressure stabilized at 4.7 psia prior to translunar injection and returned to that value after initial lunar module pressurization. Two master alarms indicating high oxygen flow occurred, however, during lunar module pressurization when the oxygen flow rate was decreasing. This condition was also experienced during ground testing. Postflight analysis has shown that this condition was caused by a malfunction of oxygen flow rate transducer (see section 16.1.5).

### 8.9.2 Particulate Back-Contamination Control

The command module oxygen systems were used for particulate lunar surface back-contamination control from final command module docking until earth landing.

At about 128 hours, the oxygen flow rate was adjusted to an indicated reading of approximately 0.6 lb/hr to establish a positive differential pressure between the two vehicles, causing the cabin pressure to increase to about 5.4 psia. The oxygen purge was terminated at 130 hours 9 minutes following the command module tunnel hatch leak check.

### 8.9.3 Thermal Control

The primary coolant system provided adequate thermal control for crew comfort and spacecraft equipment throughout the mission. The secondary coolant system was activated only during redundant component checks and the earth entry chilldown. The evaporators were not activated during lunar orbit coast, since the radiators provided adequate temperature control.

At 105 hours 19 minutes, the primary evaporator outlet temperature had dropped to 31.5° F. Normally, the temperature is maintained above 42° F by the glycol temperature control valve during cold temperature excursions of the radiator. This discrepancy is discussed in section 16.1.10.

#### 8.9.4 Water Management

Gas in the spacecraft potable water has been a problem on all manned Apollo flights. On this mission, a two-membrane water/gas separator was installed on both the water gun and the outlet at the food preparation unit. The separators allow only gas to pass through one membrane into the cabin atmosphere, while the second membrane passes only gas-free water to the outlet port for crew consumption. The crew indicated that performance of the separators was satisfactory. Water in the food bags and from the water pistol was nearly free of gas. Two interface problems were experienced while using the separators. There is no positive lock between the water pistol and the inlet port of the separator; thus, occasionally the separator did not remain in place when used to fill a food bag from the water pistol. Also, the crew commented that some provision for positively retaining the food bag to the separator outlet port would be highly desirable. For future spacecraft, a redesign of the separator will provide positive locking between the water pistol and the inlet port of the separator. Also, a change has been made in the separator outlet probe to provide an improved interface with the food bag.

#### 8.10 CREW STATION

The displays and controls were adequate except the mission clock in the lower equipment bay ran slow, by less than 10 seconds over a 24-hour period, as reported by the crew. The mission clocks have a history of slow operation, which has been attributed to electromagnetic interference. In addition, the glass face was found to be cracked. This has also been experienced in the past and is caused by stress introduced in the glass during the assembly process.

The lunar module mission clock is identical to the command module clock. Because of the lunar module clock problem discussed in section 16.2.1, an improved-design timer is being procured and will be incorporated in future command modules.

#### 8.11 CONSUMABLES

The predictions for consumables usage improved from mission to mission such that for the Apollo 11 mission, all of the command and service module consumable quantities were within 10 percent of the preflight estimates.



## 8.11.1 Service Propulsion Propellant

The service propulsion propellant usage was within 5 percent of the preflight estimate for the mission. The deviations which were experienced have been attributed to the variations in firing times (see section 8.8). In the following table, the loadings were calculated from gaging system readings and measured densities prior to lift-off.

Conditions	Actual usage, lb			Preflight planned usage, lb
	Fuel	Oxidizer	Total	
Loaded				
In tanks	15 633	24 967		
In lines	79	124		
Total	15 712	25 091	40 803	40 803
Consumed	13 754	21 985	35 739	36 296
Remaining at command module/service module separation	1 958	3 106	5 064	4 507

## 8.11.2 Reaction Control Propellant

*Service module.*- Reaction control system propellant usage predictions and flight data agreed within 5 percent. Usage was higher than expected during transposition and docking and the initial set of navigational sightings. This was balanced by efficient maneuvering of the command and service modules during the rendezvous sequence, in which the propellant consumption was less than predicted. The usages listed in the following table were calculated from telemetered helium tank pressure data using the relationship between pressure, volume, and temperature.

Condition	Actual usage, lb			Preflight planned usage, lb
	Fuel	Oxidizer	Total	
Loaded				
Quad A	110	225		
Quad B	110	225		
Quad C	110	225		
Quad D	110	225		
Total	440	900	1340	1342
Consumed	191	369	560	590
Remaining at command module/service module separation	249	531	780	752

*Command module.*- Command module reaction control system propellant usage predictions agreed with actual usage quantities within 5 percent. The usages listed in the following table were calculated from pressure, volume, and temperature relationships.

Condition	Actual usage, lb			Preflight planned usage, lb
	Fuel	Oxidizer	Total	
Loaded				
System A	44.8	78.4		
System B	44.4	78.3		
Total	89.2	156.7	245.9	245.0
Consumed				
System A	15.0	26.8		
System B	0.0	0.0		
Total	15.0	26.8	40.8	39.3
Remaining at main parachute deployment				
System A	30.8	51.6		
System B	44.4	78.3		
Total	75.2	129.9	205.1	205.7

## 8.11.3 Cryogenics

The oxygen and hydrogen usages were within 5 percent of those predicted. This deviation was caused by the loss of an oxygen tank heater element, plus a reduced reaction control system heater duty cycle. Usages listed in the following table are based on the electrical power produced by the fuel cells.

Condition	Hydrogen usage, lb		Oxygen usage, lb	
	Actual	Planned	Actual	Planned
Available at lift-off				
Tank 1	27.3		300.5	
Tank 2	26.8		314.5	
Total	54.1	56.4	615.0	634.7
Consumed				
Tank 1	17.5		174.0	
Tank 2	17.4		180.0	
Total	34.9	36.6	354.0	371.1
Remaining at command module/ service module separation				
Tank 1	9.8		126.5	
Tank 2	9.4		134.5	
Total	19.2	19.8	261.0	263.6

## 8.11.4 Water

Predictions concerning water consumed in the command and service modules are not generated for each mission because the system has an initial charge of potable water at lift-off, plus additional water is generated in the fuel cells in excess of the demand. Also, water is dumped overboard and some is consumed. The water quantities loaded, consumed, produced, and expelled during the mission are shown in the following table.

Condition	Quantity, lb
Loaded Potable water tank Waste water tank	31.7 28
Produced inflight Fuel cells Lithium hydroxide, metabolic	315 NA
Dumped overboard (including urine)	325.7
Evaporated up to command module/service module separation	8.7
Remaining at command module/service module separation Potable water tank Waste water tank	36.8 43.5

## 9.0 LUNAR MODULE PERFORMANCE

This section is a discussion of lunar module systems performance. The significant problems are described in this section and are discussed in detail in section 16, Anomaly Summary.

### 9.1 STRUCTURAL AND MECHANICAL SYSTEMS

No structural instrumentation was installed on the lunar module; consequently, the structural performance evaluation was based on lunar module guidance and control data, cabin pressure data, command module acceleration data, photographs, and analytical results.

Based on measured command module accelerations and on simulations using measured wind data, the lunar module loads are inferred to have been within structural limits during the S-IC, S-II, and S-IVB launch phase firings, and the S-IVB translunar injection maneuvers. The loads during both dockings were also within structural limits.

Command module accelerometer data show minimal structural excitation during the service propulsion maneuvers, indicating that the lunar module loads were well within structural limits.

The structural loading environment during lunar landing was evaluated from motion picture film, still photographs, postflight landing simulations, and crew comments. The motion picture film from the onboard camera showed no evidence of structural oscillations during landing, and crew comments agree with this assessment. Flight data from the guidance and propulsion systems were used in conducting the simulations of the landing (see section 5.4). The simulations and photographs indicate that the landing gear strut stroking was very small and that the external loads developed during landing were well within design values.

### 9.2 THERMAL CONTROL

The lunar module internal temperatures at the end of translunar flight were nominal and within 3° F of the launch temperatures. During the active periods, temperature response was normal and all antenna temperatures were within acceptable limits.

The crew inspected the descent stage thermal shielding after lunar landing and observed no significant damage.

### 9.3 ELECTRICAL POWER

The electrical power system performed satisfactorily. The dc bus voltage was maintained above 28.8 volts throughout the flight. The maximum observed load was 81 amperes, during powered descent initiation. Both inverters performed as expected.

The knob on the ascent engine arm circuit breaker was broken, probably by the aft edge of the oxygen purge system hitting the breaker during preparations for extravehicular activity. In any event, this circuit breaker was closed without difficulty when required prior to ascent (section 16.2.11).

At staging, the descent batteries had supplied 1055 A-h of a nominal total capacity of 1600 A-h. The difference in load sharing at staging was 2 A-h on batteries 1 and 2 and 23 A-h on batteries 3 and 4, and both of these values are acceptable.

At lunar module jettison, the two ascent batteries had delivered 336 A-h of a nominal total capacity of 592 A-h. The ascent batteries continued to supply power, for a total of 680 A-h at 28 V dc or above.

### 9.4 COMMUNICATIONS EQUIPMENT

Overall performance of the S-band steerable antenna was satisfactory. Some difficulties were experienced, however, during descent of the lunar module. Prior to the scheduled 180-degree yaw maneuver, the signal strength dropped below the tracking level and the antenna broke lock several times. After the maneuver was completed, new look angles were set in and the antenna acquired the uplink signal and tracked normally until landing. The most probable cause of the problem was a combination of vehicle blockage and multipath reflections from the lunar surface, as discussed in section 16.2.4.

During the entire extravehicular activity, the lunar module relay provided good voice and extravehicular mobility unit data. Occasional breakup of the Lunar Module Pilot's voice occurred in the extravehicular communications system relay mode. The most probable cause was that the sensitivity of the voice-operated relay of the Commander's audio center in the lunar module was inadvertently set at less than maximum specified. This anomaly is discussed in section 16.2.8.

Also during the extravehicular activity, the Network received an intermittent echo of the uplink transmissions. This was most likely caused by signal coupling between the headset and microphone. A detailed discussion of this anomaly is in section 16.2.9.

After crew ingress into the lunar module, the voice link was lost when the portable life support system antennas were stowed; however, the data from the extravehicular mobility unit remained good.

Television transmission was good during the entire extravehicular activity, both from the descent stage stowage unit and from the tripod on the lunar surface. Signal-to-noise ratios of the television link were very good. The television was turned off after 5 hours 4 minutes of continuous operation.

Lunar module voice and data communications were normal during the lift-off from the lunar surface. The steerable antenna maintained lock and tracked throughout the ascent. Uplink signal strength remained stable at approximately minus 88 dBm.

## 9.5 INSTRUMENTATION

Performance of the operational instrumentation was satisfactory with the exception of the data storage electronic assembly (onboard voice recorder). When the tape was played, no timing signal was evident and voice was weak and unreadable, with a 400-hertz hum and wideband noise background. For further discussion of this anomaly, see section 16.2.10.

## 9.6 GUIDANCE AND CONTROL

### 9.6.1 Power-Up Initialization

The guidance and control system power-up sequence was nominal except that the crew reported an initial difficulty in aligning the abort guidance system. The abort guidance system is aligned in flight by transferring inertial measurement unit gimbal angles from the primary guidance system, and from these angles establishing a direction cosine matrix. Prior to the first alignment after activation, the primary system coupling data units and the abort system gimbal angle registers must be zeroed to insure that the angles accurately reflect the platform attitude. Failure to zero could cause the symptoms reported. Another possible cause is an incorrect setting of the orbital rate drive electronics (ORDEAL) mode switch. If this switch is set in the orbital rate position, even though the orbital rate drive unit is powered down, the pitch attitude displayed on the flight director attitude indicator will be offset by an amount corresponding to the orbital rate drive resolver. No data

are available for the alignment attempt, and no pertinent information is contained in the data before and after the occurrence. Because of the success of all subsequent alignment attempts, hardware and software malfunctions are unlikely, and a procedural discrepancy is the most probable cause of the difficulty.

### 9.6.2 Attitude Reference System Alignments

Pertinent data concerning each of the inertial measurement unit alignments are contained in table 9.6-I. The first alignment was performed before undocking, and the command module platform was used as a reference in correcting for the measured 2.05-degree misalignment of the docking interface. After undocking, the alignment optical telescope was used to realign the platform to the same reference, and a misalignment equivalent to the gyro torquing angles shown in table 9.6-I was calculated. These angles were well within the go/no-go limits established preflight.

After the descent orbit insertion maneuver, an alignment check was performed by making three telescope sightings on the sun. A comparison was made between the actual pitch angle required for the sun marks and the angle calculated by the onboard computer. The results were well within the allowable tolerance and again indicated a properly functioning platform.

The inertial measurement unit was aligned five times while on the lunar surface. All three alignment options were successfully utilized, including an alignment using a gravity vector calculated by the onboard accelerometers and a prestored azimuth, one utilizing the two vectors obtained from two different star sightings, and one using the calculated gravity vector and a single star sighting to determine an azimuth.

The Lunar Module Pilot reported that the optical sightings associated with these alignments were based on a technique in which the average of five successive sightings was calculated by hand and then inserted into the computer. An analysis of these successive sightings indicated that the random sighting error was very small and that the only significant trend observed in the successive sightings was lunar rate.

The platform remained inertial during the 17.5-hour period between the third and fourth alignments. Because both of these alignments were to the same orientation, it is possible to make an estimate of gyro drift while on the lunar surface. Drift was calculated from three sources: the gyro torquing angles, or misalignment, indicated at the second alignment; the gimbal angle change history in comparison to that predicted



from lunar rate; and the comparison of the actual gravity tracking history of the onboard accelerometers with that predicted from lunar rate. The results (table 9.6-II) indicate excellent agreement for the granularity of the data utilized.

The abort guidance system was aligned to the primary system at least nine times during the mission (table 9.6-III). The alignment accuracy, as determined by the Euler angle differences between the primary and abort systems for the eight alignments available on telemetry, was within specification tolerances. In addition, the abort guidance system was independently aligned three times on the lunar surface using gravity as determined by the abort system accelerometers and an azimuth derived from an external source. The resulting Euler angles are shown in table 9.6-IV. A valid comparison following the first alignment cannot be made because the abort guidance system azimuth was not updated. Primary guidance alignments following the second alignment were incompatible with the abort guidance system because the inertial measurement unit was not aligned to the local vertical. A comparison of the Euler angles for the third alignment indicated an azimuth error of 0.08 degree. This error resulted from an incorrect azimuth value received from the ground and loaded in the abort guidance system manually. The resulting 0.08-degree error in azimuth caused an out-of-plane velocity difference between the primary and abort systems at insertion (see section 5.6).

### 9.6.3 Translation Maneuvers

All translation maneuvers were performed under primary guidance system control with the abort guidance system operating in a monitor mode. Significant parameters are contained in table 9.6-V. The dynamic response of the spacecraft was nominal during descent and ascent engine maneuvers, although the effect of fuel slosh during powered descent was greater than expected based on preflight simulations. Slosh oscillations became noticeable after the 180-degree yaw maneuver and gradually increased to the extent that thruster firings were required for damping (fig. 5-11). The effect remained noticeable and significant until after the end of the braking phase when the engine was throttled down to begin rate-of-descent control. The slosh response has been reproduced post-flight by making slight variations in the slosh model damping ratio.

The ascent maneuver was nominal with the crew again reporting the wallowing tendency inherent in the control technique used. As shown in table 9.6-V, the velocity at insertion was 2 ft/sec higher than planned. This has been attributed to a difference in the predicted and actual tail-off characteristics of the engine.

The abort guidance system, as stated, was used to monitor all primary guidance system maneuvers. Performance was excellent except for some isolated procedural problems. The azimuth misalignment which was inserted into the abort guidance system prior to lift-off and which contributed to the out-of-plane error at insertion is discussed in the previous section. During the ascent firing, the abort guidance system velocity-to-be-gained was used to compare with and to monitor the primary system velocity to be gained. The crew reported that near the end of the insertion maneuver, the primary and abort system displays differed by 50 to 100 ft/sec. A similar comparison of the reported parameter differences has been made postflight and is shown in figure 9.6-1. As indicated, the velocity difference was as large as 39 ft/sec and was caused by the time synchronization between the two sets of data not being precise. The calculations are made and displayed independently by the two computers, which have outputs that are not synchronized. Therefore, the time at which a given velocity is valid could vary as much as 4 seconds between the two systems. Both systems appear to have operated properly.

Performance of the abort guidance system while monitoring rendezvous maneuvers was also satisfactory, although residuals after the terminal phase initiation maneuver were somewhat large. The differences were caused by a 23-second late initiation of the maneuver and relatively large attitude excursions induced because of the incorrect selection of wide deadband in the primary system. The desired velocity vector in the abort guidance system is chosen for a nominal time of rendezvous. If the terminal phase initiation maneuver is begun at other than this time and the abort system is not retargeted, the maneuver direction and magnitude will not be correct.

#### 9.6.4 Attitude Control

The digital autopilot was the primary source of attitude control during the mission and performed as designed. One procedural discrepancy occurred during the 180-degree yaw maneuver after the start of powered descent. This maneuver was performed manually using the proportional rate output of the rotational hand controller. Because a low rate scale was erroneously selected for display, the maneuver was begun and partially completed at less than the desired rate of 10 deg/sec. Continuing the maneuver on the low rate scale would have delayed landing radar acquisition. After the problem was recognized, the high rate scale was selected, and the maneuver was completed as planned. The abort guidance system was used just prior to the second docking. Performance was as expected; however, some difficulty was experienced during the docking (see section 5.7).

### 9.6.5 Primary Guidance, Navigation, and Control System Performance

The inertial measurement unit was replaced 12 days before launch and exhibited excellent performance throughout the mission. Table 9.6-VI contains the preflight history of the inertial components for the inertial measurement unit. The accelerometer bias history is shown in table 9.6-VII. An accelerometer bias update was performed prior to undocking, with results as shown.

Visibility in orbit and on the lunar surface through the alignment optical telescope was as expected. Because of the relative position of the earth, the sun, and reflections off the lunar surface, only the left and right rear telescope detent positions were usable after touchdown. Star recognition and visibility through these detents proved to be adequate. The sun angle had changed by the time of lift-off, and only the right rear detent was usable. This detent proved sufficient for pre-lift-off alignments (see section 5.6).

The lunar module guidance computer performed as designed, except for a number of unexpected alarms. The first of these occurred during the power-up sequence when the display keyboard circuit breaker was closed and a 520 alarm (RADAR RUPT), which was not expected at this time, was generated. This alarm has been reproduced on the ground and was caused by a random setting of logic gates during the turn-on sequence. Although this alarm has a low probability of occurrence, it is neither abnormal nor indicative of a malfunction.

The Executive overflow alarms that occurred during descent (see section 5.3) are now known to be normal for the existing situation and were indicative of proper performance of the guidance computer. These alarms are discussed in detail in section 16.2.6.

### 9.6.6 Abort Guidance System Performance

Except for procedural errors which degraded performance to some extent, all required functions were satisfactory. Eight known state vector transfers from the primary system were performed. The resulting position and velocity differences for three of the transfers are shown in table 9.6-VIII. With the exception of one which was invalid because of an incorrect K-factor used to time-synchronize the system, all state vector updates were accomplished without difficulty.

The preflight inertial component test history is shown in table 9.6-IX. The inflight calibration results were not recorded; however, just prior to the inflight calibration (before loss of data), the accelerometer biases were calculated from velocity data and the known computer compensations.

The shift between the pre-installation calibration data and the flight measurements were as follows. (The capability estimate limits are based on current 3-sigma capability estimates with expected measurement errors included.)

Accelerometer	Accelerometer bias, $\mu\text{g}$			
	Pre-installation calibration (June 6, 1969)	Freefall (July 20, 1969)	48-day shift	Capability estimate
X	1	-65	-66	185
Y	-17	-41	-24	185
Z	-66	-84	-18	185

When telemetered data were regained after the inflight calibration and after powered ascent, excellent accelerometer stability was indicated as follows. (The capability estimate limits are based upon current 3-sigma capability estimates with expected measurement errors included.)

Accelerometer	Accelerometer bias, $\mu\text{g}$			
	Before descent	After ascent	Shift	Capability estimate
X	-34	-62	-28	60
Y	-27	-31	- 4	60
Z	-41	-62	-21	60

Inflight calibration data on the gyros were reported and two lunar surface gyro calibrations were performed with the following results. The degree of stability of the instruments was well within the expected values.

	Gyro drift, deg/hr		
	<u>X</u>	<u>Y</u>	<u>Z</u>
Pre-installation calibration on June 2, 1969	+0.27	+0.03	+0.41
Final earth prelaunch calibration on June 28, 1968	+0.10	-0.13	+0.35
Inflight calibration on July 20, 1969	+0.33	-0.07	+0.38
First lunar surface calibration on July 21, 1969	+0.34	-0.08	+0.47
Second lunar surface calibration on July 21, 1969	+0.41	-0.04	+0.50

The only hardware discrepancy reported in the abort guidance system was the failure of an electroluminescent segment in one digit of the data entry and display assembly. This is discussed in detail in section 16.2.7.

TABLE 9.6-I.- LUNAR MODULE PLATFORM ALIGNMENT SUMMARY

Time, hr:min	Type alignment	Alignment mode		Telescope detent <sup>c</sup> /star used	Star angle difference, deg	Gyro torquing angle, deg			Gyro drift, mERU		
		Option <sup>a</sup>	Technique <sup>b</sup>			X	Y	Z	X	Y	Z
100:15	P52	3	NA	2/25; -/33	0.03	-0.292	+0.289	-0.094	--	--	--
103:01	P57	3	1	NA	0.15	+0.005	-0.105	-0.225	--	--	--
103:47	P57	3	2	6/12; 4/3	0.09	-0.167	+0.186	+0.014	+4.5	-5.0	+0.4
104:16	P57	4	3	6/12; -/-	0.08	+0.228	-0.025	-0.284	--	--	--
122:17	P57	3	3	4/13; -/-	0.07	-0.699	+0.695	-0.628	+2.6	-2.6	-2.3
123:49	P57	4	3	1/10; 4/13	0.11	+0.089	+0.067	-0.041	-4.9	-3.2	-2.0
124:51	P52	3	NA	2/12; 2/25	0.00	-0.006	+0.064	+0.137	+0.4	-2.8	+8.1

<sup>a</sup>3 - REFSMMAT; 4 - Landing site.

<sup>b</sup>1 - REFSMMAT plus g; 2 - Two bodies; 3 - One body plus g.

<sup>c</sup>1 - Left front; 2 - Front; 4 - Right rear; 6 - Left rear.

S

Star names:

25 Acrux  
33 Antares  
12 Rigal  
3 Navi  
13 Capella  
10 Mirfak

TABLE 9.6-II.- LUNAR SURFACE GYRO DRIFT COMPARISON

Axis	Gyro drift, deg		
	Computer out-put (P57)	Gimbal angle change	Computed from gravity
X	0.699	0.707	0.413
Y	-0.696	-0.73	-0.76
Z	0.628	0.623	1.00

TABLE 9.6-III.- GUIDANCE SYSTEM ALIGNMENT COMPARISON

Time, hr:min:sec	Indicated difference, gimbal minus abort electronics, deg		
	X	Y	Z
Lunar Surface			
102:52:01	-0.0081	0.0066	0.0004
103:15:29	-0.0161	-0.0271	0.0004
103:50:29	-0.0063	-0.0015	0.0028
122:36:00	-0.0166	-0.0025	0.0028
122:53:00	-0.0152	-0.0071	-0.0012
122:54:30	-0.0071	-0.0101	-0.0012
Inflight			
100:56:20	-0.0019	-0.0037	0.0067
126:11:56	-0.0369	0.0104	-0.0468

TABLE 9.6-IV.- LUNAR SURFACE ALIGNMENT COMPARISON

Angle	Abort guidance	Primary guidance	Difference
Yaw, deg	13.3194	13.2275	0.0919
Pitch, deg	4.4041	4.4055	-0.0014
Roll, deg	0.5001	0.4614	0.0387



TABLE 9.6-V.- LUNAR MODULE MANEUVER SUMMARY

Condition	Maneuver					
	Descent orbit insertion	Powered descent initiation	Ascent	Coelliptic sequence initiation	Constant differential height	Terminal phase initiation
	PGMCS/DPS	PGMCS/DPS	PGMCS/APS	PGMCS/RCS	PGMCS/RCS	PGMCS/RCS
Time						
Ignition, hr:min:sec	101:36:14 <sup>a</sup>	102:33:05.01	124:22:00.79	125:19:35 <sup>a</sup>	126:17:49.6	127:03:51.6
Cutoff, hr:min:sec	101:36:44	102:45:41.40	124:29:15.67	125:20:22	126:18:29.2	127:04:14.5
Duration, sec	30.0	756.39	434.88	47.0	17.8	22.7
Velocity, ft/sec (desired/actual)		6775 total				
X	-75.8/ (b)		971.27/971.32	51.5/ (b)	2.04/2.05	-20.70/-20.62
Y	0.0/ (b)		0.22/0.18	1.0/ (b)	18.99/18.85	-13.81/-14.10
Z	+9.8/ (b)		5550.05/5551.57	0/ (b)	6.6/6.17	-4.19/-4.93
Coordinate system	Local vertical		Stable platform	Local vertical	Earth-centered inertial	Earth-centered inertial
Velocity residual after trimming, ft/sec						
X	<sup>a</sup> 0.0	Not applicable	0.4	-0.2	+0.1	-0.2
Y	-0.4		-1.0	+0.7	-0.1	0.0
Z	0.0		+1.4	-0.1	0.0	-0.1
Gimbal drive actuator, in.	(b)		Not applicable	Not applicable	Not applicable	Not applicable
Initial						
Pitch		+0.43				
Roll		-0.02				
Maximum excursion						
Pitch		+0.03				
Roll		-0.28				
Steady-state						
Pitch		+0.59				
Roll		-0.28				
Maximum rate excursion, deg/sec						
Pitch	(b)	+0.8	-16.2	(b)	-0.8	+1.2
Roll		-0.8	+1.8		-0.6	±0.8
Yaw		-0.6	+2.0		±0.2	±0.2
Maximum attitude excursion, deg						
Pitch	(b)	+1.2	+3.2	(b)	-1.6	-0.4
Roll		-1.6	-2.0		+0.8	-0.4
Yaw		-2.4	-2.0		±0.4	+3.8

<sup>a</sup>Reported by crew.<sup>b</sup>No data available.

NOTE: PGMCS - Primary guidance, navigation, and control system; DPS - Descent propulsion system; APS - Ascent propulsion system, RCS - Reaction control system.

Rendezvous maneuvers after terminal phase initiation are reported in section 5 and are based on crew reports.

Ignition and cutoff times are those commanded by the computer.

TABLE 9.6-VI.- INERTIAL COMPONENT PREFLIGHT HISTORY - LUNAR MODULE

Error	Sample mean	Standard deviation	No. of samples	Countdown value	Flight load
Accelerometers					
X - Scale factor error, ppm . . . . .	-155	111	4	-237	-270
Bias, cm/sec <sup>2</sup> . . . . .	0.60	0.09	4	0.70	0.66
Y - Scale factor error, ppm . . . . .	-1156	11	2	-1164	-1150
Bias, cm/sec <sup>2</sup> . . . . .	0.08	0.04	2	0.05	0.10
Z - Scale factor error, ppm . . . . .	-549	72	2	-600	-620
Bias, cm/sec <sup>2</sup> . . . . .	0.14	0.12	2	0.22	0.20
Gyroscopes					
X - Null bias drift, mERU . . . . .	-1.5	1.4	3	-1.3	-1.6
Acceleration drift, spin reference axis, mERU/g . . . . .	5.7	0.0	2	5.7	6.0
Acceleration drift, input axis, mERU/g . . . . .	12.8	3.5	2	15.2	10.0
Y - Null bias drift, mERU . . . . .	3.0	1.6	3	1.3	3.8
Acceleration drift, spin reference axis, mERU/g . . . . .	-4.0	1.4	2	-3.1	-5.0
Acceleration drift, input axis, mERU/g . . . . .	-2.3	6.1	2	2.0	3.0
Z - Null bias drift, mERU . . . . .	4.1	0.6	3	3.5	4.4
Acceleration drift, spin reference axis, mERU/g . . . . .	-4.7	0.4	2	-4.4	-5.0
Acceleration drift, input axis, mERU/g . . . . .	-9.3	7.7	2	-3.8	-3.0

TABLE 9.6-VII.- ACCELEROMETER BIAS FLIGHT HISTORY

Condition	Bias, cm/sec <sup>2</sup>		
	X	Y	Z
Flight load	+0.66	+0.10	+0.20
Updated value	+0.66	+0.04	+0.03
Flight average before update	+0.63	+0.04	+0.03
Flight average after update	+0.67	+0.07	-0.01

TABLE 9.6-VIII.- ABORT GUIDANCE STATE VECTOR UPDATES

Time, hr:min:sec	Abort minus primary guidance	
	Position, ft	Velocity, ft/sec
122:31:02	-137.6	0.05
124:09:12	-177.6	-0.15
126:10:14	-301.3	-2.01

TABLE 9.6-IX.- ABORT GUIDANCE SYSTEM PREINSTALLATION CALIBRATION DATA

Accelerometer bias	Sample mean, $\mu\text{g}$	Standard deviation, $\mu\text{g}$	Number of samples	Final calibration value, $\mu\text{g}$	Flight compensation value, $\mu\text{g}$
X	-53	42	15	1	0
Y	-22	9	15	-17	-23.7
Z	-79	22	15	-66	-71.2
Accelerometer scale factor		Standard deviation, ppm	Number of samples	Final calibration value, ppm	Flight compensation value, ppm
X		14	9	-430	-463.5
Y		28	9	324	299.5
Z		12	9	1483	1453.4
Gyro scale factor	Sample mean, deg/hr	Standard deviation, deg/hr	Number of samples	Final calibration value, deg/hr	Flight load value, deg/hr
X	-1048	-10	15	-1048	-1048
Y	-300	-47	15	-285	-285
Z	3456	16	15	3443	3443
Gyro fixed drift	Sample mean, ppm	Standard deviation, ppm	Number of samples	Final calibration value, ppm	Flight load value, ppm
X	0.33	0.05	15	0.27	0.27
Y	0.04	0.05	15	0.03	0.03
Z	0.51	0.07	15	0.41	0.41
Gyro spin axis mass unbalance	Sample mean, deg/hr/g	Standard deviation, deg/hr/g	Number of samples	Final calibration value, deg/hr/g	Flight load value, deg/hr/g
X	-0.67	0.12	15	-0.65	-0.65

NASA-S-69-3741

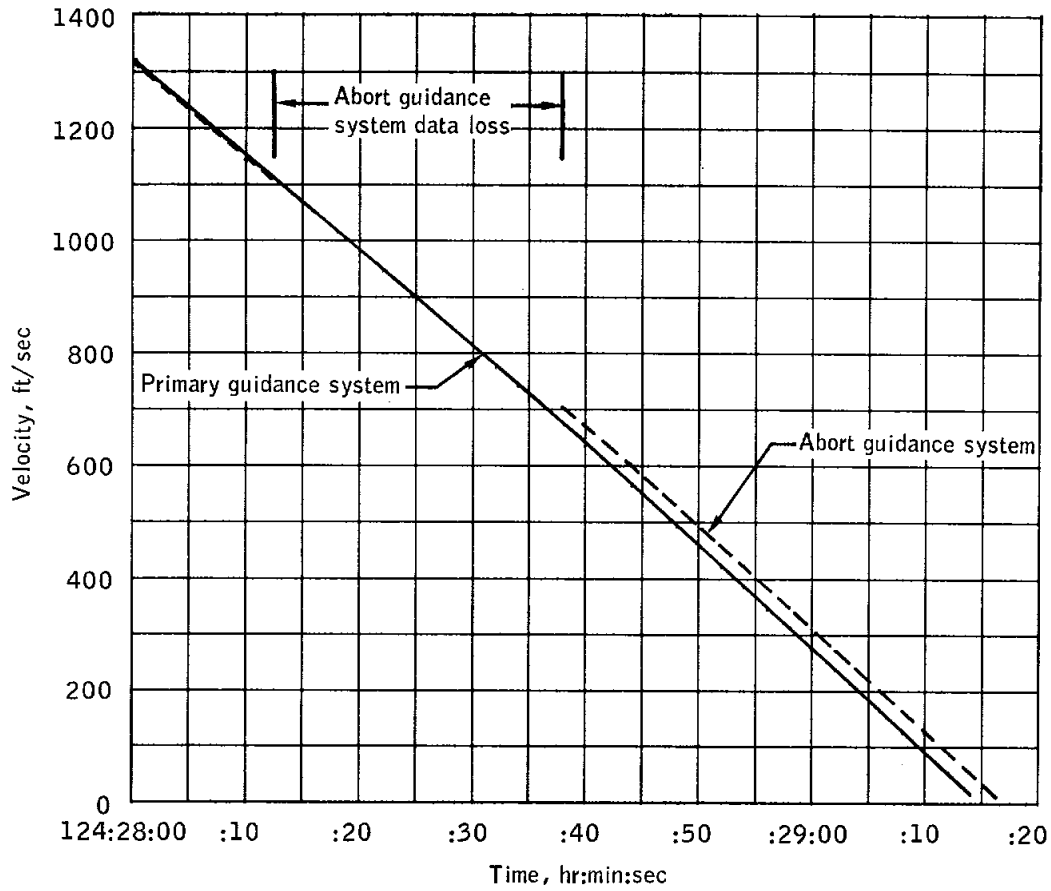


Figure 9.6-1.- Comparison of primary guidance and abort guidance system velocities during final phase of ascent.

## 9.7 REACTION CONTROL

Performance of the reaction control system was satisfactory. The system pressurization sequence was nominal, and the regulators maintained acceptable outlet pressures (between 178 and 184 psia) throughout the mission.

The crew reported thrust chamber assembly warning flags for three engine pairs. The A2 and A4 flags occurred simultaneously during lunar module station-keeping prior to descent orbit insertion. The B4 flag appeared shortly thereafter and also twice just before powered descent initiation. The crew believed these flags were accompanied by master alarms. The flags were reset by cycling of the caution and warning electronics circuit breaker. See section 16.2.14 for further discussion.

The chamber pressure switch in reaction control engine B1D failed closed approximately 8.5 minutes after powered descent initiation. The switch remained closed for 2 minutes 53 seconds, then opened and functioned properly for the remainder of the mission. The failure mode is believed to be the same as that of pressure switch failures on Apollo 9 and 10; that is, particulate contamination or propellant residue holding the switch closed. The only potential consequence of the failure would have been the inability to detect an engine failed "off."

A master alarm was noted at 126:44:00 when seven consecutive pulses were commanded on engine A2A without a pressure switch response. Further discussion of this discrepancy is contained in section 16.2.12.

Thermal characteristics were satisfactory and all temperatures were within predicted values. The maximum quad temperature was 232° F on quad 1 subsequent to touchdown. The fuel tank temperatures ranged from 68° to 71° F.

Propellant usage, based on the propellant quantity measuring device, was 319 pounds, compared with a predicted value of 253 pounds and the total propellant load of 549 pounds. About 57 of the 66 pounds above predictions were used during powered descent. Figures 9.7-1 and 9.7-2 include total and individual system propellant consumption profiles, respectively.

The reaction control system was used in the ascent interconnect mode during powered ascent. The system used approximately 69 pounds of propellant from the ascent propulsion tanks.

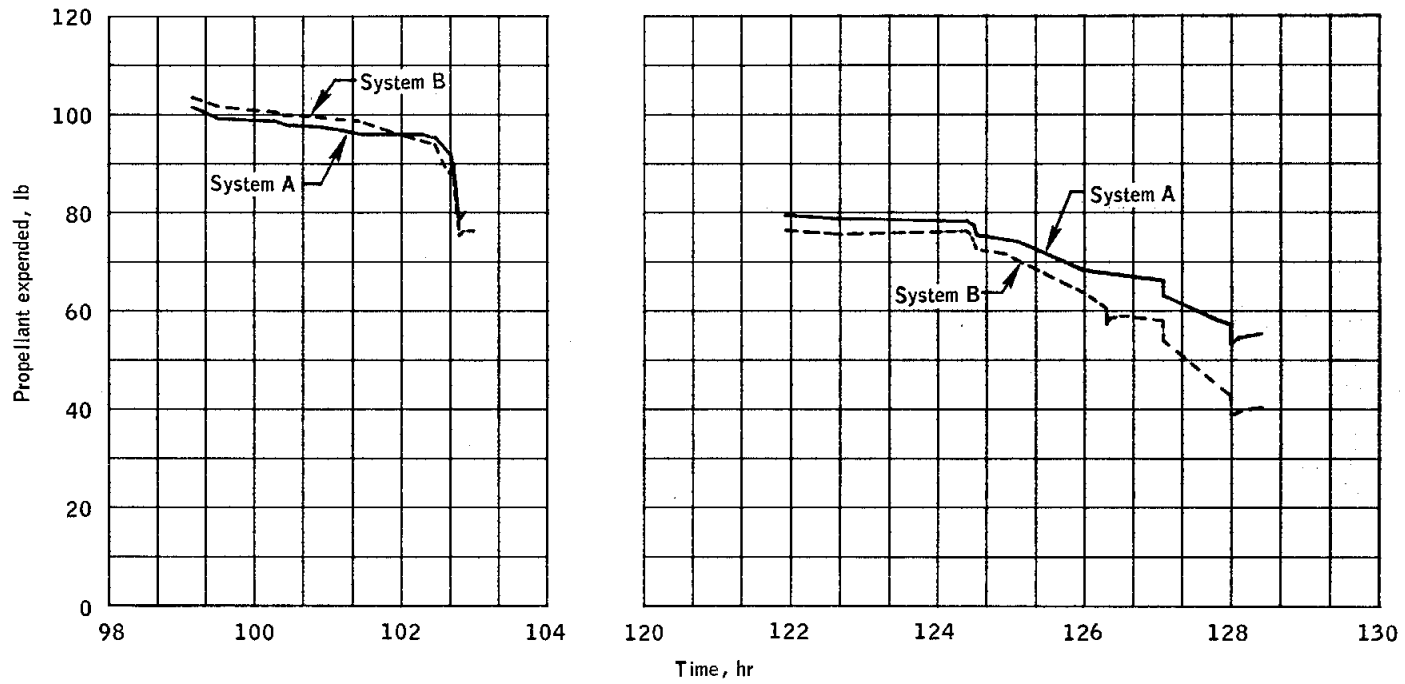


Figure 9.7-1.- Propellant consumption from each system.



NASA-S-69-3807

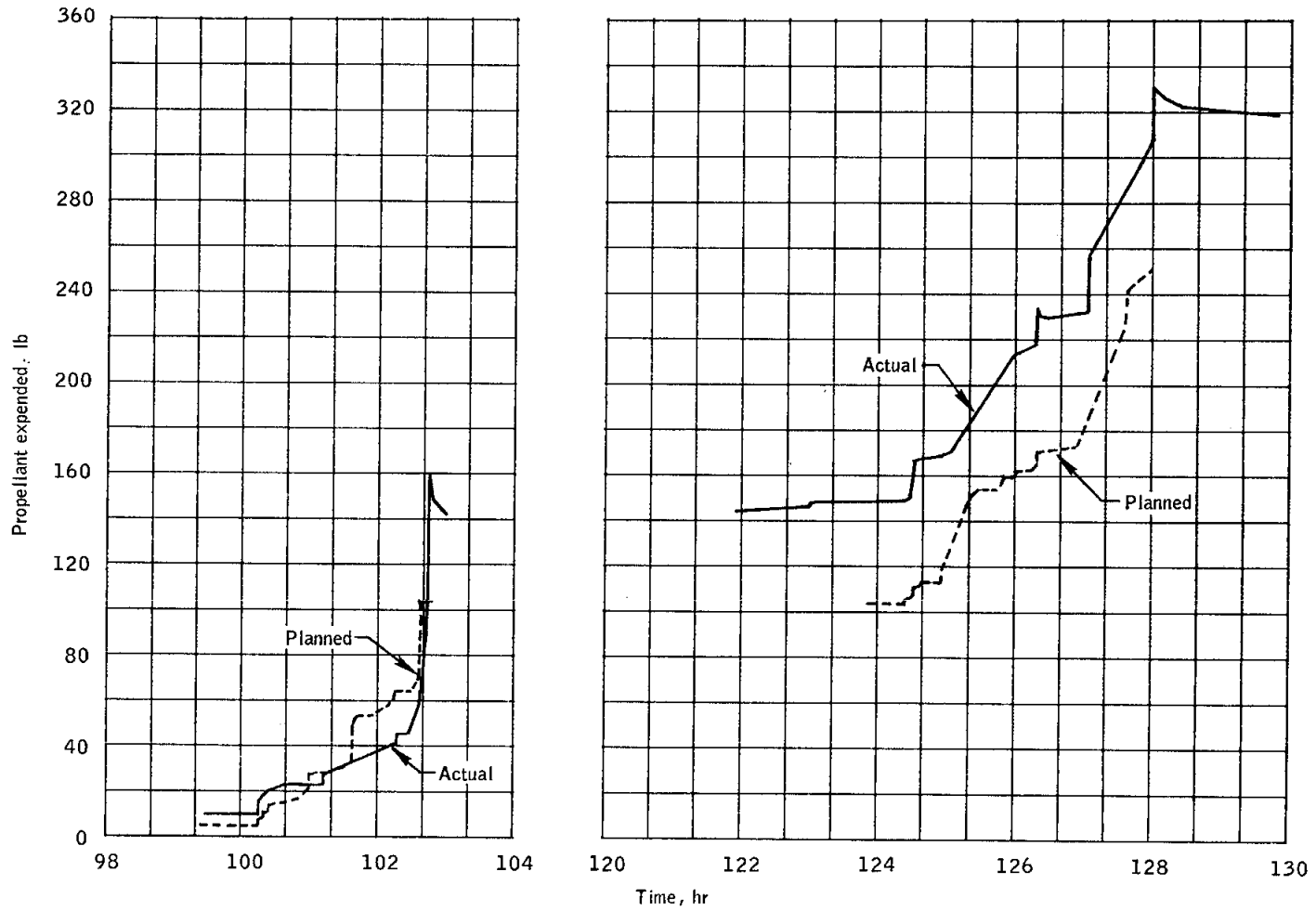


Figure 9.7-2.- Total propellant consumption.

## 9.8 DESCENT PROPULSION

The descent propulsion system operation was satisfactory for the descent orbit insertion and descent maneuvers. The engine transients and throttle response were normal.

### 9.8.1 Inflight Performance

The descent orbit insertion maneuver lasted 30 seconds; the resulting velocity change was 76.4 ft/sec. The engine was started at the minimum throttle setting of 13.0 percent of full thrust and, after approximately 15 seconds, was throttled to 40 percent thrust for the remainder of the firing.

The duration of the powered descent firing was 756.3 seconds, corresponding to a velocity change of approximately 6775 ft/sec. The engine was at the minimum throttle setting (13 percent) at the beginning of the firing and, after approximately 26 seconds, was advanced to full throttle. There was about a 45-second data dropout during this period but from crew reports, the throttle-up conditions were apparently normal. Figure 9.8-1 presents descent propulsion system pressures and throttle settings as a function of time. The data have been smoothed and do not reflect the data dropout, and the throttle fluctuations just before touchdown.

During the powered descent maneuver, the oxidizer interface pressure appeared to be oscillating as much as 67 psi peak-to-peak. These oscillations were evident throughout the firing, although of a lower magnitude (fig. 9.8-2), but were most prominent at about 50-percent throttle. The fact that oscillations of this magnitude were not observed in the chamber pressure or the fuel interface pressure measurements indicates that they were not real. Engine performance was not affected. Oscillations of this type have been observed at the White Sands Test Facility on numerous engines, on similar pressure measurement installations. The high magnitude pressure oscillations observed during the White Sands Test Facility tests were amplifications of much lower pressure oscillations in the system. The phenomenon has been demonstrated in ground tests where small actual oscillations were amplified by cavity resonance of a pressure transducer assembly, which contains a tee capped on one end with the transducer on another leg of the tee. This is similar to the interface pressure transducer installation. The resonance conditions will vary with the amount of helium trapped in the tee and the throttle setting.

### 9.8.2 System Pressurization

The oxidizer tank ullage pressure decayed from 158 to 95 psia during the period from lift-off to the first activation of the system at about 83 hours. During the period, the fuel tank ullage pressure decreased from 163 to 139 psia. These decays resulted from helium absorption into the propellants and were within the expected range.

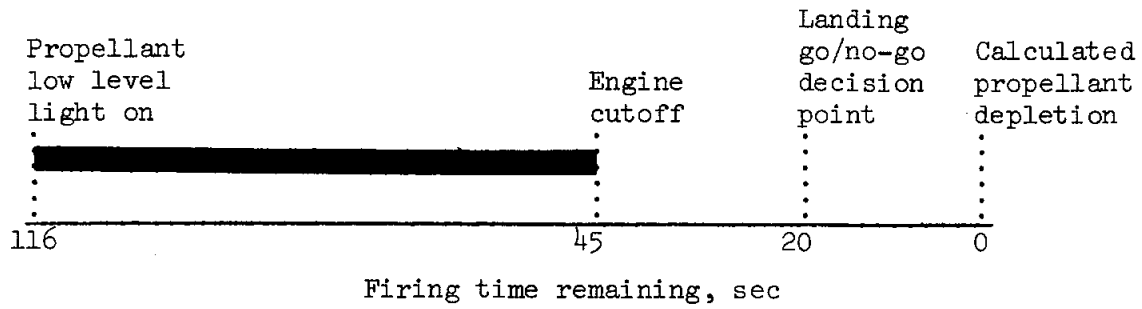
The measured pressure profile in the supercritical helium tank was normal. The preflight and inflight pressure rise rates were 8.3 and 6.4 psi/hr, respectively.

During propellant venting after landing, the fuel interface pressure increased rapidly to an off-scale reading. The fuel line had frozen during venting of the supercritical helium, trapping fuel between the pre-valve and the helium heat exchanger, and this fuel, when heated from engine soakback, caused the pressure rise. See section 16.2.2 for further discussion.

### 9.8.3 Gaging System Performance

During the descent orbit insertion maneuver and the early portion of powered descent, the two oxidizer propellant gages were indicating off-scale (greater than the maximum 95-percent indication), as expected. The fuel probes on the other hand were indicating approximately 94.5 percent instead of reading off-scale. The propellant loaded was equivalent to approximately 97.3 and 96.4 percent for oxidizer and fuel, respectively. An initial low fuel reading also had occurred on Apollo 10. As the firing continued, the propellant gages began to indicate consumption correctly. The tank 1 and tank 2 fuel probe measurements agreed throughout the firing. The tank 1 and tank 2 oxidizer probe measurements agreed initially, but they began to diverge until the difference was approximately 3 percent midway through the firing. For the remainder of the firing, the difference remained constant. The divergence was probably caused by oxidizer flowing from tank 2 to tank 1 through the propellant crossover line as a result of an offset in vehicle center of gravity.

The low level light came on at 102:44:30.4, indicating approximately 116 seconds of total firing time remaining, based on the sensor location. The propellant remaining timeline from the low level light indication to calculated propellant depletion is as follows.



The indicated 45 seconds to propellant depletion compares favorably with the postflight calculated value of 50 seconds to oxidizer tank 2 depletion. The 5-second difference is within the measurement accuracy of the system. The low level signal was triggered by the point sensor in either the oxidizer tank 2 or fuel tank 2.

NASA-S-69-3742

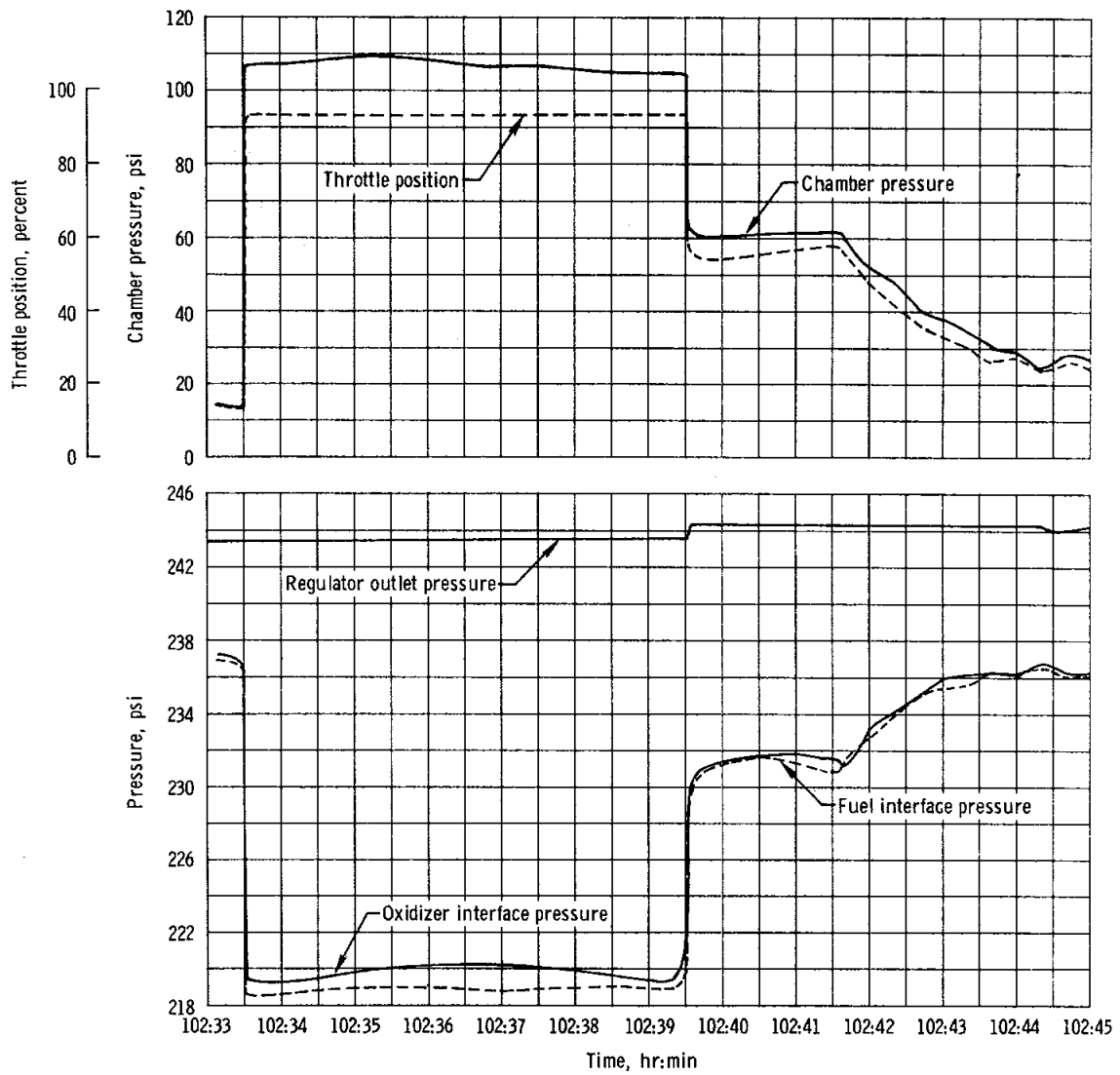


Figure 9.8-1. - Descent propulsion system performance.

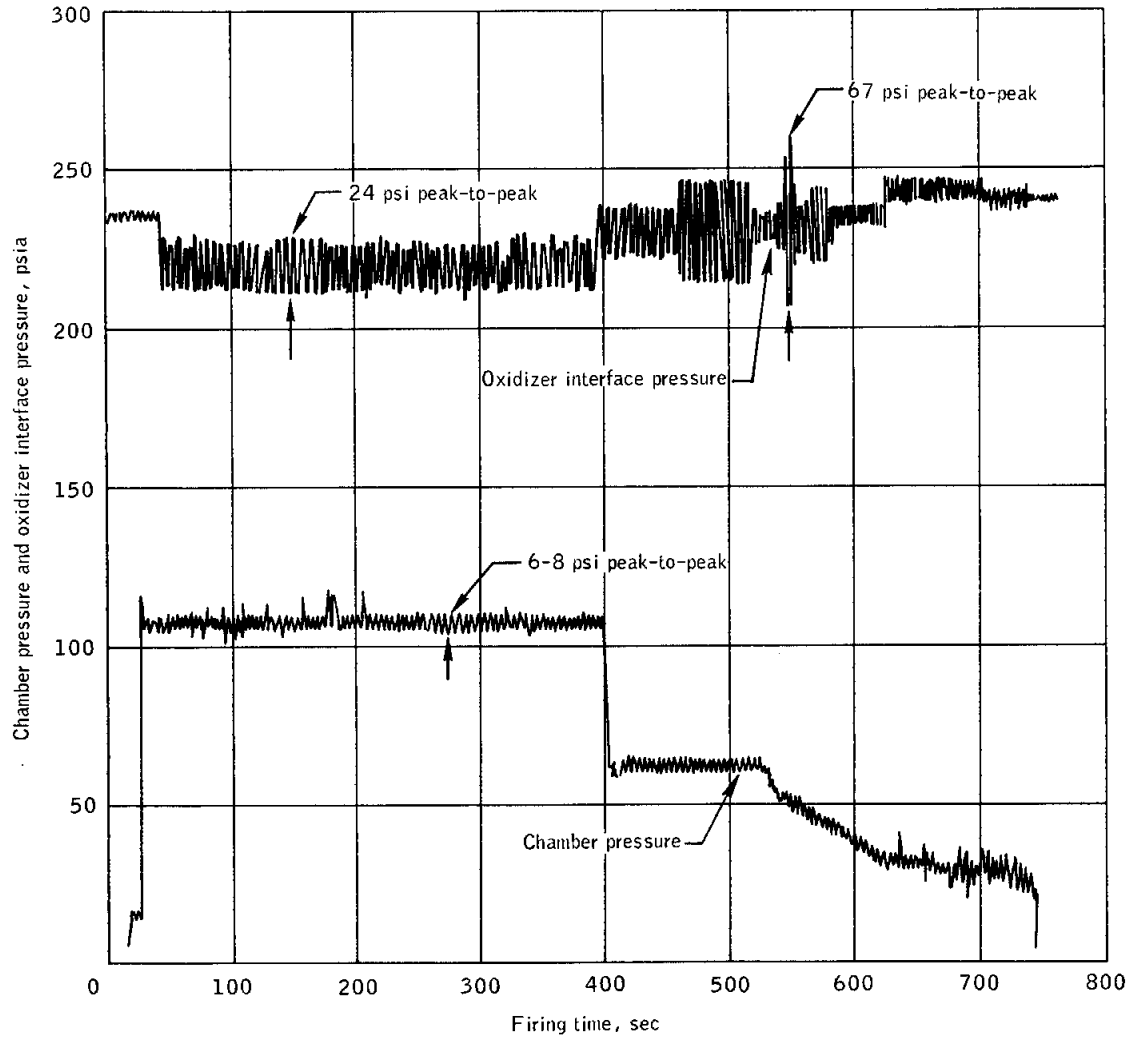


Figure 9.8-2.- Oxidizer interface pressure and chamber pressure oscillations.

## 9.9 ASCENT PROPULSION

The ascent propulsion system was fired for 435 seconds from lunar lift-off to orbital insertion. All aspects of system performance were nominal.

The regulator outlet pressure was 184 psia during the firing and returned to the nominal lock-up value of 188.5 psia after engine cutoff. Table 9.9-I presents a comparison of the actual and predicted performance. Based on engine flow rate data, the engine mixture ratio was estimated to be 1.595. The estimated usable propellant remaining at engine shutdown was 174 pounds oxidizer and 121 pounds fuel; these quantities are equivalent to 25 seconds additional firing time to oxidizer depletion.

After ascent propulsion system cutoff and during lunar orbit, the fuel and interface pressures increased from their respective flow pressures to lock-up, and then continued to increase approximately 3.6 psi for fuel and 11 to 12 psi for oxidizer. Loss of signal occurred approximately 39 minutes after engine shutdown as the vehicle went behind the moon. Pressure rises in the system were observed during both the Apollo 9 and 10 missions. This initial pressure rise after shutdown was caused by a number of contributing factors, such as, regulator lockup, heating of the ullage gas, and vaporization from the remaining propellants.

At reacquisition of signal (approximately 1 hour 29 minutes after shutdown) a drop of approximately 6 psi and 3.6 psi had occurred in the oxidizer and fuel pressures, respectively. Thereafter, the pressure remained at a constant level for the 4.5 hours that data were monitored, which rules out leakage. The apparent pressure drops had no effect on ascent propulsion system performance. The pressure drop was probably caused by a combination of ullage gas temperature cooling, pressure transducer drift resulting from engine heat soakback, and instrumentation resolution. Above 200° F, the accuracy of the pressure transducer degrades to ±4 percent (±10 psia) rather than the normal ±2 percent. A permanent shift may also occur at high temperatures. Thermal analysis indicates that the peak soakback temperatures were 200° to 235° F. Errors which may be attributed to various sources include a transducer shift of 4 percent, equivalent to ±10 psi; a pulse code modulation resolution of 2 counts, equivalent to 2 psi; and a 1 psi ullage pressure change which is effective only on the oxidizer side.

TABLE 9.9-I.- STEADY-STATE PERFORMANCE

Parameter	10 seconds after ignition		400 seconds after ignition	
	Predicted <sup>a</sup>	Measured <sup>b</sup>	Predicted <sup>a</sup>	Measured <sup>b</sup>
Regulator outlet pressure, psia . . . . .	184	184.5	184	184
Oxidizer bulk temperature, °F . . . . .	70	70.4	70	70.4
Fuel bulk temperature, °F . . . . .	70	71.0	70	71.0
Oxidizer interface pressure, psia . . . . .	170.6	170.0	169.6	169.5
Fuel interface pressure, psia . . . . .	170.4	169.3	169.5	168.8
Engine chamber pressure, psia . . . . .	122.6	122	122.5	122
Mixture ratio . . . . .	1.604	---	1.595	---
Thrust, lb . . . . .	3464	---	3439	---
Specific impulse, sec . . . . .	309.4	---	308.8	---

<sup>a</sup> Preflight prediction based on acceptance test data and assuming nominal system performance.

<sup>b</sup> Actual flight data with known biases removed.



## 9.10 ENVIRONMENTAL CONTROL SYSTEM

The environmental control system in the lunar module satisfactorily supported all lunar operations with only minor exceptions.

Routine water/glycol sampling during prelaunch activities showed the presence of large numbers of crystals which were identified as benzothiazyl disulfide. These crystals were being precipitated from a corrosion inhibitor in the fluid. The system was flushed and filtered repeatedly, but the crystals continued to be present. The fluid was then replaced with one containing a previously omitted additive (sodium sulfite), and crystals were still present but to a much lesser degree. A spacecraft pump package was run on a bench rig with this contaminated fluid, and the pump performance was shown to be unaffected, even for long durations. The filter in the test package did plug and the bypass valve opened during the test. Pump disassembly revealed no deterioration. It was then demonstrated that the crystals, while presenting an undesirable contamination, were not harmful to the system operation. The flight performance of the heat transport section was nominal. The investigation revealed that recently the corrosion inhibitor formulation was slightly modified. For future spacecraft, water/glycol with the original corrosion inhibitor formulation will be used.

Depressurization of the lunar module cabin through the bacteria filter for the extravehicular activity required more time than predicted. The data indicate that the cabin pressure transducer was reading high at the low end of its range; consequently, the crew could have opened the hatch sooner if the true pressure had been known.

During the sleep period on the lunar surface, the crew reported that they were too cold to sleep. Analysis of the conditions experienced indicated that once the crew were in a cold condition, there was not enough heat available in the environmental control system to return them to a comfortable condition. Ground tests have indicated that in addition to the required procedural changes which are designed to maintain heat in the suit circuit, blankets will be provided and the crew will sleep in hammocks.

Shortly after lunar module ascent, the crew reported that the carbon dioxide indicator was erratic, so they switched to the secondary cartridge. Also, the secondary water separator had been selected since one crewman reported water in his suit.

Evaluation of the erratic carbon dioxide indications determined that the carbon dioxide sensor had malfunctioned, and the circuit breaker was pulled. Erratic operation in the past has been caused by free water in

the optical section of the sensor. Further discussion of both the erratic carbon dioxide readings and water in the crewman's suit is contained in section 16.2.3 and 16.2.13, respectively.

## 9.11 RADAR

Performance of the rendezvous and landing radars was satisfactory, and antenna temperatures were always within normal limits. Range and velocity were acquired by the landing radar at slant ranges of approximately 44 000 and 28 000 feet, respectively. The tracker was lost briefly at altitudes of 240 and 75 feet; these losses were expected and are attributed to zero-Doppler effects associated with manual maneuvering.

## 9.12 CREW STATION

### 9.12.1 Displays and Controls

The displays and controls satisfactorily supported the mission, except that the mission timer stopped during the descent. After being deenergized for 11 hours, the timer was started again and operated properly throughout the remainder of the mission. The most probable cause of this failure was a cracked solder joint. This anomaly is discussed in greater detail in section 16.2.1.

### 9.12.2 Crew Provisions

The Commander and Lunar Module Pilot were provided with communications carrier adapter eartubes, having molded earpieces, for use in the lunar module cabin. The purpose of these earphone adapters is to increase the audio level to the ear. The Lunar Module Pilot used adapters throughout the lunar module descent and landing phase, but after landing, he found the molded earpieces uncomfortable and removed them. The Commander did not use adapters since his preflight experience indicated audio volume levels were adequate; the use of the adapters is based on crew preference. The Apollo 10 Lunar Module Pilot had used the adapters during his entire lunar module operational period and reported no discomfort. The Apollo 12 crew will also be provided adapters for optional use.

The crew commented that the inflight coverall garments would be more utilitarian if they were patterned after the standard one-piece summer flying suit. More pockets with a better method of closure, preferably zippers, were recommended and will be provided for evaluation by future crews.

The crew reported repeated fogging of the lunar module windows while the sunshades were installed. They had transferred two of the command module tissue dispensers to the lunar module and made use of them in cleaning the windows rather than using the window heaters for defogging. Tissue dispensers are being added to the lunar module stowage list.

### 9.13 CONSUMABLES

On the Apollo 11 mission, the actual usage of only three consumable quantities for the lunar module deviated by as much as 10 percent from the preflight predicted amounts. These consumables were the descent stage oxygen, ascent stage oxygen, and reaction control system propellant. The actual oxygen requirements were less than predicted because the leakage rate was lower than expected. The actual reaction control propellant requirement was greater than predicted because of the increased hover time during the descent phase.

The electrical power system consumables usage was within 5 percent of predicted flight requirements. The current usage from the descent stage batteries was approximately 8 percent less than predicted, and the ascent stage current usage was approximately 3 percent more than predicted. The deviations appear to have resulted from uncertainties in the predictions of reaction control heater duty cycles. Electrical power consumption is discussed further in section 9.3.

#### 9.13.1 Descent Propulsion System Propellant

The higher-than-predicted propellant usage by the descent propulsion system was caused by the maneuvering to avoid a large crater during the final stages of descent. Until that time, propellant usage had been nominal. Allowance for manual hover and landing point redesignation was in the preflight budget but was not considered part of the nominal usage.

The quantities of descent propulsion system propellant loading in the following table were calculated from readings and measured densities prior to lift-off.

Condition	Actual usage, lb			Preflight planned usage, lb
	Fuel	Oxidizer	Total	
Loaded	6975	11 209	18 184	18 184
Consumed				
Nominal				17 010
Redesignation				103
Margin for manual hover				114
Total	6724	10 690	17 414	17 227
Remaining at engine cutoff				
Tanks	216	458		
Manifold	35	61		
Total	251	519	770	957

#### 9.13.2 Ascent Propulsion System Propellant

The actual ascent propulsion system propellant usage was within 5 percent of the preflight predictions. The loadings in the following table were determined from measured densities prior to lift-off and from weights of off-loaded propellants. A portion of the propellants was used by the reaction control system during ascent stage operations.

Condition	Actual usage, lb			Preflight planned usage, lb
	Fuel	Oxidizer	Total	
Loaded	2020	3218	5238	5238
Consumed				
By ascent propulsion system prior to ascent stage jettison	1833	2934		
By reaction control system	23	46		
Total	1856	2980	4836	4966
Remaining at ascent stage jettison	164	238	402	272

## 9.13.3 Reaction Control System Propellant

The increased hover time for lunar landing resulted in a deviation of over 10 percent in the reaction control system propellant usage, as compared with the preflight predictions. Propellant consumption was calculated from telemetered helium tank pressure histories using the relationships between pressure, volume, and temperature. The mixture ratio was assumed to be 1.94 for the calculations.

Condition	Actual usage, lb			Preflight planned usage, lb
	Fuel	Oxidizer	Total	
Loaded				
System A	108	209		
System B	108	209		
Total	216	418	634	633
Consumed				
System A	46	90		
System B	62	121		
Total	108	211	319	253
Remaining at lunar module jettison				
System A	62	119		
System B	46	88		
Total	108	207	315	380

## 9.13.4 Oxygen

The actual oxygen usage was lower than the preflight predictions because oxygen leak rate from the cabin was less than the specification value. The actual rate was 0.05 lb/hr, as compared with the specification rate of 0.2 lb/hr. In the following table, the actual quantities loaded and consumed are based on telemetered data.

Condition	Actual usage, lb	Preflight planned usage, lb
Loaded (at lift-off)		
Descent stage	48.2	48.2
Ascent stage		
Tank 1	2.5	2.4
Tank 2	2.5	2.4
Total	5.0	4.8
Consumed		
Descent stage	17.2	21.7
Ascent stage		
Tank 1	1.0	1.5
Tank 2	0.1	0.0
Total	1.1	1.5
Remaining in descent stage at lunar lift-off	31.0	26.5
Remaining at ascent stage jettison		
Tank 1	1.5	0.9
Tank 2	2.4	2.4
Total	3.9	3.3

## 9.13.5 Water

The actual water usage was within 10 percent of the preflight predictions. In the following table, the actual quantities loaded and consumed are based on telemetered data.

Condition	Actual usage, lb	Preflight planned usage, lb
Loaded (at lift-off)		
Descent stage	217.5	217.5
Ascent stage		
Tank 1	42.4	42.4
Tank 2	42.4	42.4
Total	84.8	84.8
Consumed		
Descent stage	147.0	158.6
Ascent stage		
Tank 1	19.2	17.3
Tank 2	18.1	17.3
Total	37.3	34.6
Remaining in descent stage at		
lunar lift-off	70.5	58.9
Remaining at ascent stage jettison		
Tank 1	23.2	25.1
Tank 2	24.3	25.1
Total	46.5	50.2

## 9.13.6 Helium

The consumed quantities of helium for the main propulsion systems were in close agreement with the predicted amounts. Helium was stored ambiently in the ascent stage and supercritically in the descent stage. Helium loading was nominal, and the usage quantities in the following table were calculated from telemetered data. An additional 1 pound was stored ambiently in the descent stage for valve actuation and is not reflected in the values reported.

Condition	Descent propulsion		Ascent propulsion	
	Actual value, lb	Preflight planned value, lb	Actual value, lb	Preflight planned value, lb
Loaded	48.1	48.0	13.2	13.0
Consumed	39.5	38.4	8.8	9.4
Remaining	<sup>a</sup> 8.6	9.6	<sup>b</sup> 4.4	3.6

<sup>a</sup>At lunar landing.

<sup>b</sup>At ascent stage jettison.



## 10.0 EXTRAVEHICULAR MOBILITY UNIT PERFORMANCE

Extravehicular mobility unit performance was excellent throughout both intravehicular and extravehicular lunar surface operations. Crew mobility was very good during extravehicular activity, and an analysis of inflight cooling system data shows good correlation with ground data. The crew remained comfortable throughout the most strenuous surface operations. Because of the lower-than-expected metabolic rates, oxygen and water consumption was always below predicted levels.

The pressure garment assemblies, including helmet and intravehicular gloves, were worn during launch. The pressure garment assemblies of the Commander and Lunar Module Pilot incorporated new arm bearings, which contributed to the relatively unrestricted mobility demonstrated during lunar surface operations.

The Command Module Pilot had a problem with the fit of the lower abdomen and crotch of his pressure garment assembly, caused by the urine collection and transfer assembly flange. Pressure points resulted from insufficient size in the pressure garment assembly. On future flights, fit checks will be performed with the crewman wearing the urine collection and transfer assembly, fecal containment system, and liquid cooling garment, as applicable. In addition, the fit check will include a position simulating that which the crewman experiences during the countdown.

All three pressure garment assemblies and the liquid cooling garments for the Commander and Lunar Module Pilot were donned at approximately 97 hours in preparation for the lunar landing and surface operations. Donning was accomplished normally with help from another crewmen, as required. The suit integrity check prior to undocking was completed successfully with suit pressures decaying approximately 0.1 psi.

Wristlets and comfort gloves were taken aboard for optional use by the Commander and Lunar Module Pilot during the lunar stay. Because of the quick adaptation to 1/6-g, the light loads handled on this mission, and the short duration of the lunar surface activity, both crewmen elected to omit the use of the protective wristlets and comfort gloves. Without the protection of the wristlets, the Lunar Module Pilot's wrists were rubbed by the wrist rings, and the grasp capability of the Commander was reduced somewhat without the comfort gloves.

After attachment of the lunar module restraint, a pressure point developed on the instep of the Lunar Module Pilot's right foot because the restraint tended to pull him forward and outboard rather than straight down. However, he compensated by moving his right foot forward and outboard; this foot then took the majority of the load. The determination

of whether corrective action is required will be made after assessment of Apollo 12.

Extravehicular activity preparations proceeded smoothly. However, more time was required than planned for completing the unstowage of equipment and performing other minor tasks not normally emphasized in training exercises.

The oxygen purge system checkout was performed successfully. The crew encountered two problems during pre-egress activities: (1) difficulty in mating the remote control unit connector and (2) bumping items in the cabin because of the bulk of the portable life support system and oxygen purge system; as a result, one circuit breaker was broken and the positions of two circuit breakers were changed.

About 10 minutes was required to make each remote control unit connector. Each time the crewman thought the connector was aligned, the lock lever rotation caused the connector to cock off to one side. The problem is discussed further in section 16.3.2.

While waiting for the cabin to depressurize, the crew were comfortable even though the inlet temperature of the liquid-cooling garment reached about 90° F prior to sublimator startup. No thermal changes were noted at egress. The portable life support system and oxygen purge system were worn quite comfortably, and the back-supported mass was not objectionable in 1/6-g.

Analysis of the extravehicular activity data shows a good correlation with data from previous training conducted in the Space Environmental Simulation Laboratory facility. As expected, the feedwater pressure during the mission was slightly higher than that indicated during simulations. The difference results from the lunar gravitational effect on the head of water at the sublimator and transducer, the high point in the system. The only other discernible differences were in temperature readouts which generally indicated better performance (more cooling) than expected. Comfort in the liquid cooling garment was always adequate, although the data indicate a much higher temperature for the Commander than for the Lunar Module Pilot. This observation correlates with previous simulation experience, which shows that the Commander had a strong preference for a warmer body temperature than that desired by the Lunar Module Pilot. This parameter is controlled by each crewman to meet his comfort requirements. Operation of the extravehicular mobility unit while in the extravehicular mode was uneventful. There was never a requirement to change any of the control settings for the portable life support system other than the diverter valves, which both crewmen changed at their option for comfort.

Because of the lower-than-expected metabolic rates for the Lunar Module Pilot, and especially for the Commander, the actual oxygen and feedwater quantities consumed were lower than predicted. Consumables data are shown in the following table.

Condition	Commander		Lunar Module Pilot	
	Actual	Predicted	Actual	Predicted
Metabolic rate, Btu/hr . . .	800	1360	1100	1265
Time, min . . . . .	191	160	186	160
Oxygen, lb				
Loaded . . . . .	1.26	1.26	1.26	1.26
Consumed <sup>a</sup> . . . . .	0.54	0.68	0.60	0.63
Remaining . . . . .	0.72	0.58	0.66	0.63
Feedwater, lb				
Loaded . . . . .	8.6	8.5	8.6	8.5
Consumed <sup>b</sup> . . . . .	2.9	5.4	4.4	5.1
Remaining . . . . .	5.7	3.1	4.2	3.4
Power, W-h				
Initial charge <sup>c</sup> . . . . .	270	270	270	270
Consumed . . . . .	133	130	135	130
Remaining . . . . .	137	140	135	140

<sup>a</sup> Approximately 0.06 pound required for suit integrity check.

<sup>b</sup> Approximately 0.6 pound required for start-up and trapped water.

<sup>c</sup> Minimum prelaunch charge.

Crewman mobility and balance in the extravehicular mobility unit were sufficient to allow stable movement while performing lunar surface tasks. The Lunar Module Pilot demonstrated the capability to walk, to run, to change direction while running, and to stop movement without difficulty. He reported a tendency to tip backwards in the soft sand and noted that he had to be careful to compensate for the different location of the center of mass. The crewmen were observed to kneel down and contact the lunar surface while retrieving objects. The crew stated that getting down on one or both knees to retrieve samples and to allow closer inspection of the lunar surface should be a normal operating mode. Additional waist mobility would improve the ability to get closer to the lunar surface and, in addition, would increase downward visibility.

Each crewman raised his extravehicular visor assembly to various positions throughout the extravehicular activity and noted a back reflection of his face from the visor. The reflection was greatest with the sun shining approximately 90 degrees from the front of the visor assembly. With this reflection, it was difficult to see into shaded areas. In addition, the continuous movement from sunlight into shadow and back to sunlight required extra time because of the necessary wait for adaptation to changes in light intensity. Use of the blinders on the visor assembly could have alleviated the reflection and adaptation problem to some extent.

## 11.0 THE LUNAR SURFACE

Preflight planning for the Apollo 11 mission included a lunar surface stay of approximately 22 hours, including 2 hours 40 minutes that was allotted to extravehicular activities.

After landing, the crew performed a lunar module checkout to ascertain launch capability and photographed the landing area from the lunar module. Then, following an extensive checkout of the extravehicular mobility unit, the crewmen left the lunar module to accomplish the following activities:

- a. Inspection of the lunar module exterior
- b. Collection of a contingency sample, a bulk sample, and documented samples of lunar surface materials
- c. Evaluation of the physical characteristics of the lunar surface and its effects on extravehicular activity
- d. Deployment of the solar wind composition experiment and, at the end of the extravehicular activities, retrieval of the experiment for return to earth
- e. Deployment of the early Apollo scientific experiments package, consisting of the passive seismic experiment and the laser ranging retro-reflector.

Throughout the extravehicular activities, the crewmen made detailed observations and photographs to document the activities and lunar surface characteristics. A television camera provided real-time coverage of crew extravehicular activities.

Except for a portion of the planned documented sample collection not completed, the lunar surface activities were totally successful and all objectives were accomplished. As had been anticipated prior to flight, time did not permit exact performance of the documented sample collection. Two core samples and several loose rock samples were collected and returned. Insufficient time remained to fill the environmental and gas analysis sample containers, which were a part of the documented sampling.

Although the crewmen were operating in a new environment, they were able to complete the activities at a rate very close to that predicted before flight (see table 11-I).

Minor equipment malfunctions and operational discrepancies occurred during the extravehicular activity, but none prevented accomplishment of the respective tasks. Conversely, several operations were enhanced and equipment performance increased because of unexpected influences of the lunar environment.

The planned timeline of major surface activities compared with the actual time required is shown in table 11-I. The table lists the events sequentially, as presented in the Lunar Surface Operations Plan, and also includes several major unplanned activities. Crew rest periods, system checks, spontaneous observations, and unscheduled evaluations not necessarily related to the task being accomplished are not listed as separate activities but are included in the times shown.

During deployment of the television camera, several activities were accomplished, including some that were unplanned. The timeline provided a minimum amount of time for the Commander to remove the thermal blanket on the equipment compartment, change the camera lens, remove the tripod and camera from the compartment, and move the tripod-mounted camera to a remote location. This time also included a few minutes for viewing selected lunar features, positioning the camera to cover the subsequent surface activities, and returning to the compartment.

Throughout the extravehicular activity, both crewmen made observations and evaluations of the lunar environment, including lighting and surface features as well as other characteristics of scientific or operational interest. During the extravehicular activity, the sun angle ranged from 14-1/2 to 16 degrees. Most of the observations and evaluations will provide valuable information for future equipment design, crew training, and flight planning.

The evaluation of lunar surface experiments is contained in the following paragraphs. Photographic results, including those related to specific experiments, are discussed both in the appropriate sections and in a general description of lunar surface photography (section 11.6).

NOTE: Definitions of some scientific terms used in this section are contained in appendix E.

## 11.1 LUNAR GEOLOGY EXPERIMENT

### 11.1.1 Summary

The Apollo 11 spacecraft landed in the southwestern part of Mare Tranquillitatis at 0 degree 41 minutes 15 seconds north latitude and 23 degrees 26 minutes east longitude (fig. 11-1), approximately 20 kilometers southwest of the crater Sabine D. This part of Mare Tranquillitatis is crossed by relatively faint, but distinct, north-northwest trending rays (bright, whitish lines) associated with the crater Theophilus, which lies 320 kilometers to the southeast (ref. 4). The landing site is approximately 25 kilometers southeast of Surveyor V and 68 kilometers southwest of the impact crater formed by Ranger VIII. A fairly prominent north-northeast trending ray lies 15 kilometers west of the landing site. This ray may be related to Alfraganus, 160 kilometers to the southwest, or to Tycho, about 1500 kilometers to the southwest. The landing site lies between major rays but may contain rare fragments derived from Theophilus, Alfraganus, Tycho, or other distant craters.

About 400 meters east of the landing point is a sharp-rimmed ray crater, approximately 180 meters in diameter and 30 meters deep, which was unofficially named West crater. West crater is surrounded by a blocky ejecta (material ejected from crater) apron that extends almost symmetrically outward about 250 meters from the rim crest. Blocks as much as 5 meters across exist from on the rim to as far as approximately 150 meters, as well as in the interior of the crater. Rays of blocky ejecta, with many fragments 1/2 to 2 meters across, extend beyond the ejecta apron west of the landing point. The lunar module landed between these rays in a path that is relatively free of extremely coarse blocks.

At the landing site, the lunar surface consists of fragmental debris ranging in size from particles too fine to be resolved by the naked eye to blocks 0.8-meter in diameter. This debris forms a layer that is called the lunar regolith. At the surface, the regolith (debris layer) is porous and weakly coherent. It grades downward into a similar, but more densely packed, substrate. The bulk of the debris layer consists of fine particles, but many small rock fragments were encountered in the subsurface as well as on the surface.

In the vicinity of the lunar module, the mare surface has numerous small craters ranging in diameter from a few centimeters to several tens of meters. Just southwest of the lunar module is a double crater 12 meters long, 6 meters wide, and 1 meter deep, with a subdued raised rim. About 50 meters east of the lunar module is a steep-walled, but shallow, crater 33 meters in diameter and 4 meters deep, which was visited by the Commander near the end of the extravehicular period.

All of the craters in the immediate vicinity of the lunar module have rims, walls, and floors of relatively fine grained material, with scattered coarser fragments that occur in about the same abundance as on the intercrater areas. These craters are up to a meter deep and suggest having been excavated entirely in the regolith because of the lack of blocky ejecta.

At the 33-meter-diameter crater east of the lunar module, the walls and rim have the same texture as the regolith elsewhere; however, a pile of blocks was observed on the floor of the crater. The crater floor may lie close to the base of the regolith. Several craters of about the same size, with steep walls and shallow flat floors, or floors with central humps, occur in the area around the landing site. From the depths of these craters, the thickness of the regolith is estimated to range from 3 to 6 meters.

Coarse fragments are scattered in the vicinity of the lunar module in about the same abundance as at the Surveyor I landing site in the Ocean of Storms at 2 degrees 24.6 minutes south latitude and 43 degrees 18 minutes west longitude. They are distinctly more abundant than at the other Surveyor landing sites on the maria, including the landing site of Surveyor V northwest of the lunar module. The Surveyor I landing site was near a fresh blocky rim crater, but beyond the apron of coarse blocky ejecta, as was the Apollo 11 site. It may be inferred that many rock fragments in the immediate vicinity of the spacecraft, at both the Surveyor I and Apollo 11 landing sites, were derived from the nearby blocky rim crater. Fragments derived from West crater may have come from depths as great as 30 meters beneath the mare surface, and may be direct samples of the bedrock from which the local regolith was derived.

Rock fragments at the Apollo 11 landing site have a wide variety of shapes and most are embedded to varying degrees in the fine matrix of the regolith. A majority of the rocks are rounded or partially rounded on their upper surfaces, but angular fragments of irregular shape are also abundant. A few rocks are rectangular slabs with a faint platy (parallel fractures) structure. Many of the rounded rocks, when collected, were found to be flat or of irregular angular shape on the bottom. The exposed part of one unusual rock, which was not collected, was described by the Commander as resembling an automobile distributor cap. When this rock was dislodged, the sculptured "cap" was found to be the top of a much bigger rock, the buried part of which was larger in lateral dimensions and angular in form.

The evidence suggests that processes of erosion are taking place on the lunar surface which lead to the gradual rounding of the exposed surfaces of rocks. Several processes may be involved. On some rounded rock surfaces, the individual clasts (fragmented material) and grains



that compose the rocks and the glassy linings of pits on the surfaces have been left in raised relief by general wearing away or ablation of the surface. This differential erosion is most prominent in microbreccia (rocks consisting of small sharp fragments embedded in a fine-grained matrix). The ablation may be caused primarily by small particles bombarding the surface.

Some crystalline rocks of medium grain size have rounded surfaces that have been produced by the peeling of closely spaced exfoliation (thin, concentric flakes) shells. The observed "distributor cap" form may have developed by exfoliation or by spalling of the free surfaces of the rock as a result of one or more energetic impacts on the top surface.

Minute pits from a fraction of a millimeter to about 2 millimeters in diameter and from a fraction of a millimeter to one millimeter deep, occur on the rounded surfaces of most rocks. As described in a subsequent paragraph, many of these pits are lined with glass. They are present on a specimen of microbreccia which has been tentatively identified in photographs taken on the lunar surface and for which a preliminary orientation of the rock at the time it was collected has been obtained (see fig. 11-2). The pits are found primarily on the upper side. They clearly have been produced by a process acting on the exposed surface. They do not resemble impact craters produced in the laboratory (at collision velocities of 7 km/sec and below), and their origin remains to be explained.

#### 11.1.2 Regional Geologic Setting

Mare Tranquillitatis is a mare (refs. 5 and 6) of irregular form. Two characteristics suggest that the mare material is relatively thin: an unusual ridge ring, named Lamont, located in the southwest part of the mare, may be localized over the shallowly buried rim of a pre-mare crater; and no large positive gravity anomaly, like those over the deep mare-filled circular basins, is associated with Mare Tranquillitatis (ref. 7).

The southern part of Mare Tranquillitatis is crossed by relatively faint but distinct north-northwest trending rays and prominent secondary craters associated with the crater Theophilus. About 15 kilometers west of the landing site is a fairly prominent north-northeast trending ray. The ray may be related to either of the craters Alfraganus or Tycho, located 160 and 1500 kilometers, respectively, to the southwest.

A hill of highland-like material protrudes above the mare surface 52 kilometers east-southeast of the landing site. This structure suggests the mare material is very thin in this region, perhaps no more than a few hundred meters thick.

## 11.1.3 Analysis of Transmitted Geologic Data

*Location of the landing site.*- The landing site was tentatively identified during the lunar surface stay on the basis of observations transmitted by the crew. The Commander reported avoiding a blocky crater the size of a football field during landing, and observed a hill that he estimated to be from 1/2 to 1 mile west of the lunar module. The lunar module was tilted 4.5 degrees east (backward) on the lunar surface.

During the first command and service module pass after lunar module landing (about 1 to 1-1/2 hours after landing), the first of several different landing site locations, computed from the onboard computer and from tracking data, was transmitted to the Command Module Pilot for visual search (see section 5.5). The first such estimate of the landing site was northwest of the planned landing ellipse. The only site near this computed location that could have matched the reported description was near North crater at the northwest boundary of the landing ellipse. However, this region did not match the description very closely. Later, computed estimates indicated the landing site was considerably south of the earlier determination, and the areas near the West crater most closely fit the description. These data were transmitted to the Command Module Pilot on the last pass before lunar module lift-off, but the Command Module Pilot's activities at this time did not permit visual search. The location just west of West crater was confirmed by rendezvous radar tracking of the command module by the lunar module near the end of the lunar stay period and by the descent photography.

The crater that was avoided during landing was reported by the crew to be surrounded by ejecta containing blocks up to 5 meters in diameter and which extended 100 to 200 meters from the crater rim, indicating a relatively fresh, sharp-rimmed ray crater. The only crater in the 100- to 200-meter size range that meets the description and is in the vicinity indicated by the radar is West crater, near the southwest edge of the planned landing ellipse. A description by the Commander of a double crater about 6 to 12 meters in size and south of the lunar module shadow plus the identification of West crater, the hill to the west, and the 21- to 24-meter crater reported behind the lunar module, formed a unique pattern from which the landing site was determined to within about 8 meters. The 21 to 24 meter crater has been since identified by photometry as being 33 meters in diameter. The returned sequence-camera descent photography confirmed the landing point location. The position corresponds to coordinates 0 degree 41 minutes 15 seconds north latitude and 23 degrees 26 minutes 0 second east longitude on figure 5-10.

*Geology.*- The surface of the mare near the landing site is unusually rough and of greater geologic interest than expected before flight. Television pictures indicated a greater abundance of coarse fragmental debris than at any of the four Surveyor landing sites on the maria except that of Surveyor I (ref. 8). It is likely that the observed fragments and the

samples returned to earth had been derived from varying depths beneath the original mare surface and have had widely different histories of exposure on the lunar surface.

The major topographic features in the landing area are large craters a few hundred meters across, of which four are broad subdued features and the fifth is West crater, located 400 meters east of the landing point. Near the lunar module, the surface is pocked by numerous small craters and strewn with fragmental debris, part of which may have been generated during the impact formation of West crater.

Among the smaller craters, both sharp, raised-rim craters and relatively subdued craters are common. They range in size from a few centimeters to 20 meters. A slightly subdued, raised-rim crater (the reported 21- to 24-meter crater) 33 meters in diameter and 4 meters deep occurs about 50 meters east of the lunar module, and a double crater (the reported doublet crater) about 12 meters long and 6 meters wide lies 10 meters west of the lunar module at 260 degrees azimuth (see fig. 5-8).

The walls and floors of most of the craters are smooth and uninterrupted by either outcrops or conspicuous stratification. Rocks present in the 33-meter crater are larger than any of those seen on the surface in the vicinity of the lunar module.

The bulk of the surface layer consists of fine-grained particles which tended to adhere to the crewmen's boots and suits, as well as equipment, and was molded into smooth forms in the footprints.

The regolith is weak and relatively easily trenched to depths of several centimeters. At an altitude of approximately 30 meters prior to landing, the crewmen observed dust moving away from the center of the descent propulsion blast. The lunar module foot pads penetrated to a maximum depth of 7 or 8 centimeters. The crewmen's boots left prints generally from 3 millimeters to 2 or 3 centimeters deep. Surface material was easily dislodged by being kicked, (see fig. 11-3). The flagpole and drive tubes were pressed into the surface to a depth of approximately 12 centimeters. At that depth, the regolith was not sufficiently strong to hold the core tubes upright. A hammer was used to drive them to depths of 15 to 20 centimeters. At places, during scooping operations, rocks were encountered in the subsurface.

The crewmen's boot treads were sharply preserved and angles as large as 70 degrees were maintained in the print walls (see fig. 11-4). The surface disturbed by walking tended to break into slabs, cracking outward about 12 to 15 centimeters from the edge of footprints.

The finest particles of the surface had some adhesion to boots, gloves, suits, hand tools, and rocks on the lunar surface. On repeated

contact, the coating on the boots thickened to the point that their color was completely obscured. When the fine particles were brushed off the suits, a stain remained.

During the television panorama, the Commander pointed out several rocks west of the television camera, one of which was tabular and standing on edge, protruding 30 centimeters above the surface. Strewn fields of angular blocks, many more than 1/2 meter long, occur north and west of the lunar module. In general, the rocks tended to be rounded on top and flat or angular on the bottom.

The cohesive strength of rock fragments varied, and in some cases the crew had difficulty in distinguishing aggregates, or clods of fine debris, from rocks.

#### 11.1.4 Geologic Photography and Mapping Procedures

Television and photographic coverage of the lunar surface activities constitute most of the fundamental data for the lunar geology experiment and complement information reported by the crew. (Refer to section 11.6 for a discussion of lunar surface photography.)

Photographic documentation of the lunar surface was acquired with a 16-mm sequence camera, a close-up stereo camera, and two 70-mm still cameras (one with an 80-mm lens and the other with a 60-mm lens). The camera with the 60-mm lens was intended primarily for gathering geological data, and a transparent plate containing a 5 by 5 matrix of crosses was mounted in front of the film plane to define the coordinate system for the optical geometry.

*Photographic procedures.*- Photographic procedures planned for the lunar geologic experiment for use with the 70-mm Hasselblad with 60-mm lens were the panorama survey, the sample area survey, and the single sample survey.

The panorama survey consists of 12 pictures taken at intervals of 30 degrees in azimuth and aimed at the horizon with the lens focused at 22.5 meters. The resulting pictures, when matched together as a mosaic, form a continuous 360-degree view of the landing site from which relative azimuth angles can be measured between features of interest. The Commander took a partial panorama from the foot of the ladder immediately after he stepped to the lunar surface (fig. 11-5, part a). Also, three panoramas were taken from the vertices of an imaginary triangle surrounding the lunar module (for example, fig. 11-5, parts b and c).

The sample area survey consists of five or more pictures taken of an area 4 to 6 meters from the camera. The first picture was taken approximately down sun, and the succeeding three or more pictures were taken cross sun, with parallel camera axes at intervals of 1 to 2 meters.

The single sample survey was designed to record structures that were particularly significant to the crew. The area was photographed from a distance of 1.6 meters. As with the sample area survey, the first picture was taken approximately down sun, and the next two were taken cross sun.

*Geologic study from photographs.*- The lunar geology experiment includes a detailed study and comparison of photographs of the rock samples in the Lunar Receiving Laboratory with photographs taken on the lunar surface. The method of study involves the drawing of geologic sketch maps of faces that show features of the rock unobscured by dust and a detailed description of the morphologic (relating to former structure), structural, and textural features of the rock, together with an interpretation of the associated geologic features. The photographs and geologic sketches constitute a permanent record of the appearance of the specimens before subsequent destructive laboratory work.

A small rock, 2 by 4 by 6 centimeters, which was collected in the contingency sample has been tentatively located on the lunar-surface photographs. Photographs of the rock show a fresh-appearing vesicular (small cavity resulting from vaporization in a molten mass) lava, similar in vesicularity, texture, and crystallinity to many terrestrial basalts (see fig. 11-2).

The third largest rock in the contingency sample was collected within 2 meters of the lunar module. The rock has an ovoid shape, tapered at one end, with broadly rounded top and nearly flat bottom (see fig. 11-6). It is about 5.5 centimeters long, 2 to 3 centimeters wide, and 1-1/2 to 2 centimeters thick. Part of the top and sides are covered with fine dust but the bottom and lower sides indicate a very fine-grained clastic rock with scattered subrounded rock fragments up to 5 millimeters in diameter. The rounded ovoid shape of the top and sides of this specimen is irregular in detail. In the central part, there is a broad depression formed by many coalescing shallow irregular cavities and round pits. Adjacent to this, toward the tapered front end, round deep pits are abundant and so closely spaced that some intersect others and indicate more than one generation of pitting. The bottom is marked by two parallel flat surfaces, separated by an irregular longitudinal scarp about 1/2 to 1 millimeter high. A few small cavities are present, but no round pits of the type found on the top. An irregular fracture pattern occurs on the bottom of the rock. The fractures are short, discontinuous, and largely filled with dust. On the top of the rock near the tapered end, a set of short fractures, 3 to 9 millimeters long, is largely dust-filled and does not appear

to penetrate far into the rock. On a few sides and corners, there are short, curved fractures which may be exfoliation features. This rock is a breccia of small subangular lithic fragments in a very fine grained matrix. It resembles the material of the surface layer as photographed by the stereo closeup camera, except that this specimen is indurated.

*Photometric evaluation.*- The general photometric characteristics of the surface were not noticeably different from those observed at the Surveyor landing sites. See section 11.7 for a more detailed evaluation of the photography during lunar orbit and surface operations. The albedo of the lunar surface decreased significantly where it was disturbed or covered with a spray of fine grained material kicked up by the crew. At low phase angles, the reflectance of the fine grained material was increased noticeably, especially where it was compressed smoothly by the crewmen's boots.

#### 11.1.5 Surface Traverse and Sampling Logs

The television pictures and lunar surface photographs were used to prepare a map showing the location of surface features, emplaced instruments, and sample localities (fig. 11-7). The most distant single traverse was made to the 33-meter-diameter crater east of the lunar module.

The contingency sample was taken in view of the sequence camera just outside quad IV of the lunar module. Two scoopfuls filled the sample bag with approximately 1.03 kilograms of surface material. The areas where the samples were obtained have been accurately located on a frame (fig. 11-8) of the sequence film taken from the lunar module window. Both scoopfuls included small rock fragments (figs. 11-9 and 11-10) visible on the surface from the lunar module windows prior to sampling.

The Commander pushed the handle of the scoop apparatus 15 to 20 centimeters into the surface very near the area of the first scoop. Collection of the bulk sample included 17 or 18 scoop motions made in full view of the television camera and at least five within the field of view of the sequence camera.

The two core-tube samples were taken in the vicinity of the solar wind composition experiment. The first core location was documented by the television camera and by two individual Hasselblad photographs. The second core-tube location, as reported by the crew, was in the vicinity of the solar wind composition experiment.

Approximately 20 selected, but unphotographed, grab samples (about 6 kilograms) were collected in the final minutes of the extravehicular activity. These specimens were collected out to a distance of 10 to 15 meters in the area south of the lunar module and near the east rim of the large double crater.

The sites of three of the contingency sample rocks have been located and those of two tentatively identified by comparing their shapes and sizes from the lunar module window and surface photographs with photographs taken of the specimens at the Lunar Receiving Laboratory. Evidence for the identification and orientation of rock A (fig. 11-9) was obtained from the presence of a saddle-shaped notch on its exposed side. Rock C (fig. 11-10) was characterized by the pitlike depression visible on the photographs. Rock B (fig. 11-9) is only about 2 centimeters across and at this time has not been correlated with the specimens in the Lunar Receiving Laboratory.

During bulk sampling, rock fragments were collected primarily on the northeast rim of the large double crater southwest of the lunar module.

Photographs taken of the documented sample locality (south of the plus Z foot pad) before and after the extravehicular activity were searched for evidence of rocks that might have been included in the sample. Figures 11-11 and 11-12 illustrate that three rather large rocks (up to several tens of centimeters) were removed from their respective positions shown on the photographs taken before the extravehicular activity. A closer view of these three rocks was obtained during the extravehicular activity (fig. 11-13).

#### 11.1.6 Geologic Hand Tools

The geologic hand tools (fig. A-5) included the contingency sample container, scoop, hammer, extension handle, two core tubes, tongs, two large sample bags, weighing scale, two sample return containers, and the gnomon. Also included were small sample bags, numbered for use in documentation. All tools were used except the gnomon. The crew reported that, in general, the tools worked well.

The large scoop, attached to the extension handle, was used primarily during bulk sampling to collect rocks and fine-grained material. The large scoop was used about 22 times in collecting the bulk sample. As expected from 1/6-g simulations, some lunar material tended to fall out of the scoop at the end of scooping motion.

The hammer was used to drive the core tubes attached to the extension handle. Hard enough blows could be struck to dent the top of the extension handle. The extension handle was attached to the large scoop for bulk sampling and to the core tubes for taking core samples.

Two core tubes were driven and each collected a satisfactory sample. Each tube had an internally tapered bit that compressed the sample 2.2:1 within the inside of the tube. One tube collected 10 centimeters of

sample and the other 13 centimeters. The tubes were difficult to drive deeper than about 20 centimeters. This difficulty may have been partially caused by the increasing density of the fine grained material with depth or other mechanical characteristics of the lunar regolith. The difficulty of penetration was also a function of the tapered bit, which caused greater resistance with increased penetration. One tube was difficult to attach to the extension handle. When this tube was detached from the extension handle, the butt end of the tube unscrewed and was lost on the lunar surface. The tubes were opened after the flight and the split liners inside both were found to be offset at the bit end. The Teflon core follower in one tube was originally inserted upside down, and the follower in the other tube was inserted without the expansion spring which holds it snugly against the inside of the split tube.

The tongs were used to pick up the documented samples and to right the closeup stereo camera when it fell over on the lunar surface.

One of the large sample bags was used for stowage of documented samples. The other large bag, the weigh bag, was used for stowage of bulk samples.

The weighing scale was used only as a hook to suspend the bulk sample bag from the lunar module during the collection of bulk samples.

## 11.2 LUNAR SOIL MECHANICS EXPERIMENT

The lunar surface at the Apollo 11 landing site was similar in appearance, behavior, and mechanical properties to the surface encountered at the Surveyor maria landing sites. Although the lunar surface material differs considerably in composition and in range of particle shapes from a terrestrial soil of the same particle size distribution, it does not appear to differ significantly in its engineering behavior.

A variety of data was obtained through detailed crew observations, photography, telemetered dynamic data, and examination of the returned lunar surface material and rock samples. This information permitted a preliminary assessment of the physical and mechanical properties of the lunar surface materials. Simulations based on current data are planned to gain further insight into the physical characteristics and mechanical behavior of lunar surface materials.

### 11.2.1 Observed Characteristics

The physical characteristics of lunar surface materials were first indicated during the lunar module descent when the crew noticed a transparent sheet of dust resembling a thin layer of ground fog that moved radially outward and caused a gradual decrease in visibility.



Inspection of the area below the descent stage after landing revealed no evidence of an erosion crater and little change in the apparent topography. The surface immediately underneath the engine skirt had a singed appearance and was slightly etched (fig. 11-14), indicating a sculpturing effect extending outward from the engine. Visible streaks of eroded material extended only to a maximum distance of about 1 meter beyond the engine skirt.

During ascent, there were no visible signs of surface erosion. The insulation blown off the descent stage generally moved outward on extended flight paths in a manner similar to that of the eroded surface particles during descent, although the crew reported the insulation was, in some cases, blown for several miles.

The landing gear foot pads had penetrated the surface 2 to 5 centimeters and there was no discernible throwout from the foot pads. Figures 11-15 through 11-18 show the foot pads of the plus Y and minus Z and Y struts. The same photographs show the postlanding condition of the lunar contact probes, which had dug into and were dragged through the lunar surface, as well as some surface bulldozing by the minus Z foot pad in the direction of the left lateral motion during landing. The bearing pressure on each foot pad is 1 or 2 psi.

The upper few centimeters of surface material in the vicinity of the landing site are characterized by a brownish, medium gray, slightly cohesive, granular material that is largely composed of bulky grains in the size range of silt to fine sand. Angular to subrounded rock fragments ranging in size up to 1 meter are distributed throughout the area. Some of these fragments were observed to lie on the surface, some were partially buried, and others were only barely exposed.

The lunar surface is relatively soft to depths of 5 to 20 centimeters. The surface can be easily scooped, offers low resistance to penetration, and provided slight lateral support for the staffs, poles, and core tubes. Beneath this relatively soft surface, resistance to penetration increases considerably. The available data seem to indicate that this increase is caused by an increase in the density of material at the surface rather than the presence of rock fragments or bedrock.

Natural clods of fine-grained material crumbled under the crewmen's boots. This behavior, while not fully understood, indicates cementation and/or natural cohesion between the grains. Returned lunar surface samples in nitrogen were also found to cohere again to some extent after being separated, although to a lesser degree than observed on the lunar surface in the vacuum.

The surface material was loose, powdery, and fine-grained and exhibited adhesive characteristics. As a result, the surface material tended to stick to any object with which it came in contact, including

the crewmen's boots and suits, the television cable, and the lunar equipment conveyor. During operation of the lunar equipment conveyor, the powder adhering to it was carried into the spacecraft cabin. Also, sufficient fine-grained material collected on the equipment conveyor to cause binding.

The thin layer of material adhering to the crewmen's boot soles caused some tendency to slip on the ladder during ingress. Similarly, the powdery coating of the rocks on the lunar surface was also somewhat slippery (see section 4.0). A fine dust confined between two relatively hard surfaces, such as a boot sole and a ladder rung or a rock surface, would be expected to produce some tendency to slip.

The lunar surface provided adequate bearing strength for standing, walking, loping, or jumping, and sufficient traction for starting, turning, or stopping.

Small, fresh crater walls having slope angles of up to 15 degrees could be readily negotiated by the crew. Going straight down or up was found to be preferable to traversing these slopes sideways. The footing was not secure because the varying thickness of unstable layer material tended to slide in an unpredictable fashion.

The material on the rim and walls of larger-size craters, with wall slopes ranging up to 35 degrees appeared to be more compact and stable than that on the smaller craters which were traversed.

### 11.2.2 Examination of Lunar Material Samples

Preliminary observations were made of the general appearance, structure, texture, color, grain-size distribution, consistency, compactness, and mechanical behavior of the fine-grained material sampled by the core tubes and collected during the contingency, bulk, and documented sampling. These investigations will be reported in greater detail in subsequent science reports.

### 11.3 EXAMINATION OF LUNAR SAMPLES

A total of 22 kilograms of lunar material was returned by the Apollo 11 crew; 11 kilograms were rock fragments more than 1 centimeter in diameter and 11 kilograms were smaller particulate material. Because the documented sample container was filled by picking up selected rocks with tongs, the container held a variety of large rocks (total 6.0 kilograms). The total bulk sample was 14.6 kilograms.

The returned lunar material may be divided into the following four groups:

- a. Type A - fine-grained crystalline igneous rock containing vesicles (cavities)
- b. Type B - medium-grained vuggy (small cavity) crystalline igneous rock
- c. Type C - breccia (rock consisting of sharp fragments imbedded in a fine grained matrix) consisting of small fragments of gray rocks and fine material
- d. Type D - fines (very small particles in a mixture of various sizes).

The major findings of a preliminary examination of the lunar samples are as follows:

- a. Based on the fabric and mineralogy, the rocks can be divided into two groups: (1) fine and medium grained crystalline rocks of igneous origin, probably originally deposited as lava flows, then dismembered and redeposited as impact debris, and (2) breccias of complex history.
- b. The crystalline rocks are different from any terrestrial rock and from meteorites, as shown by the bulk chemistry studies and analyses of mineral concentration in a specified area.
- c. Erosion has occurred on the lunar surface, as indicated by the rounding on most rocks and by the evidence of exposure to a process which gives the rocks a surface appearance similar to sandblasted rocks. No evidence exists of erosion by surface water.
- d. The probable presence of the assemblage iron-troilite-ilmenite and the absence of any hydrated phase suggest that the crystalline rocks were formed under extremely low partial pressures of oxygen, water, and sulfur (in the range of those in equilibrium with most meteorites).
- e. The absence of secondary hydrated minerals suggests that there has been no surface water at Tranquility Base at any time since the rocks were exposed.
- f. Evidence of shock or impact metamorphism is common in the rocks and fines.
- g. All the rocks display glass-lined surface pits which may have been caused by the impact of small particles.

h. The fine material and the breccia contain large amounts of all noble gases with elemental and isotopic abundances that almost certainly were derived from the solar wind. The fact that interior samples of the breccias contain these gases implies that the breccias were formed at the lunar surface from material previously exposed to the solar wind.

i. The  $^{40}\text{K}/^{40}\text{Ar}$  measurements on igneous rock indicate that those rocks crystallized 3 to 4 billion years ago. Cosmic-ray-produced nuclides indicate the rocks have been within 1 meter of the surface for periods of 20 to 160 million years.

j. The level of indigenous volatilizable and/or pyrolyzable organic material appears to be extremely low (considerably less than 1 ppm).

k. The chemical analyses of 23 lunar samples show that all rocks and fines are generally similar chemically.

l. The elemental constituents of lunar samples are the same as those found in terrestrial igneous rocks and meteorites. However, several significant differences in composition occur: (1) some refractory elements (such as titanium and zirconium) are notably enriched, and (2) the alkalis and some volatile elements are depleted.

m. Elements that are enriched in iron meteorites (that is, nickel, cobalt, and the platinum group) were either not observed or were low in abundance.

n. The chemical analysis of the fines material is in excellent agreement with the results of the alpha-back-scattering measurement at the Surveyor V site.

o. Of 12 radioactive species identified, two were cosmogenic radio-nuclides of short half life, ( $^{52}\text{Mn}$  which has a half life of 5.7 days and  $^{48}\text{V}$  which has a half life of 16.1 days.

p. Uranium and thorium concentrations were near the typical values for terrestrial basalts; however, the potassium-to-uranium ratio determined for lunar surface material is much lower than such values determined for either terrestrial rocks or meteorites.

q. The observed high concentration of  $^{26}\text{Al}$  is consistent with a long cosmic-ray exposure age inferred from the rare-gas analysis.

r. No evidence of biological material has been found to date in the samples.

s. The lunar surface material at the lunar module landing site is predominantly fine grained, granular, slightly cohesive, and incompressible.

The hardness increases considerably at a depth of 6 inches. The soil is similar in appearance and behavior to the soil at the Surveyor landing sites.

#### 11.4 PASSIVE SEISMIC EXPERIMENT

The early Apollo scientific experiment package seismometer system met the requirements of the experiment for the first 2 weeks of its operation. No significant instrumental deficiencies were encountered despite the fact that maximum operating temperatures exceeded those planned for the instrument by as much as 50° F.

Analysis of calibration pulses and signals received from various crew activities indicated that all four seismometers were operating properly. Instrument response curves derived from calibration pulses are shown in figure 11-19.

During the first lunar day, data were acquired at 11:40:39 p.m. e.s.t., July 20, and transmission was stopped by command from Mission Control Center at 06:58:46 a.m. e.s.t., August 3, when the predicted rate of solar panel output power drop occurred at lunar sunset. This occurred approximately 4 hours and 40 minutes before the sunset time predicted for a flat surface, indicating an effective slope of 2 degrees 20 minutes upward to the west at the deployment site.

##### 11.4.1 Seismic Background Noise

A histogram of seismic background level recorded by the short-period seismometer is shown in figure 11-20. The high amplitude signal just after turn-on was produced in part by crew activities and in part by a signal generated within the lunar module, presumably by venting processes. The levels decreased steadily until the background had disappeared completely by July 29 (8 days after turn-on). Thus, continuous seismic background signal near 1 hertz is less than 0.3 millimicron, which corresponds to system noise. Maximum signal levels of 1.2 microns at frequencies of 7 to 8 hertz were observed during the period when the crewmen were on the surface.

Except for the occasional occurrence of transient signals, the background seismic signal level on the long period vertical component seismometer is below system noise; that is, below 0.3 millimicron over the period range from 1 to 10 seconds (see figs. 11-21 and 11-22). This is between one hundred and ten thousand times less than the average background levels observed on earth in the normal period range for microseisms (6 to 8 seconds).

Continuous background motions of relatively large amplitude (10 to 30 millimicrons peak to peak) were observed on the records from both horizontal component seismometers. The amplitude of these motions decreased below the level of the 54-second oscillation for a 2- to 3-day interval centered near lunar noon when the rate of change of external temperature with time would be at a minimum. The signals are of very low frequency (period is on the order of 20 seconds to 2 minutes). It is assumed that these signals correspond to tilting of the instruments caused by a combination of thermal distortions of the metal pallet which serves as the instrument base and a rocking motion of the pallet produced by thermal effects in the lunar surface material. However, the horizontal component of true lunar background seismic background level at shorter periods (less than 10 seconds) also appears to be less than 0.3 millimicron.

#### 11.4.2 Near Seismic Events

Four types of high frequency signals produced by local sources (within 10 to 20 kilometers of the seismic experiment package) have been tentatively identified.

Signals produced by crew activities were prominent on the short period seismometer from initial turn-on until lunar module ascent. Such signals were particularly large when the crewmen were in physical contact with the lunar module. The signal produced when the Commander ascended the ladder to reenter the lunar module is shown in figure 11-23.

The predominant frequency of all of these signals is 7.2 to 7.3 hertz. The spectrum of the signal produced by the Commander on the lunar module ladder, shown in figure 11-23, contains this prominent peak. This frequency is approximately equal to the fundamental resonant mode of vibration of the lunar module structure. The spectrum of the signal generated when one of the portable life support systems, weighing 75 pounds, struck the ground after being ejected from the lunar module is shown in figure 11-24 for comparison. The spectrum again shows the 7.2 hertz peak; however, it is important to note that the two peaks at 11.3 and 12.3 hertz would be dominant if the spectrum were corrected for instrument response. The signal at 7.2 hertz was presumably generated because the portable life support system struck the lunar module porch and the ladder as it fell to the surface.

The 7.2 hertz peak is shifted to 8.0 hertz in the spectra of signals generated after departure of the lunar module ascent stage. Resonances in the remaining descent stage structure would be expected to shift to higher frequencies when the mass of the ascent stage was removed.

Some of the signals observed had the same characteristics as did landslides on earth. The signals have emergent onsets and last up to 7 minutes for the largest trains. Low frequencies (1/10 to 1/15 hertz) associated with the largest of these trains are also observed on the seismograms from the long period, vertical component seismometer. As shown in figure 11-25, these events began on July 25 (2 days before lunar noon), subsided during the lunar noon period, and continued after lunar noon with more frequent and much smaller events. The activity is believed to be related in some way to thermal effects. More than 200 of these events were identified in total.

High frequency signals were observed from an undetermined source. These signals began with large amplitudes on the short period seismometer and gradually decreased over a period of 8 days until they disappeared completely on July 30. During the final stages of this activity, the signals became very repetitive with nearly identical structure from train to train. As mentioned previously, the predominant frequency of these signals was approximately 7.2 hertz before lunar module ascent and 8.0 hertz after lunar module ascent. The complete disappearance of these signals and their nearly identical form have led to the tentative conclusion that they were produced by the lunar module itself, presumably by venting processes.

Some of the observed high frequency signals might possibly have been from nearby meteoroid impacts. An analysis is being made of several high-frequency signals which may correspond to meteoroid impacts at ranges of a few kilometers, or less, from the passive seismic experiment package. Substantive remarks on these events cannot be made until spectra of the signals are computed.

#### 11.4.3 Distant Seismic Events

During the period from July 22 through 24, three of the recorded signals appear to be surface waves, that is, seismic waves which travel along the surface of the moon in contrast to body waves which would travel through the interior of the moon. Body waves (compressional and shear waves) produced by a given seismic source normally travel at higher velocities than surface waves and, hence, are observed on the record before the surface waves. No body waves were observed for these events. The wave trains begin with short period oscillations (2 to 4 seconds) which gradually increase in period to 16 to 18 seconds, when the train dispersed.

A wave train having similar characteristics has been observed on the long period vertical channel in association with a series of discrete pulses on the short period vertical channel. In this case, the

long period wave train observed on the record is simply the summation of transients corresponding to these pulses and, hence, is of instrumental origin. A dispersion of this type is commonly observed on earth in various types of surface waves and is well understood. The dispersion, or gradual transformation of an initial impulsive source to an extended oscillatory train of waves, is produced by propagation through a wave guide of some type. The events observed appear only on the horizontal component seismometers. Such horizontally polarized waves, when observed on earth, would be called Love waves. On earth, surface waves which have a vertical component of motion (Rayleigh waves) are usually the most prominent waves on the record from a distant event. Several possibilities are presently under study to explain these waves.

#### 11.4.4 Engineering Evaluation

From acquisition of initial data to turn-off, the passive seismic experiment package operated a total of 319 hours 18 minutes. The power and data subsystems performed extremely well, particularly in view of the abnormally high operating temperatures. The output of the solar cell array was within 1 to 2 watts of the expected value and was always higher than the 27-watt minimum design specification.

About 99.8 percent of the data from the passive seismic experiment package are preserved on tape. Several occurrences of data dropout were determined to be caused by other than the seismic experiment system.

The passive seismic experiment showed good response, detecting the crewmen's footsteps, portable life support system ejection from the lunar module, and movements by the crew in the lunar module prior to lift-off.

Data from the dust and thermal radiation engineering measurement were obtained continuously except for brief turn-off periods associated with power/thermal management.

A total of 916 commands were transmitted and accepted by the passive seismic experiment package. Most of these commands were used to level the equipment, thereby correcting for the thermal distortions of the supporting primary structure.

The downlink signal strength received from the passive seismic experiment package agree with the predictions and for the 30-foot antennas ranged from minus 135 to minus 139 dBm and for the 85-foot antennas ranged from minus 125 to minus 127 dBm.

Normal operation was initiated on the second lunar day by command from Mission Control Center at 1:00 a.m. e.s.t., August 19, approximately 20 hours after sunrise at Tranquility Base. Transmission stopped at



6:08 a.m. e.s.t., September 1, with the loss of solar panel output power at lunar sunset. The loss of transmission was disappointing, however, at the time of the loss, the passive seismic experiment package had exceeded the design objectives.

Data received, including seismometer measurements, were consistent with those recorded at corresponding sun elevation angles on the first lunar day. Operation continued until the data system did not respond to a transmitted command at 3:50 a.m. e.s.t., August 25 (approximately noon of the second lunar day). No command was accepted by the passive seismic experiment package after that time, despite repeated attempts under a wide variety of conditions.

The initial impact of the loss of command capability was the inability to re-level the long period seismic sensors. As a result, all three axes became so unbalanced that the data were meaningless; however, meaningful data continued to be received from the short period sensor.

Valid short period seismic sensor and telemetry data continued to be received and recorded during the remainder of the day. Component temperatures and power levels continued to be nominal, corresponding with values recorded at the same sun angles on the first lunar day. The passive seismic experiment was automatically switched to the standby mode of operation when the power dropped at sunset.

Downlink transmission was acquired during the third lunar day at 5:27 p.m. e.s.t., September 16. Transmission stopped at 6:31 a.m., e.s.t., October 1, with the loss of power at lunar sunset. Efforts to restore command communications were unsuccessful. The passive seismic experiment remained in the standby mode of operation, with no seismic data output. Data from the dust and thermal radiation engineering measurement went off-scale low at 10:00 p.m. e.s.t., September 16, and remained off-scale throughout the day. The downlink signal strength, component temperatures, and power levels continued to be nominal, corresponding with values recorded at the same sun angles on previous days.

#### 11.4.5 Conclusions

Tentative conclusions based on a preliminary analysis of data obtained during the first recording period (July 21 to August 3) are as follows:

a. The seismic background signal on the moon is less than the threshold sensitivity of the instrument (0.3 millimicron). Seismometers are able to operate on the lunar surface at 10 to 100 times higher sensitivity than is possible on earth.

b. Allowing for the difference in size between the earth and the moon, the occurrence of seismic events (moonquakes or impacts) is much less frequent for the moon than the occurrence of earthquakes on the earth.

c. Despite the puzzling features of the possible surface wave trains, an attempt is being made to find lunar models compatible with the data. A detailed discussion of the surface wave trains will be contained in a subsequent science report.

d. Erosional processes corresponding to landslides along crater walls may be operative within one or more relatively young craters located within a few kilometers of the passive seismic experiment package.

#### 11.5 LASER RANGING RETRO-REFLECTOR EXPERIMENT

The laser ranging retro-reflector was deployed approximately 14 meters south-southwest of the lunar module in a relatively smooth area (see fig. 11-26). The bubble was not precisely in the center of the leveling device but was between the center and the innermost division in the southwest direction, indicating an off-level condition of less than 30 minutes of arc. The shadow lines and sun compass markings were clearly visible, and the crew reported that these devices showed that the alignment was precise.

On August 1, 1969, the Lick Observatory obtained reflected signals from the laser reflector. The signal continued to appear for the remainder of the night. Between 5 and 8 joules per pulse were transmitted at 6943 angstroms. Using the 120-inch telescope, each returned signal contained, on the average, more than one photo-electron, a value that indicates that the condition of the reflector on the surface is entirely satisfactory.

On August 20, 1969, the McDonald Observatory obtained reflected signals from the reflector. The round trip signal time was found to be 2.49596311 ( $\pm 0.00000003$ ) seconds, an uncertainty equivalent to a distance variation of 4.5 meters.

These observations, made a few days before lunar sunset and a few days after lunar sunrise, show that the thermal design of the reflector permits operation during sun illuminated periods and that the reflector survived the lunar night satisfactorily. They also indicate no serious degradation of optical performance from flaked insulation, debris, dust, or rocket exhaust products which scattered during lunar module lift-off.

The scientific objectives of the laser ranging experiment — studies of gravitation, relativity, and earth and lunar physics — can be achieved only by successfully monitoring the changes in the distances from stations on earth to the laser beam reflector on the moon with an uncertainty of about 15 centimeters over a period of many years. The McDonald Observatory is being instrumented to make daily observations with this accuracy, and it is expected that several other stations capable of this ranging precision will be established.

#### 11.6 SOLAR WIND COMPOSITION EXPERIMENT

The solar wind composition experiment was designed to measure the abundance and the isotopic compositions of the noble gases in the solar wind ( $\text{He}^3$ ,  $\text{He}^4$ ,  $\text{Ne}^{20}$ ,  $\text{Ne}^{21}$ ,  $\text{Ne}^{22}$ ,  $\text{Ar}^{36}$ , and  $\text{Ar}^{38}$ ). The experiment consisted of a specially prepared aluminum foil with an effective area of 0.4 square meter (see fig. 11-27). When exposed to the solar wind at the lunar surface, solar wind particles which arrived with velocities of a few hundred kilometers per second would penetrate the foil to a depth of several millionths of a centimeter and become firmly trapped. Particle measurements would be accomplished by heating the returned foil in an ultra high vacuum system. The evolving atoms would then be analyzed in statically operated mass spectrometers, and the absolute and isotopic quantities of the particles determined.

The experiment was deployed approximately 6 meters from the lunar module. The staff of the experiment penetrated 13.5 centimeters into the surface.

The foil was retrieved after 77 minutes exposure to the lunar environment. The return unit was placed into a special Teflon bag and returned to earth in the lunar sample return container. A portion of the foil was cut out, placed into a metal gasket vacuum container, and heat sterilized at  $125^\circ\text{C}$  for 39 hours. The section of foil has been released for analysis, and results will be reported in science reports.

#### 11.7 PHOTOGRAPHY

A preliminary analysis of the Apollo 11 photographic activities is discussed in the following paragraphs. During the mission, all nine of the 70-mm and all 13 of the 16-mm film magazines carried onboard the spacecraft were exposed. Approximately 90 percent of the photographic objectives were accomplished, including about 85 percent of the requested lunar photography and about 46 percent of the targets of opportunity.

## 11.7.1 Photographic Objectives

The lunar surface photographic objectives were:

- a. Long distance coverage from the command module
- b. Lunar mapping photography from orbit
- c. Landed lunar module location
- d. Sequence photography during descent, lunar stay, and ascent
- e. Still photographs through the lunar module window
- f. Still photographs on the lunar surface
- g. Closeup stereo photography

## 11.7.2 Film Description and Processing

Special care was taken in the selection, preparation, calibration, and processing of film to maximize returned information. The types of film included and exposed are listed in the following table.

Film type	Film size, mm	Magazines	ASA speed	Resolution, lines/mm	
				High contrast	Low contrast
SO-368, color	16	5	64	80	35
	70	2			
	35	1			
SO-168, color	16	8	*	63	32
	70	2			
3400, black and white	70	5	40	170	70

\*Exposed and developed at ASA 1000 for interior photography and ASA 160 for lunar surface photography.

## 11.7.3 Photographic Results

Lunar photography from the command module consisted mainly of specified targets of opportunity together with a short strip of vertical still photography from about 170 to 120 degrees east longitude. Most of the other 70-mm command module photography of the surface consisted of features selected by the crew.

The 16-mm sequence camera photography was generally excellent. The descent film was used to determine the location of the landed lunar module. One sequence of 16-mm coverage taken from the lunar module window shows the lunar surface change from a light to a very dark color wherever the crew walked.

The quantity and quality of still photographs taken through the lunar module window and on the lunar surface were very good. On some sequences, to insure good photography the crew varied the exposures one stop in either direction from the exposure indicated. The still photography on the surface indicates that the landing site location determined by use of the 16-mm descent film is correct.

The closeup stereo photography provides good quality imagery of 17 areas, each 3 by 3 inches. These areas included various rocks, some ground surface cracks, and some rock which appears to have been partially melted or splattered with molten glass.

#### 11.7.4 Photographic Lighting and Color Effects

When the lunar surface was viewed from the command module window, the color was reported to vary with the viewing angle. A high sun angle caused the surface to appear brown, and a low sun angle caused the surface to appear slate gray. At this distance from the moon, distinct color variations were seen in the maria and are very pronounced on the processed film. According to the crew, the 16-mm photographs are more representative of the true surface color than are the 70-mm photographs. However, prints from both film types have shown tints of green and other shades which are not realistic. Underexposure contributes to the green tint, and the printing process can increase this effect. Each generation away from the original copy will cause a further increase in this tinting. On the original film, the greenish tint in the dark, or underexposed, areas is a function of spacecraft window transmission characteristics and low sun angles. For Apollo 12, the master film copies will be color corrected, which should greatly minimize unrealistic tinting.

A 16-mm film sequence from the lunar module window shows crew activities in both gray and light brown areas. As the crewmen moved, the gray area, which is apparently softer, deeper material, turned almost black. The crewmen's feet visibly sank in this gray material as they kicked moderate quantities. The light brown area did not appreciably change color with crewmen's movement.

The color pictures in which the fine grained parts of the lunar surface appear gray are properly exposed, while those pictures in which the lunar surface is light brown to light tan are generally overexposed.

The rocks appear light gray to brownish gray in pictures that are properly exposed for the rocks and vary from light tan to an off-white where overexposed. The crew reported that fine grained lunar material and rocks appeared to be gray to dark gray. These materials appeared slightly brownish gray when observed near zero phase angle. Small brownish, tan, and golden reflections were observed from rock surfaces.

The targets and associated exposure values for each frame of the lunar surface film magazines were carefully planned before flight. Nearly all of the photographs were taken at the recommended exposure settings.

Preflight simulations and training photography indicated that at shutter speeds of 1/125 second or longer, a suited crewman could induce excessive image motion during exposure. A shutter speed of 1/250 second was therefore chosen to reduce the unwanted motion to an acceptable level. Corresponding f-stops were then determined which would provide correct exposure under predicted lunar lighting conditions. At the completion of the training program, the crew was proficient at photographing different subjects under varying lighting conditions.

To simplify camera operations, f-stops of 5.6 and 11 were chosen for exposures in the cross-sun and down-sun directions, respectively. This exposure information was provided on decals attached to the film magazines and was used successfully.

The crewmen chose exposures for unusual lighting conditions. For example, the photographs of the Lunar Module Pilot descending the ladder were taken at an f-stop of 5.6 and a speed of 1/60 second, and the best photograph of the landing-leg plaque was taken at an exposure of 5.6 and 1/30 second. When a high depth of field was required, exposures were made with smaller apertures and correspondingly slower shutter speeds to maintain equivalent exposure values. The crewmen usually steadied the camera against the remote-control-unit bracket on the suit during these slower-speed exposures.

A preliminary analysis of all lunar surface exposures indicates that the nominal shutter speed of 1/250 second appears to be a good compromise between depth of field and crew-induced image motion. In those specific instances where a slower shutter speed was required, either because of depth-of-field or lighting considerations, the crew was able to minimize image motion by steadying the camera. However, the selection of the 1/250-second speed will be re-evaluated for continued general photography.

Figures 11-3, 11-4, 11-18, and 11-28 are representative of lunar surface photography.

TABLE 11-I.- COMPARATIVE TIMES FOR PLANNED LUNAR SURFACE EVENTS

Event	Planned time, min:sec	Actual time, min:sec	Difference, min:sec	Remarks
Final preparation for egress	10:00	20:45	+10:45	Approximately 8 min 30 sec spent from cabin pressure reading of 0.2 psia until hatch opening
Commander egress to surface	10:00	8:00	-2:00	
Commander environmental familiarization	5:00	2:05	-2:00	
Contingency sample collection	4:30	3:36	-0:55	Performed out of sequence with planned timeline
Preliminary spacecraft checks	6:30	6:35	+0:05	Out of sequence
Lunar Module Pilot egress to surface	7:00	7:00	0:00	Approximately 2 min 10 sec for portable life support system checks
Commander photography and observation		2:40	+2:40	
Television camera deployment (partial)	4:00	4:50	+0:50	Deployment interrupted for activity with plaque
Lunar Module Pilot environmental familiarization	6:00	15:00	+9:00	Includes assisting Commander with plaque and television camera deployment
Television camera deployment (complete)	7:00	11:50	+4:50	Includes photography of solar composition experiment and comments on lunar surface characteristics
Solar wind composition experiment deployment	4:00	6:20	+2:20	
Bulk sample and extravehicular mobility unit evaluation (complete)	14:30	18:45	+4:15	
Lunar module inspection by Lunar Module Pilot	14:00	18:15	+4:15	
Lunar Module inspection by Commander	15:30	17:10	+1:40	Includes closeup camera photographs
Off-load experiment package	7:00	5:20	-1:40	From door open to door closed
Deploy experiment package	9:00	13:00	+4:00	From selection of site to completion of photography; trouble leveling the equipment
Documented sample collection	34:00	17:50	-16:10	Partially completed
Lunar Module Pilot ingress	4:00	4:00	0:00	
Transfer sample return container	14:00	9:00	-5:00	
Commander ingress	9:30	6:14	-3:16	Includes cabin repressurization

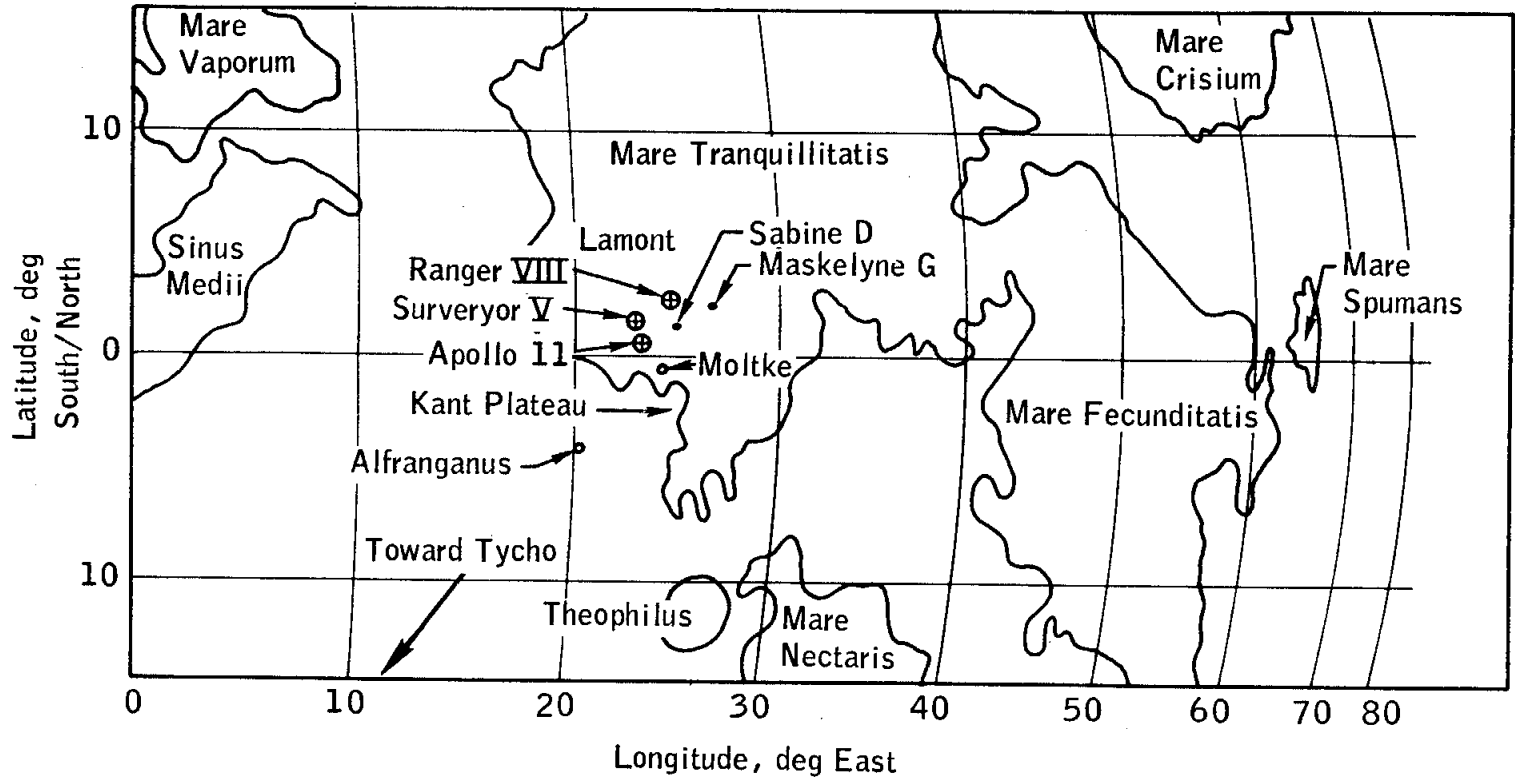


Figure 11-1.- Landing location relative to Surveyor V and Ranger VIII.



NASA-S-69-3745

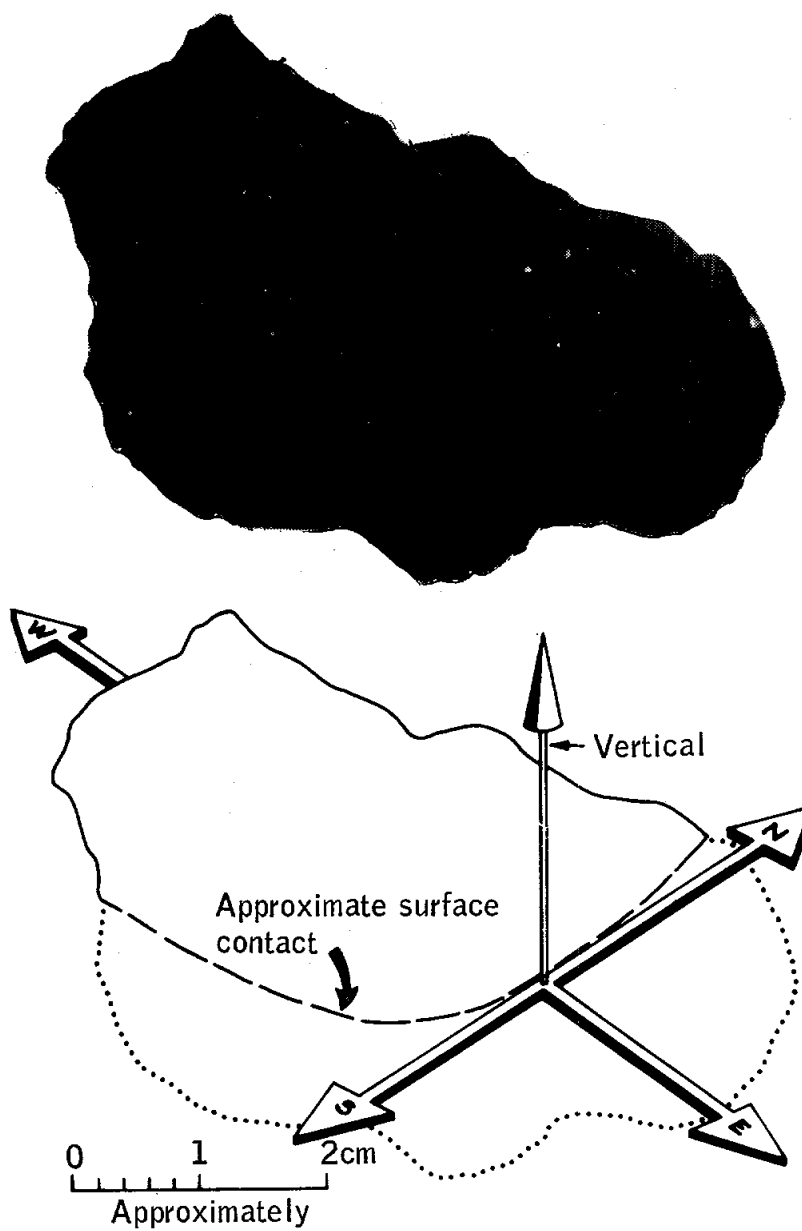


Figure 11-2.- Lunar sample and relative position on lunar surface.

NASA-S-69-3746

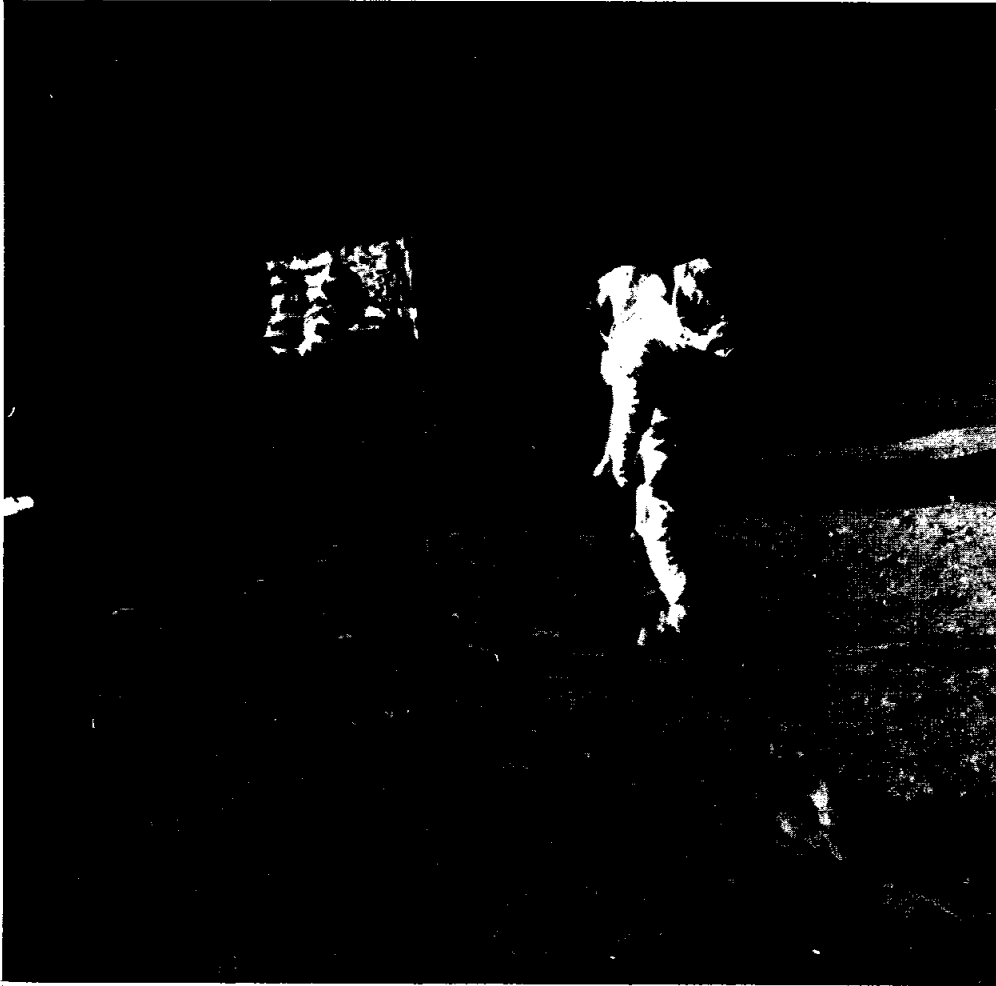


Figure 11-3.- Surface characteristics around footprints .

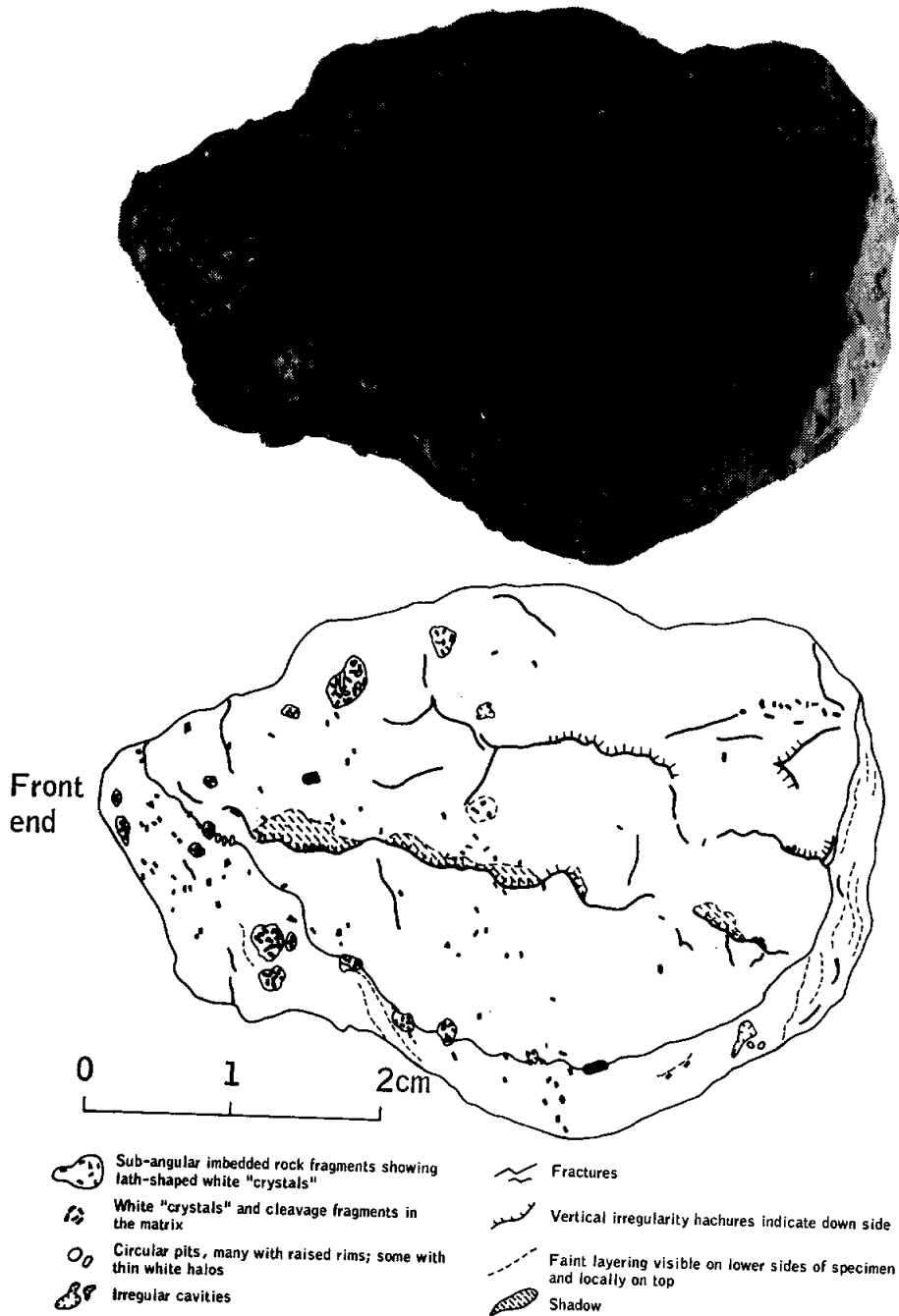
NASA-S-69-3749



(a) Top and side view.

Figure 11-6.- Detailed view of lunar rock.

NASA-S-69-3750



(b) Bottom and partial side view.

Figure 11-6.- Concluded.

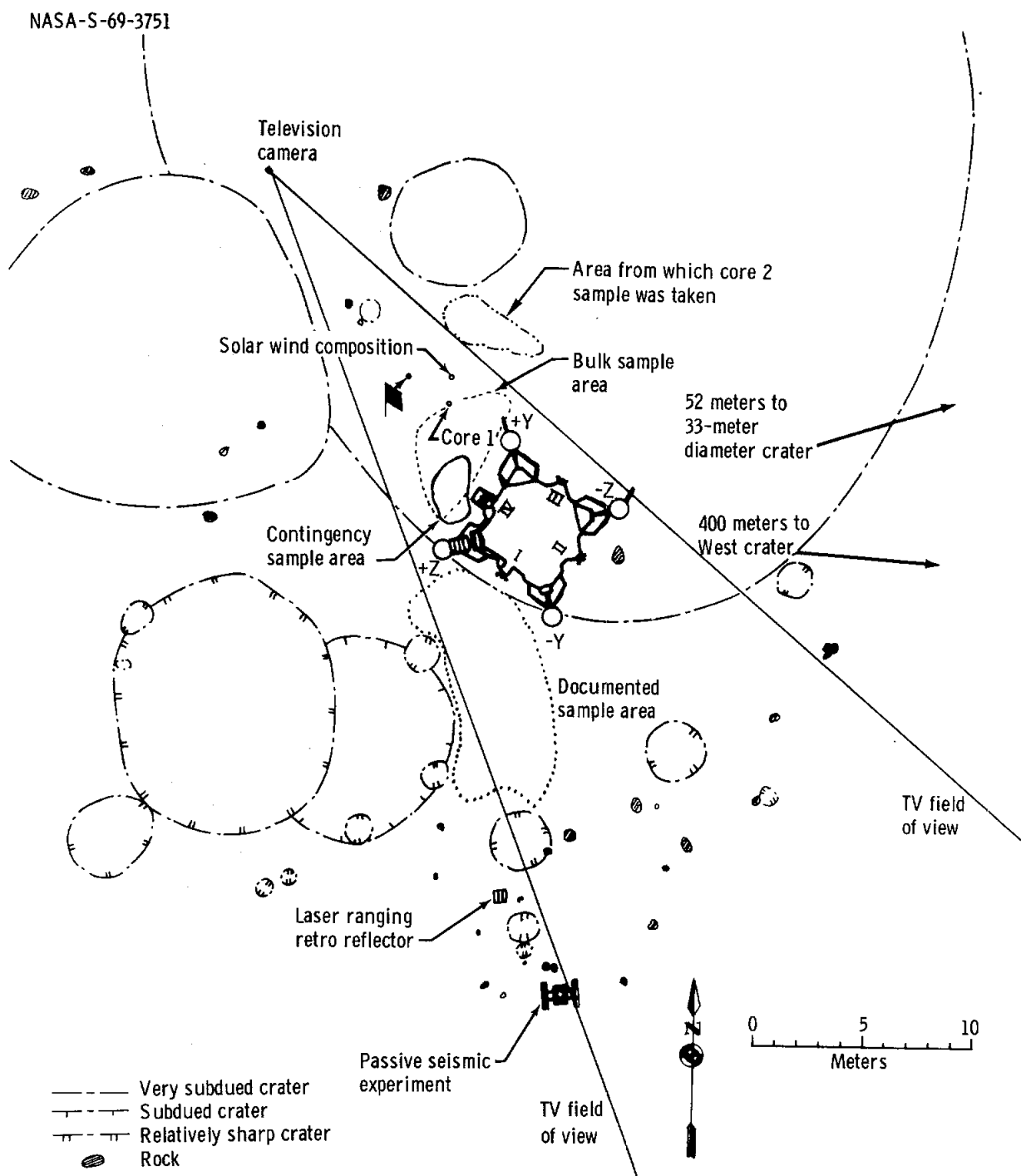


Figure 11-7. - Diagram of lunar surface activity areas.

NASA-S-69-3752

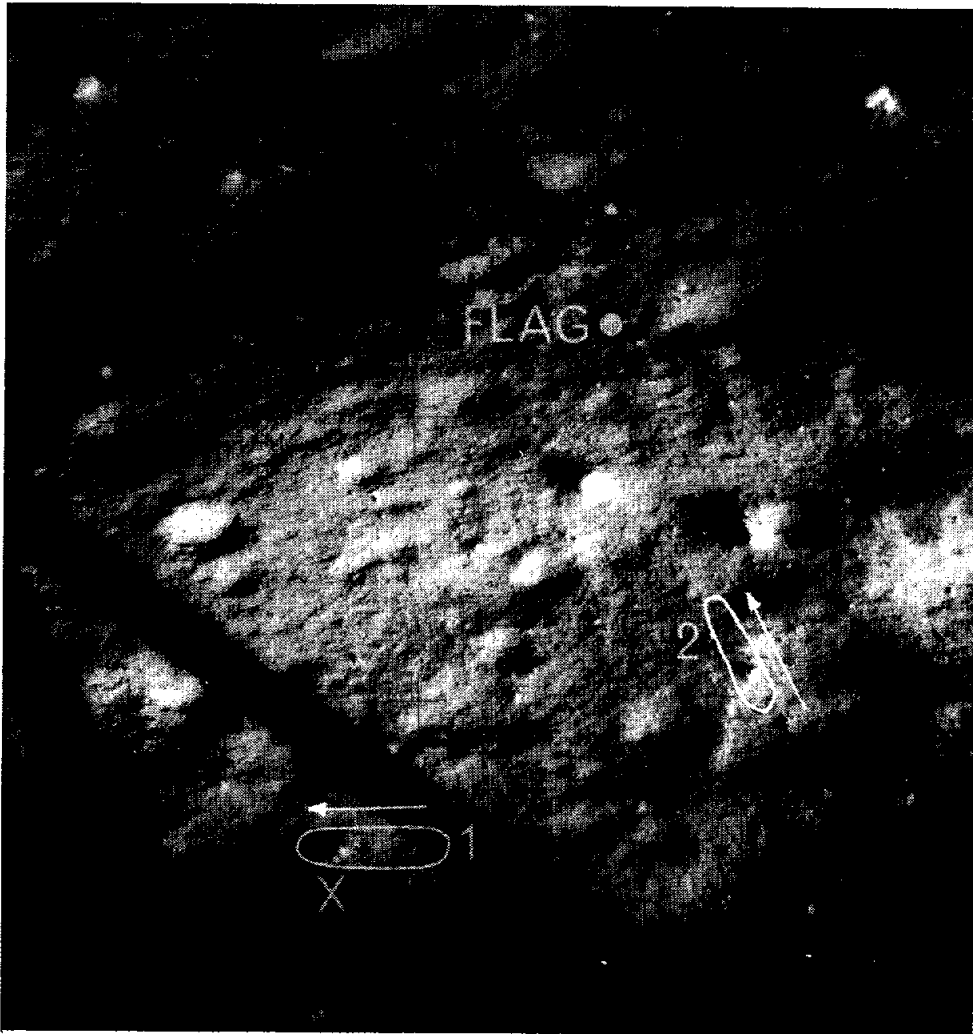


Figure 11-8.- Location of two contingency sample scoops.

NASA-S-69-3753



Figure 11-9.- Rocks collected during first contingency sample scoop.

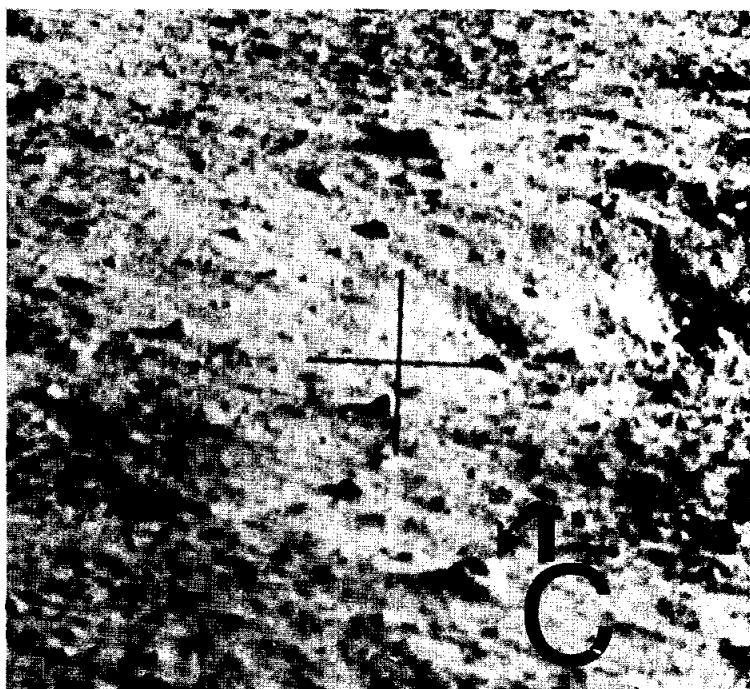


Figure 11-10.- Rock collected during second contingency sample scoop.

NASA-S-69-3754

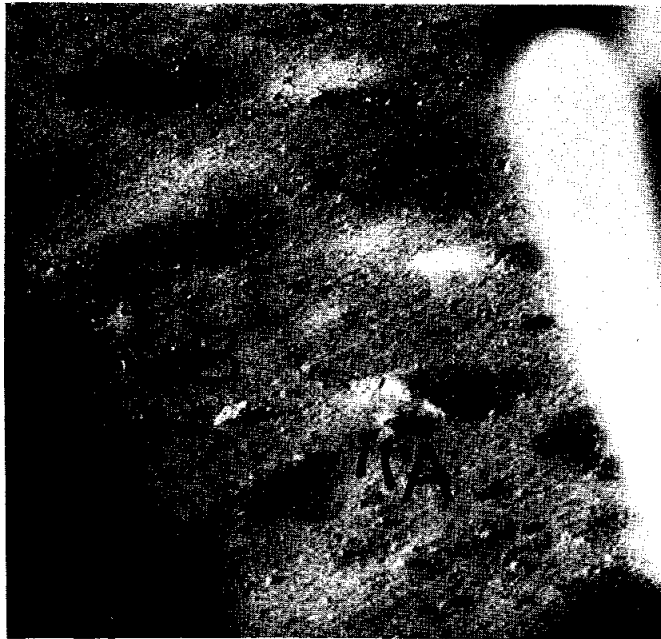


Figure 11-11. - Photograph taken prior to extravehicular activity, showing rocks collected (see figure 11-10).



Figure 11-12. - Photograph of area shown in figure 11-9 after extravehicular activity.



NASA-S-69-3755



Figure 11-13.- Photograph of area shown in figures 11-11 and 11-12, taken during extravehicular activity.

NASA-S-69-3756



Figure 11-14.- Lunar surface under descent stage engine .

NASA-S-69-3757

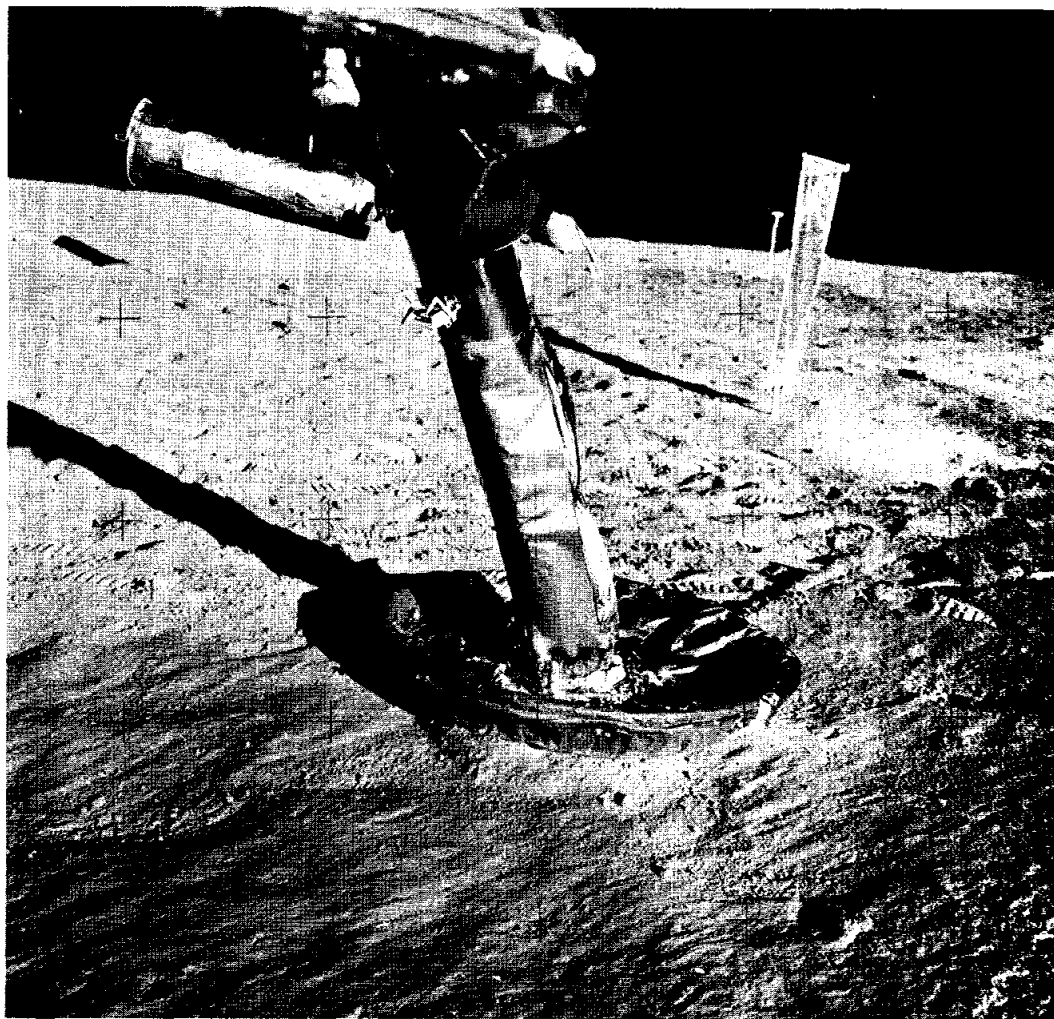


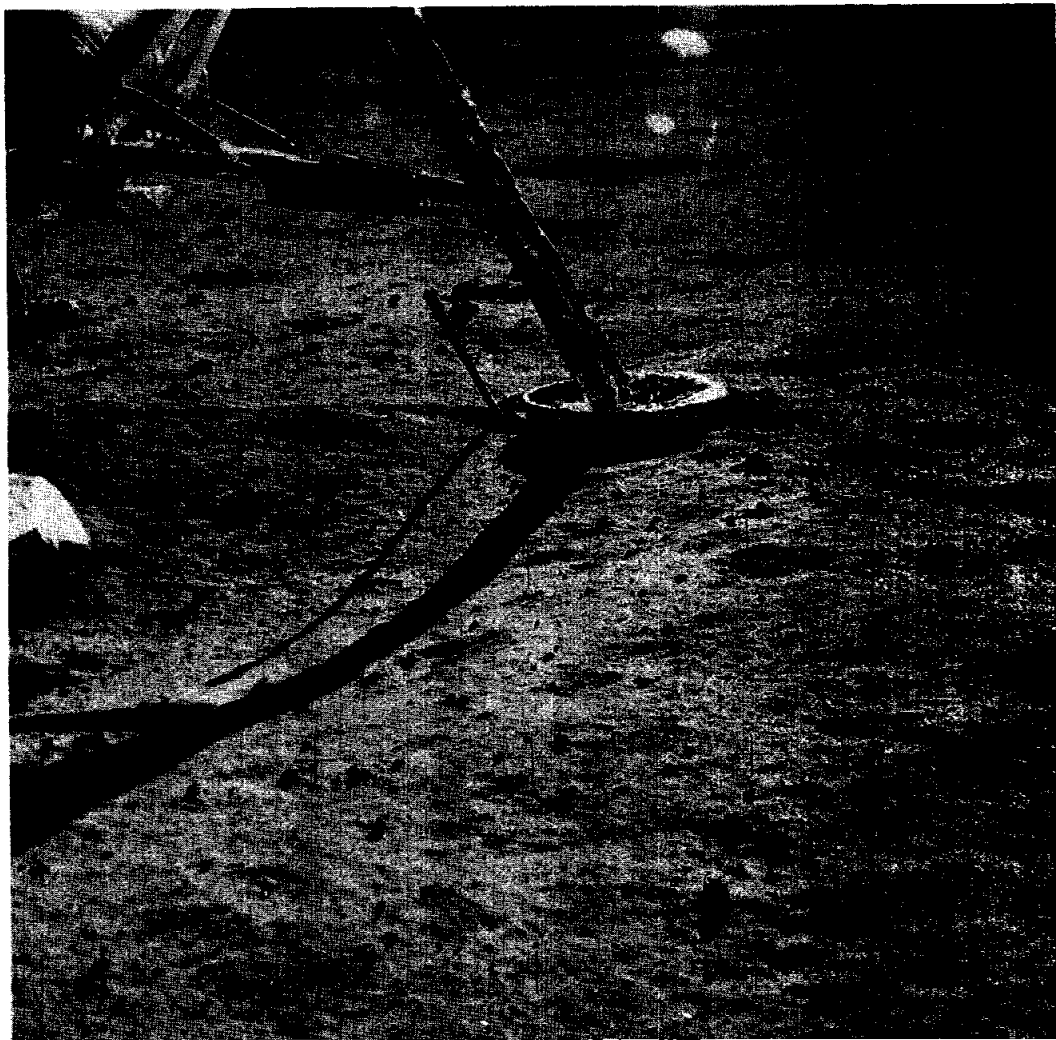
Figure 11-15.- Interaction of plus Y footpad and contact probe with lunar surface.

NASA-S-69-3758



Figure 11-16.- Interaction of the minus Z footpad with lunar surface.

NASA-S-69-3759



11-44

NASA-S-69-3760

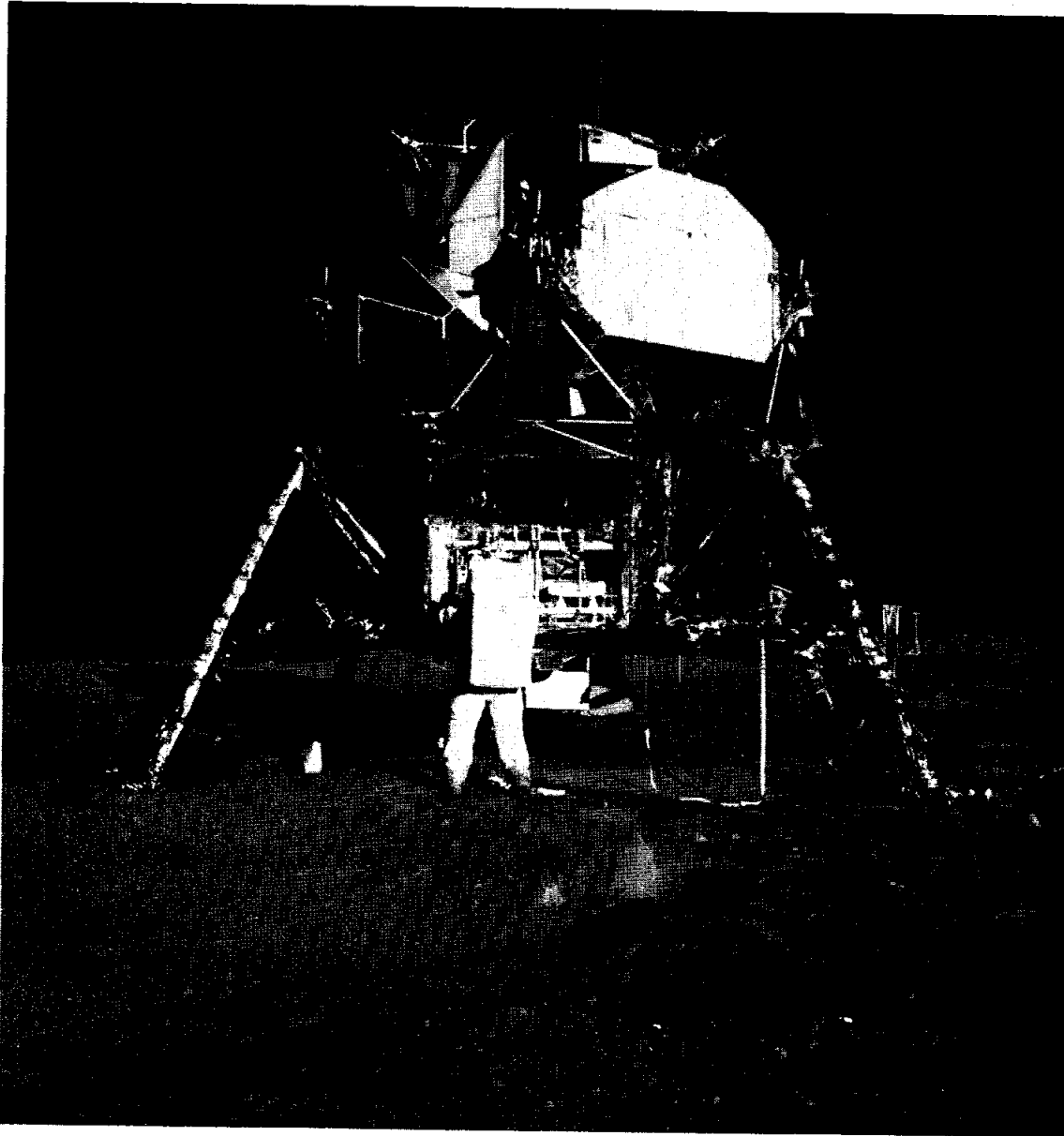


Figure 11-18.- Soil disturbance in the minus Y foot pad area.

NASA-S-69-3761

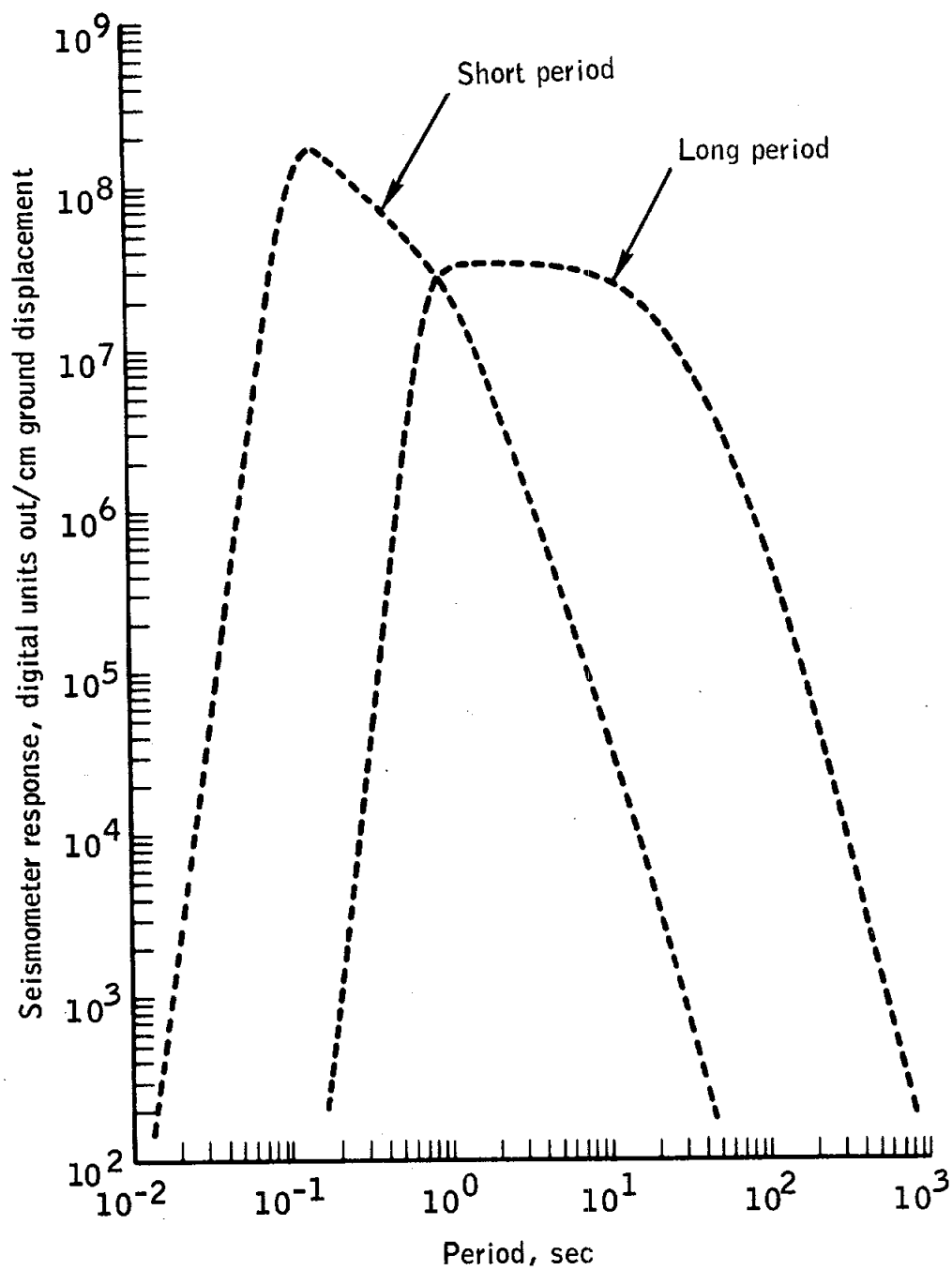


Figure 11-19.- Response from passive seismic experiment.

NASA-S-69-3762

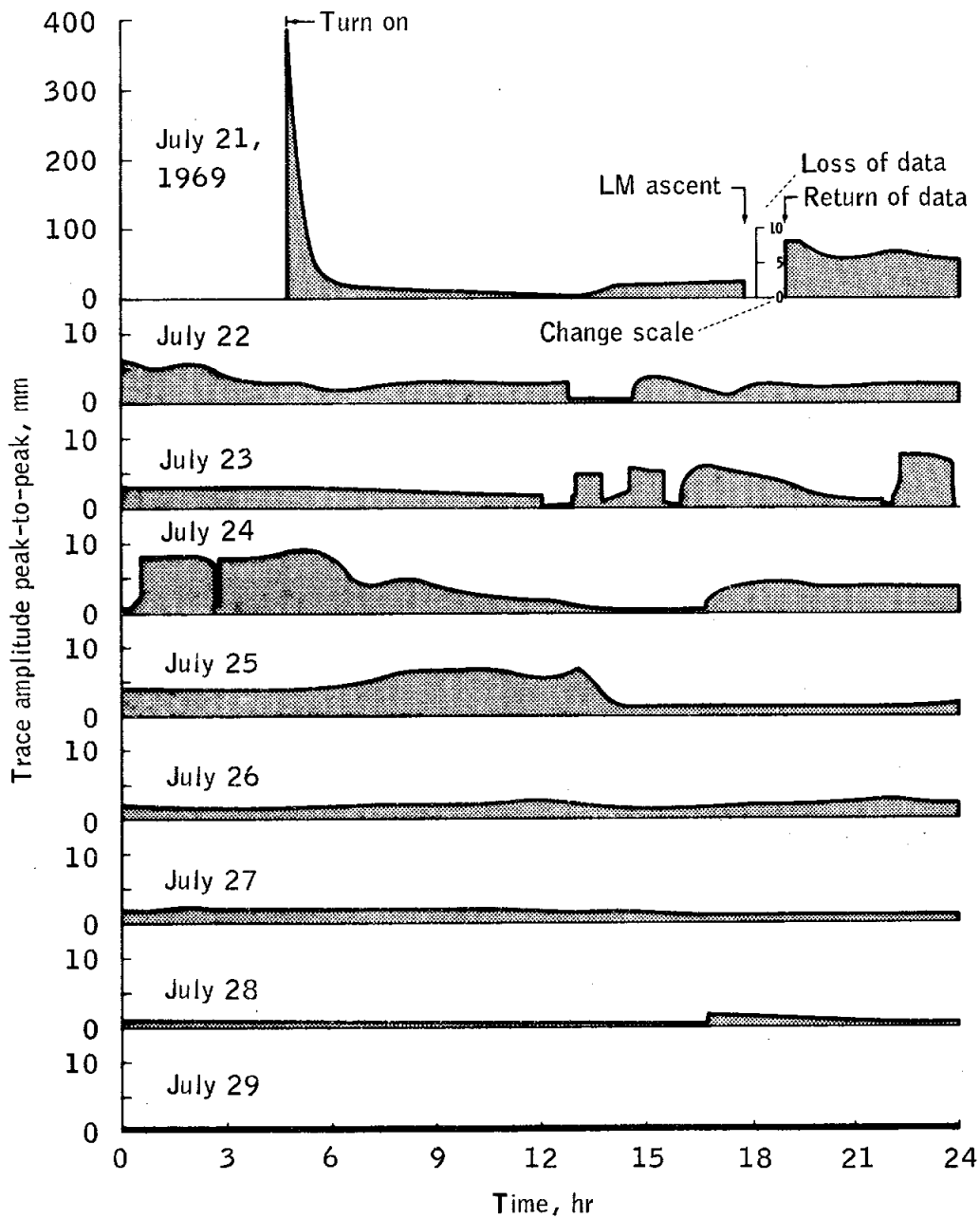


Figure 11-20.- Signal-level history from short-period Z-axis seismometer.



NASA-S-69-3763

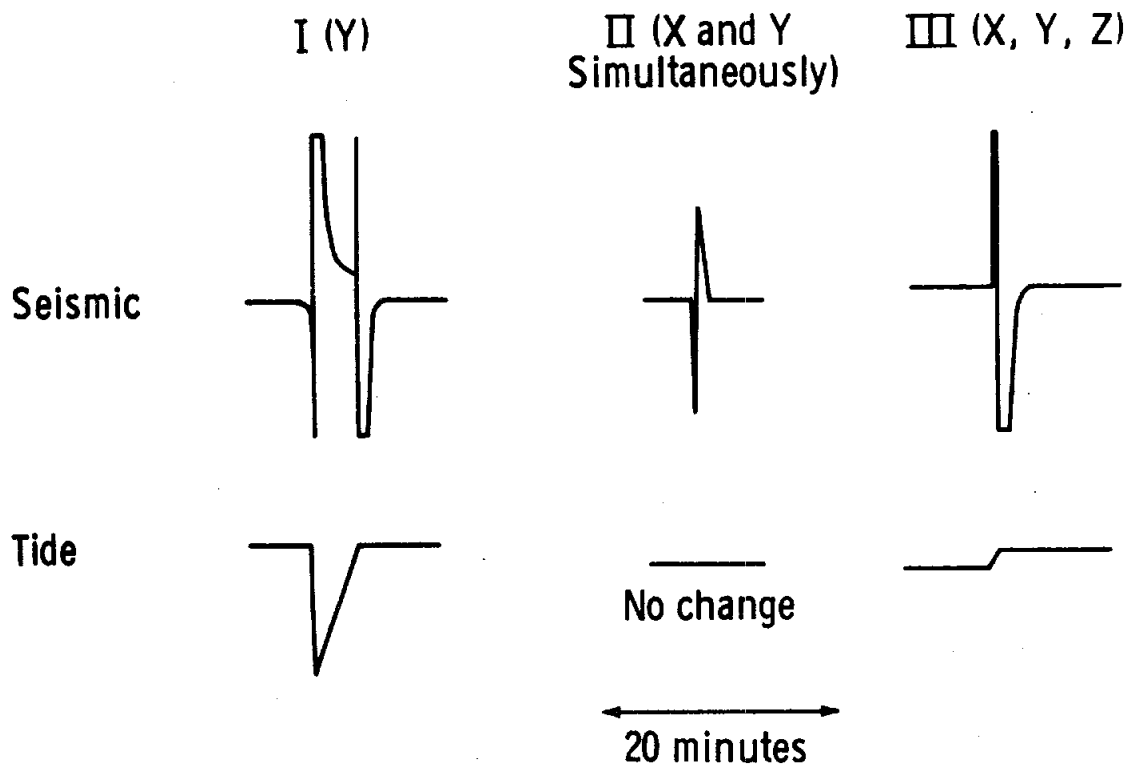


Figure 11-21.- Diagram showing types of noise transients observed on the seismic and tidal outputs from the long-period seismometers.

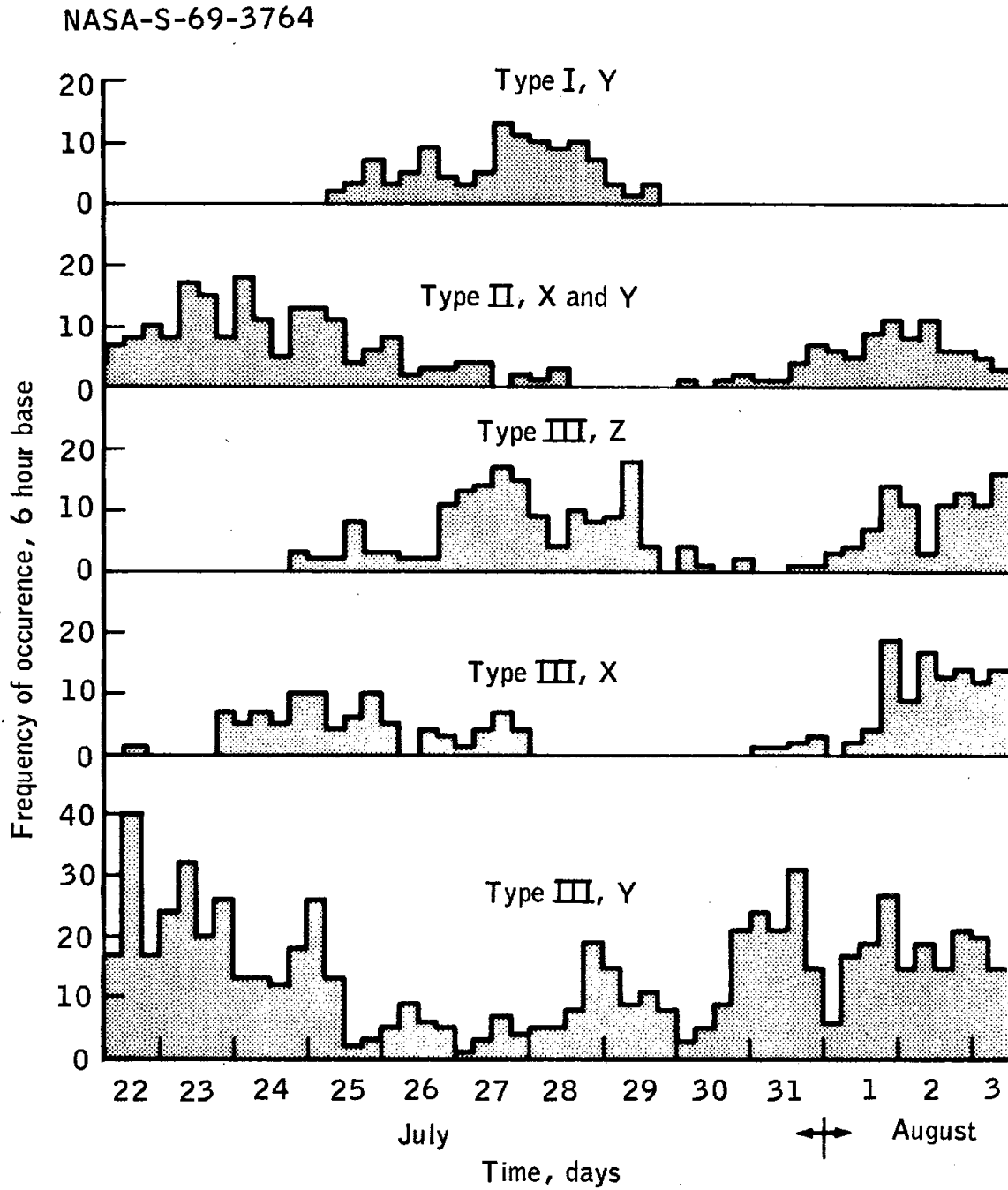


Figure 11-22.- Histogram of long-period noise transients.

NASA-S-69-3765

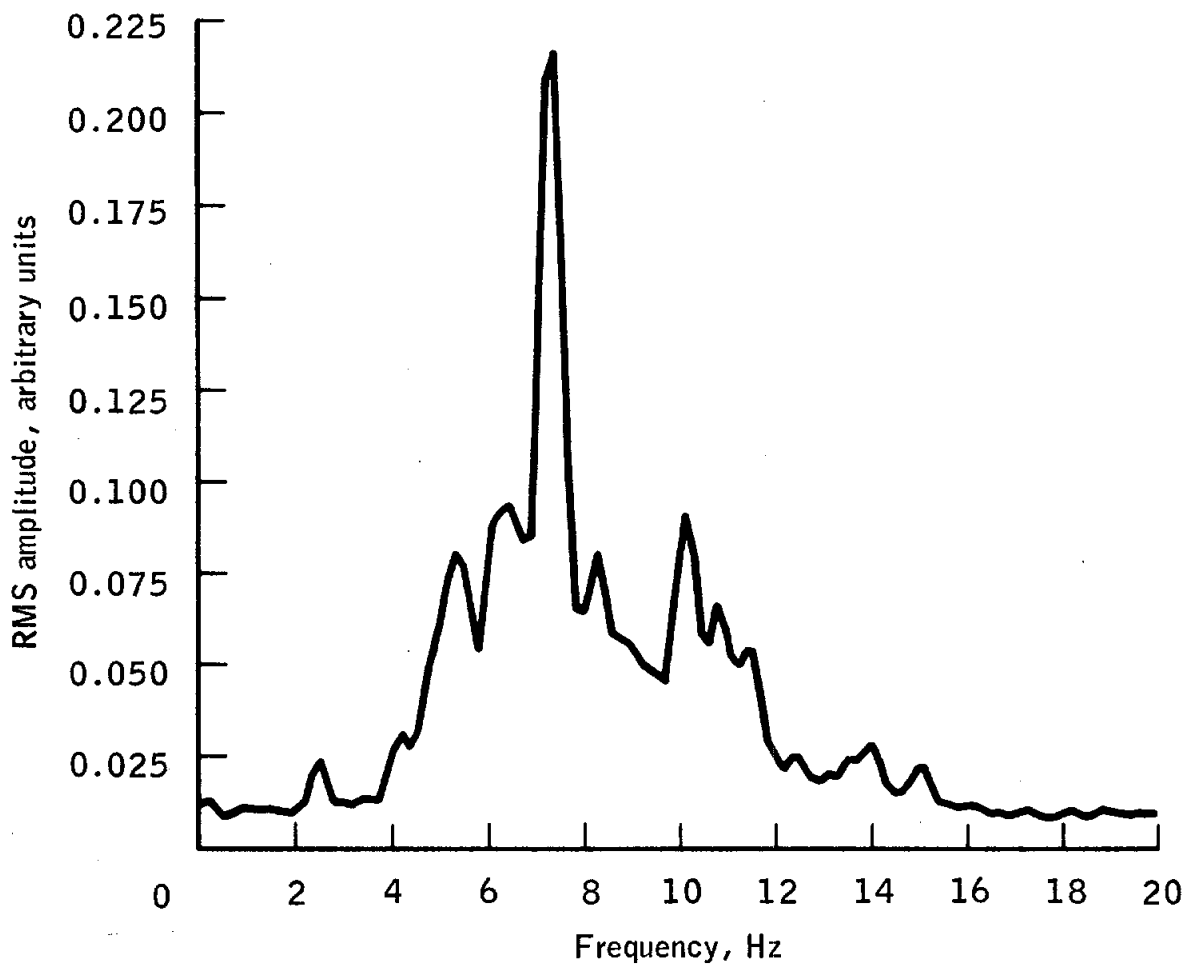


Figure 11-23.- Seismometer response while Commander was ascending ladder.

NASA-S-69-3766

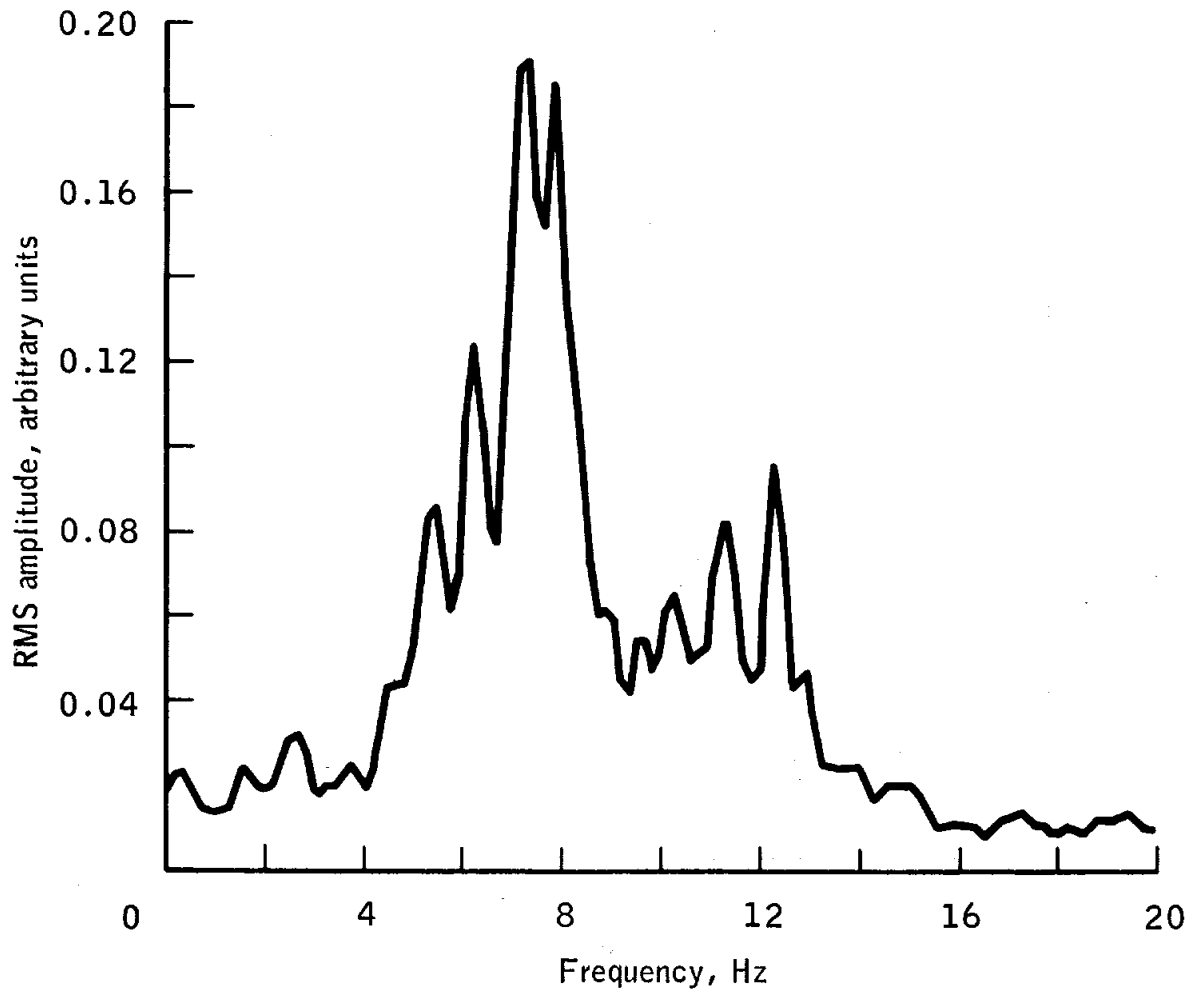


Figure 11-24.- Seismometer response from first portable life support system impacting lunar surface.

NASA-S-69-3767

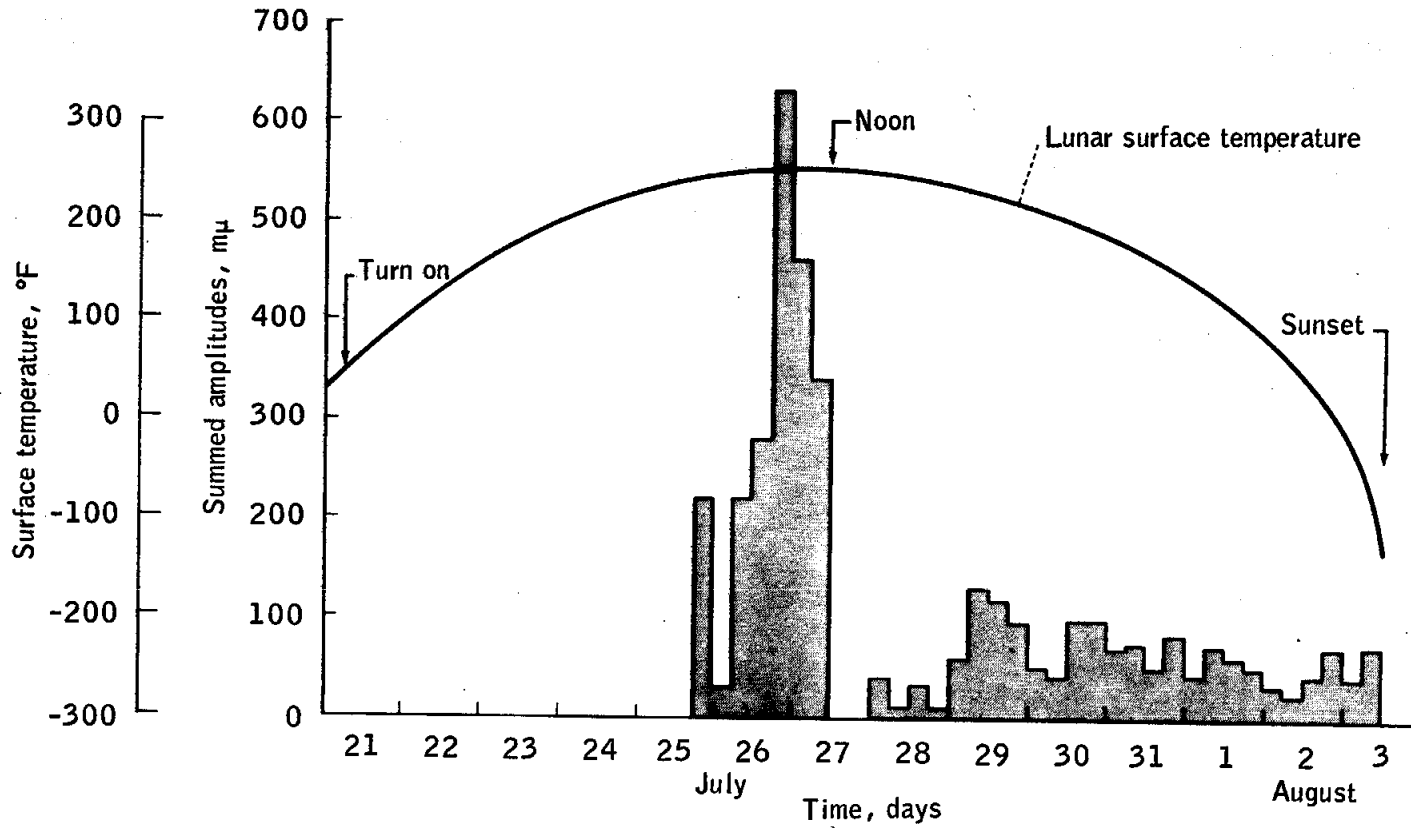


Figure 11-25.- Lunar surface temperature and seismometer output signals.

NASA-S-69-3768



Figure 11-26.- Laser ranging retro-reflector deployed.

NASA-S-69-3769



Figure 11-27.- Solar wind composition experiment deployed.

NASA-S-69-3770

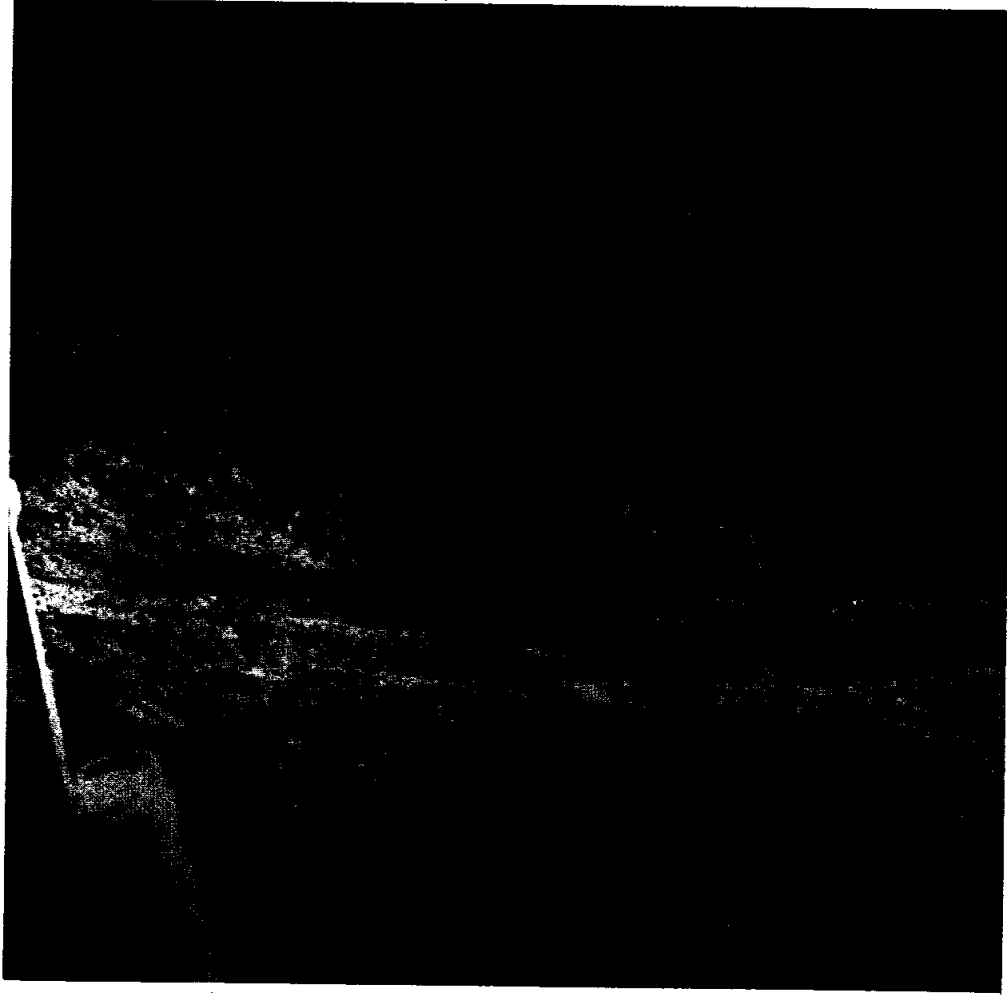


Figure 11-28.- Crater near lunar module.



## 12.0 BIOMEDICAL EVALUATION

This section is a summary of the Apollo 11 quarantine procedures and medical findings, based upon a preliminary analysis of biomedical data. More comprehensive evaluations will be published in separate medical reports.

The three crewmen accumulated 585 man-hours of space flight experience during the lunar landing mission including 2 hours 14 minutes and 1 hour 42 minutes on the lunar surface for the Commander and the Lunar Module Pilot, respectively.

The crew's health and performance were excellent throughout the flight and the 18-day postflight quarantine period. There were no significant physiological changes observed after this mission as has been the case on all previous missions, and no effects attributable to lunar surface exposure have been observed.

### 12.1 BIOINSTRUMENTATION AND PHYSIOLOGICAL DATA

The biomedical data were of very good quality. Only two minor problems occurred, both late in the flight. Data from the Command Module Pilot's impedance pneumogram became unreadable and the Lunar Module Pilot's electrocardiogram signal degraded because of drying of the electrode paste under the sensors. The Lunar Module Pilot replaced the electrocardiogram leads in his bioinstrumentation harness with the spare set from the medical kit, and proper readings were restored. No attempt was made to correct the Command Module Pilot's respiration signal because of entry preparations.

Physiological parameters were always within expected ranges, and sleep data were obtained on all three crewmen during most of the mission.

The average heart rates during the entire mission were 71, 60, and 67 beats/min for the Commander, Command Module Pilot, and Lunar Module Pilot, respectively. During the powered descent and ascent phases, the only data planned to be available were the Commander's heart rates, which ranged from 100 to 150 beats/min during descent and from 68 to 120 during ascent, as shown in figures 12-1 and 12-2, respectively.

Plots of heart rates during lunar surface exploration are shown in figure 12-3. The average heart rates were 110 beats/min for the Commander and 88 beats/min for the Lunar Module Pilot. The increase in the

Commander's heart rate during the last phases of this activity is indicative of an increased work load and body heat storage. The metabolic production of each crewman during the extravehicular activity is reported in section 12.3.

## 12.2 MEDICAL OBSERVATIONS

### 12.2.1 Adaptation to Weightlessness

The Commander reported that he felt less zero-gravity effect, such as fullness of the head, than he had experienced on his previous flight. All three crewmen commented that the lack of a gravitational pull caused a puffiness underneath their eyes and this caused them to squint somewhat, but none felt any ill effects associated with this puffiness. In donning and doffing the suits, they had no feeling of tumbling or the disorientation which had been described by the Apollo 9 crew.

During the first 2 days of the flight, the Command Module Pilot reported that half a meal was more than enough to satisfy his hunger, but his appetite subsequently returned.

### 12.2.2 Medications

The Commander and the Lunar Module Pilot each took one Lomotil tablet prior to the sleep period to retard bowel movements before the lunar module activity. They each carried extra Lomotil tablets into the lunar module but did not take them. At 4 hours before entry and again after splash-down, the three crewmen each took anti-nauseant tablets containing 0.3 mg Hyoscine and 5.0 mg Dexedrine. Aspirin tablets were also taken by the crewmen, but the number of tablets per individual was not recorded. The Lunar Module Pilot recalled that he had taken two aspirin tablets almost every night to aid his sleep.

### 12.2.3 Sleep

It is interesting to note that the crewmen's subjective estimates of amount of sleep were less than those based upon telemetered biomedical data, as shown in table 12-I. By either count, the crewmen slept well in the command module. The simultaneous sleep periods during the translunar coast were carefully monitored, and the crew arrived on the lunar surface well rested. Therefore, it was not necessary to wait until after the first planned 4-hour sleep period before conducting the extravehicular activity. The crewmen slept very little in the lunar module

following the lunar surface activity (see section 4.12.6). However, the crewmen slept well during all three transearth sleep periods.

#### 12.2.4 Radiation

The personal radiation dosimeters were read at approximately 12-hour intervals, as planned. The total integrated, but uncorrected, doses were 0.25, 0.26, and 0.28 rad for the Commander, Command Module Pilot, and Lunar Module Pilot, respectively. The Van Allen Belt dosimeter indicated total integrated doses of 0.11 rad for the skin and of 0.08 rad for the depth reading during the entire mission. Thus, the total dose for each crewman is estimated to have been less than 0.2 rad, which is well below the medically significant level. Results of the radio-chemical assays of feces and urine and an analysis of the onboard nuclear emulsion dosimeters will be presented in a separate medical report.

The crewmen were examined with a total body gamma radioactivity counter on August 10, 1969, after release from quarantine. No induced radioactivity was detected, as based on critical measurements and an integration of the total body gamma spectrum. The examination for natural radioactivity revealed the levels of potassium 40 and cesium 137 to be within the normal range.

#### 12.2.5 Inflight Exercise

The planned exercise program included isometric and isotonic exercises and the use of an exerciser. As in previous Apollo missions, a calibrated exercise program was not planned. The inflight exerciser was used primarily for crew relaxation. During transearth coast, the Lunar Module Pilot exercised vigorously for two 10-minute periods. His heart rate reached 170 and 177 beats/min, and the partial pressure of carbon dioxide increased approximately 0.6 mm Hg during these periods. The heart rates and the carbon dioxide readings rapidly returned to normal levels when exercise ceased.

#### 12.2.6 Drug Packaging

Several problems concerning drug packaging developed during the flight. All the medications in tablet and capsule form were packaged in individually sealed plastic or foil containers. When the medical kit was unstowed in the command module, the packages were blown up like balloons because insufficient air had been evacuated during packaging. This ballooning increased the volume of the medical-kit contents after it was opened and thus prevented restowage until a flap was cut away from

the kit. Venting of each of the plastic or foil containers will be accomplished for future flights and should prevent this problem from recurring. The Afrin nasal spray bubbled out when the cap was removed and was therefore unusable. The use of cotton in the spray bottle is expected to resolve this problem on future flights.

#### 12.2.7 Water

The eight inflight chlorinations of the command module water system were accomplished normally and essentially as scheduled. Analysis of the potable water samples obtained about 30 hours after the last inflight chlorination showed a free-chlorine residual of 0.8 mg from the drinking dispenser port and of 0.05 mg from the hot water port. The iodine level in the lunar module tanks, based on preflight sampling, was adequate for bacterial protection throughout the flight.

Chemical and microbiological analyses of the preflight water samples for both spacecraft showed no significant contaminants. Tests for coliform and anaerobic bacteria, as well as for yeasts and molds, were found negative during the postflight water analysis, which was delayed because of quarantine restrictions.

A new gas/water separator was used with satisfactory results. The palatability of the drinking water was greatly improved over that of previous flights because of the absence of gas bubbles, which can cause gastro-intestinal discomfort.

#### 12.2.8 Food

The food supply for the command module included rehydratable foods and beverages, wet-packed foods, foods contained in spoon-bowl packages, dried fruit, and bread. The new food items for this mission were candy sticks and jellied fruit candy; spreads of ham, chicken, and tuna salad packaged in lightweight aluminum, easy-open cans; and cheddar cheese spread and frankfurters packaged in flexible foil as wet-packed foods. A new pantry-type food system allowed real-time selection of food items based upon individual preference and appetite.

Four meal periods on the lunar surface were scheduled, and extra optional items were included with the normal meal packages.

Prior to flight, each crewman evaluated the available food items and selected his flight menus. The menus provided approximately 2300 kilocalories per man per day and included 1 gram of calcium, 0.5 gram of phosphorus, and 80 grams of protein. The crewmen were well satisfied with the quality and variety of the flight foods. They reported that their food intake met their appetite and energy requirements.

The preparation and eating of sandwiches presented no problems. Criticisms of the food systems were only that the coffee was not particularly good and that the fruit-flavored beverages tasted too sweet. The new gas/water separator was effective in reducing the amount of gas in the water and greatly improved the taste of the rehydratable foods.

### 12.3 EXTRAVEHICULAR ACTIVITY

The integrated rates of Btu production and the accumulated Btu production during the intervals of planned activities are listed in table 12-II. The actual average metabolic production per hour was estimated to be 900 Btu for the Commander and 1200 Btu for the Lunar Module Pilot. These values are less than the preflight estimates of 1350 and 1275 Btu for the respective crewmen.

### 12.4 PHYSICAL EXAMINATIONS

Comprehensive medical evaluations were conducted on each crewman at 29, 15, and 5 days prior to the day of launch. Brief physical examinations were then conducted each day until launch.

The postflight medical evaluation included the following: microbiology studies, blood studies, physical examinations, orthostatic tolerance tests, exercise response tests, and chest X-rays.

The recovery day examination revealed that all three crewmen were in good health and appeared well rested. They showed no fever and had lost no more than the expected amount of body weight. Each crewman had taken anti-motion sickness medication 4 hours prior to entry and again after landing, and no seasickness or adverse symptoms were experienced.

Data from chest X-rays and electrocardiograms were within normal limits. The only positive findings were small papules beneath the axillary sensors on both the Commander and the Lunar Module Pilot. The Commander had a mild serous otitis media of the right ear, but could clear his ears without difficulty. No treatment was necessary.

The orthostatic tolerance test showed significant increases in the immediate postflight heart rate responses, but these increases were less than the changes seen in previous Apollo crewmembers. In spite of this apparent improvement, their return to preflight values was slower than

had been observed in previous Apollo crewmen. The reasons for this slower recovery are not clear at this time; but in general, these crew members exhibited less decrement in oxygen consumption and work performed than was observed in exercise response tests after previous Apollo flights.

Follow-up evaluations were conducted daily during the quarantine period in the Lunar Receiving Laboratory, and the immunohematology and microbiology revealed no changes attributable to exposure to the lunar surface material.

## 12.5 LUNAR CONTAMINATION AND QUARANTINE

The two fundamental responsibilities of the lunar sample program were to preserve the integrity of the returned lunar samples in the original or near-original state and to make practical provisions to protect the earth's ecology from possible contamination by lunar substances that might be infectious, toxic, or otherwise harmful to man, animals, or plants.

The Public Laws and Federal Regulations concerning contamination control for lunar sample return missions are described in reference 9. An interagency agreement between the National Aeronautics and Space Administration; the Department of Agriculture; the Department of Health, Education and Welfare; the Department of the Interior; and the National Academy of Sciences (ref. 10) confirmed the existing arrangements for the protection of the earth's biosphere and defined the Interagency Committee on Back Contamination. The quarantine schemes for manned lunar missions were established by the Interagency Committee on Back Contamination (ref. 11).

The planned 21-day crew quarantine represented the period required to preclude the development of infectious disease conditions that could generate volatile epidemic events. In addition, early signs of latent infectious diseases with longer incubation periods would probably be detected through extensive medical and clinical pathological examinations. However, to provide additional assurance that no infectious disease of lunar origin is present in the Apollo 11 crewmembers, an extensive epidemiological program will continue for 1 year after their release from quarantine.

### 12.5.1 Lunar Exposure

Although each crewman attempted to clean himself and the equipment before ingress, a fairly large amount of dust and grains of lunar surface material was brought into the cabin. When the crewmen removed their helmets, they noticed a distinct, pungent odor emanating from the lunar material. The texture of the dust was like powdered graphite, and both crewmen were very dirty after they removed their helmets, overshoes, and gloves. The crewmen cleaned their hands and faces with tissues and with towels that had been soaked in hot water. The Commander removed his liquid-cooling garment in order to clean his body. One grain of material got into the Commander's eye, but was easily removed and caused no problem. The dust-like material could not be removed completely from beneath their fingernails.

The cabin cleaning procedure involved the use of a vacuum-brush device and positive air pressure from the suit supply hoses to blow remote particles into the atmosphere for collection in the lithium hydroxide filters in the environmental control system.

The concern that particles remaining in the lunar module would float in the cabin atmosphere at zero-g after ascent caused the crew to remain helmeted to prevent eye and breathing contamination. However, floating particles were not a problem. The cabin and equipment were further cleaned with the vacuum brush. The equipment from the surface and the pressure garment assemblies were placed in bags for transfer to the command module. Before transfer to the command module, the spacecraft systems were configured to cause a positive gas flow from the command module through the hatch dump/relief valve in the lunar module.

The command module was cleaned during the return to earth at 24-hour intervals using the vacuum brush and towels. In addition, the circulation of the cabin atmosphere through the lithium hydroxide filters continued to remove traces of particulate material.

### 12.5.2 Recovery Procedures

The recovery procedures were successfully conducted with no compromises of the planned quarantine techniques. The times of major post-landing events are listed in section 13.3, Recovery Operations.

After the command module was uprighted, four biological isolation garments and the decontamination gear were lowered to one of two life rafts. One of the four swimmers donned a biological isolation garment. The second life raft was then moved to the spacecraft. The protected

swimmer retired with the second life raft to the original upwind position. The hatch was opened, the crew's biological isolation garments were inserted into the command module, and the hatch was closed.

After donning the biological isolation garments, the crew egressed. The protected swimmer sprayed the upper deck and hatch areas with Beta-dine, a water-soluble iodine solution, as planned in the quarantine procedure. After the four men and the life raft were wiped with a solution of sodium hypochlorite, the three swimmers returned to the vicinity of the spacecraft to stand by during the helicopter pickup of the flight crew.

The crewmen were brought up into the helicopter without incident and remained in the aft compartment. As expected, a moderate amount of water was present on the floor after retrieval, and the water was wiped up with towels. The helicopter crewmen were also protected from possible contamination.

The helicopter was moved to the Mobile Quarantine Facility on the lower deck of the recovery vessel. The crewmen walked across the deck, entered the Mobile Quarantine Facility, and removed their biological isolation garments. The descent steps and the deck area between the helicopter and the Mobile Quarantine Facility were sprayed with glutaraldehyde solution, which was mopped up after a 30-minute contact time.

After the crewmen were picked up, the protected swimmer scrubbed the upper deck around the postlanding vents, the hatch area, and the flotation collar near the hatch with Betadine. The remaining Betadine was emptied into the bottom of the recovery raft. The swimmer removed his biological isolation garment and placed it in the Betadine in the life raft. The disinfectant sprayers were dismantled and sunk. After a 30-minute contact time, the life raft and remaining equipment were sunk.

Following egress of the flight crews and a recovery surgeon from the helicopter, its hatch was closed and the vehicle was towed to the flight deck for decontamination with formaldehyde.

The crew became uncomfortably warm while they were enclosed in the biological isolation garments in the environment (90° F) of the helicopter cabin. On two of the garments the visor fogged up because of improper fit of the nose and mouth cup. To alleviate this discomfort on future missions, consideration is being given to: (1) replacing the present biological isolation garment with a lightweight coverall, similar to whiteroom clothing, with respirator mask, cap, gloves, and booties; and (2) wearing a liquid cooling garment under the biological isolation garment.



The command module was taken aboard the USS Hornet about 3 hours after landing and attached to the Mobile Quarantine Facility through a flexible tunnel. The removal of lunar surface samples, film, data tape, and medical samples went well, with one exception. Two of the medical sample containers leaked within the inner biological isolation container. Corrective measures were promptly executed, and the quarantine procedure was not violated.

Transfer of the Mobile Quarantine Facility from the recovery ship to a C-141 aircraft and from the aircraft to the Lunar Receiving Laboratory at the Manned Spacecraft Center was accomplished without any question of a quarantine violation. The transfer of the lunar surface samples and the command module into the Lunar Receiving Laboratory was also accomplished as planned.

### 12.5.3 Quarantine

A total of 20 persons on the medical support teams were exposed, directly or indirectly, to lunar material for periods ranging from 5 to 18 days. Daily medical observations and periodic laboratory examinations showed no signs or symptoms of infectious disease related to lunar exposure.

No microbial growth was observed from the prime lunar samples after 156 hours of incubation on all types of differential media. No microorganisms which could be attributed to an extraterrestrial source were recovered from the crewmen or the spacecraft.

None of the 24 mice injected intraperitoneally with lunar material showed visible shock reaction following injection, and all remained alive and healthy during the first 10 days of a 50-day toxicity test. During the first 7 days of testing of the prime lunar samples in germ-free mice, all findings were consistent with the decision to release the crew from quarantine.

Samples from the crewmen were injected into tissue cultures, suckling mice, mycoplasma media, and 6- and 10-day old embryonated eggs. There was no evidence of viral replication in any of the host systems at the end of 2 weeks. During the first 8 days of testing the lunar material, all findings were compatible with crew release from quarantine.

No significant trends were noted in any biochemical, immunological, or hematological parameters in either the flight crew or the medical support personnel.

The personnel in quarantine and in the crew reception area of the Lunar Receiving Laboratory were approved for release from quarantine on August 10, 1969.

Following decontamination using formaldehyde, the interior of the command module and the ground servicing equipment utilized in the decontamination procedures were approved for release from quarantine on August 10, 1969.

The samples of lunar material and other items stored in the biological isolation containers in the Lunar Receiving Laboratory are scheduled for release to principal scientific investigators in September 1969.

TABLE 12-I.- ESTIMATED SLEEP DURATIONS

Time of crew report, hr:min	Estimated amount of sleep, hr:min					
	Telemetry			Crew report		
	Commander	Command Module Pilot	Lunar Module Pilot	Commander	Command Module Pilot	Lunar Module Pilot
23:00	10:25	10:10	8:30	7:00	7:00	5:30
48:15	9:40	10:10	9:15	8:00	9:00	8:00
71:24	9:35	(a)	9:20	7:30	7:30	6:30
95:25	6:30	6:30	5:30	6:30	6:30	5:30
Totals	36:10	--	32:35	29:00	30:00	25:30

<sup>a</sup>No data available.

TABLE 12-II.- METABOLIC RATES DURING LUNAR SURFACE EXPLORATION

Event	Starting time, hr:min	Duration, min	Rate, Btu/hr	Estimated work, Btu	Cumulative work, Btu
Commander					
Initial extravehicular activity	109:13	11	900	165	165
Environmental familiarization	109:24	3	800	40	205
Photography	109:27	7	875	102	307
Contingency sample collection	109:34	5	675	56	363
Monitor and photograph Lunar Module Pilot	109:39	4	850	57	420
Deploy television camera on surface	109:43	23	750	288	708
Flag and President's message	110:06	12	825	165	873
Bulk sample collection	110:18	23	850	326	1199
Lunar module inspection	110:41	18	675	203	1402
Experiment package deployment	110:59	12	775	155	1557
Documented sample collection	111:11	19	1250	396	1953
Transfer sample return containers	111:30	7	1450	169	2122
Terminate extravehicular activity	111:37	2	1400	48	2170
TOTAL		146			2170
Lunar Module Pilot					
Assist and monitor Commander	109:13	26	1200	520	520
Initial extravehicular activity	109:39	5	1950	163	683
Environmental familiarization; deploy television cable	109:44	14	1200	280	963
Deploy solar wind experiment	109:58	6	1275	128	1091
Flag and President's message	110:04	14	1350	315	1406
Evaluation of extravehicular mobility unit	110:18	16	850	227	1633
Lunar module inspection	110:34	19	875	277	1910
Experiment package deployment	110:53	18	1200	360	2270
Documented sample collection; recovery of solar wind experiment	111:11	12	1450	290	2560
Terminate extravehicular activity, ingress, and transfer sample return containers	111:23	14	1650	385	2945
Assist and monitor Commander	111:37	2	1100	37	2982
TOTAL		146			2982

NOTE: Values are from the integration of three independent determinations of metabolic rate based on heart rate, decay of oxygen supply pressure, and thermodynamics of the liquid cooling garment.

NASA-S-69-3771

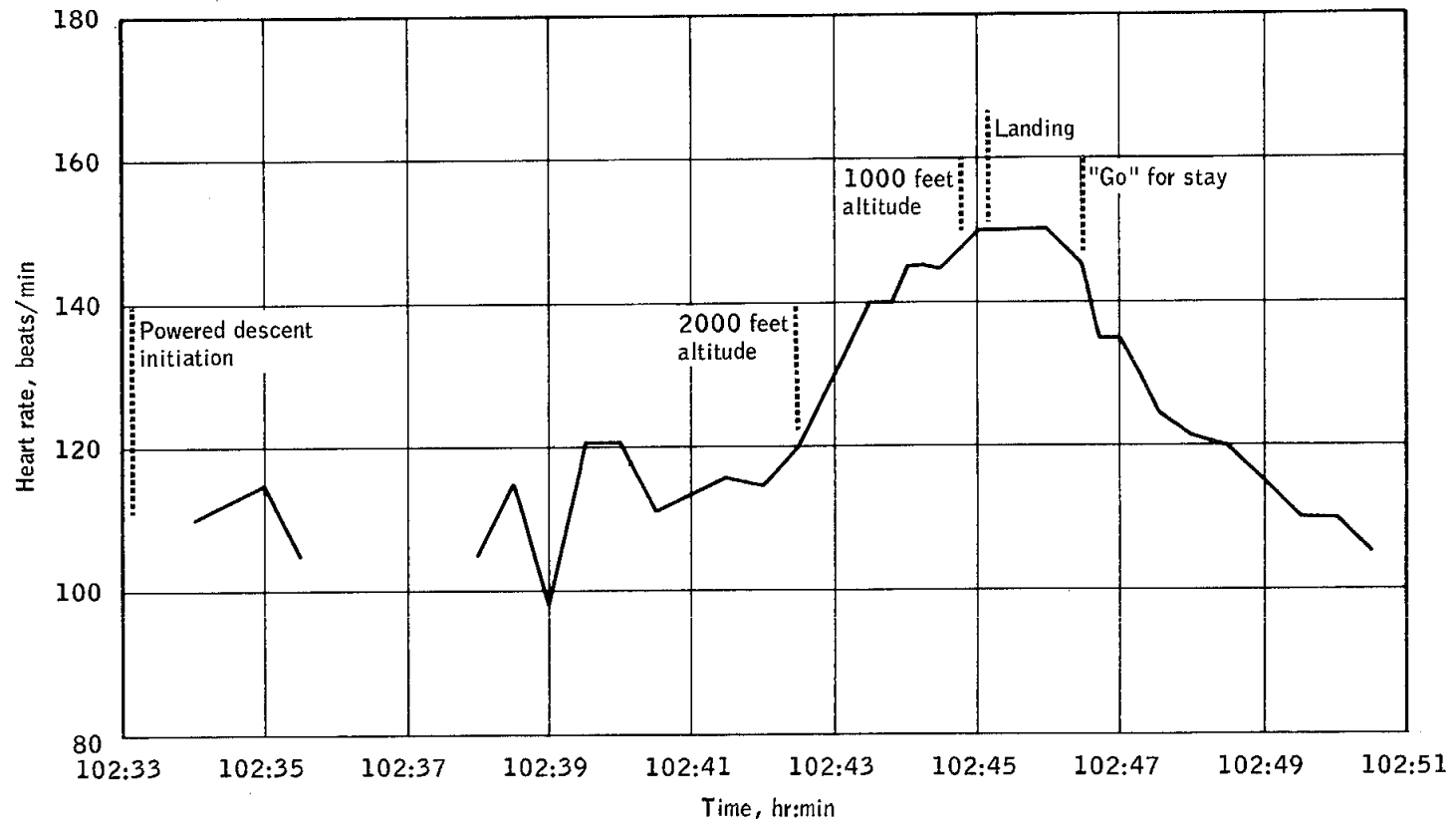


Figure 12-1.- Heart rates of the Commander during lunar descent.

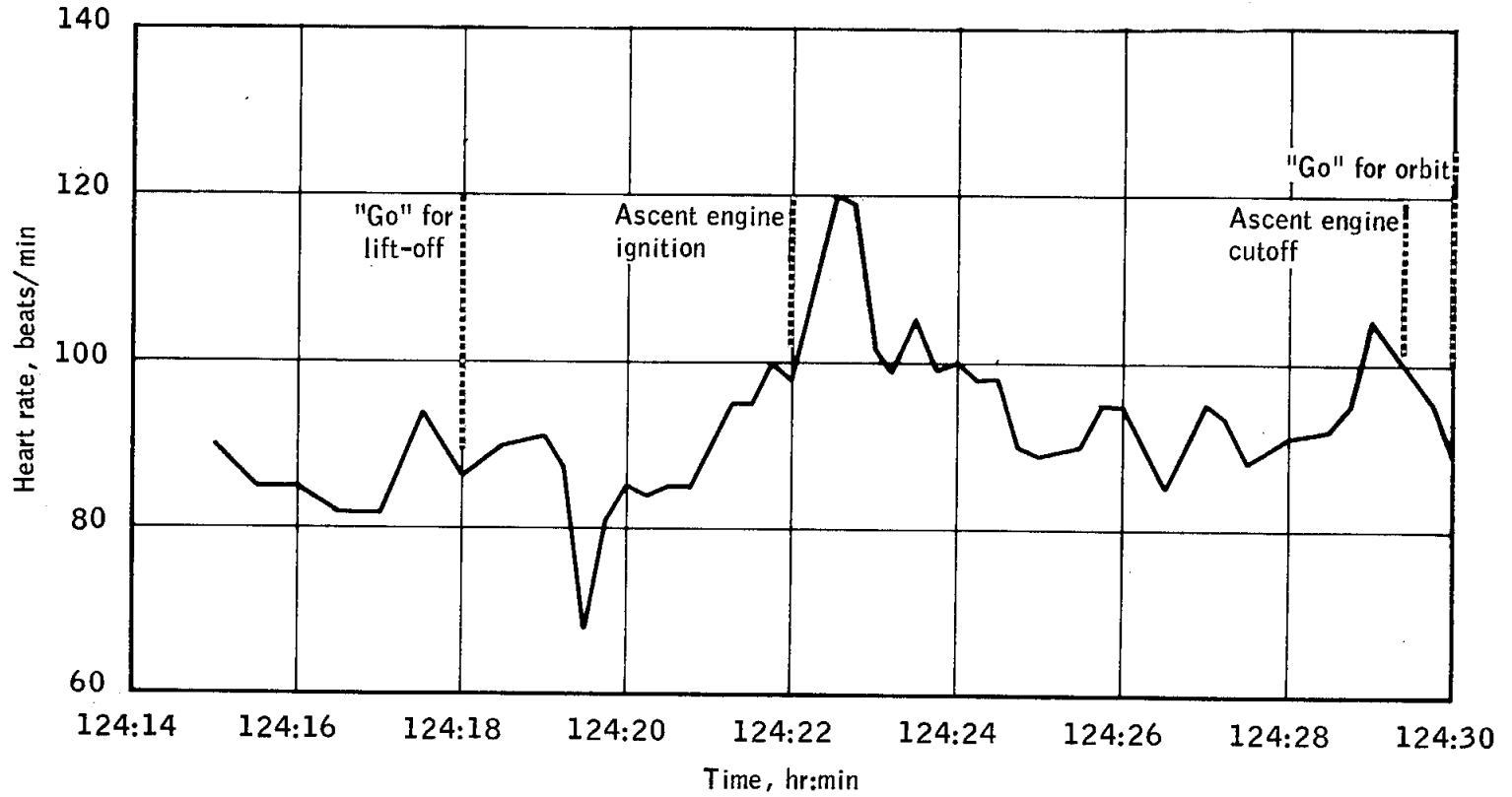
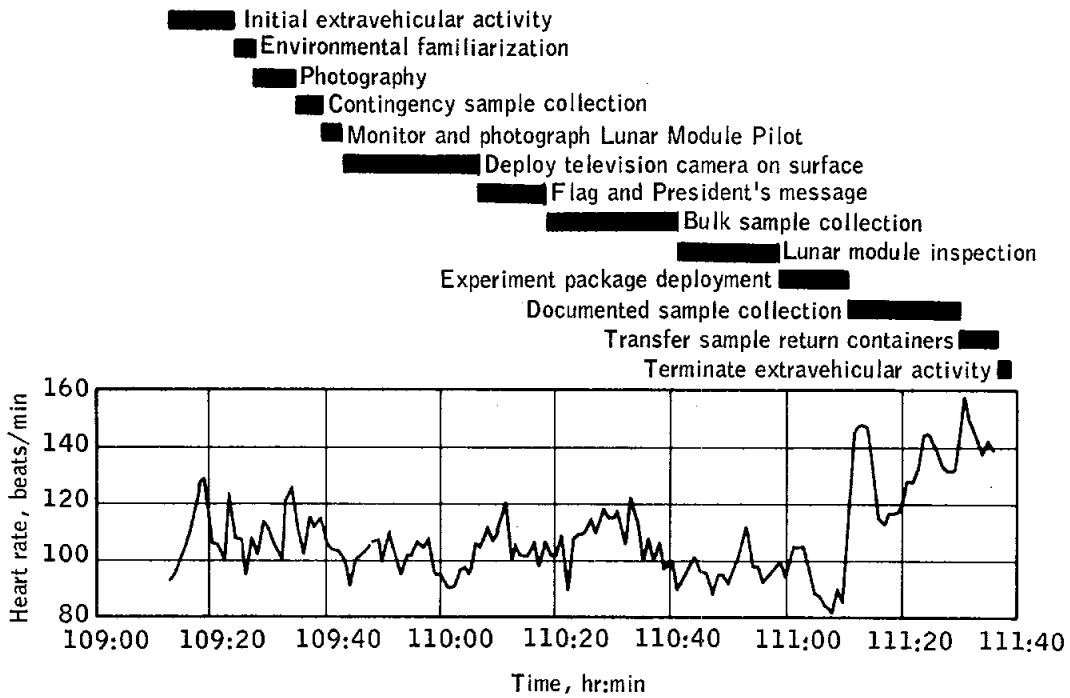
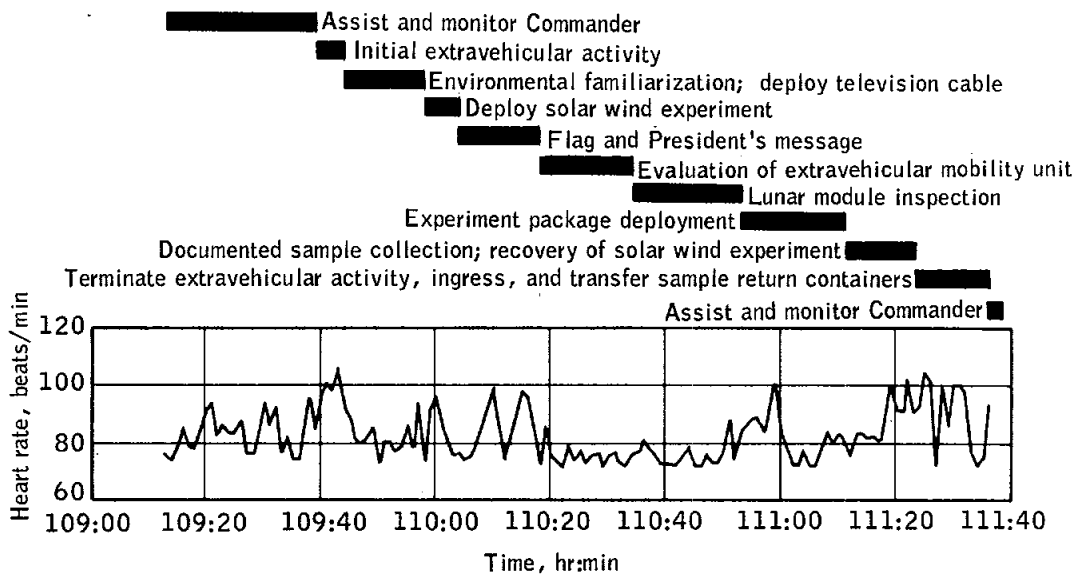


Figure 12-2.- Heart rates of the Commander during ascent.

NASA-S-69-3773



(a) Commander (CDR).



(b) Lunar Module Pilot (LMP).

Figure 12-3.- Heart rates during extravehicular activities.

## 13.0 MISSION SUPPORT PERFORMANCE

### 13.1 FLIGHT CONTROL

Preflight simulations provided adequate flight control training for all mission phases. Also, the flight controllers on the descent team supplemented this training by conducting descent simulations with the Apollo 12 crew. Interfaces between Mission Control team members and the flight crew were effective, and no major operational problems were encountered. The two-way flow of information between the flight crew and the flight controllers was effective. The overloading of the lunar module guidance computer during powered descent was accurately assessed, and the information provided to the flight crew permitted continuation of descent.

The flight control response to those problems identified during the mission was based on real-time data. Sections 8, 9, and 16 should be consulted for the postflight analyses of these problems. Three of the more pertinent real-time decisions are discussed in the following paragraphs.

At acquisition of signal after lunar orbit insertion, data showed that the indicated tank-B nitrogen pressure was about 300 psi lower than expected and that the pressure had started to decrease at 80 seconds into the maneuver (see section 16.1.1). To conserve nitrogen and to maximize system reliability for transearth injection, it was recommended that the circularization maneuver be performed using bank A only. No further leak was apparent, and both banks were used normally for transearth injection.

Five computer program alarms occurred between 5 and 10 minutes after initiation of powered descent. These alarms are symptoms of possible computer overloading. However, it has been decided before flight that bailout-type alarms such as these would not prevent continuing the flight, even though they could cause violations of other mission rules, such as velocity differences. The alarms were not continually occurring, and proper computer navigation functions were being performed; therefore, a decision was given to continue the descent.

During the crew rest period on the lunar surface, two checklist changes were recommended, based on the events of the previous 20 hours: (1) the rendezvous radar would remain off during the ascent firing, and (2) the mode-select switch would not be placed in the primary guidance position, thus preventing the computer from generating altitude and altitude rate for the telemetry display. The reason for these changes was to prevent computer overload during ascent, as had occurred during descent.



## 13.2 NETWORK PERFORMANCE

The Mission Control Center and the Manned Space Flight Network were placed on mission status on July 7, 1969, and satisfactorily supported the lunar landing mission.

Hardware, communications, and computer support in the Mission Control Center was excellent. No major data losses were attributed to these systems, and the few failures that did occur had minimal impact on support operations. Air-to-ground communications were generally good during the mission; however, a number of significant problems were experienced as a result of procedural errors.

The support provided by the real-time computer complex was generally excellent, and only one major problem was experienced. During translunar coast, a problem in updating digital-to-television displays by the primary computer resulted in the loss of all real-time television displays for approximately an hour. The problem was isolated to the interface between the computer and the display equipment.

Operations by the communications processors were excellent, and the few problems caused only minor losses of mission data.

Air-to-ground voice communications were generally good, although a number of ground problems caused temporary loss or degradation of communications. Shortly after landing on the lunar surface, the crew complained about the noise level on the S-band voice uplinked from Goldstone. This problem occurred while Goldstone was configured in the Network-relay mode. The source of the noise was isolated to a breaking of squelch control caused by high noise on the command module downlink being subsequently uplinked to the lunar module via the relay mode. The noise was eliminated by disabling the relay mode. On several occasions during the mission, spacecraft voice on the Goddard conference loop was degraded by the voice-operated gain-adjust amplifiers. In most cases the problem was cleared by disabling this unit at the remote site.

Command operations were good throughout the mission. Of the approximately 3450 execution commands transmitted during the mission, only 24 were rejected by remote-site command computers and 21 were lost for unknown reasons. Approximately 450 command loads were generated and successfully transferred to Network stations, and 58 of these were uplinked to the space vehicle.

Both C- and S-band tracking support was very good. Loss of tracking coverage was experienced during translunar injection when the Mercury ship was unable to provide high-speed trajectory data because of a temporary

problem in the central data processor. Some stations also experienced temporary S-band power amplifier failures during the mission.

Network support of the scientific experiment package from deployment through earth landing was good. A few hardware and procedural problems were encountered; however, the only significant data loss was when the S-band parametric amplifier at the Canary Island station failed just seconds before lunar module ascent. Consequently, all seismic package data were lost during this phase, since no backup stations were available for support.

Television support provided by Network and Jet Propulsion Laboratory facilities was good throughout the mission, particularly the support by the 210-foot stations at Parkes and Goldstone.

### 13.3 RECOVERY OPERATIONS

The Department of Defense provided recovery support commensurate with the probability of landing within a specified area and with any special problems associated with such a landing. Recovery force deployment was nearly identical to that for Apollo 8 and 10.

Support for the primary landing area in the Pacific Ocean was provided by the USS Hornet. Air support consisted of four SH-3D helicopters from the Hornet, three E-1B aircraft, three Apollo range instrumentation aircraft, and two HC-130 rescue aircraft staged from Hickam Air Force Base, Hawaii. Two of the E-1B aircraft were designated as "Air Boss" and the third as a communications relay aircraft. Two of the SH-3D helicopters carried the swimmers and required recovery equipment. The third helicopter was used as a photographic platform, and the fourth carried the decontamination swimmer and the flight surgeon and was used for crew retrieval.

#### 13.3.1 Command Module Location and Retrieval

Figure 13-1 depicts the Hornet and associated aircraft positions at the time of command module landing at 195:18:35 (1650 G.m.t.). The command module landed at a point calculated by recovery forces to be 13 degrees 19 minutes north latitude and 169 degrees 9 minutes west longitude.

The command module immediately went to the stable II (apex down) flotation attitude after landing. The uprighting system returned the spacecraft to the stable I attitude 7 minutes 40 seconds later. One or

two quarts of water entered the spacecraft while in stable II. The swimmers were then deployed to install the flotation collar, and the decontamination swimmer passed the biological isolation garments to the flight crew, aided the crew into the life raft, and decontaminated the exterior surface of the command module (see section 12.5.2). After the command module hatch was closed and decontaminated, the flight crew and decontamination swimmer washed each other with the decontaminate solution prior to being taken aboard the recovery helicopter. The crew arrived onboard the Hornet at 1753 G.m.t. and entered the Mobile Quarantine Facility 5 minutes later. The first lunar samples to be returned were flown to Johnston Island, placed aboard a C-141 aircraft, and flown to Houston. The second sample shipment was flown from the Hornet directly to Hickam Air Force Base, Hawaii, approximately 6-1/2 hours later and placed aboard a range instrumentation aircraft for transfer to Houston.

The command module and Mobile Quarantine Facility were offloaded in Hawaii on July 27, 1969. The Mobile Quarantine Facility was loaded aboard a C-141 aircraft and flown to Houston, where a brief ceremony was held. The flight crew arrived at the Lunar Receiving Laboratory at 1000 G.m.t. on July 28, 1969.

The command module was taken to Ford Island for deactivation. Upon completion of deactivation, the command module was shipped to Hickam Air Force Base, Hawaii and flown on a C-133 aircraft to Houston.

A postrecovery inspection showed no significant discrepancies with the spacecraft.

The following is a chronological listing of events during the recovery and quarantine operations.

<u>Event</u>	<u>Time, G.m.t.</u>
	<u>July 24</u>
Visual contact by aircraft	1639
Radar contact by USS Hornet	1640
VHF voice and recovery-beacon contact	1646
Command module landing (195:18:35)	1650
Flotation collar inflated	1704
Command module hatch open	1721
Crew egress in biological isolation garments	1729
Crew aboard Hornet	1753
Crew in Mobile Quarantine Facility	1758
Command module lifted from water	1950
Command module secured to Mobile Quarantine Facility transfer tunnel	1958
Command module hatch reopened	2005
Sample return containers 1 and 2 removed from command module	2200
Container 1 removed from Mobile Quarantine Facility	2332
	<u>July 25</u>
Container 2 removed from Mobile Quarantine Facility	0005
Container 2 and film launch to Johnston Island	0515
Container 1, film, and biological samples launched to Hickam Air Force Base, Hawaii	1145
Container 2 and film arrived in Houston	1615
Container 1, film, and biological samples arrived in Houston	2313
	<u>July 26</u>
Command module decontaminated and hatch secured	0300
Mobile Quarantine Facility secured	0435
	<u>July 27</u>
Mobile Quarantine Facility and command module offloaded	0015
Safing of command module pyrotechnics completed	0205
	<u>July 28</u>
Mobile Quarantine Facility arrived at Houston	0600
Flight crew in Lunar Receiving Laboratory	1000
	<u>July 30</u>
Command module delivered to Lunar Receiving Laboratory	2317

NASA-S-69-3774

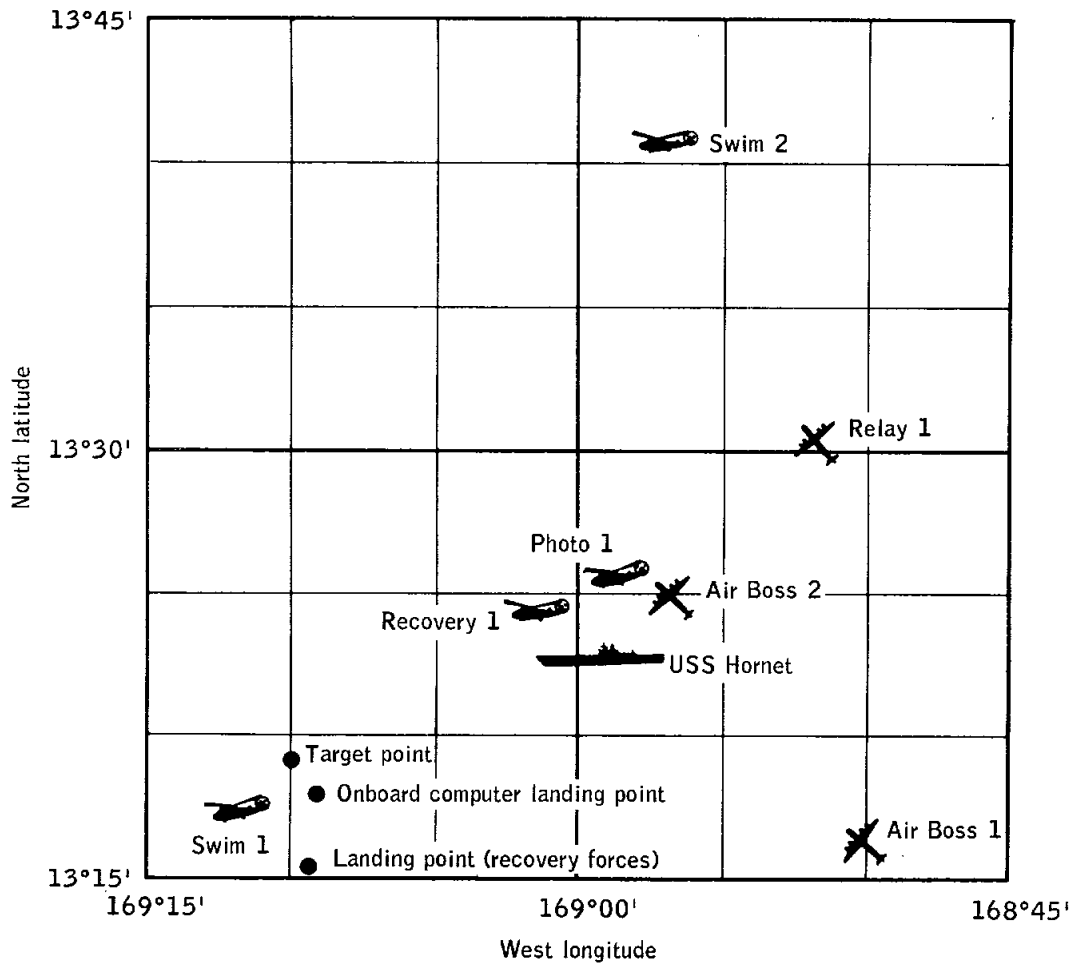


Figure 13-1.- Landing and recovery data.

## 14.0 ASSESSMENT OF MISSION OBJECTIVES

The single primary mission objective for the Apollo 11 mission, as defined in reference 12, was to perform a manned lunar landing and return safely to earth. In addition to the single primary objective, 11 secondary objectives were delineated from the following two general categories:

- a. Perform selenological inspection and sampling
- b. Obtain data to assess the capability and limitations of a man and his equipment in the lunar environment.

The 11 secondary objectives are listed in table 14-I and are described in detail in reference 13.

The following experiments were assigned to the Apollo 11 mission:

- a. Passive seismic experiment (S-031)
- b. Lunar field geology (S-059)
- c. Laser ranging retro-reflector (S-078)
- d. Solar wind composition (S-080)
- e. Cosmic ray detection (S-151)

The single primary objective was met. All secondary objectives and experiments were fully satisfied except for the following:

- a. Objective G: Location of landed lunar module.
- b. Experiment S-059: Lunar field geology

These two items were not completely satisfied in the manner planned pre-flight and a discussion of the deficiencies appear in the following paragraphs. A full assessment of the Apollo 11 detailed objectives and experiments will be presented in separate reports.

### 14.1 LOCATION OF LANDED LUNAR MODULE

It was planned to make a near real-time determination of the location of the landed lunar module based on crew observations. Observations by the lunar module crew during descent and after landing were to provide

information for locating the landing point using onboard maps. In addition, this information was to be transmitted to the Command Module Pilot, who was to use the sextant in an attempt to locate the landed lunar module. Further, if it were not possible for the Command Module Pilot to resolve the lunar module in the sextant, then he was to track a nearby landmark that had a known location relative to the landed lunar module (as determined by the lunar module crew or the ground team).

This near-real-time determination of the landed lunar module location by the lunar module crew was not accomplished because their attention was confined to the cabin during most of the visibility phase of the descent. Consequently, their observations of the lunar features during descent were not sufficient to allow them to judge their position. Their observation of the large crater near the landing point did provide an important clue to their location but was not sufficient in itself to locate the landing point with confidence.

On several orbital passes, the Command Module Pilot used the sextant in an attempt to locate the lunar module. His observations were directed to various areas where the lunar module could have landed, based on ground data. These attempts to locate the lunar module were unsuccessful, and it is doubtful that the Command Module Pilot's observations were ever directed to the area where the lunar module was actually located.

Toward the end of the lunar surface stay, the location of the landed lunar module was determined from the lunar module rendezvous radar tracking data (confirmed postflight using descent photographic data). However, the Command Module Pilot's activities did not permit his attempting another tracking pass after the lunar module location had been determined accurately.

This objective will be repeated for the Apollo 12 mission.

#### 14.2 LUNAR FIELD GEOLOGY

For the Apollo 11 mission, the documented sample collection (S-059, Lunar Field Geology) was assigned the lowest priority of any of the scientific objectives and was planned as one of the last activities during the extravehicular activity period. Two core tube samples were collected as planned, and about 15 pounds of additional lunar samples were obtained as part of this objective. However, time constraints on the extravehicular activity precluded collection of these samples with the degree of documentation originally planned.

In addition, time did not permit the collection of a lunar environment sample or a gas analysis sample in the two special containers provided. Although these samples were not obtained in their special containers, it was possible to obtain the desired results using other samples contained in the regular sample return containers.



TABLE 14-I.- DETAILED OBJECTIVES AND EXPERIMENTS

	Description	Completed
A	Contingency sample collection	Yes
B	Lunar surface extravehicular operations	Yes
C	Lunar surface operations with extravehicular mobility unit	Yes
D	Landing effects on lunar module	Yes
E	Lunar surface characteristics	Yes
F	Bulk sample collection	Yes
G	Location of landed lunar module	Partial
H	Lunar environment visibility	Yes
I	Assessment of contamination by lunar material	Yes
L	Television coverage	Yes
M	Photographic coverage	Yes
S-031	Passive seismic experiment	Yes
S-059	Lunar field geology	Partial
S-078	Laser ranging retro-reflector experiment	Yes
S-080	Solar wind composition	Yes
S-151	Cosmic ray detection	Yes
T-029	Pilot describing function	Yes

15.0 LAUNCH VEHICLE SUMMARY

The trajectory parameters of the AS-506 launch vehicle from launch to translunar injection were all close to expected values. The vehicle was launched on an azimuth 90 degrees east of north. A roll maneuver was initiated at 13.2 seconds to place the vehicle on the planned flight azimuth of 72.058 degrees east of north.

Following lunar module ejection, the S-IVB/instrument unit maneuvered to a sling-shot attitude that was fixed relative to local horizontal. The retrograde velocity to perform the lunar sling-shot maneuver was accomplished by a liquid oxygen dump, an auxiliary propulsion system firing, and liquid hydrogen venting. The vehicle's closest approach of 1825 miles above the lunar surface occurred at 78:42:00.

Additional data on the launch vehicle performance are contained in reference 1.

## 16.0 ANOMALY SUMMARY

This section contains a discussion of the significant problems or discrepancies noted during the Apollo 11 mission.

### 16.1 COMMAND AND SERVICE MODULES

#### 16.1.1 Service Propulsion Nitrogen Leak

During the lunar orbit insertion firing, the gaseous nitrogen in the redundant service propulsion engine actuation system decayed from 2307 to 1883 psia (see fig. 16-1), indicating a leak downstream of the injector pre-valve. The normal pressure decay as experienced by the primary system is approximately 50 psia for each firing. Only the one system was affected, and no performance degradation resulted. This actuation system was used during the transearth injection firing, and no leakage was detected.

The fuel and oxidizer valves are controlled by actuators driven by nitrogen pressure. Figure 16-2 is representative of both nitrogen control systems. When power is applied to the service propulsion system in preparation for a maneuver, the injector pre-valve is opened; however, pressure is not applied to the actuators because the solenoid control valves are closed. When the engine is commanded on, the solenoid control valves are opened, pressure is applied to the actuator, and the rack on the actuator shaft drives a pinion gear to open the fuel and oxidizer valves. When the engine is commanded off, the solenoid control valve vents the actuator and closes the fuel and oxidizer valves.

The most likely cause of the problem was contamination in one of the components downstream of the injector pre-valve, which isolates the nitrogen supply during nonfiring periods. The injector pre-valve was not considered a problem source because it was opened 2 minutes before ignition and no leakage occurred during that period. The possibility that the regulator and relief valve were leaking was also eliminated since pressure was applied to these components when the pre-valve was opened.

The solenoid control valves have a history of leakage, which has occurred either because of improper internal air gap adjustment or because of seal damage caused by contamination. The air gap adjustment could not have caused the leakage because an improper air gap with the pre-valves open would have caused the leak to remain constant.

Both of the solenoid control valves in the leaking system had been found to be contaminated before flight and were removed from the system, rebuilt, and successfully retested during the acceptance test cycle.

It is concluded that the leakage was due to a contamination-induced failure of a solenoid control valve. The source of contamination is unknown; however, it was apparently removed from the sealing surface during the valve closure for the first lunar orbit insertion maneuver (fig. 16-2). A highly suspect source is a contaminated facility manifold at the vendor's plant. Although an investigation of the prior failure indicated the flight valve was not contaminated, the facility manifold is still considered a possible source of the contaminants.

Spacecraft for Apollo 12 and subsequent missions have integral filters installed, and the facility manifolds are more closely controlled; therefore, no further corrective action will be taken.

This anomaly is closed.

#### 16.1.2 Cryogenic Heater Failure

The performance of the automatic pressure control system indicated that one of the two heater elements in oxygen tank 2 was inoperative. Data showing heater currents for prelaunch checkout verified that both heater elements were operational through the countdown demonstration test. However, the current readings recorded during the tank pressurization in the launch countdown showed that one heater in oxygen tank 2 had failed. This information was not made known to proper channels for disposition prior to the flight, since no specification limits were called out in the test procedure.

Manufacturing records for all block II oxygen tanks showed that there have been no thermal-switch nor electrical-continuity failures in the program; two failures occurred during the insulation resistance tests. One failure was attributed to moisture in the connector. After this unit was dried, it passed all acceptance tests. The other failure was identified in the heater assembly prior to installation in a tank. This was also an insulation problem and would not have prevented the heater from functioning normally.

The cause of the flight failure was probably an intermittent contact on a terminal board in the heater circuit. The 16-gage wiring at the board has exhibited intermittencies several times in the past. This is the same type terminal board that was found to be the cause of the control engine problem in this flight (see section 16.1.3).

Since the oxygen tank heaters are redundant, no constraints to the mission were created, other than a requirement for more frequent quantity balancing.

The launch-site test requirements have been changed to specify the amperage level to verify that both tank heaters are operational. Additionally, all launch-site procedures are being reviewed to determine whether specification limits are required in other areas.

This anomaly is closed.

### 16.1.3 Failure of Automatic Coil in One Thruster

The minus-yaw engine in command module reaction control system 1 produced low and erratic thrust in response to firing commands through the automatic coils of the engine valves. The spacecraft rates verify that the engine performed normally when fired using the direct coils.

Electrical continuity through at least one of the parallel automatic coils in the engine was evidenced by the fact that the stabilization and control system driver signals were normal. This, along with the fact that at least some thrust was produced, indicates that one of the two valves was working normally.

At the launch site, another engine undergoing checkout had failed to respond to commands during the valve signature tests. The problem was isolated to a faulty terminal board connector. This terminal board was replaced, and the systems were retested satisfactorily. Because of this incident and because of the previous history of problems with the terminal boards, these connectors were a prime suspect.

Postflight tests showed that two pins in the terminal board (fig. 16-3) were loose and caused intermittent continuity to the automatic coils of the engine valve. This type failure has previously been noted on terminal boards manufactured prior to November 1967. This board was manufactured in 1966.

The intermittent contact was caused by improper clip position relative to the bus bar counterbore. The improper positioning results in loss of some side force and precludes proper contact pressure against the bus bar. A design change to the base gasket was made to insure positively that the bus bar is correctly positioned.

The location of pre-November 1967 terminal boards has been determined from installation records, and it has been determined that none are in circuits which would jeopardize crew safety. No action will be taken for Apollo 12.

This anomaly is closed.

#### 16.1.4 Loss of Electroluminescent Segment in Entry Monitor System

An electroluminescent segment on the numeric display of the entry monitor system velocity counter would not illuminate. The segment is independently switched through a logic network which activates a silicon-controlled rectifier to bypass the light when not illuminated. The power source is 115 volts, 400 hertz.

Four cases of similar malfunctions have been recorded. One involved a segment which would not illuminate, and three involved segments which would not turn off. In each case, the cause was identified as misrouting of logic wires in the circuit controlling the rectifiers. The misrouting bent the wires across terminal strips containing sharp wire ends. These sharp ends punctured the insulation and caused shorts to ground or to plus 4 volts, turning the segment off or on, respectively.

A rework of the affected circuits took place in the process of soldering crimp joints involved in an Apollo 7 anomaly. An inspection to detect misrouting was conducted at this time; however, because of potting restrictions, the inspection was limited. A number of other failure mechanisms exist in circuit elements and leads; however, there is no associated failure history. A generic or design problem is considered unlikely because of the number of satisfactory activations sustained to date.

The preflight checkout program is being examined to identify possibilities for improvement in assuring proper operation of all segments over all operating conditions.

This anomaly is closed.

#### 16.1.5 Oxygen Flow Master Alarms

During the initial lunar module pressurization, two master alarms were activated when the oxygen flow rate was decreasing from full-scale. The same condition had been observed several times during altitude-chamber tests and during subsequent troubleshooting. The cause of the problem could not be identified before launch, but the only consequence of the alarms was the nuisance factor. Figure 16-4 shows the basic elements of the oxygen flow sensing circuit.

Note in figure 16-4 that in order for a master alarm to occur, relay K1 must hold in for 16 seconds, after which time relays K2 and K3 will close, activating a master alarm.

The capacitor shown is actually a part of an electromagnetic interference filter and is required to prevent fluctuation of the amplifier output to the voltage detector. Without the capacitor, a slow change in flow rate in the vicinity of the threshold voltage of relay K1 will cause this relay to continuously open and close (chatter).

Relay K2 has a slower dropout time than relay K1; therefore, if relay K1 is chattering, relay K2 may not be affected, so that the 16-second time delay continues to time out. Consequently, master alarms can be initiated without resetting the 16-second timer.

The filter capacitor was open during postflight tests, and the master alarms were duplicated with slow, decreasing flow rates.

There has been no previous failure history of these metalized Mylar capacitors associated with the flow sensors. No corrective action is required.

This anomaly is closed.

#### 16.1.6 Indicated Closure of Propellant Isolation Valves

The propellant isolation valves on quad B of the service module reaction control system closed during command and service module separation from the S-IVB. A similar problem was encountered on the Apollo 9 mission (see the Anomaly Summary in ref. 14). Tests after Apollo 9 indicated that a valve with normal magnetic latch forces would close at shock levels as low as 87g with an 11-millisecond duration; however, with durations in the expected range of 0.2 to 0.5 milliseconds, shock levels as high as 670g would not close the valves. The expected range of shock is 180g to 260g.

Two valves having the nominal latching force of 7 pounds were selected for shock testing. It was found that shocks of 80g for 10 milliseconds to shocks of 100g for 1 millisecond would close the valves. The latching forces for the valves were reduced to 5 pounds, and the valves were shock tested again. The shock required to close the valves at this reduced latching force was 54g for 10 milliseconds and 75g for 1 millisecond. After completion of the shock testing, the valves were examined and tested, and no degradation was noted. Higher shock levels may have been experienced in flight, and further tests will be conducted.

A review of the checkout procedures indicates that the latching force can be degraded only if the procedures are not properly implemented, such as the application of reverse current or ac to the circuit. On Apollo 12 a special test has indicated that the valve latching force has not been degraded.

Since there is no valve degradation when the valve is shocked closed and the crew checklist contains precautionary information concerning these valves, no further action is necessary.

This anomaly is closed.

#### 16.1.7 Odor in Docking Tunnel

An odor similar to burned wire insulation was detected in the tunnel when the hatch was first opened. There was no evidence of discoloration nor indications of overheating of the electrical circuits when examined by the crew during the flight. Several other sources of the odor were investigated, including burned particles from tower jettison, outgassing of a silicone lubricant used on the hatch seal, and outgassing of other components used in the tunnel area. Odors from these sources were reproduced for the crew to compare with the odors detected during flight. The crew stated that the odor from a sample of the docking hatch ablator was very similar to that detected in flight. Apparently, removal of the outer insulation (TG-15000) from the hatch of Apollo 11 (and subsequent) resulted in higher ablator temperatures and, therefore, a larger amount of outgassing odor than on previous flights.

This anomaly is closed.

#### 16.1.8 Low Oxygen Flow Rate

Shortly after launch, the oxygen flow measurement was at the lower limit of the instrumentation rather than indicating the nominal metabolic rate of 0.3 lb/hr. Also, during water separator cyclic accumulator cycles, the flow indication was less than the expected full measurement output of 1.0 lb/hr.

Analysis of associated data indicated that the oxygen flow was normal, but that the indicated flow rate was negatively biased by approximately 1.5 lb/hr. Postflight tests of the transducer confirmed this bias, and the cause was associated with a change in the heater winding resistance within the flow sensor bridge (fig. 16-5). The resistance of the heater had increased from 1000 ohms to 1600 ohms, changing the temperature of the hot wire element which supplies the reference voltage for the balance of the bridge. Further testing to determine the cause of the resistance change is not practical because of the minute size of the potted resistive element. Depotting of the element would destroy available evidence of the cause of failure. Normally, heater resistance changes have occurred early in the 100-hour burn-in period when heater stability is achieved.



A design problem is not indicated; therefore, no action will be taken.

This anomaly is closed.

#### 16.1.9 Forward Heat Shield Mortar Lanyard Untied

An apparent installation error on the forward heat shield mortar umbilical lanyard was found during postflight examination of Apollo 11 in that all but one of the tie-wrap knots were untied. This series of knots secures the tie-wraps around the electrical bundle and functions to break the wraps during heat shield jettison.

The knots should be two closely tied half-hitches which secure the tie-wrap to the lanyard (fig. 16-6). Examination of the Apollo 10 lanyard indicates that these knots were not two half-hitches but a clove hitch (see figure). After the lanyard breaks the tie-wraps, if the fragment of tie wrap pulls out of the knot, the clove hitch knot can untie, thus lengthening the lanyard. Lengthening this lanyard as the umbilical cable pays out can allow transfer of some loading into the umbilical disconnects. Should a sufficient load be transferred to the disconnect fitting to cause shear pins to fail, a disconnect of the forward heat shield mortar umbilical could result prior to the mortar firing. This would prevent deployment of the forward heat shield separation augmentation parachute, and there would be a possibility of forward heat shield recontact with the command module. Examination of the forward heat shield recovered from Apollo 10 confirmed that the mortar had fired and the parachute was properly deployed.

Spacecraft 110 and 111 were examined, and it was found that a clove hitch was erroneously used on those vehicles also.

A step-by-step procedure for correct lanyard knot tying and installation has been developed for spacecraft 112. Apollo 12 and 13 will be reworked accordingly.

This anomaly is closed.

#### 16.1.10 Glycol Temperature Control Valve

An apparent anomaly exists with the glycol temperature control valve or the related temperature control system. Temperature of the water/glycol entering the evaporator is normally maintained above 42° F by the glycol temperature control valve, which mixes hot water/glycol with water/glycol returning from the radiators (see fig. 16-7). As the radiator outlet temperature decreases, the temperature control valve opens to allow

more hot glycol to mix with the cold fluid returning from the radiator to maintain the evaporator inlet temperature at 42° to 48° F. The control valve starts to close as the radiator outlet temperature increases and closes completely at evaporator inlet temperatures above 48° F. If the automatic temperature control system is lost, manual operation of the temperature control valve is available by deactivating the automatic mode. This is accomplished by positioning the glycol evaporator temperature inlet switch from AUTO to MANUAL, which removes power from the control circuit.

Two problems occurred on Apollo 11, primarily during lunar orbit operations. First, as the temperature of the water/glycol returning from the radiators increased, the temperature control valve did not close fast enough, thus producing an early rise in evaporator outlet temperature. Second, the evaporator outlet temperature decreased to 31° F during revolution 15 as the radiator outlet temperature was rapidly decreasing (see fig. 16-8). The figure also shows normal operation of the valve and control system after the problem. Both anomalies disappeared about the time the glycol evaporator temperature inlet switch was cycled by the crew during revolution 15. The temperature control valve and related control system continued to operate satisfactorily for the remainder of the mission.

The control valve was removed from the spacecraft, disassembled, and inspected. A bearing within the gear train was found to have its retainer disengaged from the race. The retainer was interfering with the worm gear travel. The cause of the failure of the retainer is under investigation.

This anomaly is open.

#### 16.1.11 Service Module Entry

Photographic data were obtained of the service module entering the earth's atmosphere and disintegrating near the command module. Preflight predictions indicated the service module should have skipped out of the earth's atmosphere and entered a highly elliptical orbit. The crew observed the service module about 5 minutes after separation and indicated the reaction control thrusters were firing and the module was rotating about the X plane.

Based on the film, crew observation of the service module, and data from previous missions, it appears that the service module did not perform as a stable vehicle following command module/service module separation. Calculations using Apollo 10 data show that it is possible for the remaining propellants to move axially at frequencies approximately equal to the precessional rate of the service module spin axis about the X body

axis. This effect causes the movement to resonate, and the energy transfer between the rotating vehicle and the propellants may be sufficient to cause the service module to go into a flat spin about the Y or Z axis and become unstable.

Six-degree-of-freedom calculations, with a spring-mass propellant movement model, have been performed, and they do indicate that a trend toward instability is caused by propellant movement. Certain trends exist now which indicate that the service module could flip over as a result of propellant movement and attain a retrograde component of reaction control thrusting before going unstable. Service module separation instability is being reassessed to determine any change in the separation maneuver which may be desirable to better control the trajectory of the service module.

Additional analysis is continuing to determine the cause of the apparent instability.

This anomaly is open.

## 16.2 LUNAR MODULE

### 16.2.1 Mission Timer Stopped

The crew reported shortly after lunar landing that the mission timer had stopped. They could not restart the clock at that time, and the power to the timer was turned off to allow it to cool. Eleven hours later, the timer was restarted and functioned normally for the remainder of the mission.

Based on the characteristic behavior of this timer and the similarity to previous timer failures, the most probable cause of failure is a cracked solder joint. A cracked solder joint is the result of cordwood construction, where electrical components (resistors, capacitors, diodes, etc.) are soldered between two circuit boards, and the void between the boards is filled with potting compound (fig. 16-9). The differential expansion between the potting compound and the component leads causes the solder joints to crack, breaking electrical contact. Presumably, the 11-hour period the timer was off allowed it to cool sufficiently for the cracked joint to make electrical contact, and then the timer operated normally.

There is no practical solution to the problem for units which are installed for the Apollo 12 mission. However, a screening (vibration and thermal tests and 50 hours of operation) has been used to select timers for vehicle installation to decrease the probability of failure. The Apollo 11 timer was exposed to vibration and thermal tests and 36 hours of operation prior to installation.

New mission timers and event timers which will be mechanically and electrically interchangeable with present timers are being developed. These new timers will use integrated circuits welded on printed circuit boards instead of the cordwood construction and include design changes associated with the other timer problems, such as cracked glass and electromagnetic interference susceptibility. The new timers will be incorporated into the spacecraft when qualification testing is complete.

This anomaly is closed.

#### 16.2.2 High Fuel Interface Pressure After Landing

During simultaneous venting of the descent propellant and supercritical helium tanks, fuel in the fuel/helium heat exchanger was frozen by the helium flowing through the heat exchanger. Subsequent heat soakback from the descent engine caused expansion of the fuel trapped in the section of line between the heat exchanger and the engine shutoff valve (fig. 16-10). The result was a pressure rise in this section of line. The highest pressure in the line was probably in the range of 700 to 800 psia (interface pressure transducer range is 0 to 300 psia). The weak point in the system is the bellows links, which yield above 650 psia and fail at approximately 800 to 900 psia. Failure of the links would allow the bellows to expand and relieve the pressure without external leakage. The heat exchanger, which is located in the engine compartment, thawed within about 1/2 hour and allowed the line pressure to decay.

On future missions, the solenoid valve (fig. 16-10) will be closed prior to fuel venting and opened some time prior to lift-off. This will prevent freezing of fuel in the heat exchanger and will allow the supercritical helium tank to vent later. The helium pressure rise rate after landing is approximately 3 to 4 psi/hr and constitutes no constraint to presently planned missions. Appropriate changes to operational procedures will be made.

This anomaly is closed.

#### 16.2.3 Indication of High Carbon Dioxide Partial Pressure

Shortly after the lunar module ascent, the crew reported that the measurement of carbon dioxide partial pressure was high and erratic. The secondary lithium hydroxide canister was selected, with no effect on the indication. The primary canister was then reselected, and a caution and warning alarm was activated.

Prior to extravehicular activity, the environmental control system had been deactivated. This stopped the water separator and allowed the condensate that had collected in the separator to drain into a tank (fig. 16-11). The drain tank contains a honeycomb material designed to retain the condensate. If the amount of condensate exceeded the effective surface of the honeycomb, water could have been leaked through the vent line and into the system just upstream of the sensor. (Before the sensor became erratic, the Commander had noted water in his suit.) Any free water in the optical section of the sensor will cause erratic performance. The carbon dioxide content is sensed by measuring the light transmission across a stream of suit-loop gas. Any liquid in the element affects the light transmission, thus giving improper readings.

To preclude water being introduced into the sensor from the drain tank, the vent line will be relocated to an existing boss upstream of the fans, effective on Apollo 13 (see fig. 16-11).

This anomaly is closed.

#### 16.2.4 Steerable Antenna Acquisition

When the steerable antenna was selected after acquisition on revolution 14, difficulty was encountered in maintaining communications. The downlink signal strength was lower than predicted and several times decreased to the level at which lock was lost. Errors were discovered in the antenna coverage restriction diagrams in the Spacecraft Operational Data Book for the pointing angles used. In addition, the diagram failed to include the thruster plume deflectors, which were added to the lunar module at the launch site. Figure 16-12 shows the correct blockage diagram and the one that was used in the Spacecraft Operational Data Book prior to flight. The pointing angles of the antenna were in an area of blockage or sufficiently close to blockage to affect the coverage pattern.

As the antenna boresight approaches vehicle structure, the on-boresight gain is reduced, the selectivity to incoming signals is reduced, and side-lobe interference is increased.

Further, a preflight analysis showed that the multipath signal, or reflected ray (fig. 16-13), from the lunar surface to the vehicle flight trajectory alone would be sufficient to cause some of the antenna tracking losses. Also, the reduction in antenna selectivity caused by vehicle blockage increases the probability of multipath interferences in the antenna tracking circuits.

In conclusion, both the vehicle blockage and the multipath signals probably contributed to the reduced measured signal.

The nominal performance of the steerable antenna before and after the time in question indicates that the antenna hardware operated properly.

For future missions, the correct vehicle blockage and multipath conditions will be determined for the predicted flight trajectory. Operational measures can be employed to reduce the probability of this problem recurring by selecting vehicle attitudes to orient the antenna away from vehicle blockages and by selecting vehicle attitude hold with the antenna track mode switch in the SLEW or manual position through the time periods when this problem may occur.

This anomaly is closed.

#### 16.2.5 Computer Alarms During Descent

Five computer program alarms occurred during descent prior to the low-gate phase of the trajectory. The performance of guidance and control functions was not affected.

The alarms were of the Executive overflow type, which signify that the guidance computer cannot accomplish all of the data processing requested in a computation cycle. The alarms indicated that more than 10 percent of the computational capacity of the computer was preempted by unexpected counter interrupts of the type generated by the coupling data units that interface with the rendezvous radar shaft and trunnion resolvers (see fig. 16-14).

The computer is organized such that input/output interfaces are serviced by a central processor on a time-shared basis with other processing functions. High-frequency data, such as accelerometer and coupling data unit inputs, are processed as counter interrupts, which are assigned the highest priority in the time-sharing sequence. Whenever one of these pulse inputs is received, any lower priority computational task being performed by the computer is temporarily suspended or interrupted for 11.72 microseconds while the pulse is processed, then control is returned to the Executive program for resumption of routine operations.

The Executive program is the job-scheduling and job-supervising routine which allocates the required erasable memory storage for each job request and decides which job is given control of the central processor. It schedules the various repetitive routines or jobs (such as Servicer, the navigation and guidance job which is done every 2 seconds) on an open-loop basis with respect to whether the job scheduled on the previous cycle was completed. Should the completion of a job be slowed because high-frequency counter interrupts usurp excessive central processor time, the Executive program will schedule the same job again and

reserve another memory storage area for its use. When the Executive program is requested to schedule a job and all locations are assigned, a program alarm is displayed and a software restart is initiated. A review of the jobs that can run during descent leads to the conclusion that multiple scheduling of the same job produced the program alarms. The cause for the multiple scheduling of jobs has been identified by analyses and simulations to be primarily counter interrupts from the rendezvous radar coupling data unit.

The interrupts during the powered descent resulted from the configuration of the rendezvous radar/coupling data unit/computer interface. A schematic of the interface is shown in figure 16-14. When the rendezvous radar mode switch is in the AUTO or SLEW position, the excitation for the radar shaft and trunnion resolvers is supplied by a 28-volt, 800-hertz signal from the attitude and translation control assembly. When the switch is in the LGC position, the positioning of the radar antenna is controlled by the guidance computer, and the resolver excitation is supplied by a 28-volt, 800-hertz source in the primary guidance and navigation system. The output signals of the shaft and trunnion resolvers interface with the coupling data units regardless of the excitation source. The attitude and translation control assembly voltage is locked in frequency with the primary guidance and navigation system voltage through the system's control of the PCM and timing electronics frequency, but it is not locked in phase. When the mode switch is not in LGC, the attitude and translation control assembly voltage is the source for the resolver output signals to the coupling data units while the primary guidance and navigation system 800-hertz voltage is used as a reference voltage in the analog-to-digital conversion portion of the coupling data unit. Any difference in phase or amplitude between the two 800-hertz voltages will cause the coupling data unit to recognize a change in shaft or trunnion position, and the coupling data unit will "slew" (digitally). The "slewing" of the data unit results in the undesirable and continuous transmission of pulses representing incremental angular changes to the computer. The maximum rate for the pulses is 6.4 kpps, and they are processed as counter interrupts. Each pulse received by the computer requires one memory cycle time (11.7 microseconds) to process. If a maximum of 12.8 kpps are received (two radar coupling data units), 15 percent of the available computer time will be spent in processing the radar interrupts. (The computer normally operates at approximately 90 percent of capacity during peak activity of powered descent.) When the capacity of the computer is exceeded, some repetitively scheduled routines will not be completed prior to the start of the next computation cycle. The computer then generates a software restart and displays an Executive overflow alarm.

The meaningless counter interrupts from the rendezvous radar coupling data unit will not be processed by the Luminary 1B program used on future missions. When the radar is not powered up or the mode switch is not in the LGC position, the data units will be zeroed, preventing counter interrupts from being generated by the radar coupling data units. An additional change will permit the crew to monitor the descent without requiring as much computer time as was required in Luminary 1A.

This anomaly is closed.

#### 16.2.6 Slow Cabin Decompression

The decompression of the cabin prior to extravehicular activity required longer than had been anticipated.

The crew cannot damage the hatch by trying to open it prematurely. Static tests show that a handle force of 78 pounds at 0.25 psid and 118 pounds at 0.35 psid is required to permit air flow past the seal. The hatch deflected only in the area of the handle. A handle pull of 300 pounds at 2 psid did not damage either the handle or the hatch. In addition, neutral buoyancy tests showed that suited subjects in 1/6-g could pull 102 pounds maximum.

On Apollo 12 and subsequent vehicles, the bacteria filter will not be used, thus reducing the time for decompression from about 5 minutes to less than 2 minutes. In addition, the altitude chamber test for Apollo 13 included a partial cabin vent procedure which verified satisfactory valve assembly operation without the bacteria filter installed.

This anomaly is closed.

#### 16.2.7 Electroluminescent Segment on Display Inoperative

An electroluminescent segment on the numeric display of the abort guidance system data entry and display assembly was reported inoperative. The affected digit is shown in figure 16-15. With this segment inoperative, it was not possible to differentiate between the numerals 3 and 9. The crew was still able to use the particular digit; however, there was some ambiguity of the readout.

Each of the segments on the display is switched independently through a logic network which activates a silicon-controlled rectifier placed in series with the segments. The control circuit is different from that used in the entry monitor system velocity counter in this respect (see section 16.1.4), although both units are made by the same manufacturer. The power source is 115 volts, 400 hertz, and can be varied for intensity control.



One similar failure occurred on a delta qualification unit. The cause was a faulty epoxy process which resulted in a cracked and open electrode in the light emitting element.

Circuit analysis shows a number of component and wiring failures that could account for the failure; however, there is no history of these types of failure. The number of satisfactory activations of all the segments does not indicate the existence of a generic problem.

In order to ensure proper operation under all conditions, for future missions a prelaunch test will activate all segments, then the intensity will be varied through the full range while the display is observed for faults.

This anomaly is closed.

#### 16.2.8 Voice Breakup During Extravehicular Activity

Voice-operated relay operation during extravehicular activity caused breakup of voice received by the Network. This breakup was associated with both crewmen but primarily with the Lunar Module Pilot.

In ground tests, the conditions experienced during the extravehicular activity were duplicated by decreasing the sensitivity of the lunar module downlink voice-operated keying control from 9 (maximum) to 8, a decrease of about 7 dB. During chamber tests, lunar module keying by the extravehicular communications system was demonstrated when the sensitivity control was set at 9. The crew indicated that the pre-extravehicular activity adjustment should have been set in accordance with the onboard checklist (maximum increase). The crew also verified that they did not experience any voice breakup between each other or from the Network, indicating that the breakup was probably caused by marginal keying of the voice-operated keying circuits of the lunar module downlink relay.

Voice tapes obtained of the Apollo 11 crew during altitude chamber tests were used in an attempt to duplicate the problem by simulating voice modulation characteristics and levels being fed into the lunar module communications system during the extravehicular activity. These voice tapes modulated a signal generator which was received by and relayed through a breadboard (mockup) of the lunar module communication system. There was no discernible breakup of the relayed voice with the sensitivity control set at 9.

All analysis and laboratory testing to date indicates that the voice breakup experienced during the extravehicular activity was not an inherent system design problem. Testing has shown that any voice which will key the extravehicular communication system will also key the lunar module relay if the sensitivity control is set at 9.

The most probable cause of the problem is an inadvertent low setting of the Commander's sensitivity control. During extravehicular activity, both crewmen use the Commander's lunar module VOX circuit when talking to the ground. Other less likely causes are degraded modulation from the extravehicular communications system or degradation of the lunar module circuit gain between the VHF receiver and the Commander's amplifier. However, there are no known previous failures which resulted in degraded extravehicular communication modulation levels or degraded lunar module keying performance.

This anomaly is closed.

### 16.2.9 Echo During Extravehicular Activity

A voice turnaround (echo) was heard during extravehicular activity. At that time, the lunar module was operating in a relay mode. Uplink voice from the S-band was processed and retransmitted to the two extravehicular crewmen via the lunar module VHF transmitter. Crew voice and data were received by the lunar module VHF receiver and relayed to the earth via the lunar module S-band transmitter (see fig. 16-16). The echo was duplicated in the laboratory and resulted from mechanical acoustical coupling between the communications carrier earphone and microphone (fig. 16-17). The crew indicated that their volume controls were set at maximum during the extravehicular activity. This setting would provide a level of approximately plus 16 dBm into each crewman's earphones. Isolation between earphones and microphones, exclusive of air path coupling, is approximately 48 dB. The ground voice signal would therefore appear, at the microphone output, at a level of approximately minus 32 dBm. Assuming extravehicular communication keying is enabled, this signal would be processed and transmitted by the extravehicular communications system and would provide a level of approximately minus 12 dBm at the output of the lunar module VHF receiver. If the lunar module relay is enabled, this signal would be amplified and relayed to earth via S-band at a nominal output level.

When the lunar module voice-operated keying circuit is properly adjusted, any signal that keys the extravehicular communications system will also key the lunar module relay. There are indications that the lunar module voice keying sensitivity was set below maximum, as evidenced by the relayed voice breakup experienced by the Lunar Module Pilot (see section 16.2.8). Therefore, it would have been possible for the extravehicular communications system to be keyed by breathing or by suit air flow without this background noise being relayed by the lunar module. However, the uplink turnaround voice could provide the additional lunar module received audio signal level to operate the voice-operated keying circuits, permitting the signal to be returned to the earth. The crew indicated that the voice-operated keying circuits in the extravehicular

communications system were activated by suit air flow for some positions of the head in the helmet. Both voice-operated keying circuits were also keyed by bumping or rubbing of the communications carrier against the helmet. The random echo problem is inherent in the communication system design, and there does not appear to be any practical way to eliminate random voice keying or significantly reduce acoustical coupling in the communications carrier.

A procedure to inhibit the remoting of downlink voice during periods of uplink voice transmissions will be accomplished to eliminate the echo. The capsule communicator's console will be modified to allow CAPCOM simplex operation (uplink only, downlink disabled) during uplink transmissions as a backup mode of operation if the echo becomes objectionable. The ground system, however, will still have the echo of CAPCOM when using the simplex mode.

This anomaly is closed.

#### 16.2.10 Onboard Recorder Failure

The data storage electronics assembly did not record properly in flight. Postflight playback of the tape revealed that the reference tone was recorded properly; however, the voice signal was very low and recorded with a 400-hertz tone and strong background noise. Occasionally, the voice level was normal for short periods. In addition, only the 4.6-kilohertz timing signal was recorded. This signal should have switched between 4.2 and 4.6 kilohertz to record the timing code.

During postflight tests, the recorder functioned properly for the first 2 hours of operation. Then, the voice channel failed and recorded no voice or background noise, although timing and reference tones were recorded properly. This failure does not duplicate the flight results, indicating that it did not exist in flight.

Tests with the recorder installed in a lunar module were performed to determine the vehicle wiring failures that could cause the signals found on the flight tape. An open in both the timing signal return line and the voice signal line would duplicate the problem. Similar broken wires were found in LTA-8 during thermal/vacuum tests. The most likely cause of the failure was two broken wires (26 gage) in the vehicle harness to the recorder. For Apollo 12 through 15, the wire harness at the recorder connector will be wrapped with tape to stiffen it and provide protection against flexure damage. For Apollo 16 and subsequent, a sheet metal cover will be added to protect the harness.

Preflight data from the launch site checkout procedure show that both the timing inputs and the internally generated reference frequency were not within specification tolerances and may be indicative of a preflight problem with the system. The procedure did not specify acceptable limits but has now been corrected.

This anomaly is closed.

#### 16.2.11 Broken Circuit Breaker Knob

The crew reported after completion of extravehicular activity that the knob on the engine arm circuit breaker was broken and two other circuit breakers were closed. The engine arm circuit breaker was successfully closed when it was required for ascent, but loss of the knob would not allow manual opening of the breaker.

The most probable cause of the damage was impact of the oxygen purge system (aft edge) during preparation for extravehicular activities; such impact was demonstrated in simulations in a lunar module.

Circuit breaker guards will be installed on Apollo 12 and subsequent vehicles to prevent the oxygen purge system from impacting the circuit breakers.

This anomaly is closed.

#### 16.2.12 Thrust Chamber Pressure Switches

The switch used to monitor the quad 2 aft-firing engine (A2A) exhibited slow response to jet driver commands during most of the mission. During an 18-minute period just prior to terminal phase initiation, the switch failed to respond to seven consecutive minimum impulse commands. This resulted in a master alarm and a thruster warning flag, which were reset by the crew. The engine operated normally, and the switch failure had no effect on the mission. The crew did not attempt any investigative procedures to determine whether the engine had actually failed. A section drawing of the switch is shown in figure 16-18.

This failure was the first of its type to be observed in flight or in ground testing. The switch closing response (time of jet driver "on" command to switch closure) appeared to increase from an average of about 15 to 20 milliseconds during station-keeping to 25 to 30 milliseconds at the time of failure. Normal switch closing response is 10 to 12 milliseconds based on ground test results. The closing response remained at the 25- to 30-millisecond level following the failure, and the switch

continued to fail to respond to some minimum impulse commands. The switch opening time (time from jet driver "off" command to switch opening) appeared to be normal throughout the mission. In view of these results, it appears that the most probable cause of the switch failure was particulate contamination in the inlet passage of the switch. Contamination in this area would reduce the flow rate of chamber gases into the diaphragm cavity, thereby reducing the switch closing response. However, the contamination would not necessarily affect switch opening response since normal chamber pressure tailoff requires about 30 to 40 milliseconds to decrease from about 30 psia to the normal switch opening pressure of about 4 psia. The 30- to 40-millisecond time would probably be sufficient to allow the gases in the diaphragm cavity to vent such that the switch would open normally.

The crews for future missions will be briefed to recognize and handle similar situations.

This anomaly is closed.

#### 16.2.13 Water in One Suit

After the lunar module achieved orbit, water began to enter the Commander's suit in spurts (estimated to be 1 tablespoonful) at about 1-minute intervals. The Commander immediately selected the secondary water separator, and the spurts stopped after 15 to 20 minutes. The spurts entered the suit through the suit half vent duct when the crewmen were not wearing their helmets. The pressures in all liquid systems which interface with the suit loop were normal, indicating no leakage.

The possible sources of free water in the suit loop are the water separator drain tank, an inoperative water separator, local condensation in the suit loop, and leakage through the water separator selector valve. (see fig. 16-11). An evaluation of each of these possible sources indicated that leakage through the water separator selector valve was the most probable source of the free water.

The flapper type valve is located in a Y-duct arrangement and is used to select one of two water separators. Leakage of this valve would allow free water to bypass through the idle water separator and subsequently enter the suit hose. This leakage most probably resulted from a misalignment and binding in the slot of the selector valve actuation linkage (see fig. 16-19). The allowable actuation force after linkage rigging was 15 pounds. The usual actuation forces have been 7 to 8 pounds, but 12.5 pounds was required on Apollo 11. The allowable actuation force has been lowered to 10 pounds, and inspections for linkage binding have been incorporated into procedures at the factory and the launch site.

This anomaly is closed.

## 16.2.14 Reaction Control System Warning Flags

The crew reported thrust chamber assembly warning flags for three engine pairs. Quad 2 and quad 4 warning flags for system A occurred simultaneously during lunar module station-keeping prior to descent orbit insertion. Quad 4 flag for system B appeared shortly thereafter and also twice just before powered descent initiation. The crew believed these flags were accompanied by master alarms. The flags were reset by cycling of the caution and warning electronics circuit breaker. Sufficient data are not available to confirm any of the reported conditions.

One of the following may have caused the flag indications:

- a. Failure of the thrust chamber pressure switch to respond to thruster firings.
- b. Firing of opposing thrusters may have caused a thrust chamber-on failure indication.
- c. Erroneous caution and warning system or display flag operation.

The first two possible causes are highly unlikely because simultaneous multiple failures would have to occur and subsequently be corrected. The third possible cause is the most likely to have occurred where a single point failure exists. Ten of the sixteen engine pressure switch outputs are conditioned by the ten buffers in one module in the signal conditioner electronics assembly (fig. 16-20). This module is supplied with +28 V dc through one wire. In addition, the module contains an oscillator which provides an ac voltage to each of the ten buffers. If either the +28 V dc is interrupted or the oscillator fails, none of the ten buffers will respond to pressure switch closures. If engines monitored by these buffers are then commanded on, the corresponding warning flags will come up and a master alarm will occur.

If +X translation were commanded (fig. 16-21), the down-firing engines in quads 2 and 4 of system A could fire, giving flags 2A and 4A. A subsequent minus X rotation could fire the forward-firing thruster in quad 4 of system B and the aft-firing thruster in quad 2 of system A, giving flag 4B. The aft-firing engine in quad 2 of system A (A2A) is not monitored by one of the ten buffers postulated failed. The failure then could have cleared itself. The response of the vehicle to thruster firings would have been normal under these conditions. There is no history of similar failures either at package or module level in the signal conditioner electronics assembly. No corrective action will be taken.

This anomaly is closed.

## 16.3 GOVERNMENT-FURNISHED EQUIPMENT

### 16.3.1 Television Cable Retained Coiled Shape

The cable for the lunar surface television camera retained its coiled shape after being deployed on the lunar surface. Loops resulting from the coils represented a potential tripping hazard to the crew.

All the changes that have been investigated relative to changes in cable material and in stowage and deployment hardware have indicated only minimal improvement in deployed cable form, together with a weight penalty for the change. No hardware changes are planned.

This anomaly is closed.

### 16.3.2 Mating of Remote Control Unit to Portable Life Support System

During preparation for extravehicular activity, the crew experienced considerable difficulty in mating the electrical connectors from the remote control unit to the portable life support system. For rotational polarization alignment, it was necessary to grasp the cable insulation because the coupling lock ring was free for unlimited rotation on the connector shell (see fig. 16-22).

For future missions, the male half of the connector has been replaced with one which has a coupling lock ring with a positive rotational position with the connector shell and can be grasped for firm alignment of the two halves. The ring is then rotated 90 degrees to capture and lock. In addition, easier insertion has been attained with conical tipped contact pins in place of hemispherical tipped pins.

This anomaly is closed.

### 16.3.3 Difficulty in Closing Sample Return Containers

The force required to close the sample return containers was much higher than expected. This high closing force, coupled with the instability of the descent stage work table and the lack of adequate retention provisions, made closing the containers very difficult.

Because of the container seal, the force required to close the cover reduces with each closure. The crew had extensive training with a sample return container which had been opened and closed many times, resulting in closing forces lower than the maximum limit of 32 pounds.

The container used for the flight had not been exercised as had the container used for training. In addition, the cleaning procedures used by the contractor prior to delivery removed all lubricant from the latch linkage sliding surfaces. Tests with similar containers have shown that the cleaning procedure caused an increase in the closing force by as much as 24 pounds.

A technique for burnishing on the lubricant after cleaning has been incorporated. As a result, containers now being delivered have closing forces no greater than 25 pounds.

Over-center locking mechanisms for retaining the containers on the work table will be installed on a mock-up table and will be evaluated for possible incorporation on Apollo 13 and subsequent.

This anomaly is closed.



NASA-S-69-3775

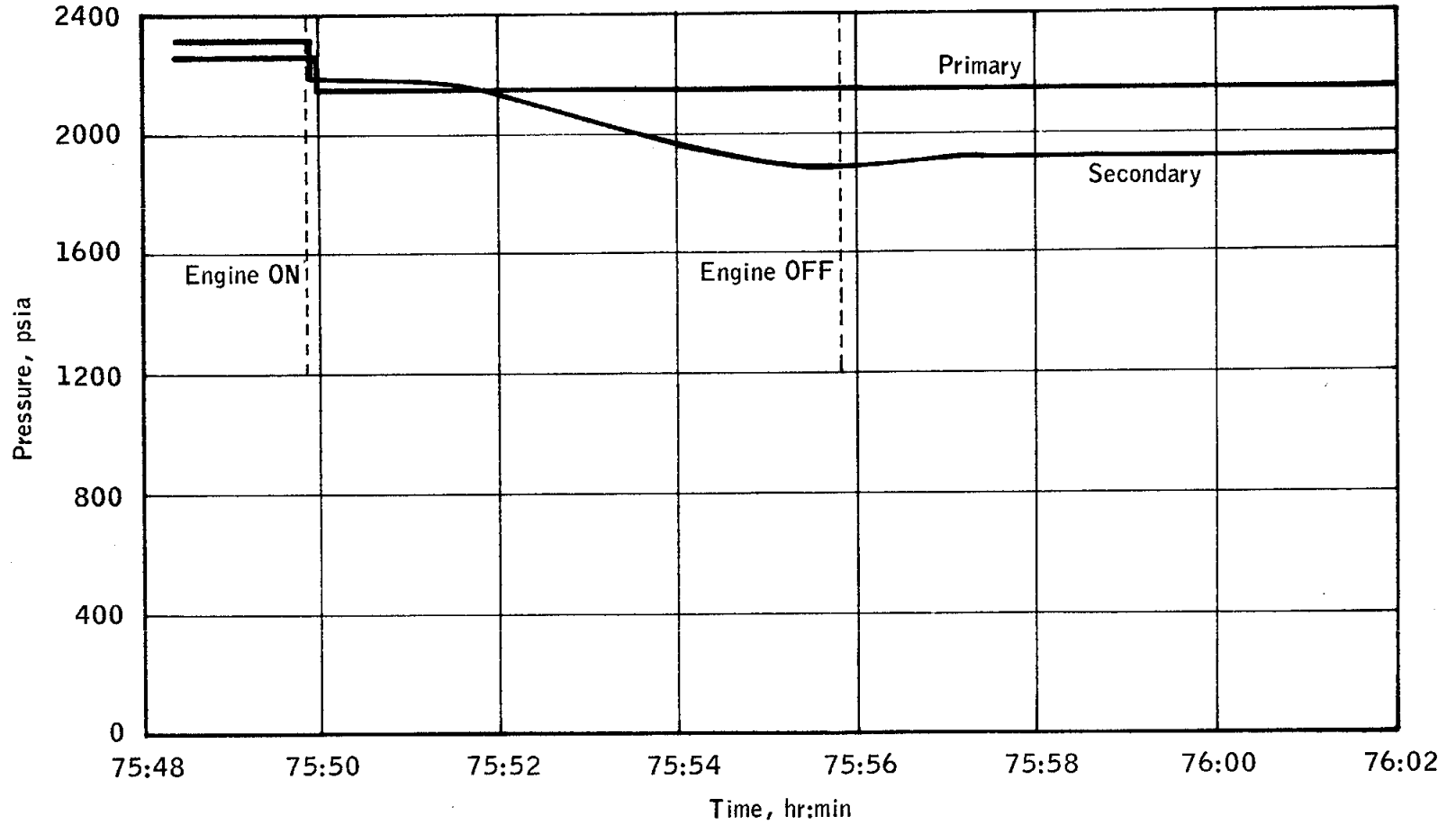


Figure 16-1.- Nitrogen pressure during initial lunar orbit insertion firing.

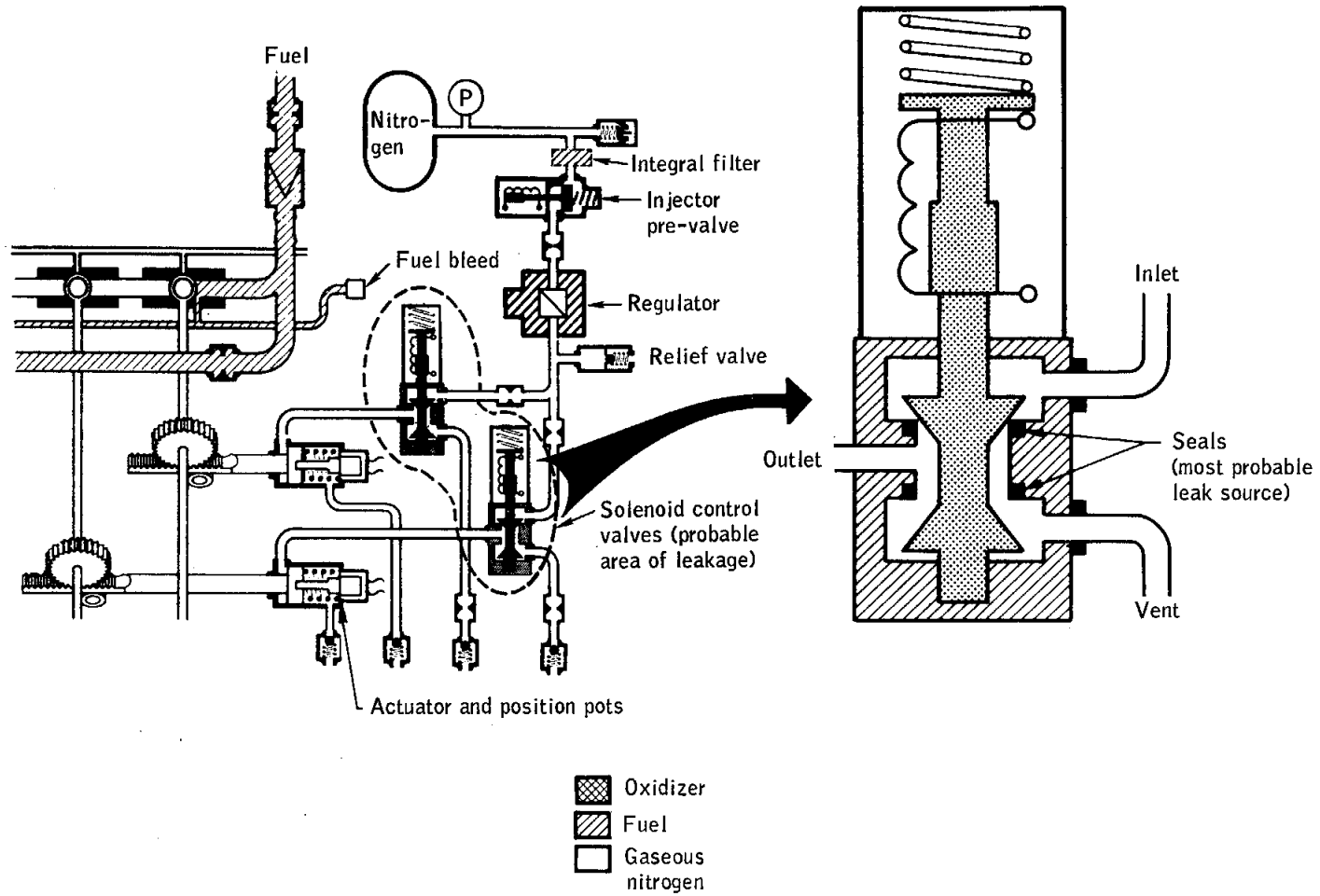


Figure 16-2.- Control for service propulsion propellants.

NASA-S-69-3777

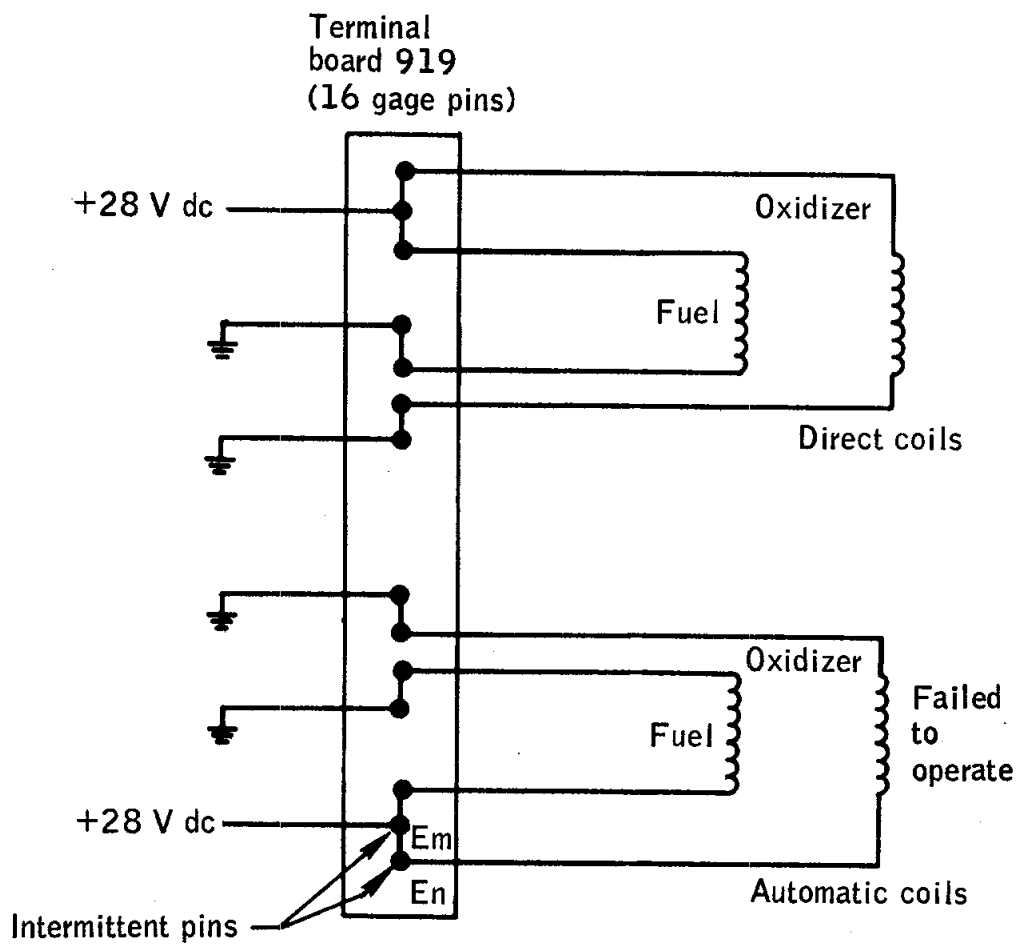


Figure 16-3.- Terminal board schematic for minus-yaw engine, command module reaction control system 1.

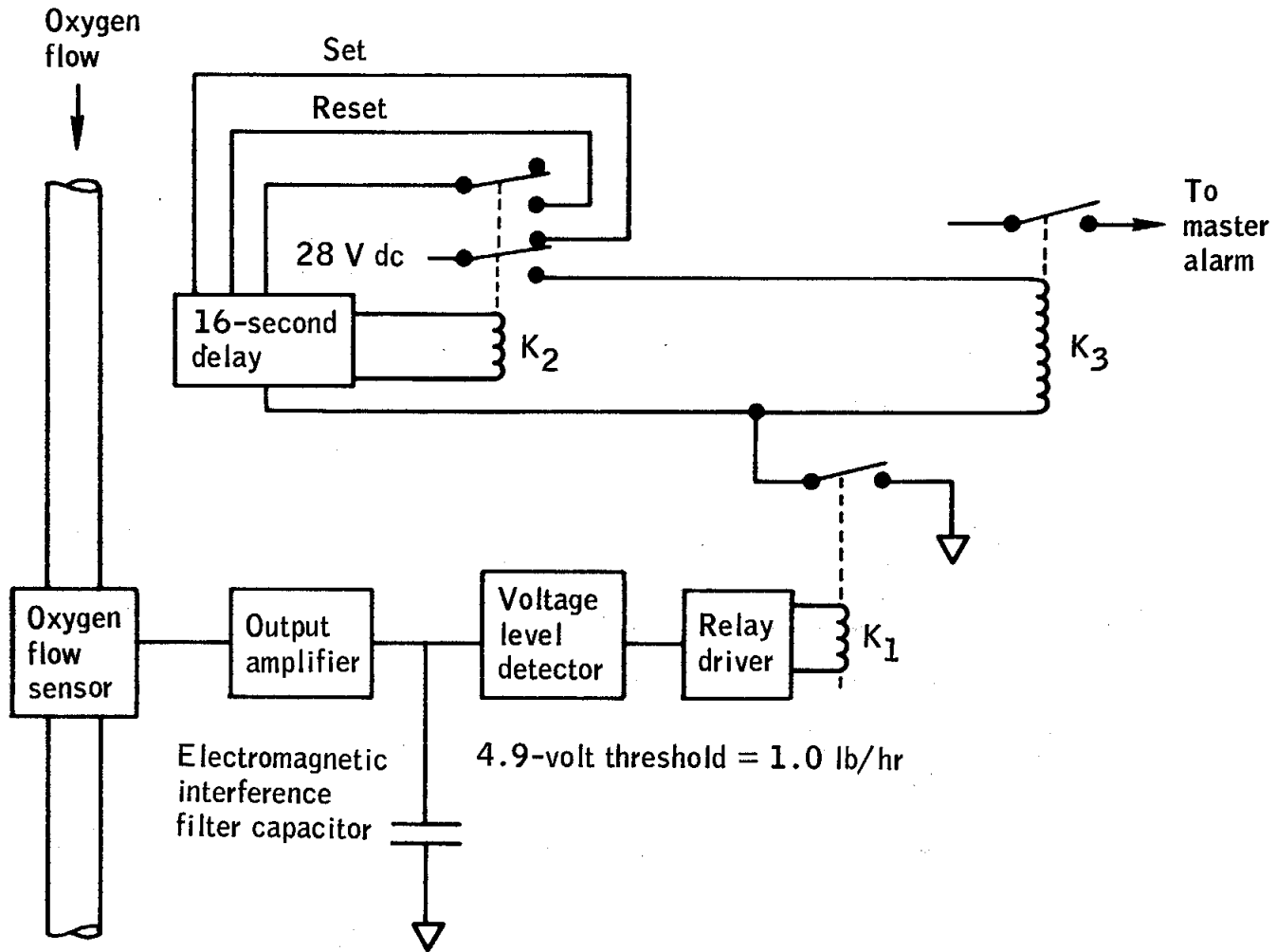


Figure 16-4.- Oxygen flow sensing circuit.

NASA-S-69-3779

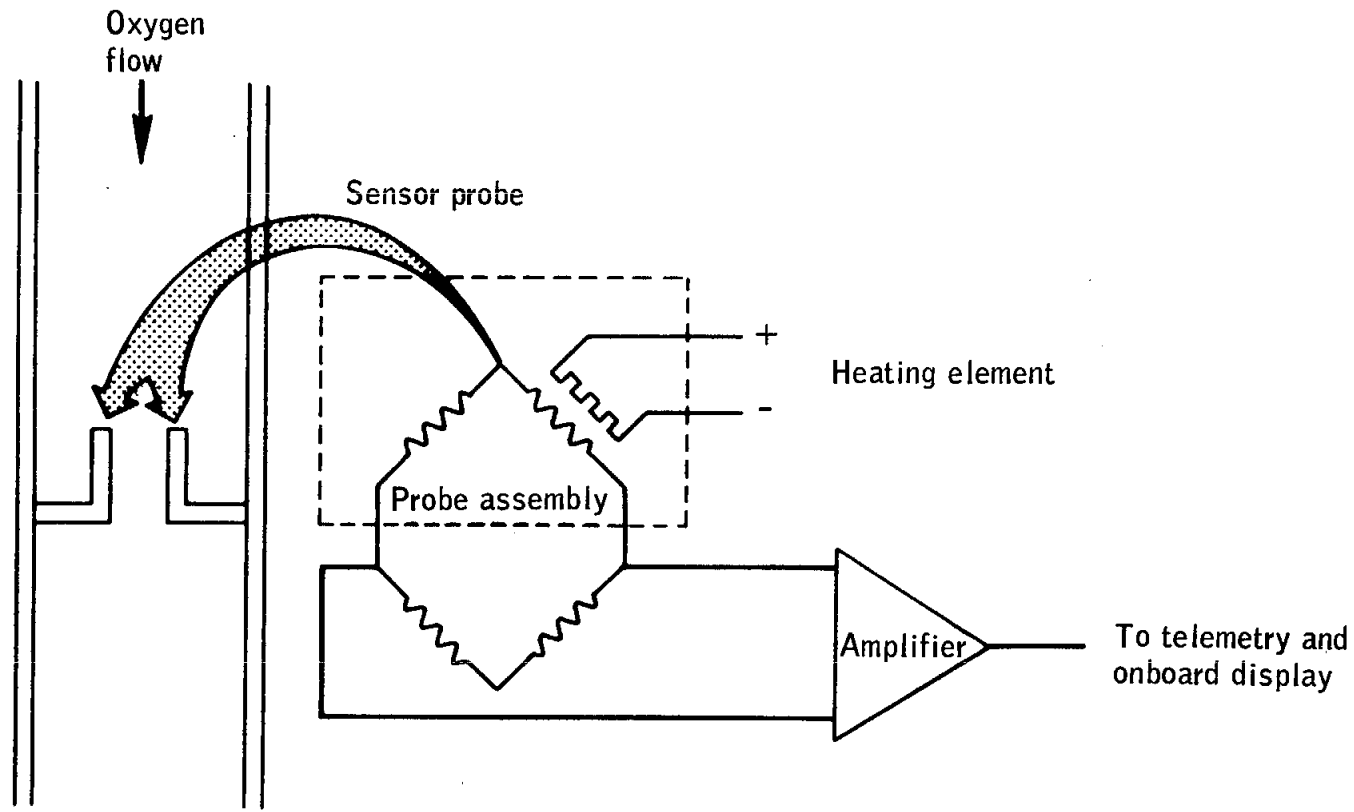


Figure 16-5.- Oxygen flow sensor.

NASA-S-69-3780

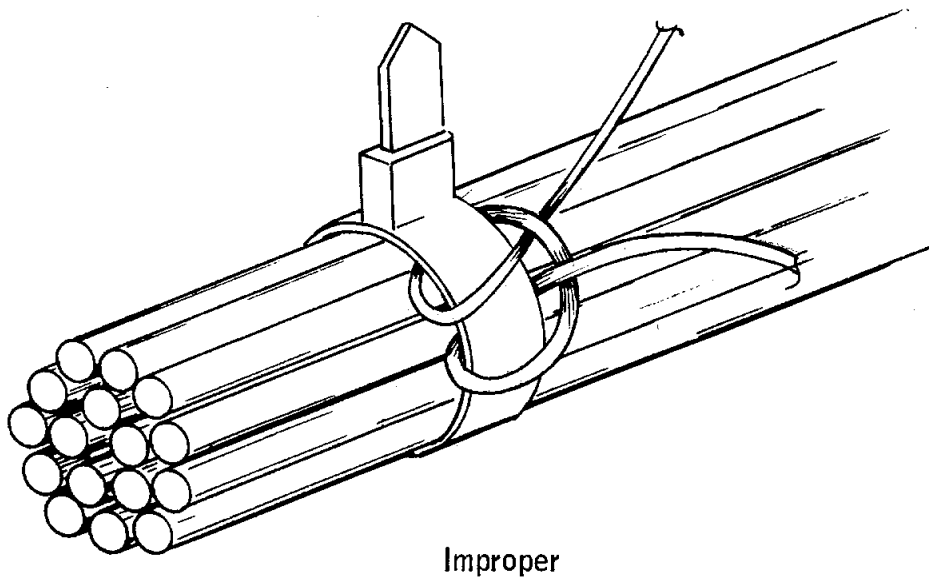
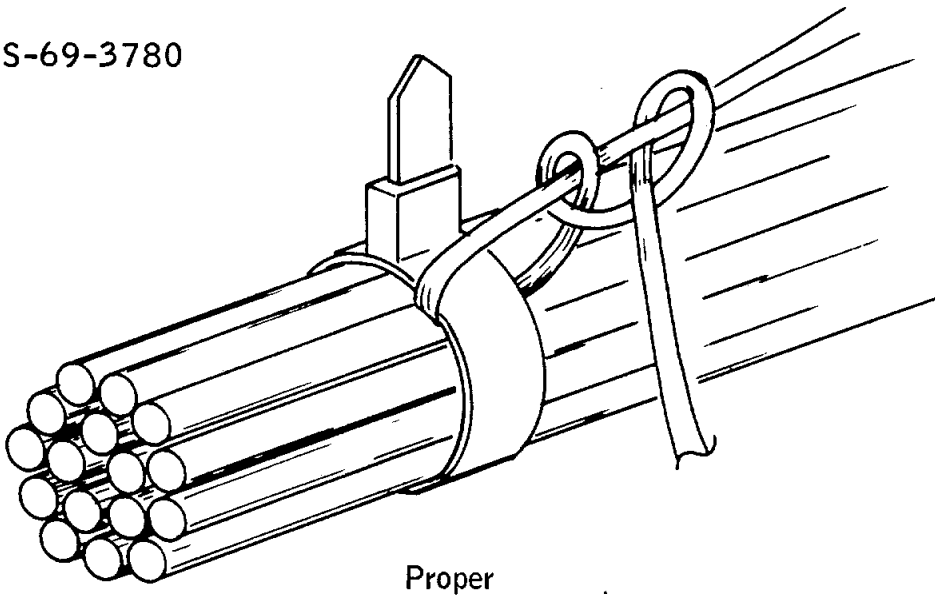


Figure 16-6.- Tie-wraps on lanyards.

NASA-S-69-3781

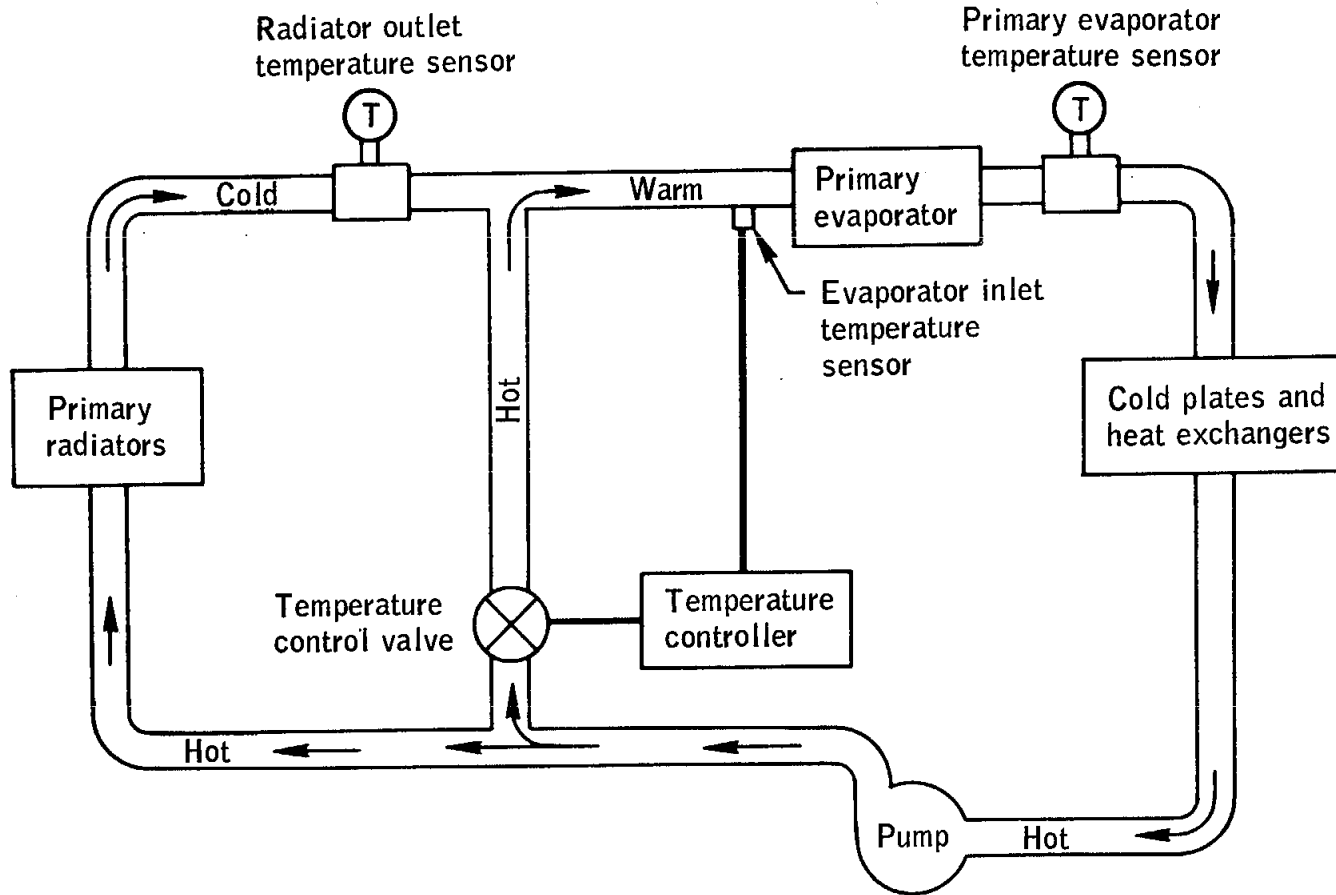


Figure 16-7.- Primary water glycol coolant loop.

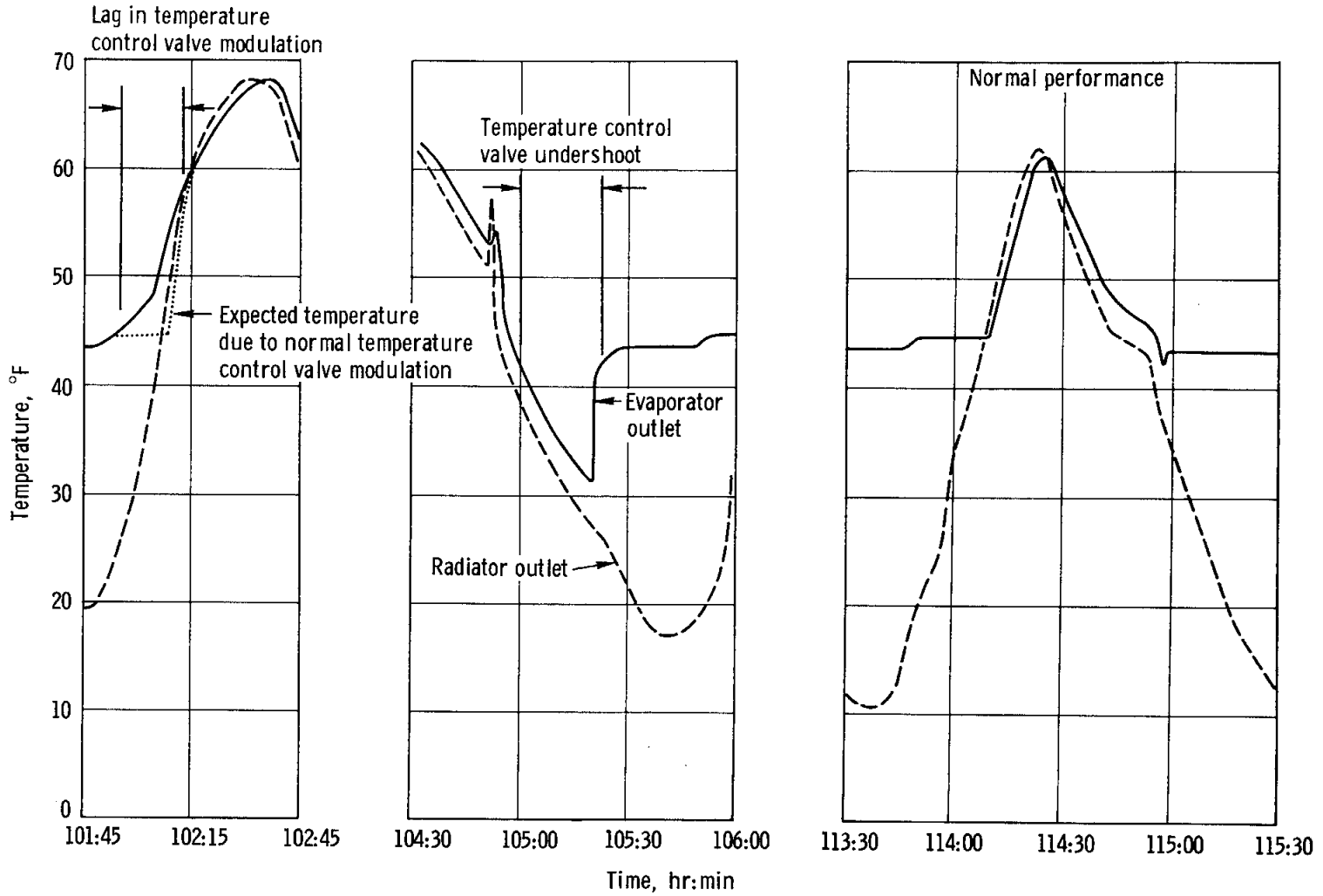


Figure 16-8. - Comparison of radiator and evaporator outlet temperatures.



NASA-S-69-3783

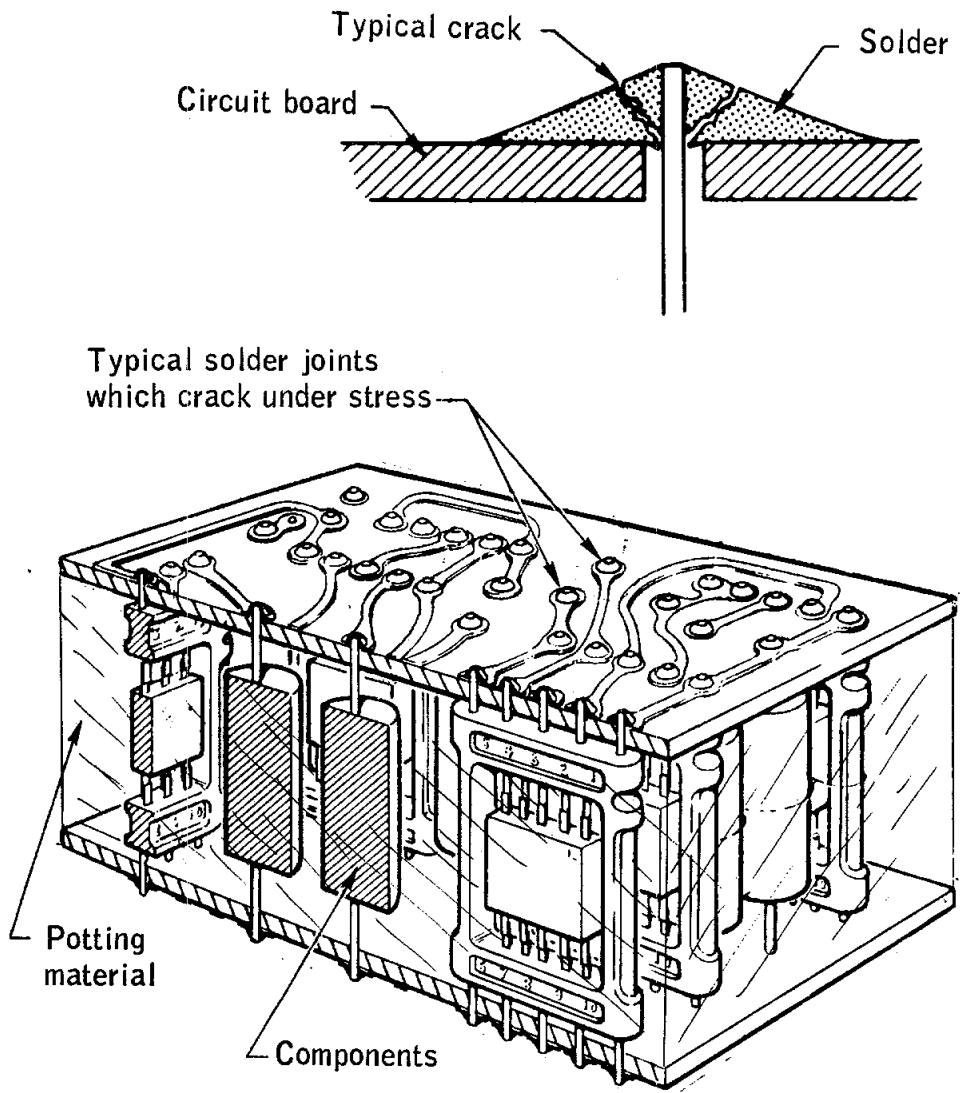


Figure 16-9.- Typical modular construction.

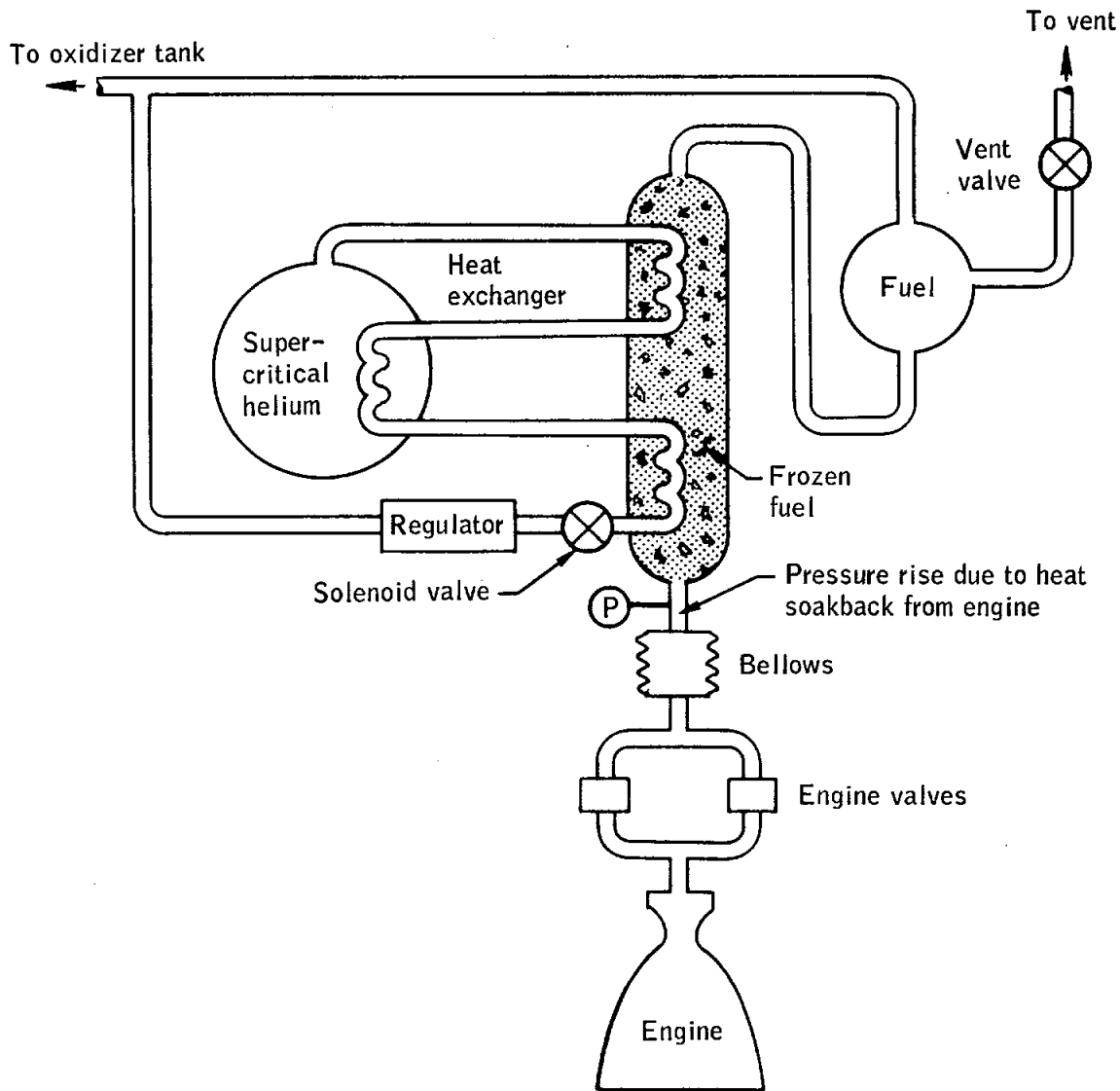


Figure 16-10.- Supercritical helium flow for descent propulsion system.

NASA-S-69-3785

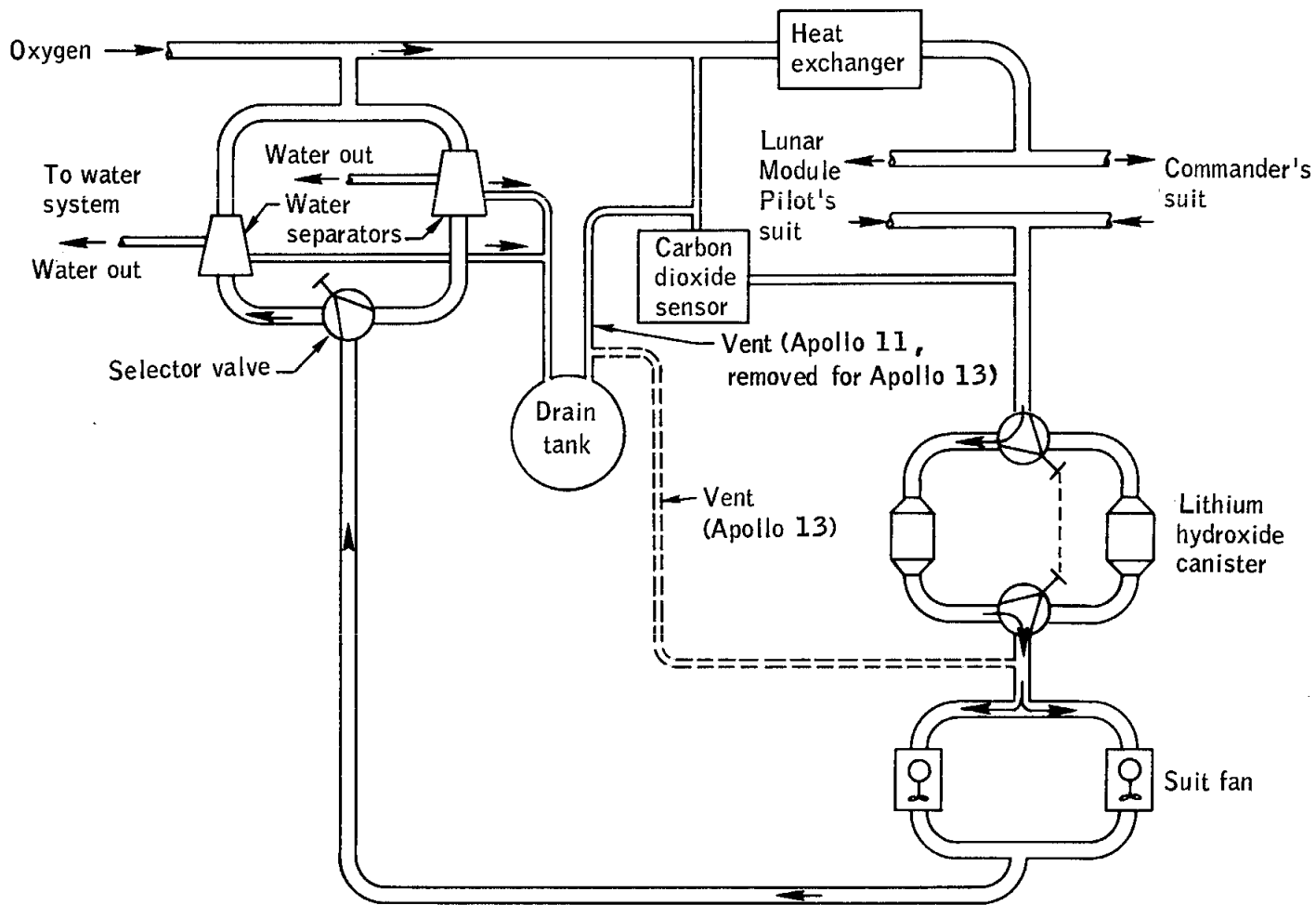


Figure 16-11.- Simplified suit loop schematic.

NASA-S-69-3786

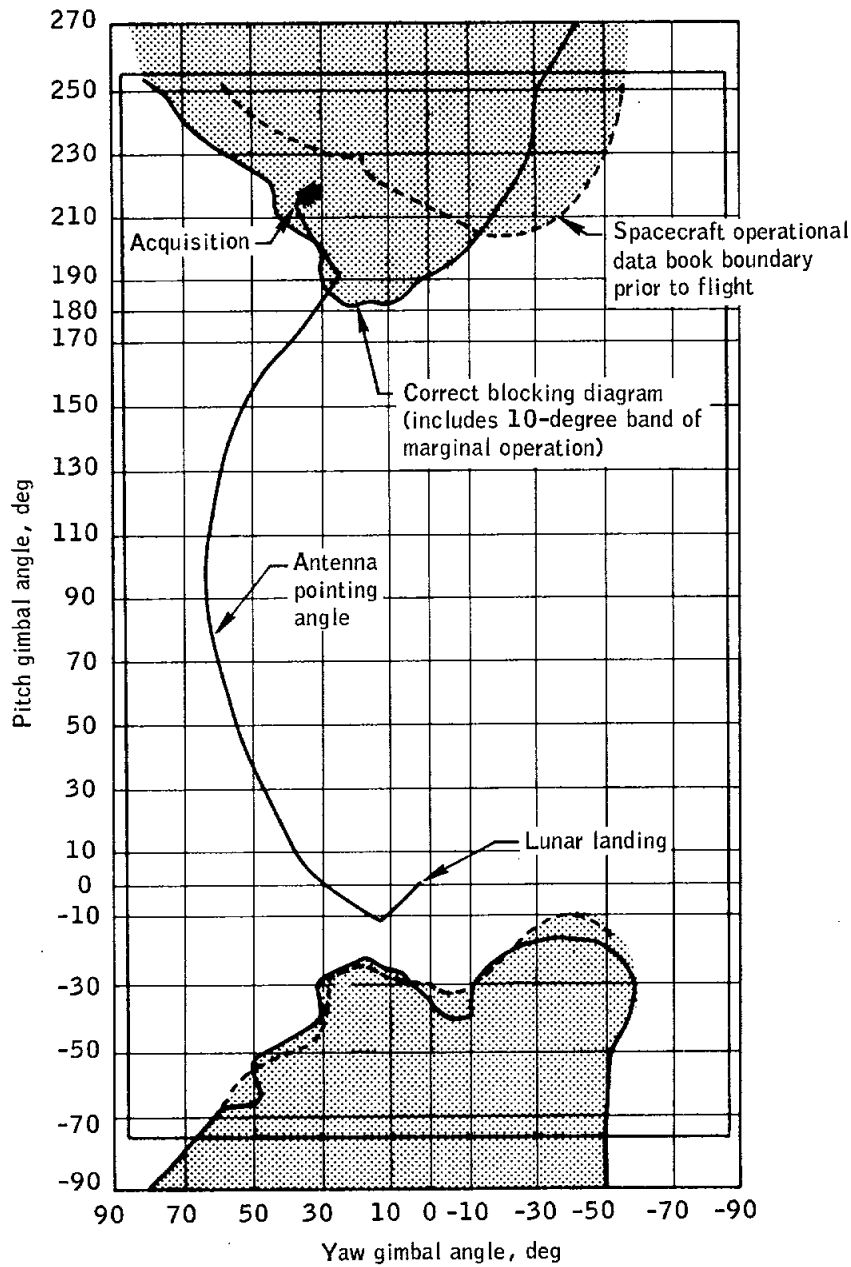


Figure 16-12.- S-band steerable antenna coverage restrictions.

NASA-S-69-3787

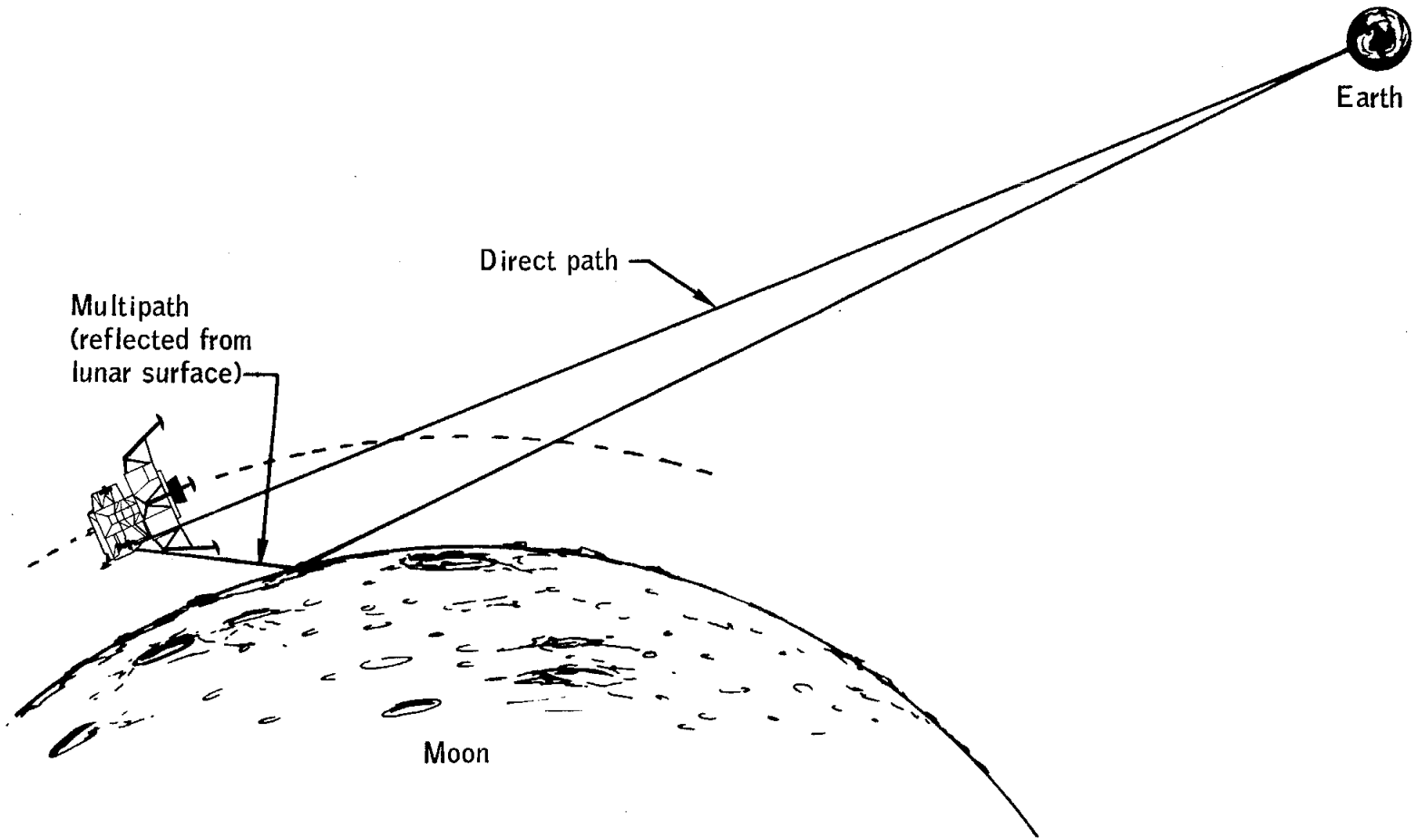


Figure 16-13.- Example of multipath.

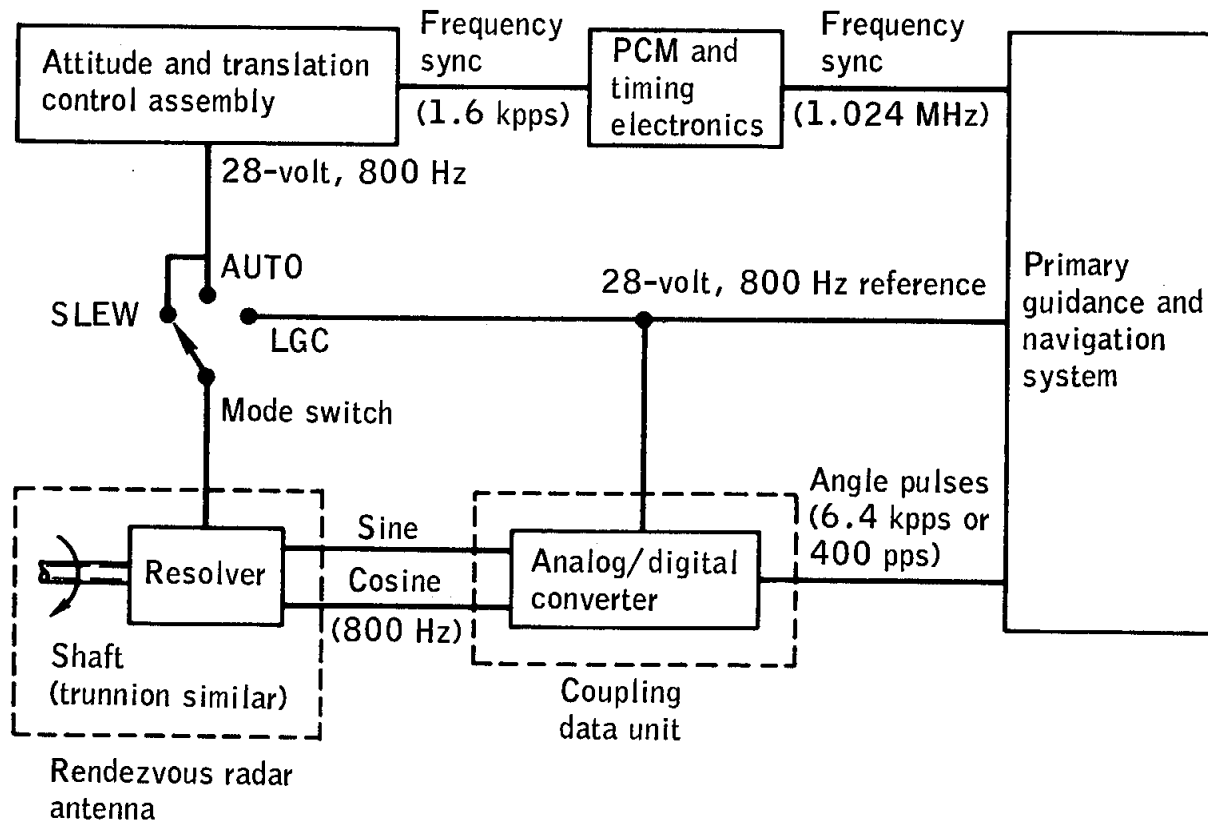


Figure 16-14.- Interfaces from rendezvous radar antenna to primary guidance system.

NASA-S-69-3789

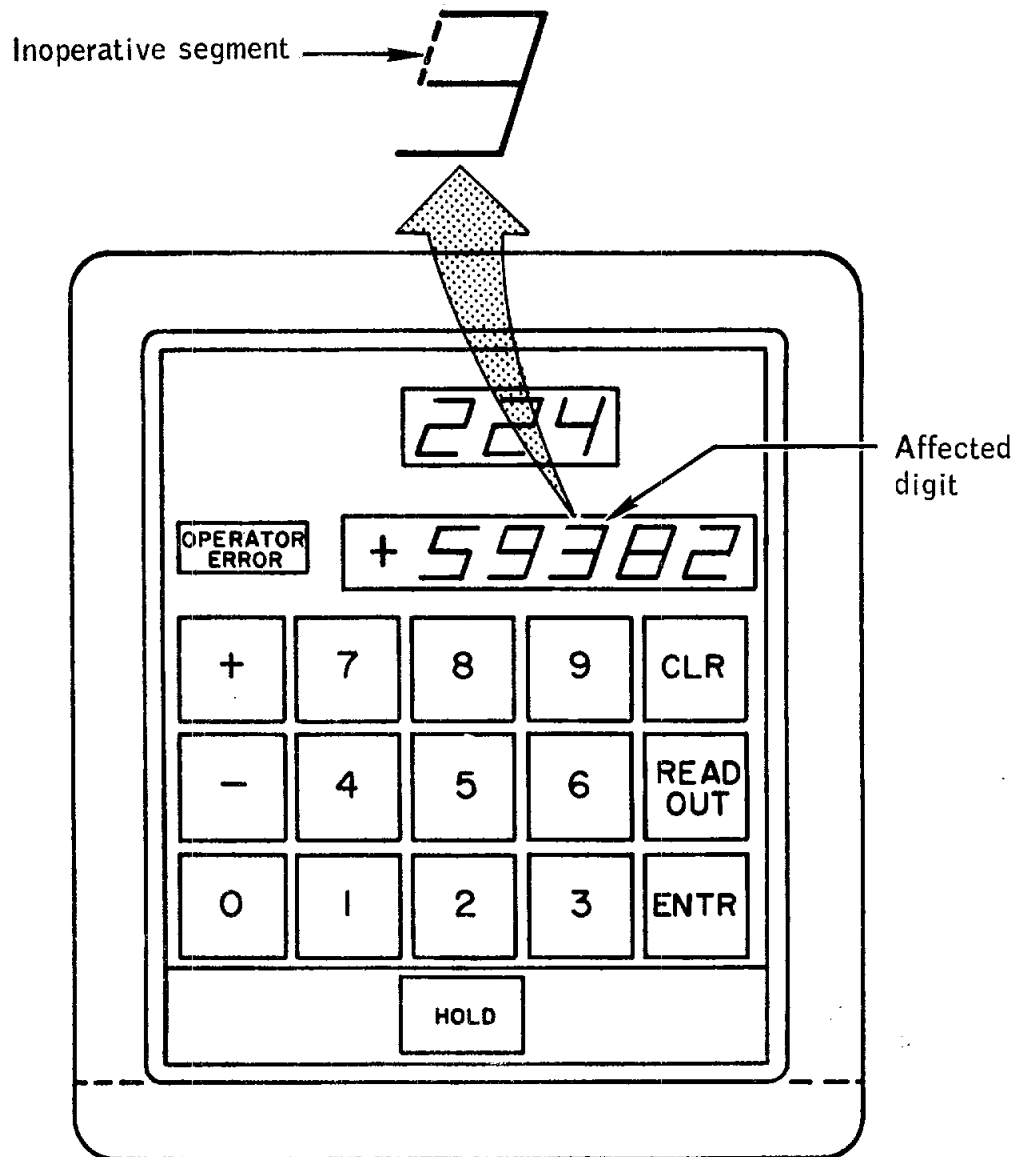


Figure 16-15.- Inoperative segment in one digit of data entry and display assembly.

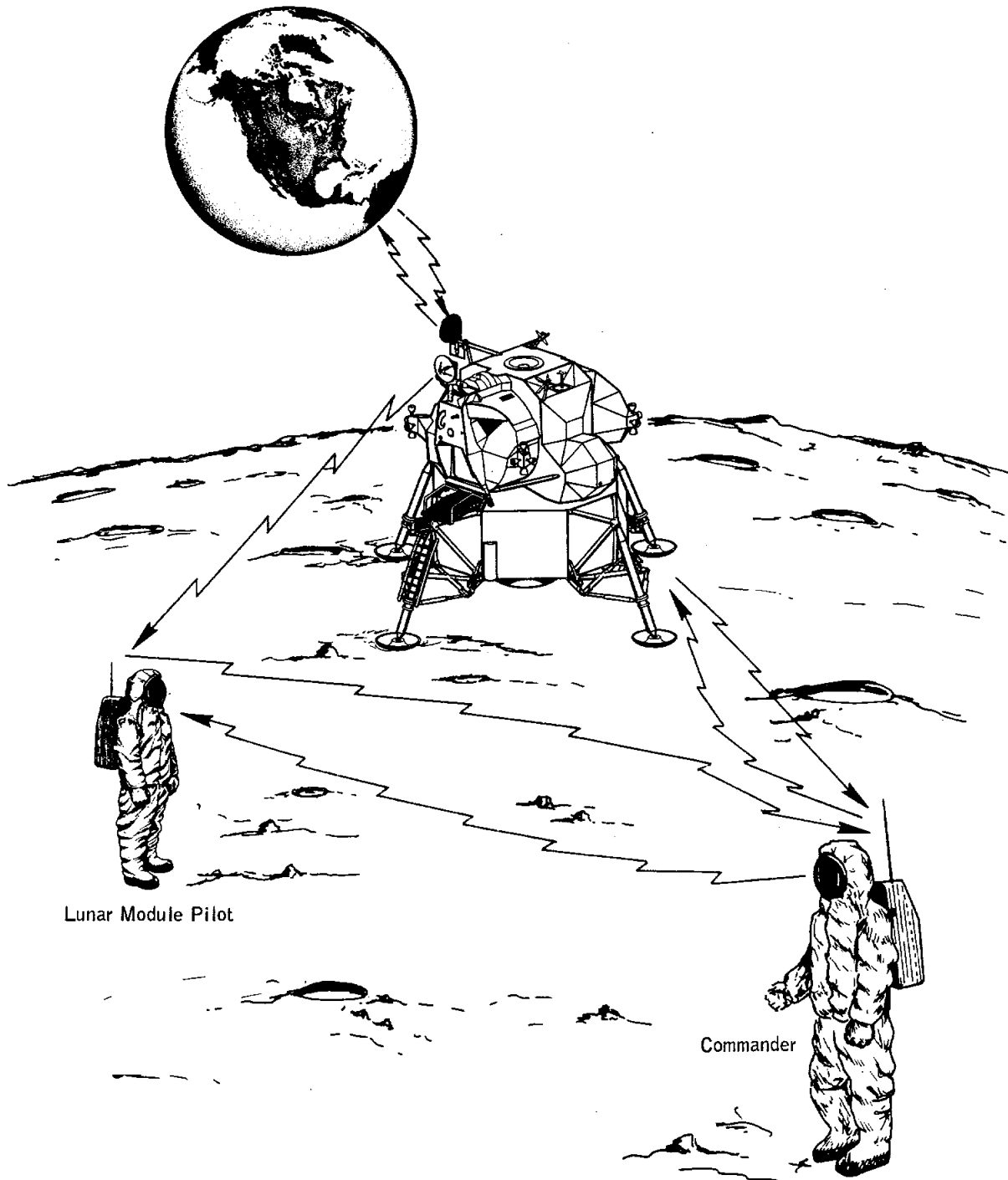


Figure 16-16.- Communications relays during extravehicular activity.



NASA-S-69-3791

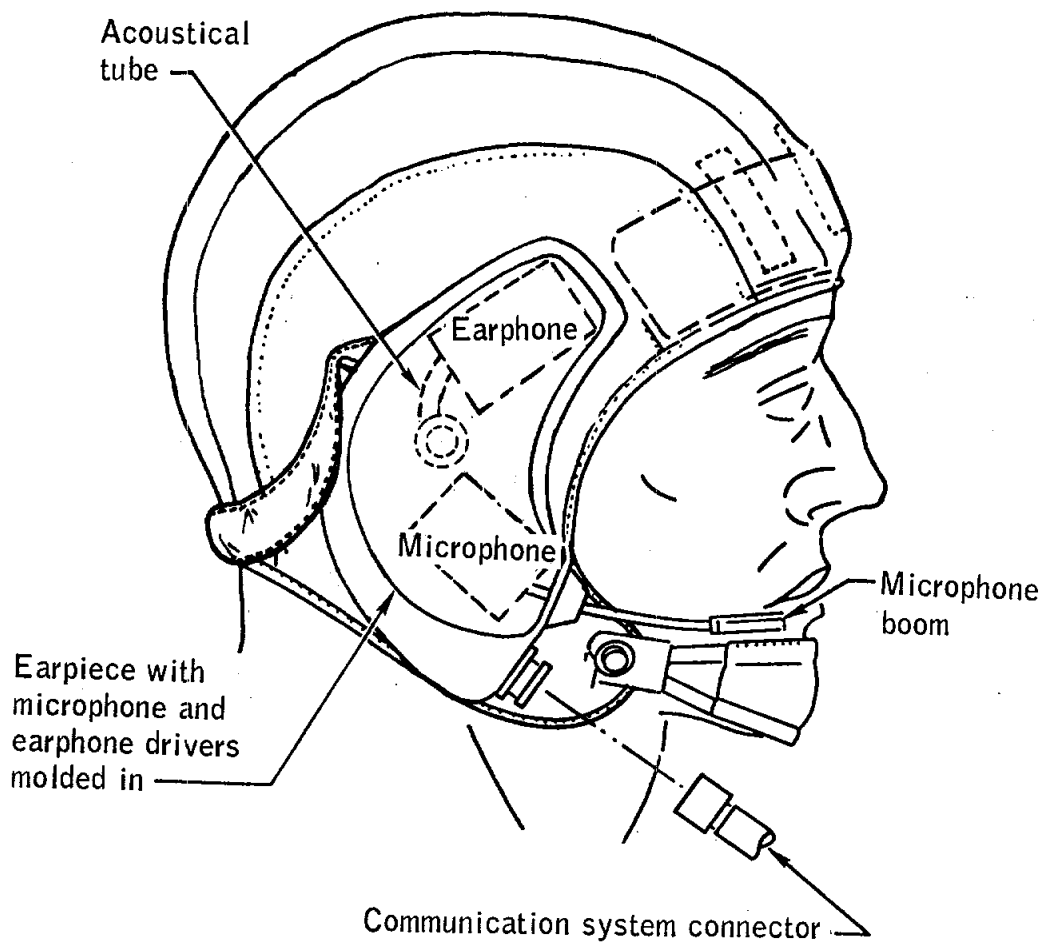


Figure 16-17.- Communications carrier.

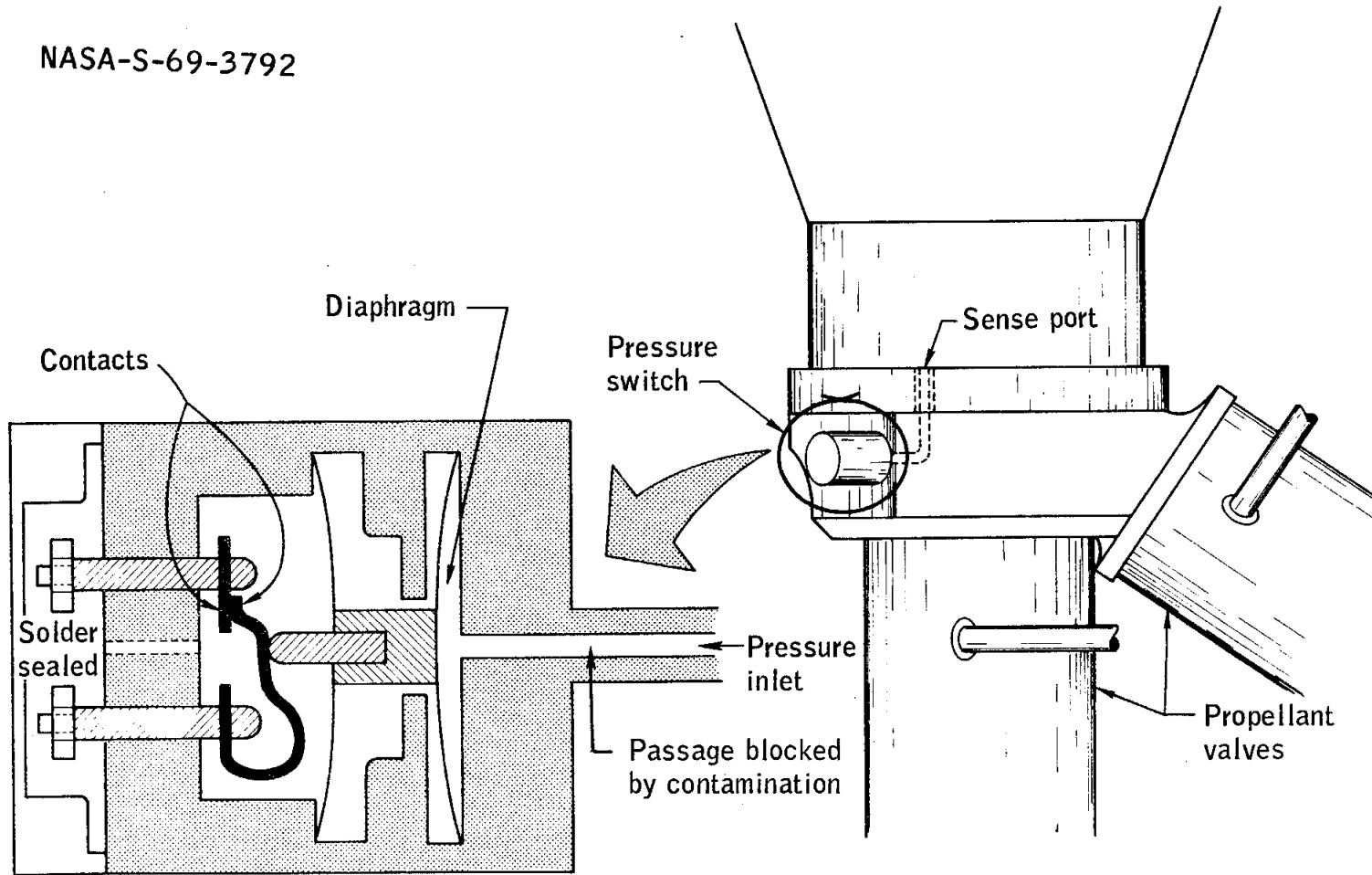


Figure 16-18.- Chamber pressure switch.

NASA-S-69-3793

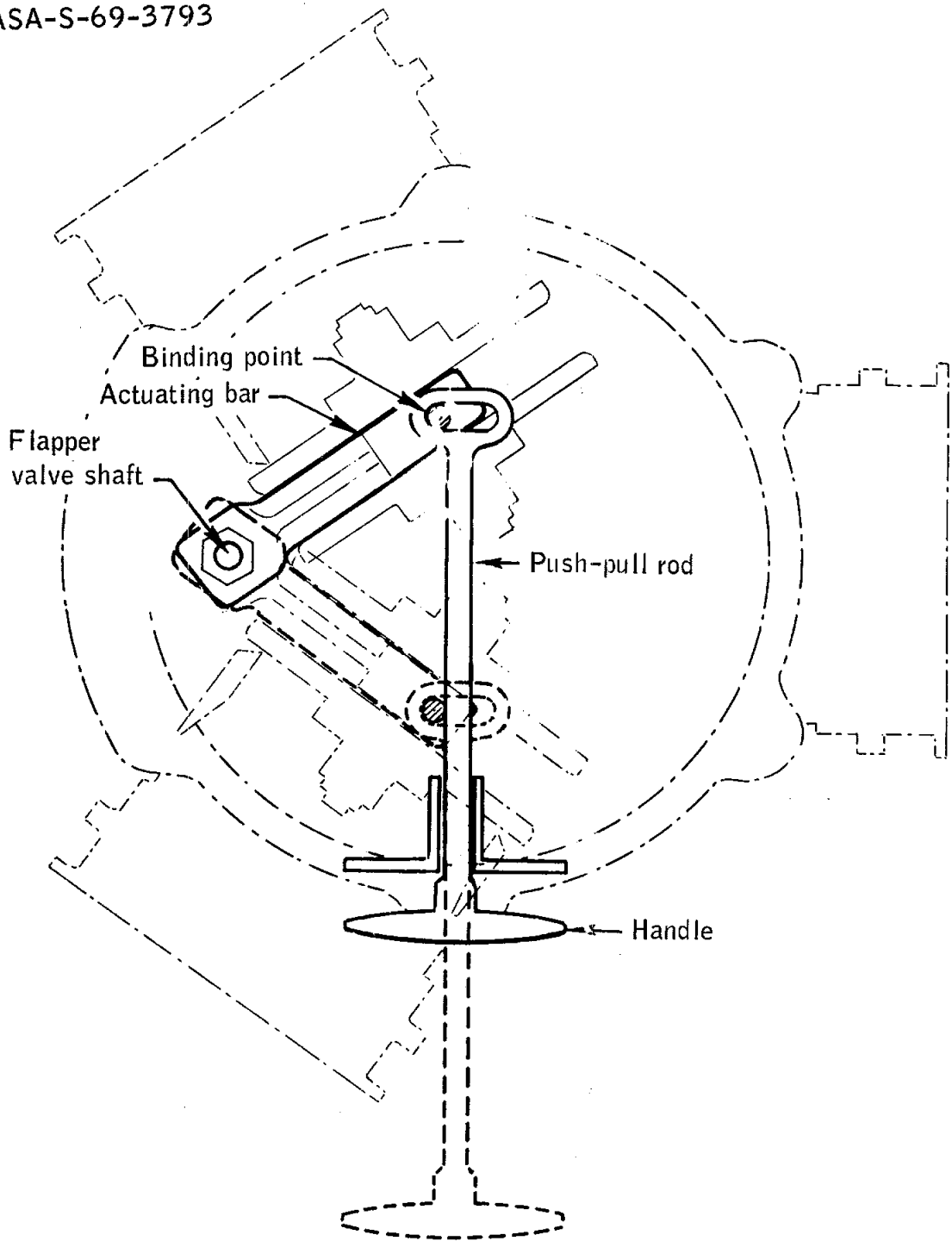


Figure 16-19.- Water separator selector valve.

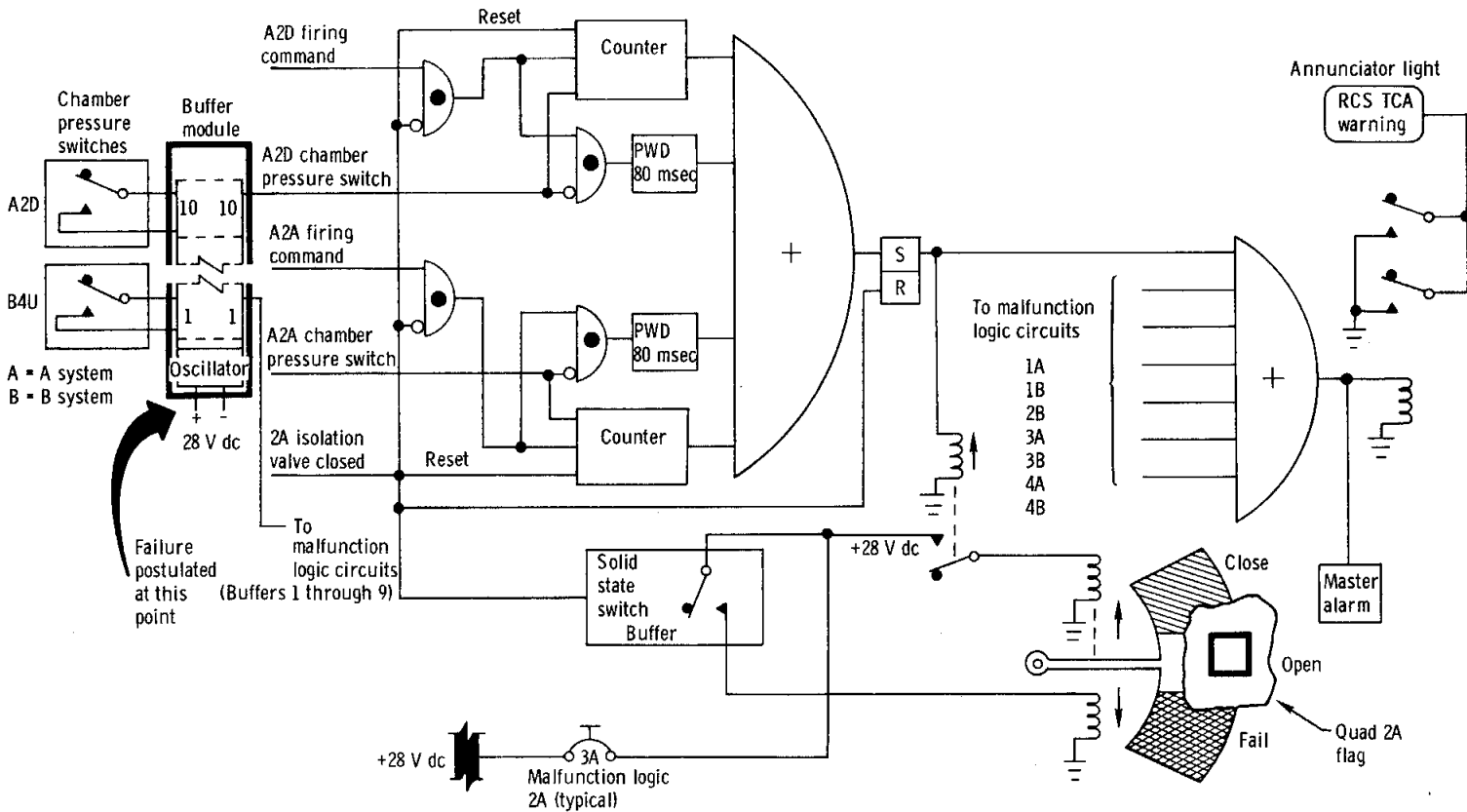


Figure 16-20. - Reaction control system malfunction detection circuits (caution and warning system).

NASA-S-69-3795

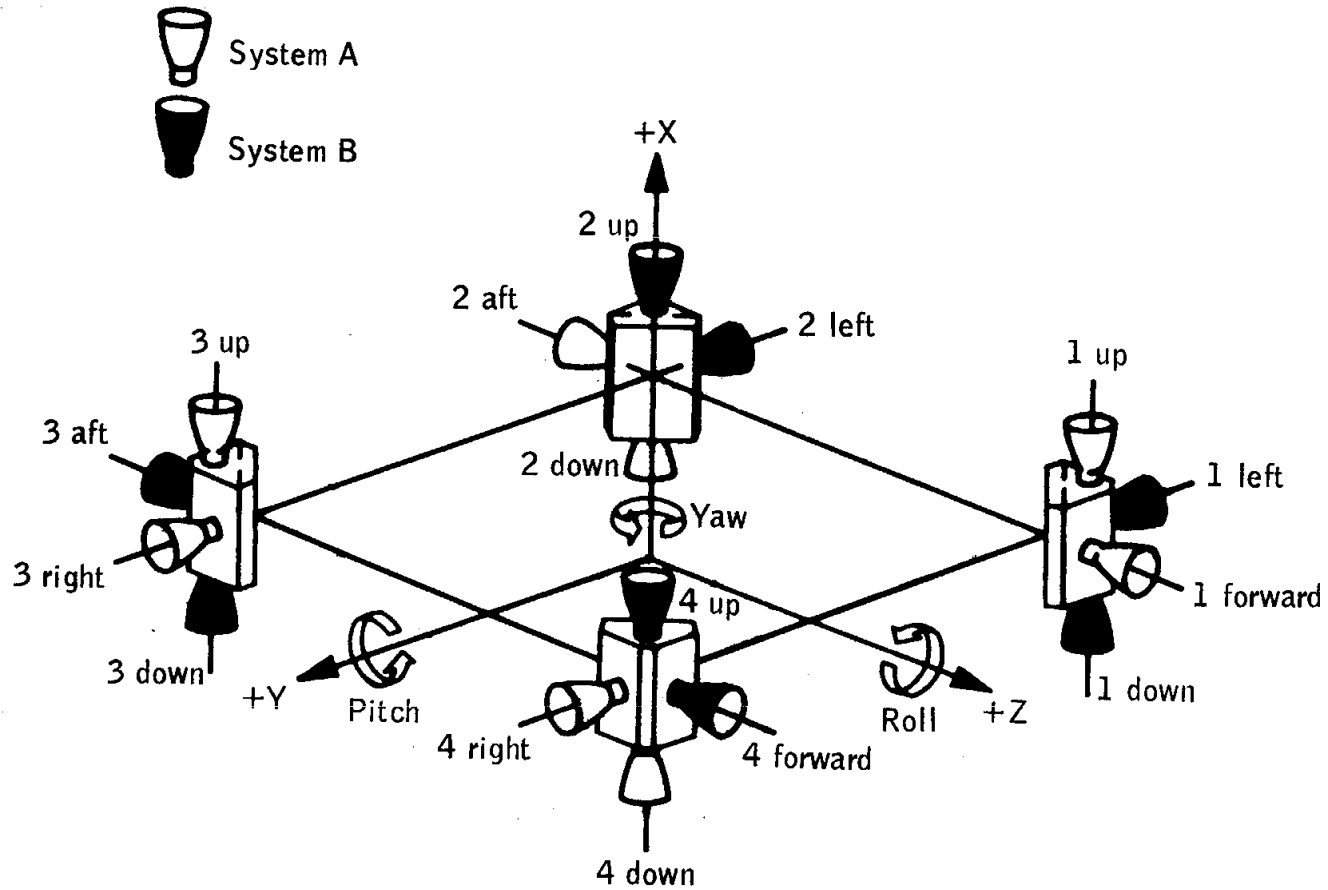


Figure 16-21.- Reaction control system geometry.

Flanged female half  
mounted on portable  
life support system

Male half mounted on  
cable to remote control  
unit

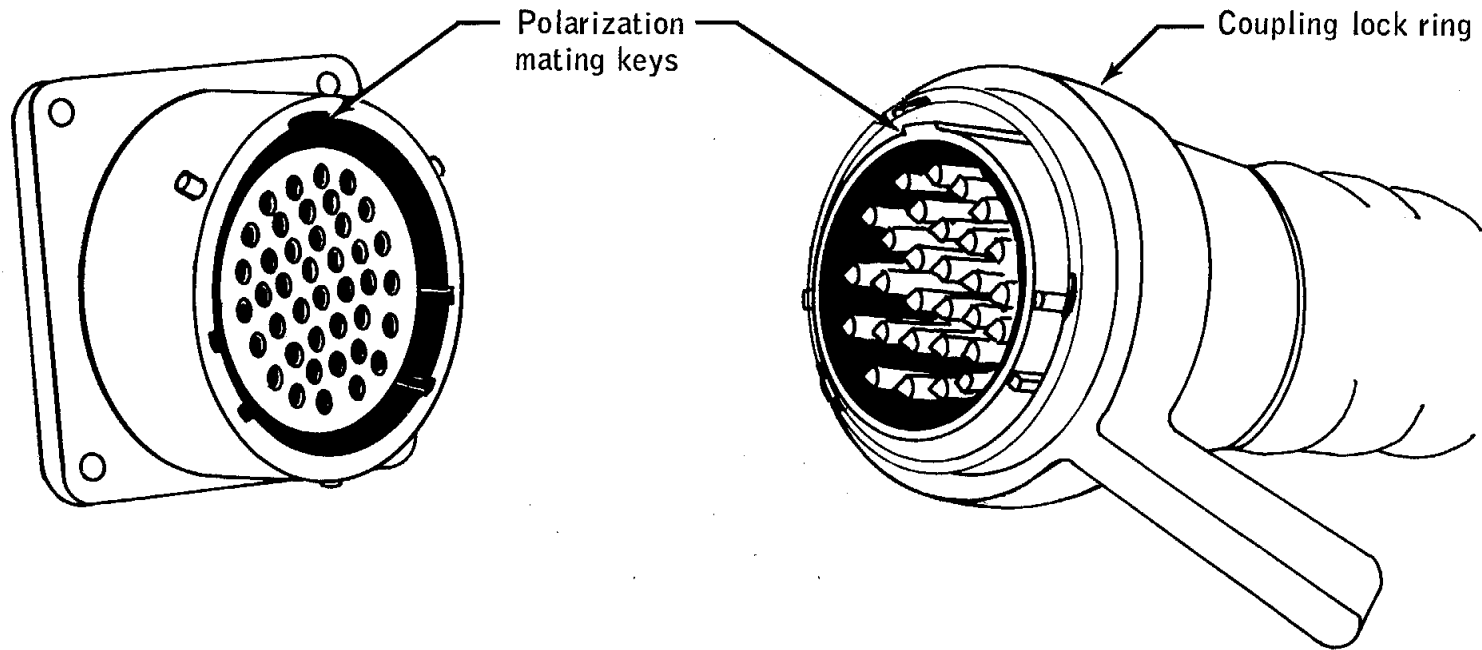


Figure 16-22.- Connector between remote control unit and portable life support system.

## 17.0 CONCLUSIONS

The Apollo 11 mission, including a manned lunar landing and surface exploration, was conducted with skill, precision, and relative ease. The excellent performance of the spacecraft in the preceding four flights and the thorough planning in all aspects of the program permitted the safe and efficient execution of this mission. The following conclusions are drawn from the information contained in this report.

1. The effectiveness of preflight training was reflected in the skill and precision with which the crew executed the lunar landing. Manual control while maneuvering to the desired landing point was satisfactorily exercised.
2. The planned techniques involved in the guidance, navigation, and control of the descent trajectory were good. Performance of the landing radar met all expectations in providing the information required for descent.
3. The extravehicular mobility units were adequately designed to enable the crew to conduct the planned activities. Adaptation to 1/6-g was relatively quick, and mobility on the lunar surface was easy.
4. The two-man prelaunch checkout and countdown for ascent from the lunar surface were well planned and executed.
5. The timeline activities for all phases of the lunar landing mission were well within the crew's capability to perform the required tasks.
6. The quarantine operation from spacecraft landing until release of the crew, spacecraft, and lunar samples from the Lunar Receiving Laboratory was accomplished successfully and without any violation of the quarantine.
7. No microorganisms from extraterrestrial source were recovered from either the crew or the spacecraft.
8. The hardware problems experienced on this mission, as on previous manned missions, were of a nature which did not unduly hamper the crew or result in the compromise of safety or mission objectives.
9. The Mission Control Center and the Manned Space Flight Network proved to be adequate for controlling and monitoring all phases of the flight, including the descent, surface activities, and ascent phases of the mission.

## APPENDIX A - VEHICLE DESCRIPTIONS

Very few changes were made to the Apollo 11 space vehicle from the Apollo 10 configuration. The launch escape system and the spacecraft/launch vehicle adapter were identical to those for Apollo 10. The few minor changes to the command and service modules, the lunar module, and the Saturn V launch vehicle are discussed in the following paragraphs. A description of the extravehicular mobility unit, the lunar surface experiment equipment, and a listing of spacecraft mass properties are also presented.

### A.1 COMMAND AND SERVICE MODULES

The insulation in the area of the command module forward hatch was modified to prevent the flaking which occurred during the Apollo 10 lunar module pressurization. The feedback circuit in the high gain antenna was slightly changed to reduce servo dither. In Apollo 10, one of the three entry batteries was modified to make use of cellophane separators. The flight results proved this material superior to the Permion-type previously used and for Apollo 11 all three entry batteries had the cellophane separators. The battery chargers were modified to produce a higher charging capacity. The secondary bypass valves for the fuel cell coolant loop were changed from an angle-cone seat design (block II) to a single-angle seat (block I) to reduce the possibility of particulate contamination. As a replacement for the water/gas separation bag which proved ineffective during Apollo 10, an in-line dual membrane separation device was added to both the water gun and the food preparation unit.

### A.2 LUNAR MODULE

#### A.2.1 Structures

The most significant structural change was the added provisions for the functional early Apollo scientific experiment package and the modular equipment stowage assembly, both of which housed the experiments and tools used during the lunar surface activities. Another change was the addition of the reaction control system plume deflectors.

Changes to the landing gear included removing the lunar surface sensing probe on the plus Z gear and lengthening the remaining probes and increasing the sliding clearance of the landing gear struts to permit full stroke at extreme temperature conditions.



### A.2.2 Thermal

A change from Kapton to Kel-F was made to the descent stage base heat shield to preclude the possibility of interference with the landing radar. Also, insulation was added to the landing gear and probes to accommodate the requirement for descent engine firing until touchdown.

### A.2.3 Communications

The major modifications to the communications systems included the addition of an extravehicular activity antenna for lunar communications between the crew, and the lunar module, and an S-band erectable antenna to permit communications through the lunar module communications system (fig. 16-16) while the crew was on the surface.

A television camera, as used on the Apollo 9 mission, was stowed in the descent stage to provide television coverage of the lunar surface activities.

### A.2.4 Guidance and Control

The major difference in the guidance and control system was the redesign of the gimbal drive actuator to a constant damping system rather than a brake. This was redesigned as a result of the brake failing in both the disengaged and engaged position. This change also required modification of the descent engine control assembly and the phase correcting network to eliminate the possibility of inadvertent caution and warning alarms.

The exterior tracking light had improvements in the flash head and in the pulse-forming network.

The pushbuttons for the data entry and display assembly were rewired to preclude the erroneous caution and warning alarms that had occurred on the Apollo 10 flight.

The guidance and navigation optics system was modified by the addition of Teflon locking rings to the sextant and the scanning telescope to prevent the rotation of eye guards under zero-g conditions.

The deletion of unmanned control capability permitted removal of the ascent engine arming assembly.

#### A.2.5 Ascent Propulsion

The injector filter for the ascent propulsion system was modified because the fine mesh in the original filter was causing a change in the mixture ratio. An additional change was the incorporation of a light-weight thrust chamber.

#### A.2.6 Environmental Control

In the environmental control system, a suit cooling assembly and water hose umbilicals were added to the air revitalization section to provide additional crew cooling capability. As a result, the cabin air recirculation assembly, the cabin temperature control valve, and the regenerative heat exchanger were deleted. Also, a redundant water regulator was added to the secondary coolant loop in the water management section.

In the environmental control system relay box in the oxygen and cabin pressure control section, a pressure transducer was replaced by a suit pressure switch to improve reliability.

#### A.2.7 Radar

The landing radar electronics assembly was reconfigured to protect against a computer strobing pulse that was providing what appeared to be two pulses to the radar. Another modification permitted the crew to break tracker lock and to start a search for the main beam in the event the radar pulse locked onto the structure or onto a side lobe. The lunar reflectivity attenuation characteristics were updated in the radar electronics to account for the updated Surveyor data and landing radar flight tests. To permit correlation between the inertial measurement unit of the primary guidance system and the Network, a logic change permitted the lateral velocity to be an output signal of the landing radar. A further design change was made to prevent the landing radar from accepting noise spikes as a pulse in the velocity bias error signal train.

The rendezvous radar design changes included a new self-test segment to provide low temperature stability with the low-frequency and mid-frequency composite signal. In addition, heaters were added to the gyro assembly and the cable wrap to accommodate the lunar stay temperature requirements. A manual voting override switch permitted the crew to select either the primary or secondary gyro inputs.

### A.2.8 Displays and Controls

Circuit breakers were added for the abort electronics assembly and the utility light. A circuit breaker was added for the abort electronics assembly to protect the dc bus, and another circuit breaker was added to accommodate the transfer of the utility light to the dc bus to provide redundant light.

The circuit breaker for the environmental control system suit and cabin repressurization function was deleted in conjunction with the modification of the suit cooling assembly. In addition, a low-level caution and warning indication on the secondary water glycol accumulator has been provided.

Changes to the caution and warning electronics assembly included the inhibiting of the landing radar temperature alarm and the prevention of a master alarm during inverter selection and master alarm switching.

Master alarm functions which were eliminated include the descent helium regulator warning prior to pressurization with the descent engine control assembly; the reaction control system thrust chamber assembly warning with quad circuit breakers open; the rendezvous radar caution when placing the mode select switch in the auto-track position; and the deletion of the reaction control system quad temperature alarm.

Caution and warning functions which were deleted include the landing radar velocity "data no-good" and the descent propellant low-level quantity which was changed to a low-level quantity indication light only.

A further change included the added capability of being able to reset the abort electronics assembly caution and warning channel with the water quantity test switch.

A modification was made to the engine stop switch latching mechanism to insure positive latching of the switch.

### A.2.9 Crew Provisions

The waste management system was changed to a one-large and five-small urine container configuration.

Additional stowage included provisions for a second Hasselblad camera, a total of two portable life support systems and remote control units, two pairs of lunar overshoes, and a feedwater collection bag. The Commander had an attitude controller assembly lock mechanism added.

### A.3 EXTRAVEHICULAR MOBILITY UNIT

The extravehicular mobility unit provides life support in a pressurized or unpressurized cabin and up to 4 hours of extravehicular life support.

In its extravehicular configuration the extravehicular mobility unit was a closed-circuit pressure vessel that enveloped the crewman. The environment inside the pressure vessel consisted of 100-percent oxygen at a nominal pressure of 3.75 psia. The oxygen was provided at a flow rate of 6 cubic feet per minute. The extravehicular life support equipment configuration is shown in figure A-1.

#### A.3.1 Liquid Cooling Garment

The liquid cooling garment was worn by the crewmen while in the lunar module and during all extravehicular activity. It provided cooling during extravehicular and intravehicular activity by absorbing body heat and transferring excessive heat to the sublimator in the portable life support system. The liquid cooling garment was a one piece, long sleeved, integrated stocking undergarment of netting material. It consisted of an inner liner of nylon chiffon, to facilitate donning, and an outer layer of nylon Spandex into which a network of Tygon tubing was woven. Cooled water, supplied from the portable life support system or from the environmental control system, was pumped through the tubing.

#### A.3.2 Pressure Garment Assembly

The pressure garment assembly was the basic pressure vessel of the extravehicular mobility unit. It would have provided a mobile life support chamber if cabin pressure had been lost due to leaks or puncture of the vehicle. The pressure garment assembly consisted of a helmet, torso and limb suit, intravehicular gloves, and various controls and instrumentation to provide the crewman with a controlled environment.

#### A.3.3 Torso and Limb Suit

The torso and limb suit was a flexible pressure garment that encompassed the entire body, except the head and hands. It had four gas connectors, a multiple water receptacle, an electrical connector, and a urine transfer connector. The connectors had positive locking devices and could be connected and disconnected without assistance. The gas connectors comprised an oxygen inlet and outlet connector, on each side of the suit front torso. Each oxygen inlet connector had an integral ventilation diverter

valve. The multiple water receptacle, mounted on the suit torso, served as the interface between the liquid cooling garment multiple water connector and portable life support system multiple water connector and the environmental control system water supply. The pressure garment assembly electrical connector, mated with the vehicle or portable life support system electrical umbilical, provided a communications, instrumentation, and power interface to the pressure garment assembly. The urine transfer connector was used to transfer urine from the urine collection transfer assembly to the waste management system.

The urine transfer connector on the suit right leg, permitted dumping the urine collection bag without depressurizing the pressure garment assembly. A pressure garment assembly pressure relief valve on the suit sleeve, near the wrist ring, vented the suit in the event of overpressurization. The valve opened at approximately 4.6 psig and reseated at 4.3 psig. If the valve did not open, it could have been manually overridden. A pressure gage on the other sleeve indicated suit pressure.

#### A.3.4 Helmet

The helmet was a Lexan (polycarbonate) shell with a bubble type visor, a vent pad assembly, and a helmet attaching ring. The vent pad assembly permitted a constant flow of oxygen over the inner front surface of the helmet. The crewman could turn his head within the helmet neck ring area. The helmet did not turn independently of the torso and limb suit. The helmet had provisions on each side for mounting an extravehicular visor assembly.

#### A.3.5 Communications Carrier

The communications carrier was a polyurethane foam headpiece with two independent earphones and microphones which were connected to the suit 21-pin communications electrical connector. The communications carrier could be worn with or without the helmet during intravehicular operations. It was worn with the helmet during extravehicular operations.

#### A.3.6 Integrated Thermal Micrometeoroid Garment

The integrated thermal micrometeoroid garment was worn over the pressure garment assembly, and protected the crewman from harmful radiation, heat transfer, and micrometeoroid activity. The integrated thermal micrometeoroid garment was a one piece, form fitting multilayered garment that was laced over the pressure garment assembly and remained with it. The extravehicular visor assembly, gloves, and boots were donned separately. From the outer layer in, the integrated thermal micrometeoroid

garment consisted of a protective cover, a micrometeoroid-shielding layer, a thermal-barrier blanket (multiple layers of aluminized Mylar), and a protective liner. A zipper on the integrated thermal micrometeoroid garment permitted connecting or disconnecting umbilical hoses. For extravehicular activity, the pressure garment assembly gloves were replaced with the extravehicular gloves. The extravehicular gloves were made of the same material as the integrated thermal micrometeoroid garment to permit handling intensely hot or cold objects outside the cabin and for protection against lunar temperatures. The extravehicular boots were worn over the pressure garment assembly boots for extravehicular activity. They were made of the same material as the integrated thermal micrometeoroid garment. The soles had additional insulation for protection against intense temperatures.

#### A.3.7 Extravehicular Visor Assembly

The extravehicular visor assembly provided protection against solar heat, space particles, and radiation, and helped to maintain thermal balance. The two pivotal visors of the extravehicular visor assembly could be attached to a pivot mounting on the pressure garment assembly helmet. The lightly tinted (inner) visor reduced fogging in the helmet. The outer visor had a vacuum deposited, gold-film reflective surface, which provided protection against solar radiation and space particles. The extravehicular visor assembly was held snug to the pressure garment assembly helmet by a tab-and-strap arrangement that allowed the visors to be rotated approximately 90° up or down, as desired.

#### A.3.8 Portable Life Support System

The portable life support system (see figure A-2) contained the expendable materials and the communication and telemetry equipment required for extravehicular operation. The system supplied oxygen to the pressure garment assembly and cooling water to the liquid cooling garment and removed solid and gas contaminants from returning oxygen. The portable life support system, attached with a harness, was worn on the back of the suited crewman. The total system contained an oxygen ventilating circuit, water feed and liquid transport loops, a primary oxygen supply, a main power supply, communication systems, displays and related sensors, switches, and controls. A cover encompassed the assembled unit and the top portion supported the oxygen purge system.

The remote control unit was a display and control unit chest-mounted for easy access. The controls and displays consisted of a fan switch, pump switch, space-suit communication-mode switch, volume control, oxygen quantity indicator, and oxygen purge system actuator.

The oxygen purge system provided oxygen and pressure control for certain extravehicular emergencies and was mounted on top of the portable life support system. The system was self-contained, independently powered, and non-rechargeable. It was capable of 30 minutes of regulated ( $3.7 \pm 0.3$  psid) oxygen flow at 8 lb/hr to prevent excessive carbon dioxide buildup and to provide limited cooling. The system consisted of two interconnected spherical 2-pound oxygen bottles, an automatic temperature control module, a pressure regulator assembly, a battery, oxygen connectors, and the necessary checkout instrumentation. The oxygen purge system provided the hard mount for the VHF antenna.

#### A.4 EXPERIMENT EQUIPMENT

##### A.4.1 Solar Wind Composition

The purpose of the solar wind composition experiment was to determine the elemental and isotopic composition of noble gases and other selected elements present in the solar wind. This was to be accomplished by trapping particles of the solar wind on a sheet of aluminum foil exposed on the lunar surface.

Physically, the experiment consisted of a metallic telescoping pole approximately 1-1/2 inches in diameter and approximately 16 inches in length when collapsed. When extended, the pole was about 5 feet long. In the stowed position, the foil was enclosed in one end of the tubing and rolled up on a spring-driven roller. Only the foil portion was recovered at the end of the lunar exposure period, rolled on the spring-driven roller, and stowed in the sample return container for return to earth.

##### A.4.2 Laser Ranging Retro-Reflector

The laser ranging retro-reflector experiment (fig. A-3) was a retro-reflector array of fused silica cubes. A folding support structure was used for aiming and aligning the array toward earth. The purpose of the experiment was to reflect laser ranging beams from earth to their point of origin for precise measurement of earth-moon distances, center of moon's mass motion, lunar radius, earth geophysical information, and development of space communication technology.

Earth stations that can beam lasers to the experiment include the McDonald Observatory at Fort Davis, Texas; the Lick Observatory in Mount Hamilton, California; and the Catalina Station of the University of Arizona. Scientists in other countries also plan to bounce laser beams off the experiment.

#### A.4.3 Passive Seismic Experiment Package

The passive seismic experiment (fig. A-4) consisted of three long-period seismometers and one short-period vertical seismometer for measuring meteoroid impacts and moonquakes and to gather information on the moon's interior; for example, to investigate for the existence of a core and mantle. The passive seismic experiment package had four basic subsystems: the structure/thermal subsystem to provide shock, vibration, and thermal protection; the electrical power subsystem to generate 34 to 46 watts by solar panel array; the data subsystem to receive and decode Network uplink commands and downlink experiment data and to handle power switching tasks; and the passive seismic experiment subsystem to measure lunar seismic activity with long-period and short-period seismometers which could detect inertial mass displacement. Also included in the package were 15-watt radioisotope heaters to maintain the electronic package at a minimum of 60° F during the lunar night.

A solar panel array of 2520 solar cells provided approximately 40 watts to operate the instrument and the electronic components, including the telemetry data subsystem. Scientific and engineering data were to be telemetered downlink while ground commands initiated from the Mission Control Center were to be transmitted uplink utilizing Network remote sites.

#### A.4.4 Lunar Field Geology

The primary aim of the Apollo lunar field geology experiment was to collect lunar samples, and the tools described in the following paragraphs and shown in figure A-5 were provided for this purpose.

A calibrated Hasselblad camera and a gnomon were to be used to obtain the geometric data required to reconstruct the geology of the site, in the form of geologic maps, and to recover the orientation of the samples for erosion and radiation studies. The sample bags and camera frame numbers would aid in identifying the samples and relating them to the crew's description.

Core tubes, in conjunction with hammers, were to provide a sample in which the stratigraphy of the uppermost portion of the regolith would be preserved for return to earth.

A sample scoop was provided for collecting particulate material and individual rock fragments and for digging shallow trenches for inspection of the regolith. The tongs were provided for collecting rock fragments and for retrieving tools that might have been dropped.



Lunar environment and gas analysis samples were to be collected, sealed in special containers, and returned for analysis.

#### A.5 LAUNCH VEHICLE

Launch vehicle AS-506 was the sixth in the Apollo Saturn V series and was the fourth manned Apollo Saturn V vehicle. The AS-506 launch vehicle was configured the same as AS-505, used for the Apollo 10 mission, except as described in the following paragraphs.

In the S-IC stage, the prevalve accumulator bottles were removed from the control pressure system, and various components of the research and development instrumentation system were removed or modified.

In the S-II stage, the components of the research and development instrumentation were removed, and excess weld doublers were removed from the liquid oxygen tank aft bulkhead.

In the S-IVB stage, five additional measurements were used to define the low-frequency vibration that had occurred during the Apollo 10 mission. In the propulsion system, a liner was added to the liquid hydrogen feed duct, an oxygen/hydrogen injector was changed, the shutoff valve on the pneumatic power control module was modified by the addition of a block point, and new configuration cold helium shutoff and dump valves and a pneumatic shutoff valve solenoid were installed.

In the instrument unit, the FM/FM telemetry system was modified to accommodate the five added S-IVB structural vibration measurements. Tee sections, clamps, and thermal switch settings were minor modifications in the environmental control system. The flight program was changed to accommodate the requirements of the Apollo 11 mission.

#### A.6 MASS PROPERTIES

Spacecraft mass properties for the Apollo 11 mission are summarized in table A-I. These data represent the conditions as determined from postflight analyses of expendable loadings and usage during the flight. Variations in spacecraft mass properties are determined for each significant mission phase from lift-off through landing. Expendables usage is based on reported real-time and postflight data as presented in other sections of this report. The weights and centers of gravity of the individual command and service modules and of the lunar module ascent and descent stages were measured prior to flight, and the inertia values were calculated. All changes incorporated after the actual weighing were monitored, and the spacecraft mass properties were updated.

TABLE A-I.- MASS PROPERTIES

Event	Weight, lb	Center of gravity, in.			Moment of inertia, slug-ft <sup>2</sup>			Product of inertia, slug-ft <sup>2</sup>		
		X <sub>A</sub>	Y <sub>A</sub>	Z <sub>A</sub>	I <sub>XX</sub>	I <sub>YY</sub>	I <sub>ZZ</sub>	I <sub>XY</sub>	I <sub>XZ</sub>	I <sub>YZ</sub>
Lift-off	109 666.6	847.0	2.4	3.9	67 960	1 164 828	1 167 323	2586	8 956	3335
Earth orbit insertion	100 756.4	807.2	2.6	4.1	67 108	713 136	715 672	4745	11 341	3318
Transposition and docking										
Command & service modules	63 473.0	934.0	4.0	6.5	34 445	76 781	79 530	-1789	-126	3148
Lunar module	33 294.5	1236.2	0.2	0.1	22 299	24 826	24 966	-508	27	37
Total docked	96 767.5	1038.0	2.7	4.3	57 006	532 219	534 981	-7672	-9 240	3300
Separation maneuver	96 566.6	1038.1	2.7	4.3	56 902	531 918	534 766	-7670	-9 219	3270
First midcourse correction										
Ignition	96 418.2	1038.3	2.7	4.2	56 770	531 482	534 354	-7711	-9 170	3305
Cutoff	96 204.2	1038.4	2.7	4.2	56 667	531 148	534 113	-7709	-9 147	3274
Lunar orbit insertion										
Ignition	96 061.6	1038.6	2.7	4.2	56 564	530 636	533 613	-7785	-9 063	3310
Cutoff	72 037.6	1079.1	1.7	2.9	44 117	412 855	419 920	-5737	-5 166	382
Circularization										
Ignition	72 019.9	1079.2	1.8	2.9	44 102	412 733	419 798	-5745	-5 160	386
Cutoff	70 905.9	1081.5	1.6	2.9	43 539	407 341	413 864	-5403	-5 208	316
Separation	70 760.3	1082.4	1.8	2.8	44 762	407 599	414 172	-5040	-5 404	286
Docking										
Command & service modules	36 847.4	943.6	2.8	5.5	20 747	57 181	63 687	-2094	833	321
Ascent stage	5 738.0	1168.3	4.9	-2.4	3 369	2 347	2 873	-129	54	-354
Total after docking										
Ascent stage manned	42 585.4	973.9	3.1	4.5	24 189	113 707	120 677	-1720	-1 018	-50
Ascent stage unmanned	42 563.0	972.6	2.9	4.5	24 081	110 884	117 804	-2163	-811	-28
After ascent stage jettison	37 100.5	943.9	2.9	5.4	20 807	56 919	63 417	-2003	730	305
Transearth injection										
Ignition	36 965.7	943.8	3.0	5.3	20 681	56 775	63 303	-1979	709	336
Cutoff	26 792.7	961.4	-0.1	6.8	15 495	49 843	51 454	-824	180	-232
Command & service module separation										
Before	26 656.5	961.6	0.0	6.7	15 406	49 739	51 338	-854	228	-200
After										
Service module	14 549.1	896.1	0.1	7.2	9 143	14 540	16 616	-837	885	-153
Command module	12 107.4	1040.4	-0.2	6.0	6 260	5 470	4 995	55	-403	-47
Entry	12 095.5	1040.5	-0.2	5.9	6 253	5 463	4 994	55	-400	-47
Drogue deployment	11 603.7	1039.2	-0.2	5.9	6 066	5 133	4 690	56	-375	-48
Main parachute deployment	11 318.9	1039.1	-0.1	5.2	5 933	4 947	4 631	50	-312	-28
Landing	10 873.0	1037.1	-0.1	5.1	5 866	4 670	4 336	45	-322	-27
Lunar Module										
Lunar module at launch	33 297.2	185.7	0.2	0.2	22 304	25 019	25 018	228	454	77
Separation	33 683.5	186.5	0.2	0.7	23 658	26 065	25 922	225	705	73
Descent orbit insertion										
Ignition	33 669.6	186.5	0.2	0.8	23 649	26 045	25 899	224	704	71
Cutoff	33 401.6	186.5	0.2	0.8	23 480	25 978	25 871	224	704	71
Lunar landing	16 153.2	213.5	0.4	1.6	12 582	13 867	16 204	182	555	74
Lunar lift-off	10 776.6	243.5	0.2	2.9	6 808	3 475	5 971	20	214	45
Orbit insertion	5 928.6	255.3	0.4	5.3	3 457	3 082	2 273	17	135	43
Coelliptic sequence initiation	5 881.5	255.0	0.4	5.3	3 437	3 069	2 246	17	137	44
Docking	5 738.0	254.4	0.4	5.4	3 369	3 044	2 167	18	141	50
Jettison	5 462.5	255.0	0.1	3.1	3 226	3 039	2 216	28	119	35

NASA-S-69-3797

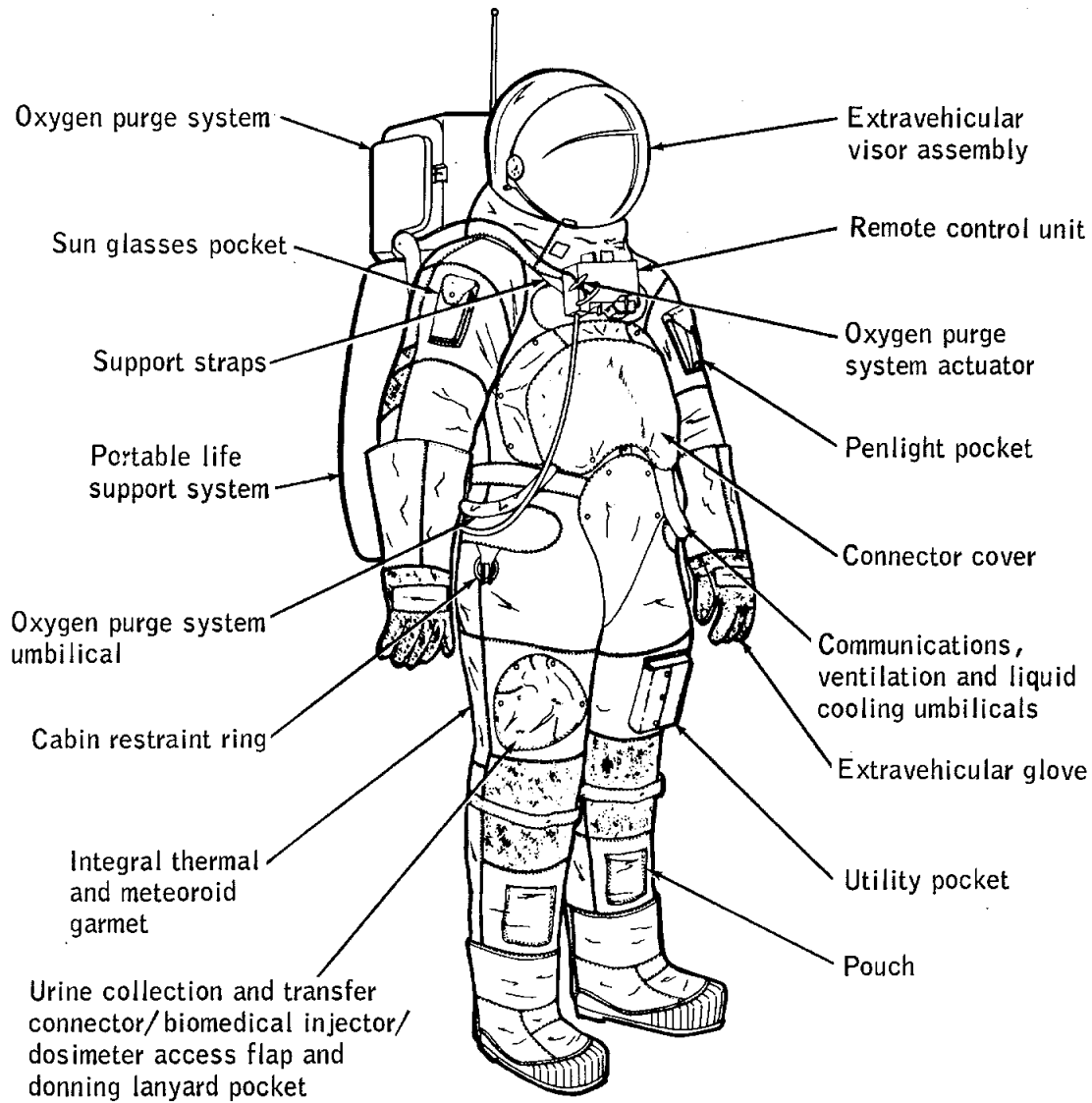


Figure A-1.- Extravehicular mobility unit.

NASA-S-69-3798

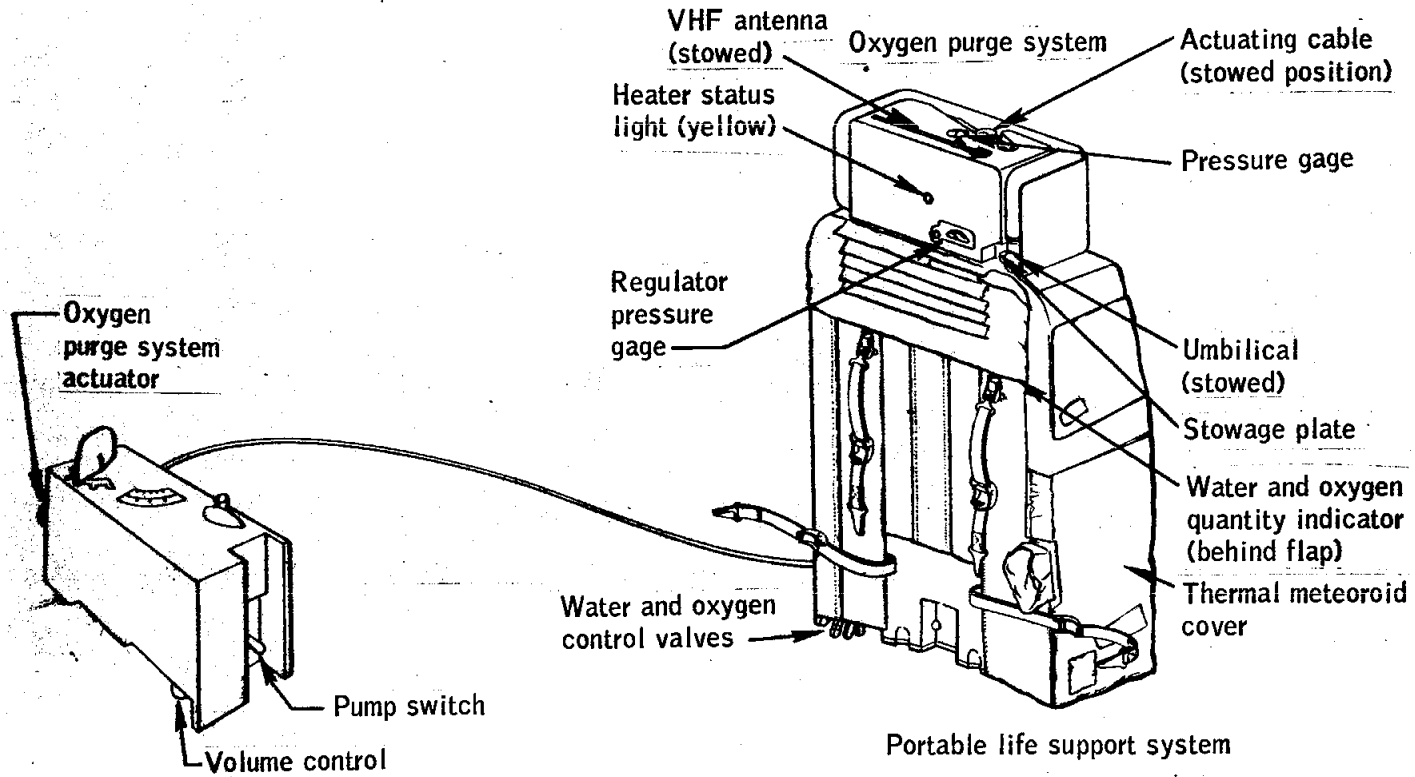


Figure A-2.- Portable life support system.

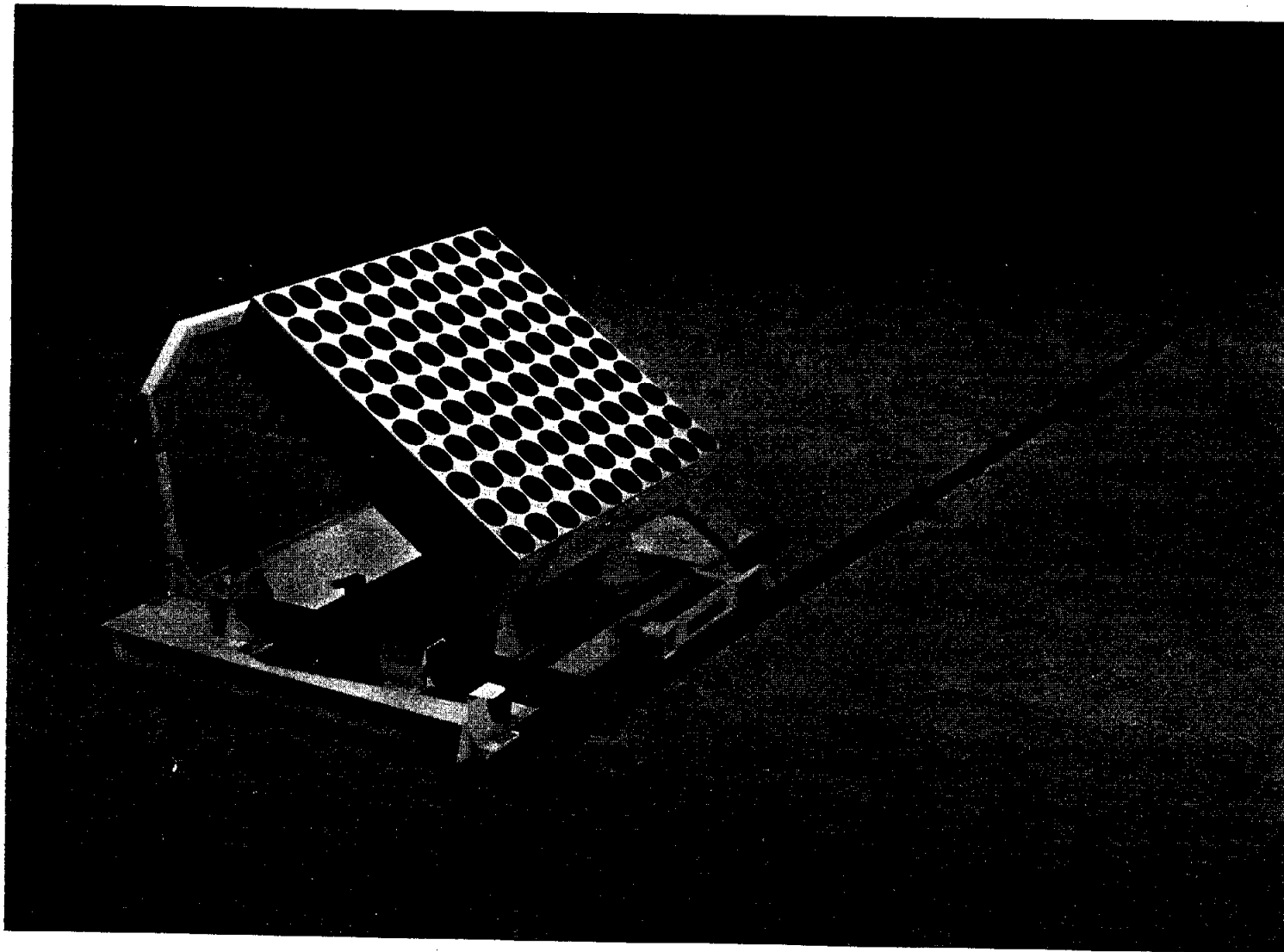


Figure A-3.- Laser reflector experiment deployment.

NASA-S-69-3800

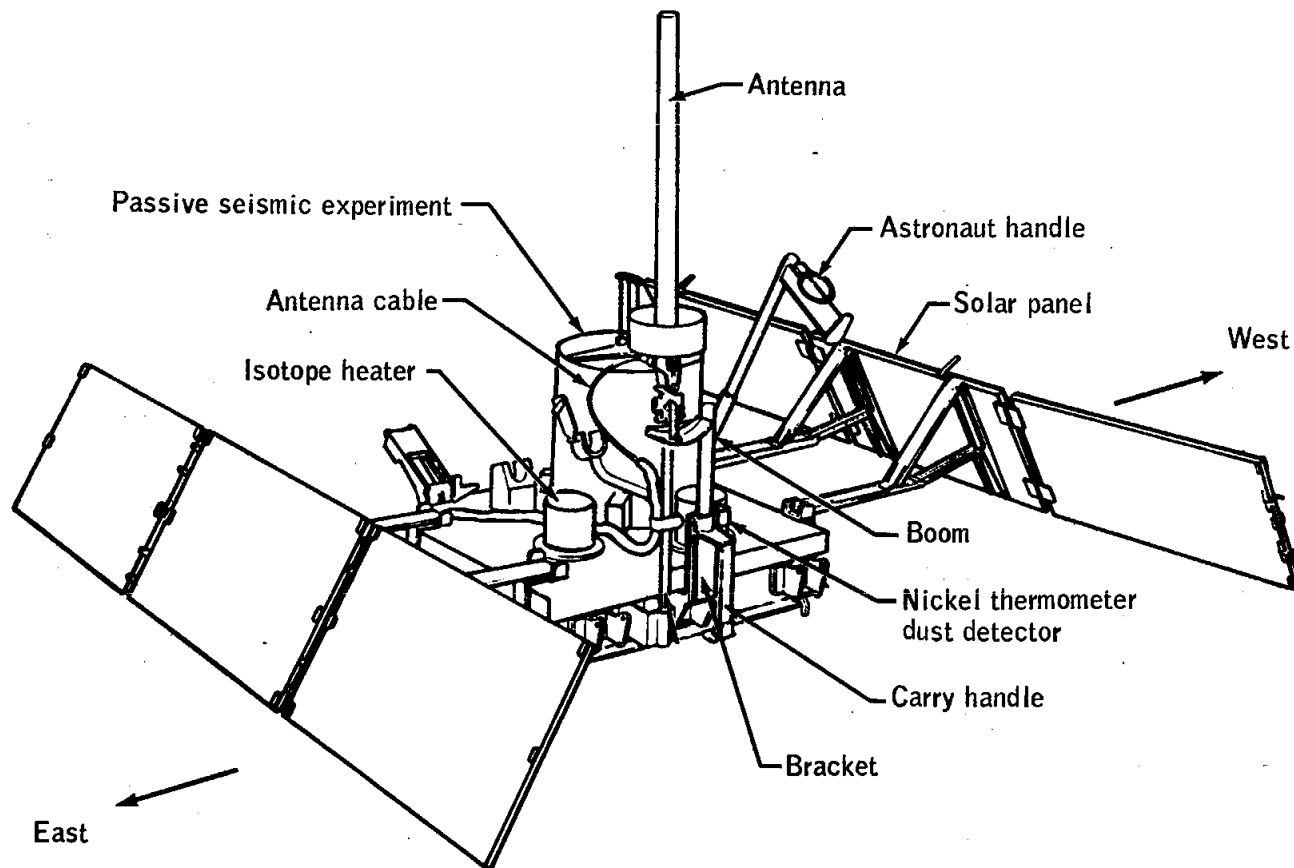


Figure A-4.- Passive seismic experiment package deployed configuration showing dust detector geometry.

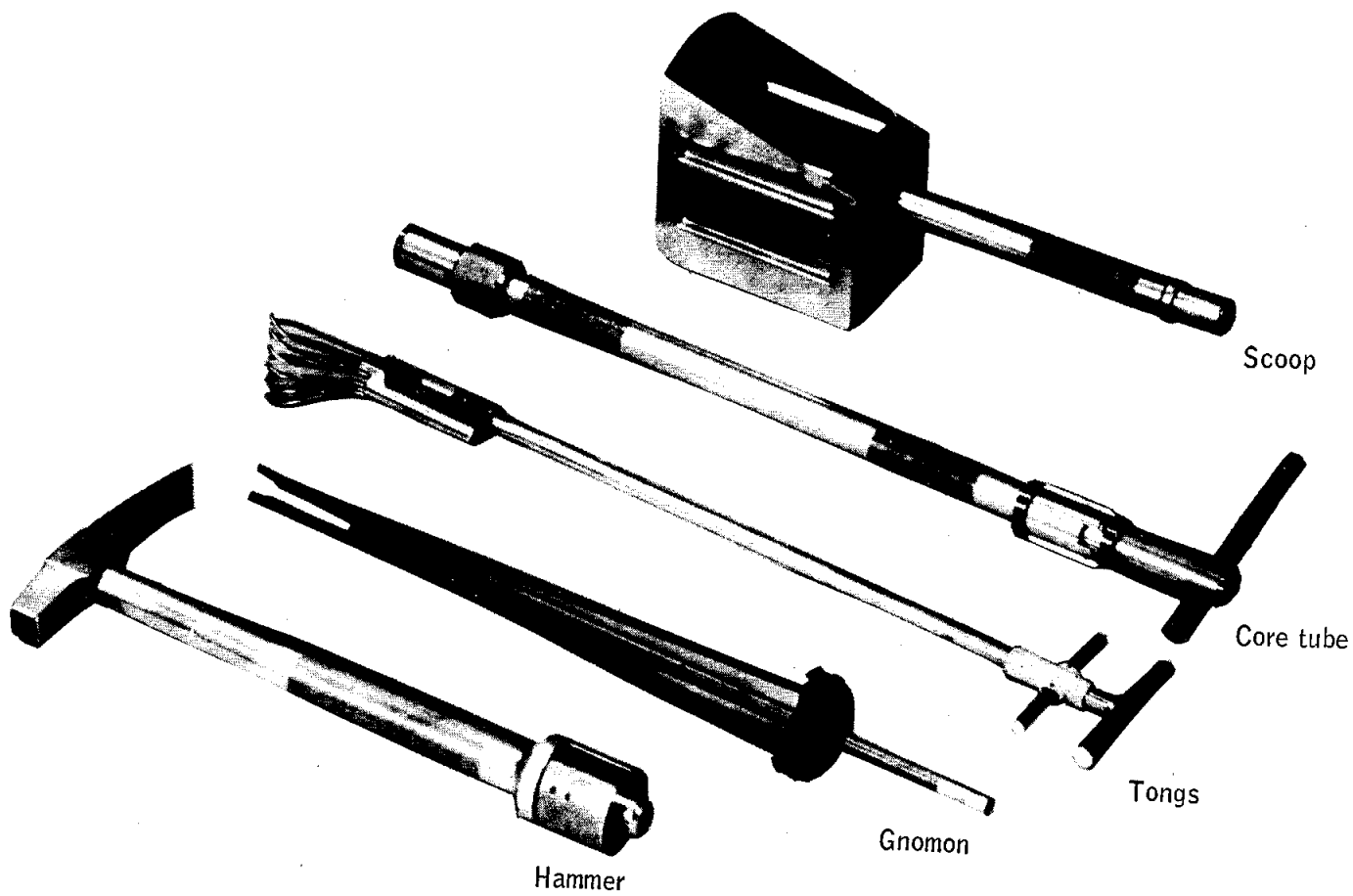


Figure A-5.- Geological sampling tools.

APPENDIX B - SPACECRAFT HISTORIES

The history of command and service module (CSM 107) operations at the manufacturer's facility, Downey, California, is shown in figure B-1, and the operations at Kennedy Space Center, Florida, in figure B-2.

The history of the lunar module (LM-5) at the manufacturer's facility, Bethpage, New York, is shown in figure B-3, and the operations at Kennedy Space Center, Florida, in figure B-4.



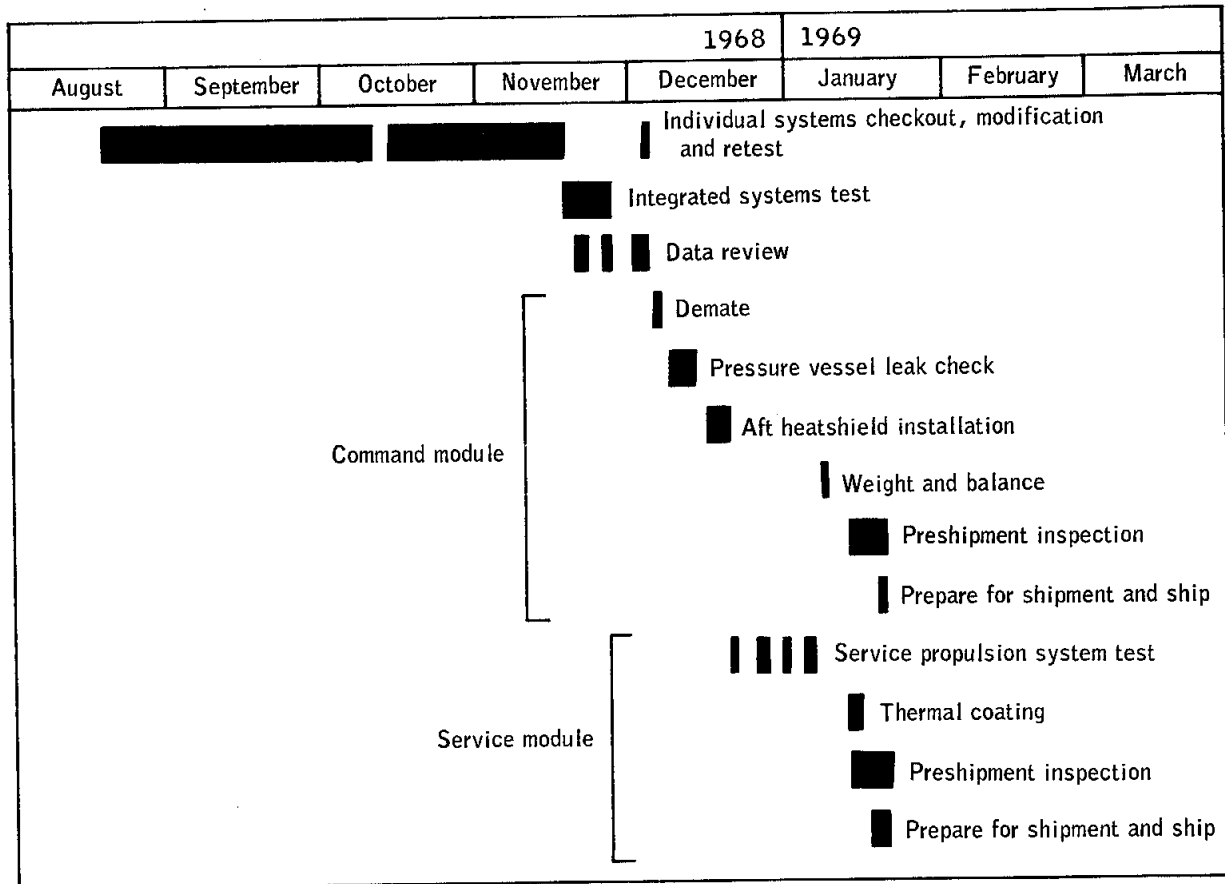


Figure B-1.- Factory checkout flow for command and service modules at contractor facility.

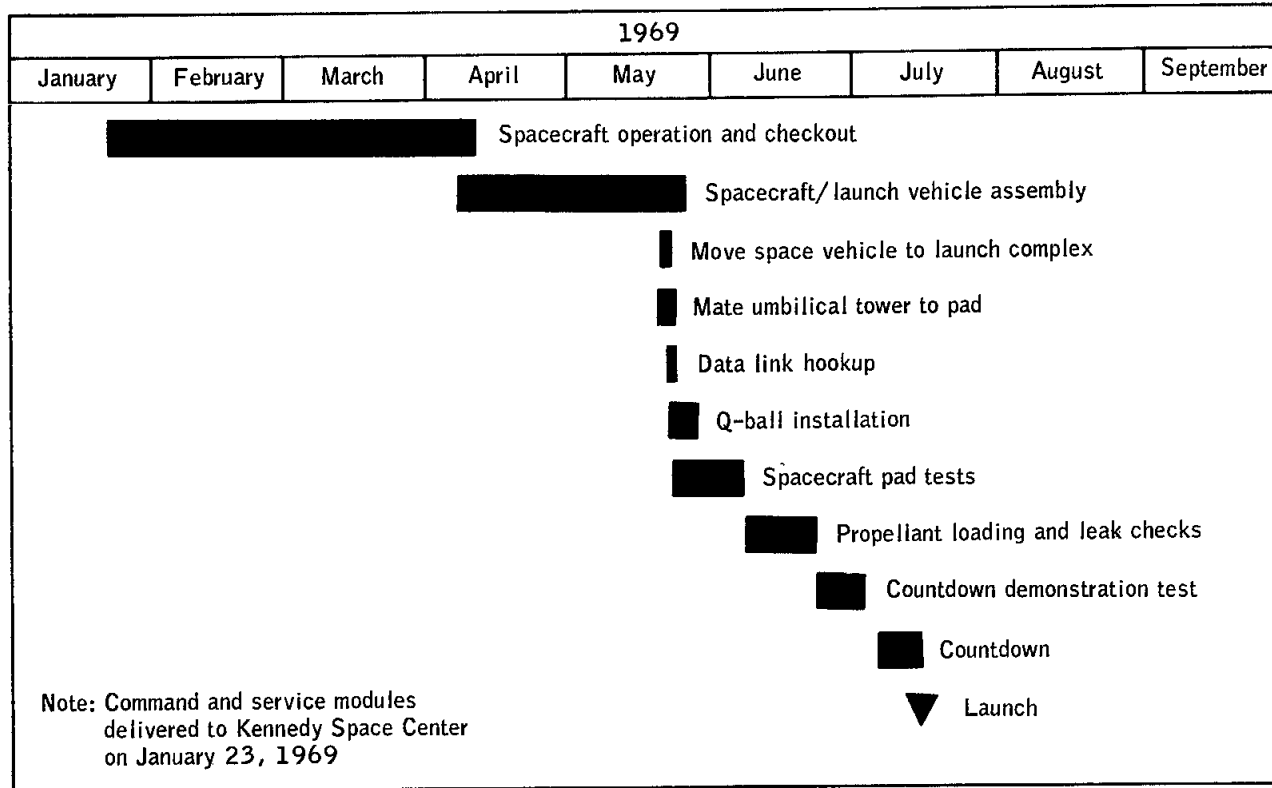


Figure B-2.- Spacecraft checkout history at Kennedy Space Center.

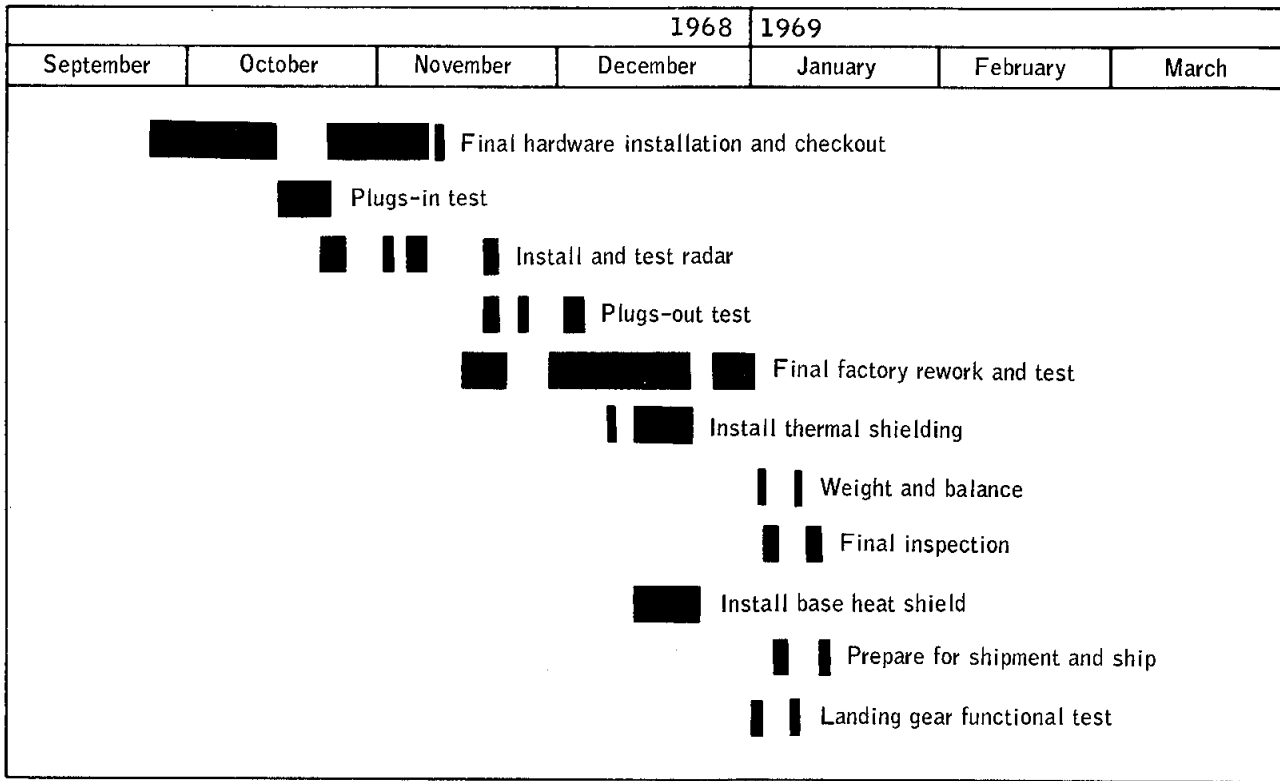


Figure B-3.- Factory checkout flow for lunar module at contractor facility.

NASA-S-69-3805

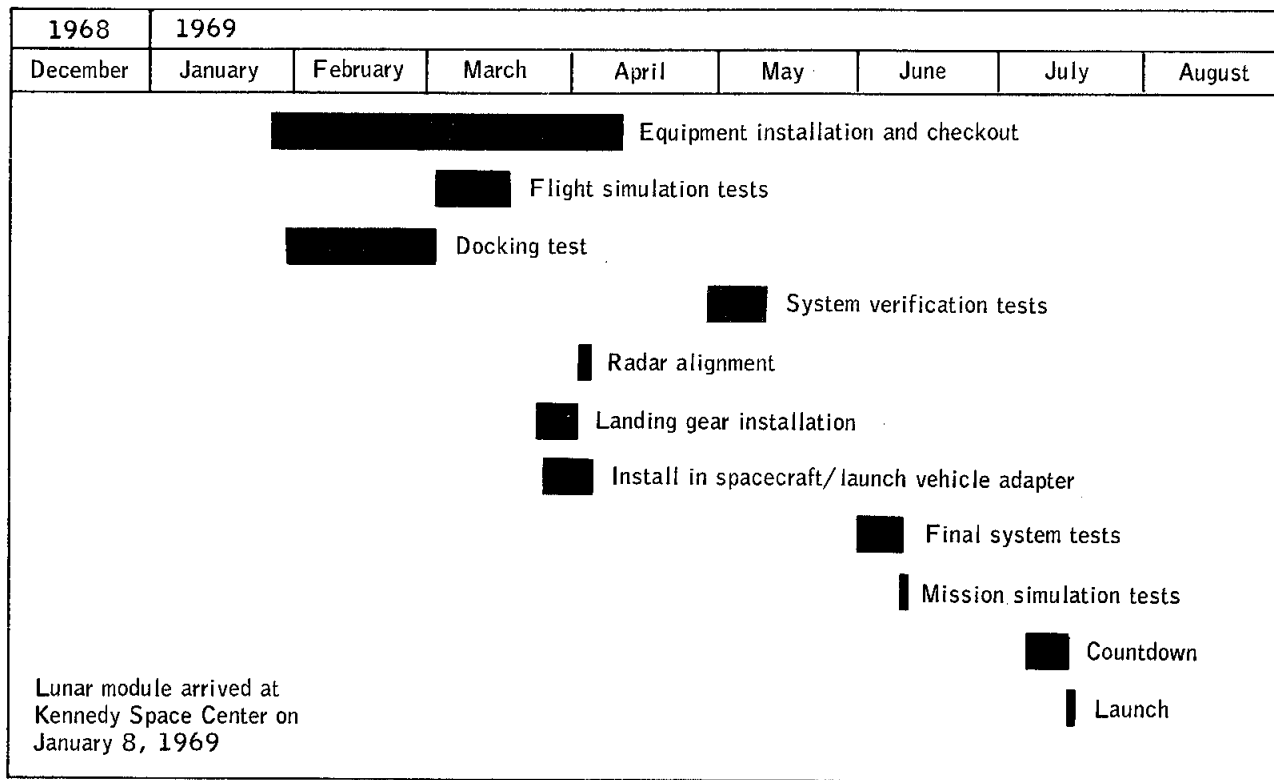


Figure B-4.- Lunar module checkout history at Kennedy Space Center.

APPENDIX C - POSTFLIGHT TESTING

The command module arrived at the Lunar Receiving Laboratory, Houston, Texas, on July 30, 1969, after reaction control system deactivation and pyrotechnic safing in Hawaii. After decontamination and at the end of the quarantine period, the command module was shipped to the contractor's facility in Downey, California, on August 14. Postflight testing and inspection of the command module for evaluation of the inflight performance and investigation of the flight irregularities were conducted at the contractor's and vendor's facilities and at the Manned Spacecraft Center in accordance with approved Apollo Spacecraft Hardware Utilization Requests (ASHUR's). The tests performed as a result of inflight problems are described in table C-I and discussed in the appropriate systems performance sections of this report. Tests being conducted for other purposes in accordance with other ASHUR's and the basic contract are not included.

TABLE C-I.- POSTFLIGHT TESTING SUMMARY

ASHUR no.	Purpose	Tests performed	Results
Environmental Control			
107001	To determine the cause of the downshift in oxygen flow reading and its remaining at the lower limit except for periods of high flow	End-to-end resistance and continuity check of the flow rate transducer calibration; calibration check and failure analysis	A capacitor in the electromagnetic interference filter was open and the resistance of the heater element on one of the two air stream probes was 600 ohms above the requirement.
107019	To determine the cause for the decrease in the primary glycol accumulator quantity	Leak test on the primary water/glycol system; leak test on the glycol reservoir valves	System was found to be tight and well within specification. Indication was that the glycol reservoir inlet valve was not fully closed during flight and allowed leakage into the reservoir.
107503	To determine the cause for high and low water/glycol temperatures sensed at the evaporator outlet during mixing mode operation in lunar orbit	Measure the glycol temperature controller deadband and determine response to a simulated glycol temperature sensor	All resistances and deadband proper. Control valve bound closed.
107039	To determine the cause for high and low water/glycol temperatures sensed at the evaporator outlet during mixing mode operation in lunar orbit	Remove control valve from spacecraft and perform electrical and mechanical acceptance tests. Disassemble control valve.	Broken bearing found interfering with gear train assembly. Analysis incomplete.
Reaction Control			
107014	To determine the cause of the malfunction of the command module negative yaw thruster	Circuit continuity verification	Continuity test determined that an intermittent existed on a terminal board. Wiring was found to be proper.
107016	To verify command module circuit associated with service module propellant isolation valves for quad B	Circuit continuity verification	Control circuit for service module reaction control quad B propellant isolation valves and indicators was proper through the command module to the circuit interrupter interface.

TABLE C-I.- POSTFLIGHT TESTING SUMMARY - Concluded

ASHUR no.	Purpose	Tests performed	Results
Crew Equipment			
107028	To determine the cause of high closing forces on the sample return containers	Examine the seal for comparison with ground test. Re-roll seal and measure latching forces.	Vacuum seal satisfactory. Latching force above maximum specification limits because of lubrication removal. Application of lubrication on similar latches, using Apollo 12 procedures, resulted in closing forces below maximum specification limits.
107030	To investigate the loose handle on the medical kit and overpressurization of pill containers	Visual inspection. Determine whether pin holes will prevent overpressurization	The handle was not attached to right end; only barely attached to left end. Unvented pill packages expand about 300 percent at 5 psia from ambient. Vented packages (two needle holes in film) do not expand at 5 psia from ambient.
107034	To investigate the voice turnaround problem during extravehicular activity	Turnaround test with extravehicular communications system packs and Commander and Lunar Module Pilot headsets in all possible connectors.	No defective circuits or components in either carrier. Up-voice turnaround was present in both headsets but always acquired with the Lunar Module Pilot carrier, regardless of position of connection. Turnaround was caused by audio/mechanical coupling, and could be acquired or eliminated by control of mechanical isolation of headset and earphone output level.
107038	Investigate leak in riser of liquid cooling garment.	X-ray and visually inspect hose and manifold. Verify corrective action.	During preflight adjustment of the liquid cooling garment, the spring reinforced riser hose was improperly drawn over the manifold nipple, cutting the inner wall of the hose between the spring and the nipple. Water/glycol leaked through the inner wall hole and ruptured the outer wall of the Lunar Module Pilot's garment during postflight tests at the qualification level of 31 psig. No leakage was found in the Commander's garment because the inner wall was sealed against the nipple by the spring behind the cut. Proper installation with the necessary between the nipple and spring will preclude cuts in the inner wall.

APPENDIX D - DATA AVAILABILITY

Tables D-I and D-II are summaries of the data made available for systems performance analyses and anomaly investigations. Table D-I lists the data from the command and service modules, and table D-II, the lunar module. Although the tables reflect only data processed from Network magnetic tapes, Network data tabulations and computer words were available during the mission with approximately a 4-hour delay. For additional information regarding data availability, the status listing of all mission data in the Central Metric Data File, building 12, MSC, should be consulted.



TABLE D-I.- COMMAND MODULE DATA AVAILABILITY

Time, hr:min		Range station	Event	Standard bandpass	Special bandpass	Computer words	Special programs	O'graphs or Brush recordings	Special plots or tabs
From	To								
-04:30	+00:23	ALDS		X	X				
+00:00	00:12	MILA	X	X	X	X	X	X	X
00:02	00:13	BDA	X	X	X	X		X	X
00:06	04:18	CATS		X	X				
00:09	00:15	VAN		X		X			
00:16	00:23	CYI				X			
00:28	01:30	D/T		X		X			
00:52	00:58	CRO		X					
00:59	01:05	HSK		X					
01:28	01:35	GDS		X					
01:33	01:45	MILA		X					
01:42	01:49	VAN		X					
01:50	01:55	CYI		X					
01:54	02:25	D/T		X					
02:25	02:32	CRO		X					
02:40	02:46	RED	X		X	X		X	
02:44	03:25	D/T	X	X	X	X	X	X	X
02:45	02:54	MER	X		X	X		X	X
02:49	03:15	HAW	X	X	X	X		X	
03:10	03:16	HAW	X	X	X	X	X	X	
03:15	03:25	D/T		X	X		X	X	
03:25	03:37	GDS	X	X		X		X	
04:02	04:57	GDS	X	X	X	X		X	
04:55	05:05	GDS	X	X	X	X		X	
05:24	05:43	GDS		X		X			
06:00	06:42	GDS				X			
06:35	07:45	CATS		X					
06:42	08:38	GDS				X			
08:04	11:38	CATS		X					
09:22	09:39	GDS	X			X			
10:39	10:57	GDS				X			
12:35	12:42	GDS				X			
14:45	16:19	CATS		X					
16:19	19:01	CATS		X					
17:23	17:34	D/T					X		
19:01	25:06	CATS		X					
24:00	24:19	MAD	X			X		X	
24:28	25:50	MAD				X			
25:06	27:05	CATS		X					
26:24	26:49	MAD	X	X	X	X	X	X	
26:48	27:00	MAD				X			
27:06	38:34	CATS		X					
27:15	27:35	MAD				X			
28:17	28:50	GDS	X						
29:14	30:50	GDS				X			
34:24	34:30	GDS				X			
35:39	36:01	GDS				X			
36:35	38:00	GDS				X			
38:34	42:23	CATS		X	X				
42:23	47:19	CATS		X	X				
44:23	44:33	HSK		X					
47:00	48:00	MAD				X			
47:19	53:49	CATS		X					
52:50	53:06	MAD				X			
53:49	56:50	CATS		X	X				
54:52	55:17	GDS	X	X					

TABLE D-I.- COMMAND MODULE DATA AVAILABILITY - Continued

Time, hr:min		Range station	Event	Standard bandpass	Special bandpass	Computer words	Special programs	O'graphs or Brush recordings	Special plots or tabs
From	To								
56:50	58:10	CATS		X	X				
57:15	57:30	GDS				X			
57:30	57:45	GDS		X		X			
58:10	73:09	CATS		X	X				
73:15	73:48	MAD			X			X	X
73:48	75:48	MAD						X	
75:48	75:57	D/T	X	X		X		X	
75:57	76:15	D/T		X		X			
77:39	78:24	GDS		X					
78:24	79:09	GDS	X			X		X	
78:41	80:22	MSFN		X	X				
79:07	79:47	GDS	X		X		X		
79:54	80:37	GDS		X			X		
80:10	80:43	D/T	X	X		X		X	
80:22	85:41	MSFN		X	X				
81:40	83:11	D/T		X					
83:43	84:30	D/T		X					
85:00	85:30	GDS					X		
85:41	86:32	D/T		X					
85:42	89:11	MSFN		X					
87:39	88:27	D/T		X					
88:32	89:41	HSK				X			
89:37	90:25	D/T		X					
90:25	93:07	MSFN		X	X				
90:29	91:39	HSK				X			
91:36	92:29	D/T		X		X			
92:30	92:40	HSK				X			
93:26	99:07	MSFN		X	X		X		
93:34	94:31	D/T		X				X	
94:22	94:34	MAD			X				X
95:32	96:20	D/T		X				X	
96:30	98:20	MSFN				X			
97:30	98:52	D/T		X		X			
98:20	100:00	MSFN				X			
98:50	99:00	MAD	X					X	
99:29	100:32	D/T		X		X			
100:35	100:45	MAD	X	X		X		X	
100:44	101:19	MSFN				X			
100:55	102:45	MSFN		X	X				
101:15	101:27	MAD				X			
101:27	102:14	D/T		X		X			
102:15	102:48	MAD				X			
102:49	106:48	MSFN		X	X	X			
103:25	104:19	D/T		X					
105:23	106:11	D/T		X					
106:28	110:21	MSFN		X	X				
107:21	108:10	D/T		X					
109:17	110:09	D/T		X					
110:31	113:16	MSFN		X	X				
111:18	112:38	D/T		X					
112:06	113:00	MSFN				X			
113:11	117:02	MSFN		X	X				
113:18	114:04	D/T		X					
115:17	116:02	D/T		X					
117:13	118:01	D/T		X					
118:00	122:06	MSFN		X	X				

TABLE D-I.- COMMAND MODULE DATA AVAILABILITY - Concluded

Time, hr:min		Range station	Event	Standard bandpass	Special bandpass	Computer words	Special programs	O'graphs or Brush recordings	Special plots or tabs
From	To								
119:11	119:58	D/T		X					
121:09	121:57	D/T		X					
122:12	124:37	MSFN				X			
122:26	126:26	MSFN		X	X				
123:06	124:20	D/T		X		X			
124:20	125:06	MSFN				X			
125:06	125:53	D/T				X			
126:29	130:23	MSFN		X	X				
126:37	127:07	GDS	X						
127:01	127:59	D/T		X		X			
127:52	128:10	GDS				X			
129:01	129:50	D/T		X					
130:00	130:12	GDS	X			X		X	
130:22	130:40	GDS		X			X		
130:23	134:26	MSFN		X	X				
131:00	131:48	D/T		X					
132:58	133:46	D/T		X					
134:26	137:42	MSFN		X	X				
134:27	134:58	MSFN				X			
134:58	135:35	D/T		X		X	X		
135:22	135:28	D/T	X	X	X	X		X	
135:38	135:49	HSK	X	X	X			X	
136:45	137:00	MSFN				X			
137:42	142:20	MSFN		X	X				
137:50	138:50	MSFN			X				
142:20	150:16	MSFN		X	X				
149:12	149:24	MSFN				X			
150:16	151:45	MSFN		X	X				
150:20	150:30	MAD	X	X	X		X	X	
151:40	152:31	GDS				X	X		
151:45	170:29	MSFN		X	X				
152:31	152:50	GDS				X	X		
170:29	174:19	MSFN		X	X				
170:40	171:39	MAD						X	
172:22	173:40	MAD				X	X		
177:00	177:40	GDS				X	X		
186:24	194:26	MSFN		X	X				
189:55	190:30	HSK	X						
192:04	192:30	MSFN				X			
194:09	194:34	HSK						X	
194:40	195:09	HSK	X	X	X	X	X	X	X
195:03	195:11	ARIA	X	X	X	X	X	X	X

TABLE D-II.- LUNAR MODULE DATA AVAILABILITY

Time, hr:min		Range station	Event	Standard bandpass	Special bandpass	Computer words	Special programs	O'graphs or Brush recordings	Special plots or tabs
From	To								
-04:30	-02:30	ALDS		X	X				
95:55	99:07	MSFN		X		X			
96:17	96:38	MAD	X						
96:37	96:48	MAD	X						
96:46	97:33	MAD	X						
98:16	99:08	MAD	X					X	
98:55	99:10	MAD						X	
99:07	99:20	MAD	X					X	
99:08	100:55	MSFN		X		X			
99:18	99:32	MAD	X					X	
99:30	99:48	D/T	X	X					
100:12	100:17	D/T	X	X					
100:15	100:44	MAD	X				X	X	
100:20	100:25	MAD		X					
100:43	100:53	MAD	X					X	
100:52	101:30	MAD	X					X	
100:53	102:16	MSFN		X		X			
101:30	102:13	D/T	X	X			X		
102:13	102:53	GDS	X	X	X	X	X	X	X
102:45	106:28	MSFN		X	X	X			X
102:52	103:03	GDS	X					X	
103:03	103:59	GDS	X	X			X		
103:57	104:04	MAD	X						
104:02	104:10	MAD	X						
104:10	104:57	GDS	X						
106:28	110:31	MSFN		X	X	X			
107:49	108:13	GDS	X						X
108:14	108:27	GDS	X						X
108:25	109:24	GDS			X				
110:31	113:16	MSFN		X	X	X			
113:11	117:48	MSFN		X	X	X			
113:30	114:00	HSK			X				
113:59	114:10	MSFN							X
114:08	114:21	HSK			X				
114:20	115:20	HSK			X				
118:00	122:06	MSFN		X		X			
121:35	121:45	MAD	X	X					
122:00	123:08	MAD	X			X		X	
122:18	122:25	MAD		X					
122:22	126:26	MSFN		X		X			
122:33	122:45	MAD			X				
123:08	124:08	MAD	X						
124:07	125:09	MAD	X	X		X		X	
124:20	124:35	MAD			X		X	X	
125:07	125:13	MAD	X						
125:51	126:29	MAD	X		X	X	X	X	
126:00	126:15	MAD		X					
126:15	126:29	GDS	X	X	X	X	X	X	X
126:27	126:35	MAD	X	X					
126:28	126:40	GDS	X					X	
126:29	130:23	MSFN		X		X			
126:37	127:07	GDS	X	X	X	X	X	X	
127:51	128:20	GDS	X	X	X				
128:19	129:04	GDS	X						
129:48	130:47	GDS						X	
130:00	130:25	GDS	X	X	X	X	X	X	

TABLE D-II.- LUNAR MODULE DATA AVAILABILITY - Concluded

Time, hr:min		Range station	Event	Standard bandpass	Special bandpass	Computer words	Special programs	O'graphs or Brush recordings	Special plots or tabs
From	To								
130:23	134:24	MSFN		X		X			
130:46	131:03	GDS	X				X		
132:43	133:02	GDS	X				X		
133:46	134:45	GDS	X				X		
134:24	137:42	MSFN		X		X			
134:44	135:01	GDS	X				X		
135:33	135:48	GDS	X				X		
135:44	135:58	GDS	X				X		
135:57	136:58	GDS	X				X		
137:48	137:54	MSFN		X		X			

APPENDIX E - GLOSSARY

The following definitions apply to terms used in section 10.

ablation	removal; wearing away
albedo	ratio of light reflected to light incident on a surface
basalt	generally, any fine-grained dark-colored igneous rock
breccia	see microbreccia
clast	rock composed of fragmental material of specified types
diabase	a fine-grained, igneous rock of the composition of a gabbro, but having lath-shaped plagioclase crystals enclosed wholly or in part in later formed augite
ejecta	material thrown out as from a volcano
euhebral	having crystals whose growth has not been interfered with
exfoliation	the process of breaking loose thin concentric shells or flakes from a rock surface
feldspar	any of a group of white, nearly white, flesh-red, bluish, or greenish minerals that are aluminum silicates with potassium, sodium, calcium, or barium
feldspathic	pertaining to feldspar
gabbro	a medium or coarse-grained basic igneous rock-forming intrusive bodies of medium or large size and consisting chiefly of plagioclase and pyroxene
gal	unit of acceleration equivalent to 1 centimeter per second per second
gnomon	instrument used for size and color comparison with known standards
igneous	formed by solidification from a molten or partially molten state
induration	hardening

lithic	stone-like
microbreccia	rock consisting of small sharp fragments embedded in any fine-grained matrix
mophologic	study of form and structure in physical geography
olivine	mineral; a magnesium-iron silicate commonly found in basic igneous rocks
peridotites	any of a group of granitoid igneous rocks composed of olivine and usually other ferromagnesian minerals but with little or no feldspar
plagioclase	a triclinic feldspar
platy	consisting of plates or flaky layers
pyroxene	a family of important rock-forming silicates
pyroxenites	an igneous rock, free from olivine, composed essentially of pyroxene
ray	any of the bright, whitish lines seen on the moon and appearing to radiate from lunar craters
regolith	surface soil
terra	earth
vesicle	small cavity in a mineral or rock, ordinarily produced by expansion of vapor in the molten mass

## REFERENCES

1. Marshall Space Flight Center: Saturn V Launch Vehicle Flight Evaluation Report AS-506 Apollo 11 Mission (publication number and date not assigned).
2. Boeing Company, Seattle, Washington: Lunar Gravitational Model Analysis for Apollo. December 5, 1968.
3. Manned Spacecraft Center: Apollo 10 Mission Report. Section 15.0 Anomaly Summary. MSC-00126. August 1969.
4. U.S. Geological Survey: Geologic Map of Theophilus Quadrangle of the Moon; Geologic Atlas of the Moon, Scale 1:1,000,000. I-546 (LAC 78). 1968
5. California Institute of Technology, Jet Propulsion Laboratory: Ranger VII, Pt. II, Experimenters Analysis and Interpretations. 32-700. 1965.
6. Journal Geophysics: Color Differences on the Lunar Surface by T. B. McCord. V.74, n.12, pp 3131-3142. 1969.
7. Science: Mascons: Lunar Mass Concentrations by P. M. Muller and W. L. Sjogren. V.161, pp 680-684. 1968.
8. California Institute of Technology, Jet Propulsion Laboratory: 1968 Surveyor Project Final Report Pt II Science Results, Section III Television Observations from Surveyor.
9. Government Printing Office: Interagency Committee on Back Contamination: Excerpts of Federal Regulation Pertinent to Contamination Control for Lunar Sample Return Missions. GPO 927-742.
10. NASA Headquarters: Protection of the Earth's Biosphere from Lunar Sources of Contamination; An Interagency Agreement Between the National Aeronautics and Space Administration; the Department of Agriculture; the Department of Health, Education, and Welfare; the Department of the Interior; and the National Academy of Sciences. August 24, 1967.
11. NASA Headquarters: Interagency Committee on Back Contamination; Quarantine Schemes for Manned Lunar Missions.
12. NASA Headquarters: Apollo Flight Mission Assignments. OMSF M-D MA 500-11 (SE 010-000-1). July 11, 1969.



13. NASA Headquarters: Mission Requirements, G-type Mission (Lunar Landing). SPD 9-R-039. April 17, 1969.
14. Manned Spacecraft Center: Apollo 9 Mission Report. MSC-PA-R-69-2. May 1969.

APOLLO SPACECRAFT FLIGHT HISTORY

(Continued from inside front cover)

<u>Mission</u>	<u>Spacecraft</u>	<u>Description</u>	<u>Launch date</u>	<u>Launch site</u>
Apollo 4	SC-017 LTA-10R	Supercircular entry at lunar return velocity	Nov. 9, 1967	Kennedy Space Center, Fla.
Apollo 5	LM-1	First lunar module flight	Jan. 22, 1968	Cape Kennedy, Fla.
Apollo 6	SC-020 LTA-2R	Verification of closed-loop emergency detection system	April 4, 1968	Kennedy Space Center, Fla.
Apollo 7	CSM 101	First manned flight; earth-orbital	Oct. 11, 1968	Cape Kennedy, Fla.
Apollo 8	CSM 103	First manned lunar orbital flight; first manned Saturn V launch	Dec. 21, 1968	Kennedy Space
Apollo 9	CSM 104 LM-3	First manned lunar module flight; earth orbit rendezvous; EVA	Mar. 3, 1969	Kennedy Space Center, Fla.
Apollo 10	CSM 106 LM-4	First lunar orbit rendezvous; low pass over lunar surface	May 18, 1969	Kennedy Space Center, Fla.
Apollo 11	CSM 107 LM-5	First lunar landing	July 16, 1969	Kennedy Space Center, Fla.
Apollo 12	CSM 108 LM-6	Second lunar landing	Nov. 14, 1969	Kennedy Space Center, Fla.